A MORPHOLOGICAL STUDY OF THE ORAL CAVITY, PHARYNGEAL CAVITY AND OESOPHAGUS OF THE NILE CROCODILE, *CROCODYLUS NILOTICUS* (LAURENTI, 1768)

by

JOHN FRASER PUTTERILL

Submitted in partial fulfilment of the requirements for the degree MSc

DEPARTMENT OF ANATOMY AND PHYSIOLOGY

FACULTY OF VETERINARY SCIENCE

UNIVERSITY OF PRETORIA

PRETORIA

2002

Supervisor: Professor J.T. Soley

Department of Anatomy and Physiology

Faculty of Veterinary Science

University of Pretoria

Pretoria

DECLARATION

I declare that the dissertation which I hereby submit for the degree Master of Science at the University of Pretoria is my own work and has not been submitted by me for a degree at another university.

To my wife Helena, my sons, Brandon and Dale, for their love, patience

and support…

and to that wonderful creature,

the Nile crocodile!

CONTENTS

ACKNOWLEDGEMENTS

The sustained encouragement and professional guidance from my supervisor, mentor and friend, Professor John Soley is sincerely appreciated.

I am also deeply indebted to Mr. and Mrs. Kuhlmann, of the Izintaba Croco Farm, De Wildt, Northwest Province, South Africa, who unselfishly allowed me access to their farm and supplied me with numerous and very valued specimens for this study.

The following persons and institutions are also thanked for their generous and skilful assistance:

From the Onderstepoort Veterinary Institute (OVI) of the Agricultural Research Council:

The staff of the Histology Laboratory, Pathology Division

Dr Fritz Huchzermeyer, Pathology Division (retired)

The staff of the Library

The staff of the Computer Centre

From the Faculty of Veterinary Science, University of Pretoria:

The staff of the Department of Anatomy and Physiology

The staff of the Electron Microscopy Unit

The staff of the Histology Laboratory, Department of Pathology

Ms Estelle Mayhew of the Graphics Department

The staff of the Centre for Microscopy and Microanalysis, University of Pretoria

Ms Louise Coetzee of the National Museum, Bloemfontein

Dr Harald Krenn of the Institut für Zoologie, Universität Wien, Austria

Mrs Priscilla Maartens, Electron Microscope Unit, University of Natal, Durban

Finally, throughout this study, I have endeavoured to adopt and work by a credo. The following text, written by Henry Baker in 1742, sums up my approach during this study:

"Beware of determining and declaring your opinion suddenly on any object; for imagination often gets the start of judgement, and makes people believe they see things, which better observations will convince them could not possibly be seen; therefore assert nothing till after repeated experiments and examinations in all lights and positions.

When you employ the microscope, shake off all prejudice, nor harbor any favourite opinions; for if you do, 'tis not unlikely fancy will betray you into error, and make you see what you wish to see.

Remember that truth alone is the matter that you are in search after; and if you have been mistaken, let not vanity seduce you to persist in your mistake.

Pass no judgement upon things over-extended by force, or contracted by dryness, or in any manner out of their natural state, without making suitable allowances.

There is no advantage in examining any object with a greater magnifier than what shows the same distinctly."

Henry Baker, 1742. Chapter 15, "Cautions in Viewing Objects", in *The Microscope Made Easy*. Obtained from ProjectMicro Website at the following www address: http://www.msa.microscopy.com/ProjectMicro/QuotesMicroscopes.html

SUMMARY

A MORPHOLOGICAL STUDY OF THE ORAL CAVITY, PHARYNGEAL CAVITY AND OESOPHAGUS OF THE NILE CROCODILE, *CROCODYLUS NILOTICUS* (LAURENTI, 1768)

by

JOHN FRASER PUTTERILL

SUPERVISOR: Professor J.T. Soley

DEPARTMENT: Department of Anatomy and Physiology, Faculty of Veterinary Science, University of Pretoria, Private Bag X04, Onderstepoort, 0110, Republic of South Africa.

DEGREE: MSc

In view of the paucity of detailed information in the literature relevant to the upper digestive tract of the Nile crocodile, this study describes the morphological and histological features of the oral cavity (gingivae, palate and tongue), pharyngeal cavity and oesophagus of the Nile crocodile, *Crocodylus niloticus* (Laurenti, 1768) using light microscopy. The findings, which were supplemented by scanning electron microscopy, were compared with published information. The ciliated component of the oesophagus was also examined using transmission electron microscopy.

The oral cavity had the form of a triangle and was dorso-ventrally flattened. The dorsal limit was formed by the palate and the ventral limit by the broad-based tongue. The close proximity of the tongue and palate severely limited the space within the cavity. The caudal border of the cavity was formed by the dorsal and ventral components of the gular valve. The epithelium of the palate, gingivae and tongue was stratified squamous in nature and appeared lightly keratinised. Specialised epithelial structures in the palate, gingivae and tongue, revealed by both light microscopy (LM) and scanning electron microscopy (SEM),

bore characteristics resembling structures responsible for pressure and taste reception. Glandular tissue in the tongue was arranged in a triangular formation in the posterior region and displayed morphological features ascribed to salt secreting glands described in other Crocodilia. There were no palatine glands in the oral region of the palate, except that the oral surface of the dorsal gular fold contained branched tubular mucus secreting glands.

The pharyngeal cavity was also dorso-ventrally flattened and was bordered rostrally by the flaccid dorsal gular fold, which displayed a median apical notch, and the ventral gular fold, which was supported internally by the broad rostral tip of the basihyal plate (hyaline cartilage). In the occluded mouth, the dorsal gular fold and the more rostrally positioned ventral component of the gular valve isolated the pharyngeal cavity. This arrangement is essential in preventing the crocodile from drowning (flooding of the pharyngeal cavity) while capturing prey. The roof of the pharyngeal cavity was characterised by the opening to the internal nares (an extension of the nasal passage from the external nares), the fibrous Eustachian plug sealing the common opening to the paired Eustachian ducts and a nodular tonsillar region, which was situated caudo-laterally to the Eustachian plug. Throughout this region, the epithelium was typically ciliated with goblet cells. However, the tonsillar nodules displayed regions of partial or no ciliation on their surface. SEM and stereomicroscopic observations showed fine longitudinal mucosal folding throughout the pharynx the distension of which, together with the large capacity for mucus production (produced by intraepithelial glands and mucus secreting glands), would facilitate the swallowing of large chunks of food in the living state. The ventrally situated laryngeal mound containing the slit-like glottis also displayed longitudinal folds and a ciliated epithelium.

Anatomically, the oesophagus could be divided into two clear regions. The cranial, approximate two-thirds appeared broad and flabby. At the tracheal bifurcation, the oesophagus narrowed significantly and indicated a greater muscular content, confirmed by light microscopy. LM and SEM examination of the oesophagus, however, revealed three regional components, *viz*., the cranial, mid- and caudal regions. In the cranial region, the epithelium was densely ciliated with intervening goblet cells being present. In the mid-region the ciliated component decreased with a concomitant increase in the goblet cell component. In the caudal region there was a further decrease in the number of ciliated cells and a higher concentration of goblet cells. Transmission electron microscopy (TEM) of the ciliated component of the oesophagus showed typical ultrastructural features of both the ciliated and goblet cells.

CHAPTER 1

GENERAL INTRODUCTION

ORIGIN OF THE CROCODILIA

The Crocodilia evolved over 200 million years ago, beginning in the late Triassic period when other important reptilian groups (turtles, lizards and dinosaurs) were starting to dominate (Bellairs, 1987). The Crocodilians belong to the group of "ruling reptiles" or archosaurs which also include the extinct and most primitive earliest members, the thecodonts. The thecodonts included the dinosaurs and the pterosaurs, or flying reptiles, and the ancestors of birds (Bellairs, 1987). The Cretaceous period (140 to 65 million years ago) saw the appearance of the most advanced Crocodilians, including the present-day crocodiles, belonging to the suborder Eusuchia (Bellairs, 1987). The genus *Crocodylus* appeared in the Early Tertiary period, probably in the Eocene (55 – 37 million years ago) or Oligocene (37 – 25 million years ago) (Buffetaut, 1979).

The family Crocodylidae has three subfamilies; the Crocodylinae (genera *Crocodylus* and *Osteolaemus*), Alligatorinae (genera *Alligator*, *Caiman*, *Paleosuchus* and *Melanosuchus*) and Gavialinae (genera *Gavialis* and possibly *Tomistoma*, the "false gharial" were previously thought to belong in the subfamily Crocodylinae [Taplin, 1984]). Ross and Magnusson (1989) place *Tomistoma* (the “false gharial”) in the subfamily Crocodylinae.

DISTRIBUTION AND BREEDING BIOLOGY OF *Crocodylus niloticus*

The Nile crocodile, *Crocodylus niloticus* (Laurenti, 1768), is widely distributed throughout Africa south of the Sahara, except in the extreme south and southwest. Its distribution extends northwards along the Nile River as far as Lake Nasser and it is also found on Madagascar (Groombridge, 1987). Historical distribution has included the Mediterranean coast (from Tunisia to Syria) and isolated groups have also been known to occur

in lakes and waterholes in Mauritania, SE Algeria and NE Chad, in the Sahara Desert (Ross & Magnusson, 1989). *C. niloticus* is regarded as a large animal, ranging from 3.5 to 5 m in length and is found in a variety of wetland habitats, *viz.,* rivers, lakes and swamps. They mature sexually from 12 to 15 years of age at a length of 2 – 3 m. Nests are made in holes in the ground with clutches of eggs being laid seasonally and averaging about 50 eggs per clutch. Both parents tend the young hatchlings for about 8 weeks (Groombridge, 1987). The diet of the Nile crocodile varies with age. Young animals will eat insects and spiders or small vertebrates like frogs, fish, snakes and lizards. The adult crocodiles eat antelope, zebra, warthog, wildebeest and humans (Ross & Magnusson, 1989).

ECONOMIC IMPORTANCE

The Nile crocodile is increasingly being utilised on an intensive scale in the farming industry. To date, approximately 40 crocodile farms exist in both South Africa and Zimbabwe. The economic importance of the crocodile lies almost exclusively in the skin trade and, to an increasing extent, in meat production, Chinese medicines (feet, heads and organs) and also the ethnic "muti" trade. Meat from carcasses is normally supplied to the local restaurant trade, with some being exported in the form of whole tails or "stir-fry" from off-cuts from the rib cage and legs. Some farms, not being equipped for hygienic carcass processing, simply feed the carcasses back to the adult breeding stock. No figures pertaining to the total value of the crocodile meat trade could be obtained. The commercial utilisation of this animal has focused attention on the ecology and biology of the Crocodilia. Commercial crocodile farming in South Africa forms a small but viable industry and continued research into nutrition and physiology is vital to its continuance. The world economy and its ability to absorb luxury goods made from crocodile skin also plays an important role. The recent world economic recession in 1998 had a very damaging effect on this industry, resulting in the closure of a number of crocodile farms.

Worldwide production of skins is divided into “wild-harvested” skins and “ranched” skins. There are five crocodilian species being utilised for wild-harvesting of skins, *viz*., *Alligator mississippiensis*, *Caiman* sp., *Crocodylus porosus*, *Crocodylus niloticus* and *Crocodylus novaeguineae* and four species being used for ranched skins *viz*., *Alligator mississippiensis*, *Crocodylus porosus*, *Crocodylus niloticus* and *Crocodylus novaeguineae* (MacGregor, 2001). The total estimated world production of skins from all the above species from 1977 – 1999 was 10.5 million wild-harvested skins and 2.44 million ranched skins (MacGregor, 2001).

Total wild-harvested skins in 1977 numbered 0.43 million and only 0.07 million in 1999, peaking between 1983 - 1985 at approximately 1.4 million per year. Ranched skins, on the other hand, have shown an encouraging increase in production from figures of only 1258 in 1977 to 0.256 million in 1999 (figures extrapolated from MacGregor, 2001). No figures for this period for South African/Zimbabwean production, or percentage of the totals, were available, except that during 1988 South Africa provided less than 2 % of the total world production of crocodile skins suitable for the skin industry and only 5.3 % of the total world production of Nile crocodile skins (Marais & Smith, 1990).

The reasons for this poor performance by the South African crocodile industry are multi-factorial. South Africa is a member of the Convention on International Trade in Endangered Species of Fauna and Flora (CITES). South African crocodiles are classified under CITES Appendix I regulations which prevents the harvesting of eggs and hatchlings from the wild. Originally listed on CITES Appendix I, the Zimbabwean population was transferred to CITES Appendix II in 1983 and a number of other African countries including Madagascar, were transferred to Appendix II in 1985. CITES Appendix II listing provides for legal trade of wild-caught animals with set quotas (Groombridge, 1987). Secondly, breeding stock is not readily available. At present the South African crocodile industry is in a phase where brood-stock is being accumulated and little is being produced in the way of skins. Market trends also play a major role in determining the number of animals slaughtered. The crocodile farm from which material for this study was collected only slaughtered 250 to 400 animals on a weekly basis. Other farms only slaughter on demand, i.e., when orders for skins have been received (F.W. Huchzermeyer, personal communication, 2000).

SOURCE AND COLLECTION OF MATERIAL

Clinically healthy *C. niloticus* specimens of either sex were obtained from Izintaba Croco Farm, Brits District, Northwest Province, South Africa, where they were slaughtered commercially for their skins and meat. The operation on the farm revolves around the two breeding dams (Fig. 1A) which have laying pens constructed around their perimeters. Eggs, which are laid seasonally in ground nests, are harvested from the laying pens on a daily basis and removed for incubation. Hatchlings are further incubator raised to slaughter age (2.5 – 3 year-old and 1.2 - 1.5 m in length). Slaughter age animals are randomly selected and shot in the brain (Fig. 1B) at close range using a .22 calibre rifle. Shot carcasses are then removed to the abattoir for further processing. Although death was instantaneous, there was a

mandatory waiting period of approximately 45 minutes to allow carcasses to overcome post mortem tremor before commencing the skinning process. As the animals were slaughtered for their skins, any sudden reflex movement by the carcass during the skinning process might have caused a nick or cut to the skin, thus reducing its market value.

After the skinning process, tails are removed using a band saw and the head and torso suspended from the angle of the mandible in preparation for evisceration (Fig. 1C). During evisceration (Fig. 1D), the oesophagus is cut at the caudal pharyngeal limit and clamped to prevent contamination of meat by ingesta and the viscera are cut away from the thoracic and abdominal cavities. Eviscerated carcasses are then further processed into pieces and vacuum packaged prior to being deep-frozen. The skins, after being cleaned of attached muscle tissue, are salted, packaged and refrigerated for export.

AIM OF THIS STUDY

The nutrition of captive crocodilia is non-natural, and a balanced diet is continually being investigated. However, little information is currently available regarding the histology of the alimentary tract of the Nile crocodile, *C. niloticus* and existing data mainly refer to the gross anatomy of the American alligator or caiman. A number of studies have detailed the macroscopic and microscopic morphology of the digestive tract of various reptilian species including representatives of the *Crocodilia* (reviewed by Luppa, 1977). Other workers have concentrated on descriptions of the internal relief of the reptilian digestive tract (see Parsons and Cameron, 1977). Many of these studies provided scant and sometimes erroneous information as they were based on a limited number of specimens which, in earlier studies, may not have been optimally preserved (Parsons and Cameron, 1977). In recent years (1992 – 2002) a few light microscopic and scanning electron microscopic (SEM) studies of the digestive tract of *C. niloticus* have been published (Kotzé, van der Merwe, van Aswegen & Smith, 1992; Kotzé & Soley, 1995). However, with the exception of some preliminary reports (Putterill, van der Merwe & Soley, 1991; Putterill & Soley, 1998a; Putterill & Soley, 1998b; Putterill & Soley, 2001; Putterill & Soley, 2002), these publications fail to provide meaningful data on the morphology of the upper digestive tract.

This study presents a macroscopic and light-microscopical study of the mouth cavity (gingivae, palate and tongue), pharyngeal cavity and oesophagus of the Nile crocodile, *Crocodylus niloticus* (Laurenti, 1768). Light microscopy will concentrate on a description of the various tissue layers of the above-

mentioned regions of the upper digestive tract and will be supplemented by a detailed scanning electron microscopic (SEM) study of the appropriate surface features. SEM provides a convenient overall view of surface features and is valuable in correlating data obtained by other microscopic techniques. Transmission electron microscopy (TEM) will be utilised to describe the ultrastructure of the ciliated epithelium seen throughout the upper digestive tract, particularly in the oesophagus and pharynx. The results are compared with published information on this and other crocodilian species. The study provides a normal data base for histopathological examination of the tissues described and also creates a basis for further studies into the digestive physiology of the crocodile.

REFERENCES

BELLAIRS, A. d'A., 1987. The crocodilia, in *Wildlife management: crocodiles and alligators*, edited by G.J.W. Webb, S.C. Manolis, & P.J. Whitehead. Surrey Beatty and Sons Pty. (Ltd), in association with The Conservation Commission of the Northern Territory, Chipping Norton, NSW: 5-7.

BUFFETAUT, E. 1979. The evolution of the crocodilians. *Scientific American*, 241:124-132.

GROOMBRIDGE, B. 1987. The distribution and status of world crocodilians, in *Wildlife management: crocodiles and alligators*, edited by G.J.W. Webb, S.C. Manolis, & P.J. Whitehead. Surrey Beatty and Sons Pty. (Ltd) in association with The Conservation Commission of the Northern Territory, Chipping Norton, NSW: 9-18.

KOTZÉ, S.H. & SOLEY, J.T. 1995. Scanning electron microscopic study of intestinal mucosa of the Nile crocodile (*Crocodylus niloticus*). *Journal of Morphology*, 225:169-178.

KOTZÉ, S.H., VAN DER MERWE, N.J., VAN ASWEGEN G. & SMITH, G.A. 1992. A light microscopical study of the intestinal tract of the Nile crocodile (*Crocodylus niloticus*, Laurenti 1768). *Onderstepoort Journal of Veterinary Research*, 59:249-252.

LUPPA, H. 1977. Histology of the digestive tract, in *Biology of the Reptilia*, *Morphology E*, edited by C. Gans, & T.S. Parsons. London: Academic Press: Volume 6:225-313.

MACGREGOR, J. 2001. International trade in Crocodilian skins: Review and analysis of the economic issues for conservation. Report submitted to Florida Department of Agriculture and Consumer Affairs, contract # 005923, and Louisiana Department of Wildlife and Fisheries CMF # 567716, USA:130 pp.

PARSONS, T.S. & CAMERON, J.E. 1977. Internal relief of the digestive tract, in *Biology of the Reptilia*, *Morphology E*, edited by C. Gans, & T.S. Parsons. London: Academic Press: Volume 6:159-223.

PUTTERILL, J.F. & SOLEY J.T. 1998a. Histology of the tongue of the Nile crocodile, *Crocodylus niloticus*

(Laurenti, 1768). *Proceedings of the Microscopical Society of Southern Africa*, 28:89.

PUTTERILL, J.F. & SOLEY J.T. 1998b. Histology of the gular valve of the Nile crocodile, *Crocodylus niloticus* (Laurenti, 1768). *Proceedings of the Microscopical Society of Southern Africa*, 28:90.

PUTTERILL, J.F. & SOLEY, J.T. 2001. Morphology of the roof of the pharyngeal cavity of the Nile crocodile, *Crocodylus niloticus* (Laurenti, 1768). *Proceedings of the Microscopical Society of Southern Africa*, 31:69.

PUTTERILL, J.F. & SOLEY, J.T. 2002. Morphology of the pharyngeal cavity of the Nile crocodile, *Crocodylus niloticus* (Laurenti, 1768). *Proceedings of the 15th International Congress on Electron Microscopy*: *Life Sciences*, Durban, South Africa, 1 – 6 September 2002, Volume 2:591-592.

PUTTERILL, J.F., VAN DER MERWE, N.J. & SOLEY, J.T. 1991. Scanning electron and light microscopy of the oesophagus of the Nile crocodile, *Crocodylus niloticus*. *Proceedings of the Electron Microscopy Society of Southern Africa*, 21:235-236.

ROSS, C.A. & MAGNUSSON, W.E. 1989. Living crocodilians, in *Crocodiles and alligators*, edited by C.A. Ross and S. Garnett. London: Merehurst Press: 58-67.

MARAIS, J., & SMITH, G.A. 1990. (Eds). The world skin trade and South Africa, in *Crocodilian News*, Pretoria: The Crocodilian Study Group of Southern Africa: 1:7-11.

TAPLIN, L. 1984. Evolution and zoogeography of crocodilians: a new look at an ancient order, in *Vertebrate Evolution and Zoogeography in Australia*, edited by M. Archer and G. Clayton. Perth: Hesperian Press: 361-370.

FIGURE 1: THE BREEDING FARM AI[illegible]IG OF CARCASSES

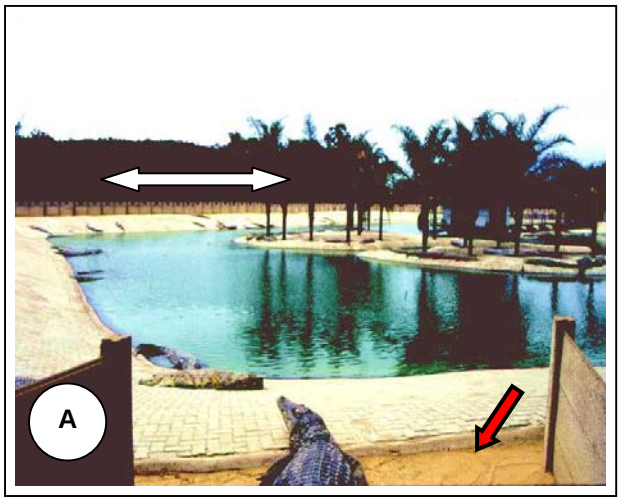

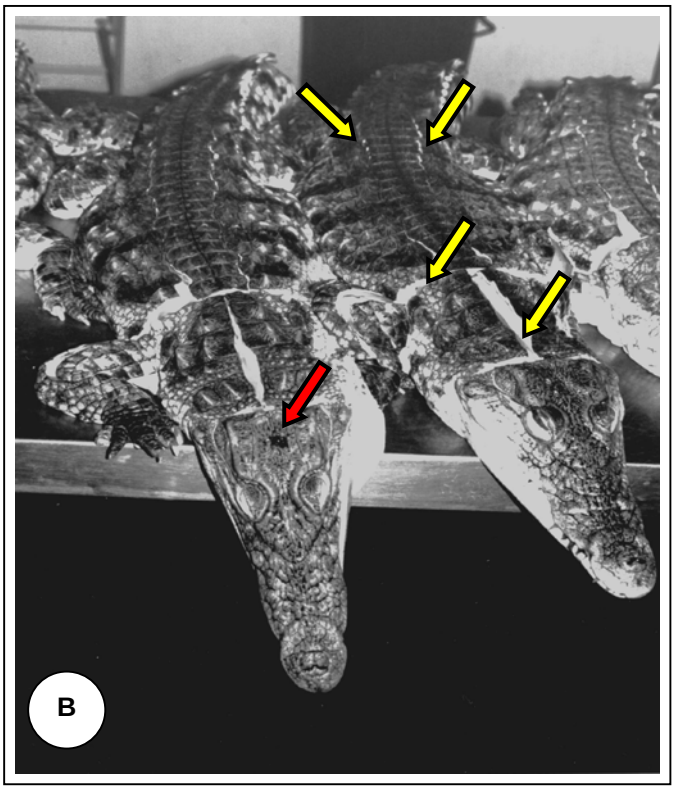

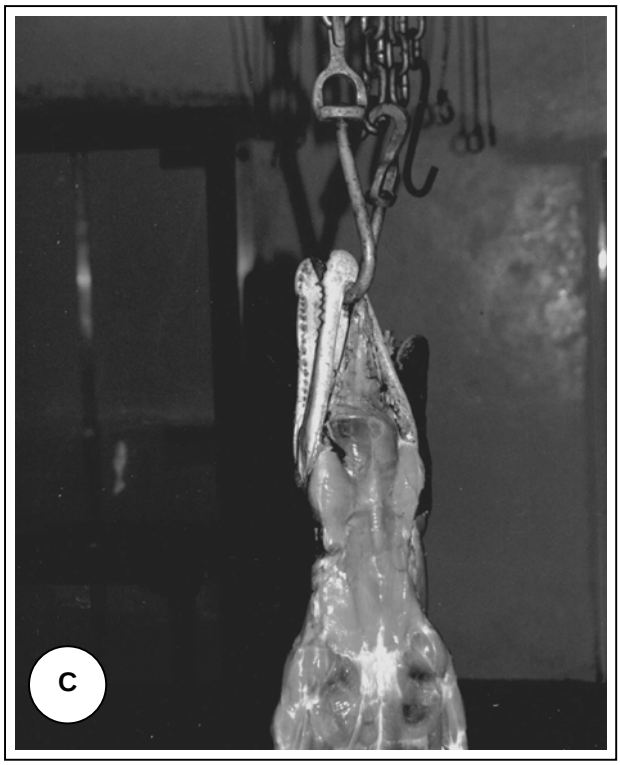

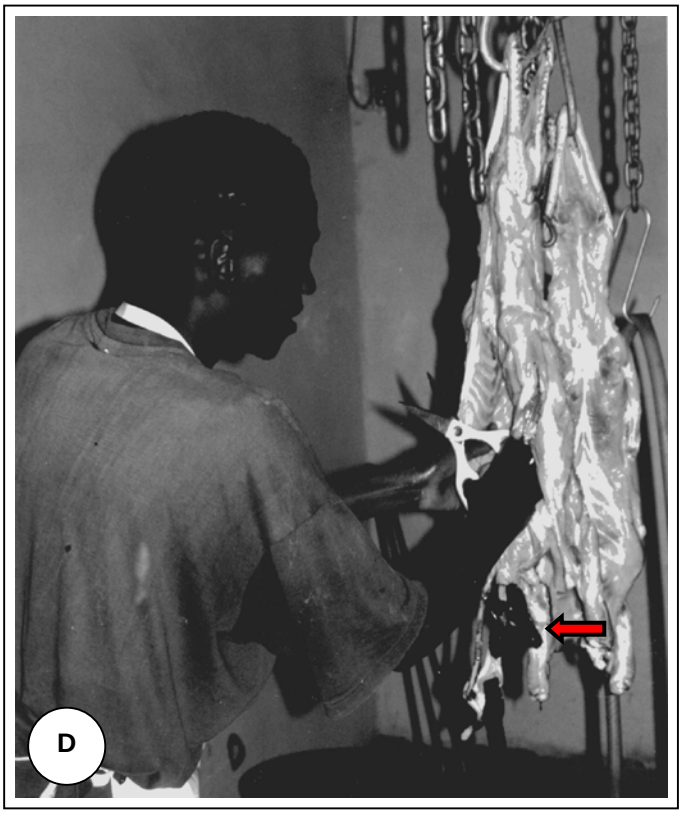

FIG. 1A: Eggs are laid seasonally in ground nests and harvested from laying pens (red arrow) on a daily basis for incubation. Laying pens extend around the perimeter (double headed arrow) of the dam enclosure.

FIG. 1B: After raising young crocodiles to slaughter age (2.5 – 3 year-old), animals are shot in the brain (red arrow) and prepared in the abattoir for the skinning process (yellow arrows).

FIG. 1C: After the skinning process, tails are removed using a band saw and the head and torso suspended from the angle of the mandible in preparation for evisceration.

FIG. 1D: During evisceration of the torso, the oesophagus is cut at the caudal pharyngeal limit and clamped to prevent contamination of meat by ingesta. In the photograph, the clamped oesophagus (arrow) is seen hanging with the rest of the GIT at the caudal aspect of the abdomen prior to being removed from the carcass. This procedure prevented the use of some regions of the oesophagus, due to bruising.

CHAPTER 2

MORPHOLOGY OF THE ORAL CAVITY – TONGUE, PALATE AND GINGIVAE

INTRODUCTION

The morphology and microscopic anatomy of the reptilian oral cavity has received much attention in the literature (for a review see Luppa, 1977), with most of these studies concentrating on the description and location of glandular tissue, taste receptors and epithelial specialisation of the region. Attention has also been given to the embryological and evolutionary development of these specialisations. Similarly, most studies on the oral cavity of Crocodilians have concentrated on specific morphological features of this region. Gaupp (1888, cited by Röse, 1893) described lingual glands (*glandulae linguales*) in crocodilians and Röse (1893) reported the presence of glandular tissue situated in pits between the teeth of the maxilla (*glandulae palatinae*) in *Crocodylus porosus* and elucidated further on the embryological development of these glands. A more recent investigation by Chen, Tang, Wei and Zhang (1989) examined the lingual glands of the Chinese alligator, *Alligator sinensis*. Lingual salt secreting glands in *Crocodylus porosus* were reported by Taplin and Grigg (1981) after intraperitoneal injection of methacholine chloride. Taplin, Grigg and Beard (1985) subsequently also used methacholine chloride to stimulate lingual gland secretion in several other species of Crocodylinae (*Crocodylus acutus, C. johnsoni, C. acutus*, *C. palustris*, *C. cataphractus*, *C. niloticus* and *Osteolaemus tetraspis*) and Alligatorinae (*Alligator mississippiensis* and *Caiman crocodilus*) and reported that in all instances the animals possessed functional lingual glands, but that only the Crocodylinae secreted significant concentrations of Na^+, indicating the presence of salt secreting glands.

Bath (1905, 1906) described the histology of taste receptors in the oral cavity, pharynx and oesophagus of *Crocodilus niloticus* (*sic*.) and *Aligator mississipiensis* (*sic*.), finding no clear distinction between those seen in these species and those of higher animals. Hulanicka (1913) investigated the innervation of the

tongue, palate and the skin of *Crocodylus niloticus* and *Alligator mississippiensis* and described five different nerve endings in the regions studied.

Fuchs (1908, cited by Barge, 1937) postulated the formation of the secondary palate in the Crocodilia and compared this formation to other reptiles, concluding that the secondary palate of crocodiles was unique amongst the reptiles. Barge (1937) described the embryological development and phylogeny of the secondary palate in crocodiles. Ferguson (1979) investigated the developmental mechanisms in normal and abnormal palate formation in the American alligator (*Alligator mississippiensis*) and stated that "the Crocodilia exhibit characteristics which are part mammalian and part reptilian, and this unique combination makes them a particularly useful model in which to study palatogenesis."

Dentition in Crocodilia has also received much attention in the literature. Of note is the paper by Poole (1961) who described tooth replacement in *C. niloticus*, the studies by Westergaard and Ferguson (1986, 1987) who described the development of dentition in hatchling and juvenile *A. mississippiensis* and the article by Kieser, Klapsidis, Law, and Marion (1993) who examined heterodonty and patterns of tooth replacement in *C. niloticus*. Sues (1989), who also described the process of tooth replacement in crocodilians, however, concluded that the teeth were isodont in nature. Edmund (1962, 1969) also made a major contribution to studies on dentition in the Reptilia, including the Crocodilia, describing the sequence and rate of tooth replacement in these reptiles.

Although detailed descriptions of specific components of the crocodilian oral cavity have been presented, only a few studies have reported on the general histological features of this region. Reese (1913) studied the histology of the enteron of the Florida alligator, which included the oral cavity. Reese's description, however, concerned histological differences between hibernating and feeding, captive animals. Taguchi (1920) compared similar regions of the oral cavity to those examined by Reese (1913) in three species of Crocodilia, namely, *Alligator sinensis*, *Krokodilus porosus* and *Krokodilus vulgaris* (*K. vulgaris* is believed to represent the Nile crocodile, *Crocodylus niloticus* – see *http://www.flmnh.ufl.edu/natsci/herpetology/turtcroclist/chklst2.htm*. When referring to the findings of Taguchi (1920) throughout this dissertation, "*Krokodilus*" is referred to as "*Crocodylus*" and "*K. vulgaris*" as "*C. niloticus*"). In Chiasson's (1962) publication on the anatomy of the alligator, only the component regions of the oral cavity (palate and tongue) are mentioned without any further detail being given. Parsons

& Cameron (1977) examined the relief of the gastro-intestinal tract, but only start their description from the oesophagus, disregarding the morphology of the oral and pharyngeal cavities.

In view of the paucity of information pertaining to the general histological features of this part of the upper digestive tract, this chapter presents a description of the macroscopic and microscopic features of the tongue, palate and gingiva of the Nile crocodile, *Crocodylus niloticus* (Laurenti, 1768) and compares the results with published information on this species and other Crocodilia. The histological features are supplemented by information supplied by scanning electron microscopy (SEM).

MATERIALS AND METHODS

Experimental animals

Nine clinically healthy 2.5 - 3 year-old *C. niloticus* specimens of either sex were obtained from a breeding farm where they were slaughtered commercially for their skins and meat. The lengths of the animals sampled ranged from 1.2 - 1.5 m. Animals were shot in the brain (see Chapter 1 - Fig. 1B) at close range using a .22 calibre rifle. Although death was instantaneous, carcasses were left until all obvious signs of post mortem tremor had ceased before commencing the skinning process. There was therefore an unavoidable delay of approximately 45 minutes before tissues could be fixed for microscopy. The heads were removed from the skinned carcasses and immersion fixed in a large volume of 10 % phosphate-buffered formalin in plastic buckets for two hours after which six of the heads were removed to allow sampling of the tongues as indicated below. These heads were re-immersed in fixative and all nine heads were further immersion fixed for a minimum period of 48 hours. Care was taken to exclude air by wedging a small block of wood in the angle of the mouth prior to immersion in the fixative. Samples from the palate and gingivae were removed from the appropriate six heads after the minimum fixation period of 48 hours and processed for LM and SEM examination according to the procedures detailed below.

Topography

The three formalin-fixed heads with tongues *in situ* were utilised for a description of the gross anatomical features and topographical relationships of the structures in the oral cavity. Macrophotographs were recorded digitally using a Nikon Coolpix 995 (Nikon, Tokyo, Japan) digital camera or on 35 mm film

using a Chinon X-7 (Chinon, Tokyo, Japan) single lens reflex camera, respectively. The oral cavities of these heads were also examined and micrographed using a stereomicroscope (Wild M-400 Photomakroskop, Heerbrugg, Switzerland) to obtain higher magnification micrographs of specific topographical features.

A dried skull from a five-year-old (approximate age) specimen was used to confirm the position and naming of teeth in the maxilla and mandible as well as to provide supporting evidence for the anatomical description. Teeth were named and numbered according to Kieser *et al*. (1993).

Light microscopy (LM)

As noted above, the tongues were removed from six heads after a short fixation period of two hours. This pre-fixation was deemed necessary to firm the relatively soft tissue of the organ prior to it being cut into the various segments for light microscopy and scanning electron microscopy. These tongues were freed from the mandible by cutting through the peripheral membrane and the tissue mass at the base of the tongue. The ventral half of the tongue was removed and discarded and the remaining dorsal surface was divided longitudinally into left and right halves down the midline. Identical transverse sections from the regions indicated in Fig. 1A were taken from each half of the tongue for LM and SEM, respectively. Both sets of samples were fixed for a minimum period of 48 hours in fresh 10 % buffered formalin.

Samples of the gingiva from the mandible were removed from the various regions indicated in Fig. 1A and were based on the position of the incisor and canine teeth. The portion of gingiva caudal to the indicated regions, i.e., the region involving the molar teeth, was too firmly attached to the underlying bone to permit reasonable samples to be taken. The mucosa of the palate was also sampled according to the dental arrangement of the teeth, i.e., from regions I 1 to I 5, C 1 to C 5 and M 1 to M 8 as shown in Fig. 1B. As the gingiva of the maxilla appeared macroscopically to be continuous with the palate, these specimens were removed together with the samples of the palate. A similar set of specimens (adjacent tissue) from all the indicated regions of the mandible and palate was taken at the same time for scanning electron microscopy.

LM samples were dehydrated through 70, 80, 96 and 2X 100 % ethanol and further processed through 50 : 50 ethanol : xylol, 2X xylol and 2X paraffin wax (60 - 120 minutes per step) using a Shandon model 2LE Automatic Tissue Processor (Shandon, Pittsburgh, PA, USA). Tissue samples were finally embedded

manually into paraffin wax in brass moulds. Sections were cut at 4 - 6 μm, stained with haematoxylin and eosin (H&E) (Luna, 1968) or periodic acid-Schiff (PAS) (Pearse, 1985) and viewed and micrographed using a Reichert Polyvar (Reichert, Austria) compound light microscope fitted with a differential interference contrast (DIC) prism.

Scanning electron microscopy (SEM)

The samples of the tongue, gingiva and palate obtained as indicated above, had been fixed in 10 % phosphate-buffered formalin for a minimum of 48 hours after which they were rinsed for several hours in water to remove traces of phosphate buffer. These samples were routinely dehydrated through an ascending ethanol series (50, 70, 90, 95 and 3X 100 % - 60 minutes per step) and critical point dried from 100 % ethanol through liquid-CO_2 in a Polaron Critical Point Drier (Polaron, Watford, England). The samples were then mounted onto brass or aluminium viewing stubs (to expose the epithelial surface) with a conductive paste (carbon dag) and sputter coated with gold using a Balzers 020 Sputter Coater (Balzers Union, Liechtenstein). Specimens were viewed and photographed using a Hitachi S-2500 Scanning Electron Microscope (Hitachi, Tokyo, Japan) operated at 8 kV.

RESULTS

Macroscopic Features

The oral cavity had the form of an isosceles triangle and was dorso-ventrally flattened, severely limiting the space within the cavity (see Fig. 1 – Chapter 3 & Figs. 1A & B - this Chapter). The roof of the cavity was formed exclusively by the palate and the indistinct gingiva with which it was continuous. The caudal limit of the roof was demarcated by the notched dorsal component of the gular valve (see Chapter 3 - Figs. 2C & D & 3A & C), whereas the rostral limit of the palate was occasionally characterised by the presence of two deep pits which accommodated the first two incisors of the mandible. Between the two pits (or at the base of the two I 1 teeth) was a small, rigid, conically-shaped process (Fig. 1B) which emerged from a low-profiled ridge above the anterior palatine foramen. The tip of this process was housed within a shallow depression in the mandible at the base of the first two mandibular incisors (Fig. 1A). The surface of the palate had a cobbled appearance (Fig. 1B) due to the presence of numerous, raised, cobble-like structures. The cobbles on the rostral two-thirds of the palate were large, whereas those occupying the caudo-lateral aspects of the

palate were smaller, had a lower profile, but were densely arranged. Between the latter two regions were paired elliptical areas, devoid of cobbles, and which merged medially along the midline of the palate (Fig. 1B). These smooth areas corresponded to the positioning of the left and right posterior palatine foraminae which were formed by the caudal edges of the maxillary, the lateral edges of the palatine, a small region of the rostral edge of the pterygoid and the medial edge of the transpalatine bones. Along the mid-line of the palate were a series of closely positioned cobbles forming a clearly defined median ridge. This ridge extended from the conical process mentioned above to the base of the dorsal fold of the gular valve. However, the part of the ridge dividing the two smooth elliptical areas above the posterior palatine foraminae was less distinct in nature. The base of the palate adjacent to the dorsal fold of the gular valve displayed a variable number of transverse mucosal folds which closely followed the contours of the dorsal fold across its entire breadth (Fig. 1B).

The gingiva of the maxilla was continuous with the palate and could practically be considered to be part of it (Fig. 1B). A relatively wide (4 – 5 mm), clearly demarcated zone of smooth mucosa (possibly representing the palatal aspect of the gingiva) separated the cobbled portion of the palate from the maxillary teeth, from approximately C 3 to M 8. From approximately C 2 rostrally, the surface of the gingiva also had a cobbled appearance similar to that of the palate and the boundary between the latter and the gingiva was not clearly defined. The teeth of the maxilla reflected the dental formula described by Kieser *et al.* (1993) and were carried in the premaxillary and maxillary bones. In the occluded mouth, the teeth of the maxilla were accommodated in grooves to the outside of the mandible, between the teeth of the lower jaw. The tips of the teeth of the mandible were accommodated in pits situated between the teeth of the maxilla.

The floor of the oral cavity was formed by the tongue and a wide, rostral mucosal plate continuous with the gingiva. This plate represented the mucosa-covered surface of the widened rostral tips of the paired dentary bones of the mandible where they met at the dentary symphysis. This plate extended from the rostrally-positioned first two incisors to a point approximately midway between C 1 and C 2 (Figs. 1A & 2A). The relatively long tongue was roughly triangular in shape, being much broader caudally than at its tip (Fig. 1A). It occupied the greater part of the floor of the oral cavity (apart from the rostral plate over the symphysis of the dentary bones) and was bordered peripherally by a loose, highly folded, continuous, fibrous membrane. This membrane attached the ventro-lateral aspect of the tongue to the ventro-medial aspect of the mandible. The membrane was more complexly folded around the rostral tip of the tongue.

In the specimens examined the tip of the tongue was always pulled away (in a caudal direction) from the apex formed by the rostral fusion of the paired dentary bones, revealing the highly folded membrane attaching the tongue to the mandible (Figs. 1A & 2A). Pigmentation varied amongst specimens examined and where present, occurred peripherally in the loosely folded membrane and on occasion, superficially on the surface of the tongue (see Fig. 1A). Pigmentation was also often evident at the angle of the tongue and the oral surface of the ventral fold of the gular valve which also formed the ventro-caudal border of the oral cavity. The dorsal surface of the tongue displayed numbers of large, dome-shaped structures which were concentrated in a triangular formation in the posterior two-thirds of the tongue (Figs. 1A & 2B). These elevated structures revealed a centrally-positioned, darkly pigmented opening which on histology proved to represent the duct opening of large branched coiled tubular glands situated deeply below the tongue surface (see Figs. 9A-C). Stereomicroscopy revealed small, nipple-like surface extensions scattered between the duct openings (Fig. 2C). Smaller, more discrete, non-pigmented units were observed on the lateral and rostral aspects of the tongue surface (Figs. 2B). Two isolated concentrations of similar structures were situated at the caudo-lateral aspect of the tongue, at the base of the ventral fold of the gular valve (Fig. 2D). The non-pigmented units differed from the more obvious pigmented units in that they did not display a duct opening. The centrally positioned structure typical of these units represented a flattened disc of thickened epithelium which on LM proved to be possible taste receptors (see below). The tip of the tongue displayed deep transverse/oblique grooves which possibly represented a shrinkage or fixation artifact (Figs. 1A & 2A). The surface of the tongue was generally creamy-yellow in colour and had a slightly spongy texture (even in the fixed specimens), probably due to the underlying glandular component identified histologically.

The gingiva of the mandible was more clearly defined than that of the maxilla, having a low profiled, cobbled appearance from approximately C 3 rostrally. There was close attachment of the gingiva to the mandibular (dentary and splenial) bones, especially in the region of C 3 (or C 4) to M 7 (or M 8). The rostral tip of the dentary bones formed a broad shelf or plateau (the rostral dentary shelf) which was divided medially by the dentary symphysis. In this region the gingiva had a slightly spongy texture, although the surface also had a cobbled appearance (Fig. 2A). The teeth of the mandible were carried in the paired dentary bones and also reflected the dental formula described by Kieser *et al*. (1993) (see Fig. 1A). From M 4 (or M 5) to M 7 (or M 8) the dentary bone and the medially situated splenial bone were in close association, although the mandibular teeth were clearly housed in the dentary bone.

Light microscopy

The Palate

H&E-stained sections of the palate revealed a keratinised stratified squamous epithelium of variable thickness in all the regions examined. The stratum basale was composed of a single layer of cuboidal to columnar cells resting on a basement membrane. The basement membrane was most obvious in PAS-stained sections and varied in prominence from conspicuous to barely visible. The nuclei of the basal layer of cells were pale, vesicular and round to oval in shape (Figs. 3A1 & A2). Where oval, the nuclei were oriented vertically to the surface of the epithelium. The stratum spinosum consisted of 3 - 6 layers of cells. The cells adjacent to the stratum basale were cuboidal in shape, while the more superficial cells were horizontally flattened. All the cells of this layer displayed the characteristic inter-linking cytoplasmic bridges connecting the individual components. The nuclei of these cells resembled those of the stratum basale. A thin (3 - 4 layers) stratum granulosum was present above the stratum spinosum. Cells in this layer were spindle shaped or flattened and oriented horizontally. The nuclei were pycnotic, flattened and oriented in the same plane as the cells, while the cytoplasm was filled with strongly basophilic-staining keratohyaline granules (Figs. 3A1, A2 & 3B). The stratum corneum varied in thickness and was composed of a number of compressed layers of cells in which no nuclei were apparent. In some areas, particularly towards the gingiva of the teeth and in convoluted regions of the epithelium, a stratum disjunctum consisting of a loose layer of keratinised cells was present (Figs. 3A1 & 3B).

The epithelium was supported by a thick layer of irregular dense connective tissue with prominent bundles of variably oriented collagen fibres being the most prominent feature (Figs. 3A1, B, D & E). Sandwiched between the deeper regions of the irregular dense supporting connective tissue and the periosteum of the palatine bones was a well-developed plexus of blood vessels, lymphatics and nerves (medullated and non-medullated). Deeply situated striated muscle bundles were noted only in the region of the posterior palatine foraminae, stretching from the posterior third of the palate to the base of the dorsal gular fold. No other muscular tissue was observed. Immediately beneath the basement membrane was a thin layer of fine connective tissue which in places displayed a vacuolated, spongy appearance. This region demonstrated a rich capillary blood supply which was intimately associated with the overlying epithelium. No glandular tissue was ever observed in any of the specimens during histological examination of the palate. Lymphocytic aggregations were also not apparent in these sections.

Melanocytes were observed in the connective tissue a short distance beneath the stratum basale, but never within the epithelial layer. The cells were typically dendritic in nature and displayed large numbers of brown to black melanin granules (melanosomes). The melanocytes were concentrated around the capillary plexus beneath the epithelium and also around the larger blood vessels and nerves more deeply positioned within the connective tissue stroma. In some areas the melanocytes formed a diffuse but definite layer beneath the epithelium. The presence of melanin varied amongst individual specimens examined and in some cases was found to be entirely absent.

Mast cells occurred either singly or in small groups throughout the connective tissue layer with concentrations of five or more cells sometimes being observed. The Mast cells were large, round and often observed in the vicinity of blood vessels. The pale, round to oval vesicular nucleus was centrally positioned within the cytoplasmic mass which displayed small fine, evenly distributed basophilic granules. Prominent Pacinian-like corpuscles were randomly scattered throughout the connective tissue layer a short distance beneath the epithelium (Figs. 3B & C). These structures typically consisted of a variable number of connective tissue lamellae surrounding an inner core representing the terminal portion of the innervating nerve. The corpuscle was surrounded by a prominent, dense connective tissue capsule (Fig. 3C) and large medullated nerves were observed in the vicinity of the corpuscles.

Three types of surface specialisations were observed in the sections studied. The first type comprised small pointed elevations of the epithelial lining supported by a core of fine connective tissue (Figs. 3A1 & A2). In some instances these elevations presented as a series of small localised projections giving the surface of the palate a scalloped appearance. These structures probably represented the epithelial folds observed by SEM (see below). The remaining two types of specialised structures were characterised by modification of both the epithelium and the underlying connective tissue. Both structures (Figs. 3D & E) displayed a localised thickening of the epithelium due mainly to an increase in the number of layers of the stratum spinosum. The keratinised layer in the region of the epithelial thickening was generally thinner than that of the adjacent tissue. The localised epithelial thickenings were most commonly found in the form of an elevated dome-shaped structure due primarily to the presence of a diffuse, ellipsoid or conical-shaped mass of loosely arranged connective tissue situated immediately beneath the epithelium (Fig. 3D). These regions were more lightly stained (H&E-stain) than the surrounding connective tissue (due to a reduction in size and number of the collagen bundles) and caused localised protrusion of the overlying epithelium into the mouth cavity. The morphological features of the specialised regions varied. In some instances the diffuse

connective tissue core contained a basophilic cell-rich mass situated immediately adjacent to the basal lamina. In other regions, the connective tissue core displayed a paucity of cells, possibly due to the plane of section. Associated with the modified regions of connective tissue were Pacinian-like corpuscles which were either found in or adjacent to this zone. Nerve tissue featured prominently within the modified connective tissue and large medullated nerves and blood vessels were observed entering/leaving at the base of the connective tissue core. The dome-shaped specialisations were distributed throughout the palate but appeared to be more numerous on the rostral aspect up to the rostral border of the posterior palatine foraminae (see Fig. 1B).

A small number of localised epithelial thickenings appeared flattened in contrast to the dome-shaped structures and were either positioned level with the adjoining epithelial surface or slightly raised above it. The floor of these epithelial specialisations jutted into the underlying connective tissue layer. Epithelial cells towards the middle of the specialisation adopted a vertical orientation, forming a large elliptical structure reminiscent of a taste bud (Figs. 3E & F). Some of the vertically inclined cells revealed dense, somewhat elongated nuclei, particularly towards the periphery of the elliptical structure, and were similar in appearance to the supporting cells of the mammalian taste-bud. Similarly inclined cells with more vesicular nuclei were seen among the supporting cells and may have represented neuro-epithelial cells. A modified connective tissue core similar to that seen beneath the dome-shaped structures was also evident but did not appear to be specifically associated with Pacinian-like corpuscles. Attendant medullated nerves, however, were much in evidence. The taste receptors described above appeared to be concentrated on the more lateral aspects of the palate although they were occasionally encountered towards the midline.

SEM examination confirmed the cobbled appearance of the palate seen macroscopically. It should be noted, however, that individual variation existed in the specimens examined regarding the prominence of the cobbling. Each clearly demarcated cobbled unit displayed a centrally positioned dome-shaped structure or papilla surrounded by an expanse of loosely attached surface epithelial cells. Desquamation of these cells was particularly obvious at the perimeter of the dome-shaped structure (Fig. 4B). In much of the palate (roughly corresponding to the surface in contact with the dorsum of the tongue) the epithelial surface surrounding the papillae was thrown into a number of conspicuous folds which branched and anastomosed (Fig. 4A). The folds displayed a rostro-caudal or slightly oblique alignment. However, towards the periphery of the palate bordering the gingivae and the dorsal fold of the gular valve, as well as in the smooth region of

the palate overlaying the posterior palatine foraminae, the cobbled units displayed a featureless surface around the domed papillae.

Some of the domed papillae revealed a small centrally positioned depression and radiating grooves (Fig. 4C). These structures appeared to occur more commonly in the rostro-lateral regions of the palate. All regions of the palate were characterised by distinct desquamation of the superficial cells of the epithelium. This phenomenon was possibly accentuated by the critical point drying (CPD) process used for SEM sample preparation. Cracking of the epithelial layer was evident in some specimens examined (see Fig. 4C) and was also attributed to the CPD process. Higher magnification of the epithelial surface using SEM imaging revealed the typical polygonal outline of the individual cells, although the borders were not always clearly demarcated. The keratinised surfaces had a coarse, matted appearance (Fig. 4D).

The Gingivae

The composition and structure of the gingival mucosa was similar in general appearance to that of the palate, although some variations in structure were apparent. The epithelial surface was more undulating than that of the palate, with occasional elevated structures protruding from the surface (Fig. 5A). The epithelium itself was thinner than that of the palate, with the stratum corneum and stratum disjunctum forming the most prominent layers. The stratum spinosum was extremely thin and only obvious in regions of localised thickening. Below the basement membrane was a thin layer of vacuolated, spongy connective tissue which was continuous with a thick layer of irregular dense connective tissue. The occurrence, appearance and organisation of mast cells, melanocytes, vascular and nerve plexuses was similar to that seen in the palate. Surface specialisations similar to those seen in the palate were evident in the gingiva, namely, the small, pointed epithelial elevations and the larger specialised structures displaying modification of the epithelium and the underlying connective tissue. These structures were particularly obvious at the rostral aspect of the mandible although they were found throughout the gingivae. The small epithelial projections probably represent the conical processes seen by SEM (see Fig. 5D). The raised, dome-shaped structures with a thickened epithelium were, as in the palate, associated with Pacinian-like corpuscles situated in the vicinity of the modified connective tissue core. However, the Pacinian-like corpuscles appeared to be more abundant in the gingivae, with three to four sometimes being associated with each specialisation. The thickened, non-elevated epithelial specialisations typically also displayed structures

resembling taste buds. The “taste bud” was generally situated in the centre of the thickened epithelial lining, although pairs of “taste buds” were sometimes observed (Figs. 5B & E).

SEM of the gingivae revealed a series of raised, dome-shaped structures each of which was surrounded by two concentric rows of smaller, raised conical projections (Fig. 5D). These structural units appeared most concentrated on the shelf above the dentary symphysis (rostral dentary shelf) of the mandible and showed smaller concentrations at the base of each tooth (see Fig. 5C), from I 1 to C 5, but progressively reduced in numbers caudally on the lingual surfaces of the dentary and splenial bones. The gingiva of the maxilla also displayed a reduced number of these structural units. Situated between some of these units were small, flattened and slightly depressed, circular areas, often displaying a centrally situated pore (Fig. 5D). Pairs of closely associated pores were also occasionally seen (Fig. 5E). Higher magnification of the flattened discs sometimes showed a mass of fimbriae protruding from the pore (Figs. 5E & F). The pores were believed to represent the opening on the surface of the underlying “taste buds” and were sometimes difficult to observe by SEM due to occlusion of the pore by cellular debris. The flattened areas did not occur constantly between the domed units described above and also did not appear to be arranged in any sequence or pattern, but their occurrence was most common on the rostral dentary shelf. On occasion they also occurred isolated from any other epithelial specialisations, although they displayed similar morphological features. Desquamation of the surface cells was much in evidence and the surface features of the cells were similar to those seen in the palate (see Fig. 4D).

Examination of fresh specimens from the palate and gingiva showed that the cobbled units described above did not display epithelial folding as prominently as formalin-fixed or critical point dried specimens. This phenomenon was presumed to be associated with the shrinking effect of fixation and the processing of the tissue samples for SEM observation.

The Tongue

Cross-sections of the rostral region of the tongue revealed a relatively thin, lightly keratinised stratified squamous epithelium supported by a thick layer of irregular dense fibrous connective tissue (Fig. 6A). The epithelium on the dorsum of the tongue displayed a few shallow folds, but these rapidly increased in number and complexity towards the lateral borders of the tongue. The epithelial folds were supported by the underlying connective tissue and primary, secondary and occasionally tertiary folds could be distinguished.

The epithelium in the highly folded lateral zone appeared more heavily keratinised and a distinct layer of desquamated cells (stratum disjunctum) was generally evident (Fig. 7C). At the ventro-medial aspect of the tongue the epithelium, supported by a substantial layer of more loosely arranged irregular dense connective tissue, was reflected laterally towards the medial surface of the mandible with which it was continuous. The loosely arranged, highly folded membrane thus formed, connected the ventro-lateral aspects of the tongue to the mandible. Beneath the connective tissue layer was a clearly demarcated adipose tissue core containing large adipocytes, strands of fibrous connective tissue and variably sized bundles of striated muscle fibres. A large plexus of blood and lymphatic vessels was situated between the irregular dense connective tissue and the adipose tissue core. A large vascular and lymphatic plexus was also situated at the angle of the tongue and the ventral fold of the gular valve. These vessels were sandwiched between the thick sub-epithelial connective tissue layer and the adipose tissue core (Fig. 7B). More caudal cross-sections of the tongue displayed a similar arrangement of the basic tissue layers outlined above. In addition, however, a dense mass of striated lingual musculature was evident ventral to the adipose core, and large branched coiled tubular glands associated with prominent duct openings characterised the dorsal sub-epithelial layer of connective tissue (Fig. 8B).

The lightly keratinised stratified squamous epithelium varied in thickness (3 – 6 cell layers) and, in PAS-stained sections was seen to rest on a prominent basement membrane. The shape, appearance and orientation of the cells and their nuclei was similar to that described for the palate and gingivae. The stratum spinosum was poorly developed in the thinner regions of the epithelium and was only clearly defined in the areas of localised epithelial thickening associated with the glandular openings and specialised sensory structures (see Figs. 6C, 7A & 8C).

In addition to ubiquitous epithelial folds, the epithelial lining of the tongue demonstrated randomly distributed localised thickenings associated with ellipsoid intra-epithelial structures resembling taste buds (Figs. 6A-C & 7A-C). Structurally, this type of epithelial specialisation resembled the non-raised epithelial thickenings containing taste buds observed in the palate and gingivae described above. As in both these regions, the underlying connective tissue contained conspicuously less collagen fibres and formed a conical or dome-shaped zone associated with medullated nerve fibres. Small lymphocytic aggregations were often associated with the epithelial specialisations (Fig. 6B). The taste receptors appeared to be most numerous on the dorso-lateral aspects of the tongue and also in the epithelium lining the lateral wall of the organ. Not all sections of the epithelial thickenings, however, revealed the intraepithelial, ellipsoid structures and

Pacinian-like corpuscles were occasionally seen in the vicinity of the modified connective tissue core, particularly towards the tip of the tongue. This may indicate that some of the specialisations represent touch or pressure receptors in addition to the more commonly encountered taste receptors (see SEM results below). It is also possible that individual sections did not always pass through the centrally positioned taste bud, creating the erroneous impression that it was absent.

Immediately beneath the epithelium was a narrow layer of fine connective tissue followed by a diffuse yet prominent layer containing melanin pigment (Figs. 8A-C). The melanocytes appeared to be concentrated around capillaries present in this region and was also observed in the deeper parts of the connective tissue stroma in the vicinity of larger blood vessels and nerves. The sub-epithelial capillary supply was sparse in comparison to that seen in the gingivae and palate. However, in addition to the vascular and lymphatic plexuses mentioned above, numerous large blood and lymphatic vessels and attendant medullated and non-medullated nerves, were observed throughout the deeper lying layer of irregular dense connective tissue.

The caudal two-thirds of the tongue were dominated by the presence of large collections of glandular tissue (lingual salivary glands) and masses of associated lymphoid tissue (Figs. 8A & B). The more centrally positioned glands were generally larger and more complex than those situated more laterally. In oblique or transverse sections the glandular tissue exhibited features typical of compound tubular glands and appeared to be composed of lobes and lobules separated by tracts of connective tissue. When sectioned in the longitudinal plane, however, it was obvious that the glands were branched, coiled tubular in nature with each branch leading to an elaborately coiled secretory endpiece. Each secretory endpiece formed a distinct glandular unit. The various branches were linked to a single secretory duct which opened onto the dorsum of the tongue. The main secretory duct was lined by a stratified squamous epithelium originating from the stratum germinativum of the surface epithelium with which it was continuous. The epithelial cells, however, were vertically oriented with the final layer lining the duct appearing typically columnar in nature. The epithelium of the main duct thinned rapidly to form a relatively narrow tube lined by three to four layers of cells before dividing from the surface inwards into a number of smaller branches. These branches were lined by a simple columnar epithelium which was continuous with the coiled secretory endpieces of the gland. The point of exit of the secretory duct onto the surface of the tongue was marked by a distinct depression or pore. Intra-epithelial structures resembling taste buds were often located within the wall of the pore (Fig. 8A-C).

The secretory portions of the glands were coiled tubular in nature and lined by a simple columnar epithelium. The nuclei of the secretory cells were generally round or oval and although situated towards the base of the cell, were not compressed. PAS-positive granules were identified in cells lining some tubular profiles, generally towards the periphery of the glands, while most of the secretory tubules showed a light staining reaction or none at all. The tubular lumen was wide and individual secretory profiles were separated by delicate bands of connective tissue. Each individual secretory unit was separated from neighbouring units by relatively wide tracts of connective tissue.

The individual units of the lingual salivary glands were generally situated in the deeper lying tissue of the sub-epithelial connective tissue, close to the border of the adipose tissue core (Figs. 9B). Between the glandular tissue and the surface of the tongue, and initially associated with the secretory duct, were large aggregations of lymphoid tissue which formed lingual tonsils. Although the lymphoid masses displayed diffuse infiltration into the thickened stratified epithelium of the secretory duct, obliteration of the epithelium was not observed. Loosely arranged collections of lymphoid tissue were also sometimes associated with the glandular tissue itself.

The glandular tissue was richly supplied with blood vessels and the vascular and lymphatic plexuses present at the junction of the irregular dense connective tissue and adipose tissue layers were often positioned close to the glandular units (Fig. 9B). Non-medullated nerves were associated with the glandular tissue.

Scanning electron microscopy of the tongue surface confirmed the LM observation that the dorsum of the tongue was composed of a number of clearly demarcated round to angular units. The various units appeared to be elevated and were surrounded by deep, sometimes wide, clefts which accentuated individual units. The exaggerated division of the units was attributed to shrinkage caused by the drying process for SEM. The round to polygonal-shaped units occupying the triangular glandular region situated in the posterior two-thirds of the tongue (see Fig. 2B) exhibited a relatively low profile and smooth surface features. A centrally positioned pore which was frequently filled with debris/glandular secretions and which was shown by LM to represent the opening of the main secretory duct of the underlying lingual salivary glands, was the most prominent feature. A number of grooves (probably representing epithelial folds) radiated outwards from the pore. The grooves varied in length and occasionally extended the entire diameter of the unit (Fig. 10A & inset Fig. 10A). Situated towards the

periphery of the units were small, spherical, low-profiled, dome-shaped protrusions (Fig. 10A & inset Fig. 10A) which appeared to represent the nipple-like surface extensions seen by stereomicroscopy (see Fig. 2C). Occasional flattened discs (see below) with a random distribution were also observed. More discrete surface units were observed laterally on the tongue surface (see Fig. 2B) and also in the smaller paired triangular areas situated caudo-laterally at the base of the tongue (Fig. 2D). The surface of the discrete units presented a rough, corrugated appearance with epithelial folds of variable depth creating a mosaic-like pattern (Figs. 10B & C). Centrally, and occasionally excentrically, positioned on each unit were clearly defined, flattened, disc-shaped structures. More than one disc-shaped structure was seen on some units (Fig. 10C). At the centre of each disc was a small pore which in many cases was obscured by cell debris and/or bacteria. In pores not filled with debris, a variable number of short processes were observed to protrude from the opening. The processes often displayed clavate tips (Fig. 11C). Based on LM observations, the pores with their processes, would appear to represent the superficial component of the “taste buds” located within localised epithelial specialisations (see Fig. 6C). The pore itself was surrounded by concentric arrangements of desquamating surface cells (Figs. 11A & B). Individual cells were polygonal in shape and displayed a complicated array of microridges, giving the surface a sponge-like appearance (Figs. 11B & C). Occasional dome-shaped structures similar to those described in the glandular area were sometimes observed.

DISCUSSION

Meaningful gross morphological descriptions of the oral cavity of the Crocodilia are not available in the literature and it appears that only specific specialisations and structures (glands, dentition, the development and structure of the palate and osteology) have been described. Although illustrated in a number of papers, the cobbled appearance of the epithelium of the palate and parts of the gingivae have not drawn any comment by the authors. Certainly, the small, rigid, conically shaped process (Fig. 1B) which emerged from a low-profiled ridge above the anterior palatine foramen has not been described. The true structure and function of this process is unknown and was not specifically examined in this study, but may well prove an interesting topic for further investigation. Similarly, the description of the clearly defined median ridge, comprising a series of closely positioned cobbles along the mid-line of the palate, appears also to have drawn no attention from previous authors. The presence of a broad dentary shelf forming the rostral aspect of the mandible, and which is richly supplied with sensory structures, is likewise not specifically mentioned in the literature.

In his generalised description of the reptilian oral cavity, Luppa (1977) states that "the epithelial lining of the oral cavity (of reptiles) shows considerable variation, both regional and specific" and that within a single species, there may be found "compound squamous epithelium, ciliated epithelium, goblet cells and simple non-ciliated columnar epithelium." This study revealed that the epithelium of the oral cavity (including the surface of the tongue) varied little in structure except for the lining of the oral aspect of the dorsal and ventral folds of the gular valve. Throughout the oral cavity the epithelium was a lightly keratinised stratified squamous epithelium which showed slight localised variation in thickness.

A relatively thin stratified squamous epithelium lined all aspects of the palate. However, towards the base of the dorsal fold and on the oral surface of the ventral fold of the gular valve, there was a sharp transition from the lightly keratinised epithelium to a thick, non-keratinised stratified squamous epithelium with prominent epithelial and connective tissue papillae (Personal observation). A ciliated epithelium associated with goblet cells and glandular tissue also made an appearance on the oral surface of the dorsal fold of the gular valve (see full description of this epithelium and the dorsal fold of the gular valve in Chapter 3). This transition of epithelial types was described by Taguchi (1920) as mucus metamorphosis ("Schleimmetamorphose") and it was observed in all three species of crocodile he examined.

Throughout the palate, the epithelium was supported by a thick layer of irregular dense connective tissue at the base of which, adjacent to the periosteum of the palatal bones, were well developed plexuses of blood vessels, lymphatic vessels and nerves. Adjacent to the basement membrane was a layer of melanocytes. Variation in density was apparent amongst specimens examined and in some cases no melanin appeared to be present. This region is similarly described by Taguchi (1920) who also mentions a scattered presence of "pigmented cells", presumably melanin containing cells. Luppa (1977) also describes these features in the oral cavity, but generalises regarding their occurrence in the Reptilia.

The general composition of the epithelium of the gingivae appeared very similar to that of the palate, although the gingivae had a more undulating surface. The epithelium itself was slightly thinner than that of the palate, with the stratum corneum and stratum disjunctum forming the most prominent layers, particularly in the immediate vicinity of the teeth.

The occurrence of glands and the presence of taste receptors (sensory neuro-epithelial cells, [Luppa, 1977] or "Schmeckzellen" of Krause, 1922 [cited by Luppa, 1977]) appear to dominate descriptions amongst authors who have examined the histology or morphology of the oral cavity of crocodiles. Kochva (1978) extensively describes glandular tissue in reptiles, but only fleetingly refers to the Crocodilia (*Caiman* sp., *A. mississippiensis* and *C. niloticus*) noting only that "A cursory examination of some slides of *Crocodylus niloticus* reveals no sublingual glands". In an earlier study Woerdeman (1920) observed that, “while the buccal cavity of reptiles is very rich in glands, the crocodiles are an exception and different researchers have stated that they did not find any glands in the buccal cavity.” Woerdeman (1920) also reviewed earlier literature (ca. 1888 to 1914) on the subject and emphasised discrepancies amongst the authors regarding the presence or absence of oral glands in Crocodilia. Gaupp (1888, cited by Woerdeman, 1920) described the presence of small *Glandulae linguales* but concluded that *Glandulae sublinguales* and *Glandulae palatinae* were absent. Stannius (no reference cited by Woerdeman, 1920) stated that crocodiles did not have any salivary glands. Gegenbaur (1901, cited by Woerdeman, 1920) reported the absence of labial glands in crocodiles. Schimkewitsch (1910, cited by Woerdeman, 1920) however, describes medial and lateral glandular groups in the palate of crocodiles. These *Glandulae palatinae*, according to Schimkewitsch (1910), were the equivalent of the intermaxillary glands in amphibians.

Farenholz (1937) reported two areas in the palate in which glands occur, *viz*., median palatine glands, found in *Caiman* and small glands at the median aspect of the maxillary teeth, found in *Caiman* sp. and *A. mississippiensis*. Woerdeman (1920), while investigating tooth development of *Crocodylus*, found that the development of glands, previously described by Röse (1893), was closely associated with the development of the dental system. These glands were observed to open into pits situated between the maxillary teeth and into which fit the tips of the mandibular teeth. The glands are medially situated in the pits and are surrounded by soft connective tissue and covered by a stratified squamous epithelium. The region between the maxillary teeth (i.e., the pits into which fit the tips of the mandibular teeth) was not examined during this study and it is thus not possible to comment on the presence or absence of any glandular tissue in this region. However, Taguchi (1920) found glandular tissue “in the submucosa of the caudal part of the palate and the oral surface of the velum” in all three species he examined and described the glands as being branched tubulo-alveolar mucus glands. This statement indicates that Taguchi found two clear zones of glands, albeit in close proximity to each other. This investigation clearly indicated that there was no glandular tissue in the palate “proper” and that glandular tissue (as described by Taguchi

[1920]) only occurred on the oral surface of the dorsal fold of the gular valve ("oral surface of the velum" of Taguchi [1920]).

Pressure receptors are noted by Pooley and Gans (1976) to occur "between the teeth and (in) the jaws" of the Nile crocodile and that they function to gauge the intensity of a bite. They do not, however, give any histological description of these receptors, but do state that similar receptors are found in mammals, including man. This investigation revealed that lamellated, Pacinian-like receptors were frequently observed in the palate and the gingivae (see Figs. 3B & C & 5A). These structures were observed in the lateral and rostral regions of the palate and also occurred in the gingiva covering the rostral dentary shelf (Fig. 1A). Andres and von Düring (1973), von Düring (1973) and von Düring and Miller (1979) made significant contributions to the study of sensory innervations in vertebrates, including the Crocodilia. Von Düring (1973) stated that "in Caiman, the lamellae (inner core) of the encapsulated receptors with a capsule space have a structure similar to that of the inner core of the Vater-Pacinian corpuscle." Illustrations given in the papers of Andres and von Düring (1973), von Düring (1973) and von Düring and Miller (1979) also support the finding in this study that the lamellated structures seen in the oral cavity are of the Pacinian-type of corpuscles. Furthermore, Jackson, Butler, & Youson (1996) studied integumentary sense organs (ISO's) of *Crocodylus porosus* using LM, SEM and TEM. Although no TEM studies of these receptors were carried out in this investigation, there are clear similarities between the LM and SEM findings by Jackson *et al*. (1996) and this study (see Figs. 3D, 4B & 5A). Conclusions by Jackson *et al*. (1996) were that the ISO's possibly had a mechanosensory or chemosensory function and that further physiological studies would have to be performed to determine their true function.

Hulanicka (1913) examined the nerve endings in the tongue, palate and the skin of two species of crocodile, *viz*., *Crocodylus niloticus* (eight young specimens examined, 25 – 45 cm in length) and *Alligator mississippiensis* (three young specimens examined, 65 – 110 cm in length) and described five types of nerve endings in the tongue, palate and the abdominal skin. These were free nerve endings (in the palate), touch cells (in the stroma of the tongue, dermis of the skin, stroma of the stomach, chin and jaws), tactile papillae (in the skin and in the mucosa of the tongue and palate), tactile corpuscles (in the stroma of the tongue, the palate and in the dermis of the skin) and taste buds as described by Bath (1905; 1906). Bath studied the structure as well as the distribution of taste receptors in the Nile crocodile (*C. niloticus*) and the alligator (*A. mississippiensis*), and reported taste receptors in the oral cavity, pharyngeal cavity and upper region of the oesophagus of *C. niloticus*. Hulanicka (1913), however,

disputed some of Bath's findings regarding the structure of taste receptors in the species he examined, specifically the association between support cells and the nerve fibres innervating the taste bud.

The diagrammatic representations of sensory nerve endings and the distribution of nerves in the tongue of the Nile crocodile presented by Hulanicka (1913), correspond to the general form of the light-staining connective tissue cores underlying the sensory epithelial structures seen in micrographs presented in this study (see Figs. 3D & E, 5A & B, 6B & C, 9C). Although the specific innervation of the oral cavity was not examined during this study, it was found, as described above, that the palate and gingivae were rich in Pacinian-type corpuscles.

Luppa (1977), who generalised his description of the histological composition in the reptilian oral cavity, stated that “taste buds were scattered throughout the oral epithelium in reptiles and that in *Lacerta* they were most numerous laterally and on the palatal folds.” Luppa (1977) further reported that reptilian taste buds showed no significant differences in their cellular composition from those of mammals and that sensory neuro-epithelial cells (= Schmeckzellen of Krause, 1922, cited by Luppa, 1977) and supportive cells occurred in both mammals and reptilians. Sensory areas observed during this study, and presumed to be taste buds, in the epithelium of the palate, gingivae and the tongue, were of similar morphology to those described by Bath (1905, 1906) and Taguchi (1920). These structures displayed typical longitudinally oriented supportive and neuro-epithelial cells and were observed to be associated with medullated nerve concentrations situated in the connective tissue at the base of the taste receptors. In addition, this study graphically illustrated by SEM the cuticular processes of the neuro-epithelial cells where they emerged through the taste pore (see Figs. 11 B & C).

The tongue of Crocodilia has been discussed in a number of publications, mainly in regard to the presence of lingual glands and their participation in salt secretion (Dunson, 1976, 1982; Ellis, 1981; Taplin & Grigg, 1981; Taplin, Grigg, Harlow, Ellis & Dunson, 1982; Mazzotti & Dunson, 1984; Taplin, 1984, 1988; Taplin, Grigg & Beard, 1985; Taplin & Loveridge, 1988; Chen, *et al*., 1989; Steel, 1989; Taylor, Franklin & Grigg, 1995). These papers, however, give very little information on the basic structure of the tongue of crocodiles and appear to be based primarily on physiological studies regarding salt balance, tolerance to saline conditions and salt secretion. Some morphological information, however, has been presented (Taguchi, 1920; Gabe & Saint Girons, 1972; Luppa, 1977; Kochva, 1978; Taplin & Grigg, 1981; Minnich, 1982; Grigg & Gans, 1993), although, with the exception of the paper by Taguchi

(1920) and to a lesser extent that of Kochva (1978), very little descriptive information of the true structure of the lingual salivary glands is provided.

Earlier literature (Röse, 1893; Bath, 1905; 1906; Reese, 1913; Taguchi, 1920; Woerdeman, 1920; Krauss, 1922, cited by Luppa, 1977; Luppa, 1977) made no mention of salt secretion, except for the fact that glandular tissue did occur in the tongues of specimens examined. Reese (1913) studied the histology of the enteron of the Florida alligator and described the glandular tissue in the tongue as "... probably mucus or slime secreting". Taguchi (1920) made a comparative histological study of the digestive tract, including the tongue, of three crocodilian species (*A. sinensis, C. niloticus* and *C. porosus*) and described tongue glands. These glands, identified by Taguchi (1920) as being of the branched tubular type appear to be typical of the glandular tissue observed during this study. Although Taguchi (1920) did not specify a mucus secretion as such, he did state that the secretory cells appeared to be filled with fine granular material.

In more recent studies the tongues of the marine or estuarine crocodile (*C. porosus*) and the American crocodile (*Crocodylus acutus*) have received most attention, seemingly due to the animals' salt water or estuarine habitat and the implication of the lingual glands in salt secretion during osmoregulation or electrolyte homeostasis (Taplin and Grigg, 1981). Steel (1989) reported that the marine or estuarine crocodile (*C. porosus*) is "quite at home in a marine environment" and "ranges far out into the open ocean." He further states that *C. porosus* "has up to 40 complex tubular salt glands on its tongue that secrete a concentrated solution of sodium chloride when a saltwater crocodile is in saline surroundings." This information has been substantiated by other authors (Taplin & Grigg, 1981; Taplin, *et al*., 1982; Taplin, *et al.*, 1985; Taplin, 1988; Grigg & Gans, 1993). Taplin & Grigg (1981) describe the glands in this species as compound tubular glands having "a broad, shallow duct which leads down to a series of smaller ducts that branch repeatedly into lobules of the gland. The larger branches are lined with columnar to cuboidal epithelium which passes into squamous epithelium in the smaller branches. Each lobule of the gland is densely packed with branching secretory tubules lined almost entirely by columnar epithelial cells." According to Taplin (1988), the ultrastructural features of the salt secreting glands revealed by TEM were the "characteristically complex interdigitations of lateral cell membranes, expanded intercellular spaces, abundant mitochondria, and extensive network of blood vessels and unmyelinated nerve fibres."

Chen, *et al*., (1989) examined the lingual glands of the Chinese alligator, *Alligator sinensis*, and report that the glands are either simple tubular or complex acinotubular glands. Chen, *et al*., conclude that the glands, which number about 100 throughout the tongue, appear in the posterior two-thirds of the tongue and further state that these glands function as salt secreting glands and also serve to lubricate food (data extrapolated from an English abstract of Chen, *et al*., [1989]). This investigation on the Nile crocodile identified glandular tissue in a triangular area occupying the posterior two-thirds of the tongue. Each lingual salivary gland was demarcated by a raised, domed unit with a centrally positioned, pigmented pore which indicated the opening of the secretory duct (Figs. 1A & 2B & C). There were approximately 40 pores present which is similar in number to those seen in the saltwater crocodile by Taplin and Grigg (1981). However, in species of Alligatorinae, many more pores are present with 100 being reported in *A. sinensis* by Chen *et al*. (1989) and 200 or more in *A. mississippiensis* (Taplin *et al*., 1982).

Taplin and Grigg (1981) and Taplin, *et al.* (1985) used methacholine chloride to stimulate lingual gland secretion in various species of Crocodylinae (*Crocodylus acutus, C. johnsoni, C. acutus*, *C. palustris*, *C. cataphractus*, *C. niloticus* and *Osteolaemus tetraspis*), Alligatorinae (*Alligator mississippiensis* and *Caiman crocodilus*) and in *Gavialis gangeticus* (Family Gavialidae), and reported that in all instances the animals possessed functional lingual glands, but that only the Crocodylinae secreted significant concentrations of Na^+, indicating the presence of salt secreting glands. These lingual salt secreting glands open through pores in the posterior region of the tongue and secrete a solution of Na^+ and Cl^- at concentrations similar to that of seawater (Taplin and Grigg, 1981; Steel, 1989). Steel (1989) states that "alligators and caimans do have minute pores on the back of their tongues and in the palatal epithelia around the buccal valve, but it would seem that these are primarily salivary glands, although some Na^+ and K^+ is excreted at a low rate." Taplin (1988), Grigg and Gans (1993) and Grigg and Beard (unpublished observation, as cited by Grigg and Gans, 1993) state that salt glands have not been found in any members of the Alligatoridae, and a study of captive *Alligator mississippiensis* suggests that this species cannot maintain homeostasis in hyperosmotic water (Lauren, 1985). Steel (1989) postulated that the "subfamily (Crocodylinae) originated in a marine environment and subsequently colonised a freshwater habitat, or conversely, that all crocodylid subfamilies were of freshwater origin but only the Crocodylinae acquired a saltwater adaption." Bellairs (1987) also suggested that modern crocodylines had ancestors with "markedly marine habits" and cites Taplin (1984). From illustrations presented by Taplin and Grigg (1981), Minnich (1982), Taplin (1988), Grigg and Gans (1993), it may be deduced that

the pores seen by them represent the region of glandular tissue observed in *C. niloticus* during this study.

No physiological examination of the glands in the tongue of *C. niloticus* was carried out during this study and it is therefore not possible to unequivocally identify them as "salt secreting". However, the histological structure of the lingual glands observed in the Nile crocodile is similar to that described in *C. porosus*, despite the difference in classification of the glands as "branched coiled tubular (*C. niloticus* – this study) or compound tubular glands (*C. porosus* - Taplin & Grigg, 1981). A noteworthy difference was that the ducts connecting the main secretory duct to the secretory units was lined by a simple columnar epithelium in the Nile crocodile as opposed to the simple squamous epithelium identified in *C. porosus* (Taplin & Grigg, 1981). The additional observation that not all the acini in the glands of *C. niloticus* demonstrate a positive PAS reaction may support the statement of Chen, *et al*. (1989) that the lingual glands of *A. sinensis* function as salt secreting glands and also serve to lubricate the passage of food.

It was noted in the present study that lymphoid tissue was closely associated with the glandular tissue, particularly with the large ducts linking the glands to the surface of the tongue. A similar observation was made by Taguchi (1920) in the three species he examined (*A. sinensis*, *C. niloticus* and *C*. *porosus*) and he describes lymph follicles in close proximity to the secretory ducts of the lingual glands as well as lymphocytic penetration of the epithelial layer of the ducts. These lymphoid aggregations prompted Taguchi (1920) to state that they "remind one of tongue tonsilli of higher animals."

No muscular tissue, apart from sheets of striated muscle in the deeper lying regions above the posterior palatine foraminae, and lingual musculature of the tongue was observed in the oral cavity. Taguchi (1920) noted in his specimen of *C. porosus* that striated muscular tissue occurred close to the nasal surface of the velum (oral surface of the dorsal gular fold), which he described as the equivalent of musculus pharyngopalatinus of higher animals. Taguchi noted further that this muscle traversed the velum (dorsal gular fold) from one side of the lateral wall of the pharynx to the other. Numerous sections of the dorsal gular fold of *C. niloticus* examined during this investigation revealed no muscular tissue.

Although dentition was only superficially examined during this study in the Nile crocodile, it became important when sampling methods of the palate and gingivae of the lower and upper jaws were considered. Teeth were therefore named and numbered according to Kieser, *et al*. (1993), who

concluded that the Nile crocodile was heterodont and had five premaxillary incisors, five canines and six or more post canines (molar) teeth in the maxilla. The dental arrangement in the mandible was three premandibular incisors, five canines and six or more post canines (molar). The conclusions of Kieser, *et al*. (1993) stemmed from an investigation involving ontogenetic developmental studies of serially sectioned crocodile (*C. niloticus*) embryos and three-dimensional, computer-generated reconstruction of lateral radiographs of dried, one-year-old skulls. They further concluded from this study that "three morphogenetic zones of tooth initiation were identifiable" and that "the Nile crocodile was hetero- rather than homodont" (isodont). This is in contrast to the opinion of Sues (1989) who stated that the dentition of crocodiles is "more or less isodont" as "all the teeth are similar in size and shape". This study on 2.5 to 3 year-old *Crocodylus niloticus* specimens clearly supported the heterodont nature of the dentition described by Kieser *et al*. (1993) (see Figs. 1A & B).

The teeth of the mandible were accommodated in the paired dentary bones which united at the rostral, elongated dentary symphysis (see Iordansky, 1973 for osteology of the crocodilian skull). Each tooth emerged from its own alveolus in the dentary bone. The caudal region of the splenial bone, situated medially to the dentary bone, was in close association to molar teeth M 4 to M 7 (or M 8), but did not form part of the accommodation of the teeth in the jaw. This is in contrast to the findings of Chiasson (1962) who examined the alligator and stated that the dentary bone "bears the first 14 – 15 teeth in individual alveoli on each side, the remaining 5 – 6 teeth being held in a common groove between the dentary and splenial bones." The teeth of the maxilla were similarly accommodated in individual alveoli in the premaxilla and maxillary bones, which also formed the major portion of the palate. Chiasson (1962) stated that in the alligator there were "15 to 16 maxillary teeth on each side. The first few of these are held in individual alveolar sockets but the posterior series are set side by side in a common groove."

REFERENCES

ANDRES, K.H. & VON DÜRING, M. 1973. Morphology of cutaneous receptors, in *Handbook of Sensory Physiology*, edited by H. Autrum, R. Jung, W.R. Loewenstein, D.M. MacKay and H.L. Teuber, Springer Verlag: Berlin: Volume 2:3-28.

BARGE, J.A.J. 1937. Mundhöhlendach und Gaumen, in *Handbuch der vergleichenden Anatomie der Wirbeltiere,* edited by L. Bolk, E. Göppert, E. Kallius and W. Lubosch. Berlin: Urban and Schwarzenberg: Volume 3:29-48.

BATH, W. 1905. Über das Vorkommen von Geschmacksorganen in der Mundhöhle von *Krokodilus niloticus* Laur. (Abstract) *Zoologisches Anzeiger*, 29:352-353.

BATH, W. 1906. Die Geschmacksorgane der Vögel und Krokodile, *Archiv für Biontologie*, 1:4-52.

BELLAIRS, A. d'A. 1987. The crocodilia, in *Wildlife management: crocodiles and alligators*, edited by G.J.W. Webb, S.C. Manolis, & P.J. Whitehead, Chipping Norton, NSW: Surrey Beatty and Sons Pty. (Ltd), in association with The Conservation Commission of the Northern Territory: 5-7.

CHEN, B., TANG. J., WEI, Y. & ZHANG, Z. 1989. The lingual glands of the Chinese alligator. *Acta Zoologica Sinica*, 35:28-32. (In Chinese with English and Chinese summary).

CHIASSON, R.B. 1962. *Laboratory anatomy of the alligator*. Dubuque, Iowa: WM.C. Brown Company Publishers. 3-38.

DUNSON, W.A. 1976. Salt glands in reptiles, in *Biology of the Reptilia*, *Physiology A*, edited by W.R. Dawson & C. Gans. London: Academic Press: Volume 5:413-445.

DUNSON, W.A. 1982. Salinity relations of crocodiles in Florida Bay. *Copeia*, 2:374-385.

EDMUND, A.G. 1962. Sequence and rate of tooth replacement in the crocodilia. *Contributions. Life Sciences Division, Royal Ontario Museum, Toronto*, 56:1-42.

EDMUND, A.G. 1969. Dentition, in *Biology of the Reptilia*, *Morphology C*, edited by C. Gans, A.A. Bellairs & T.S. Parsons. London: Academic Press: 115-200.

ELLIS, T.M. 1981. Tolerance of sea water by the American crocodile, *Crocodylus acutus. Journal of Herpetology*, 15:187-192.

FARENHOLZ, C. 1937. Drüsen der Mundhöhle, in *Handbuch der vergleichenden Anatomie der Wirbeltiere*, edited by L. Bolk, E. Göppert, E. Kallius and W. Lubosch. Berlin: Urban and Schwarzenberg: 3:115-210.

FERGUSON, M.W.J. 1979. The American alligator (*Alligator mississippiensis*): A new model for investigating developmental mechanisms in normal and abnormal palate formation. *Medical Hypotheses*, 5:1079-1090.

GABE, M. & SAINT GIRONS, H. 1972. Contribution à l'histologie de l'estomac des lépidosauriens (Reptiles). *Zoologisches Jahrbuch zur Anatomie*, 89:579-599.

GRIGG, G.C. & GANS, C. 1993. Morphology and physiology of the crocodilia, in *Fauna of Australia, Amphibia and Reptilia*, edited by C.J. Glasby, G.J.B. Ross & P.L. Beesley. Canberra: Australian Government Publishing Service: Volume 2A:326-336.

HULANICKA, R. 1913. Recherches sur les terminaisons nerveuses dans la langue, le palais, et la peau du crocodile. *Archives de Zoologie Expérimentale et Générale*, 53:1-14.

IORDANSKY, N.N. 1973. The skull of the crocodilia, in *Biology of the Reptilia*, edited by C. Gans & T. Parsons. London, Academic Press: Volume 4:201-262.

JACKSON, K., BUTLER, D.G. & YOUSON, J.H. 1996. Morphology and ultrastructure of possible integumentary sense organs in the Estuarine crocodile (*Crocodylus porosus*). *Journal of Morphology*, 229:315-324.

KIESER, J.A., KLAPSIDIS, C., LAW, L. & MARION, M. 1993. Heterodonty and patterns of tooth replacement in *Crocodylus niloticus*. *Journal of Morphology*, 218:195-201.

KOCHVA, E. 1978. Oral glands of the reptilia, in *Biology of the Reptilia*, *Physiology B*, edited by C. Gans, & T.S. Parsons. London: Academic Press: Volume 8:43-161.

LAUREN, D.J. 1985. The effect of chronic saline exposure on the electrolyte balance, nitrogen metabolism and corticosterone titer in the American alligator, *Alligator mississippiensis. Comparative Biochemistry and Physiology*, 81A, 217-223.

LUNA, L.G. (Ed.) 1968. *Manual of histologic staining methods of the Armed Forces Institute of Pathology.* 3rd ed. American Registry of Pathology. New York: McGraw-Hill Book Company.

LUPPA, H. 1977. Histology of the digestive tract, in *Biology of the Reptilia*, *Morphology E,* edited by C. Gans & T.S. Parsons. London: Academic Press: Volume 6:225-313.

MAZZOTTI, F.J. & DUNSON, W.A. 1984. Adaption of *Crocodylus acutus* and *Alligator* for life in saline water. *Comparative Biochemistry and Physiology*, 79A, 641-646.

MINNICH, J.E. 1982. The use of water, in *Biology of the Reptilia, Physiology C*, edited by C. Gans & F.H. Pough. London: Academic Press: Volume 12:374-395.

PARSONS, T.S. & CAMERON, J.E. 1977. Internal relief of the digestive tract, in *Biology of the Reptilia*, *Morphology E*, edited by C. Gans, & T.S. Parsons. London: Academic Press: Volume 6:159-223.

PEARSE, A.G.E. 1985. *Histochemistry. Theoretical and applied*. *Analytical technology*. 4th ed. Volume 2, New York: Churchill Livingston.

POOLE, D.F.G. 1961. Notes on tooth replacement in the Nile crocodile, *Crocodylus niloticus*. *Proceedings. Zoological Society of London*, 136:131-160.

POOLEY, A.C. & GANS, C. 1976. The Nile crocodile. *Scientific American*, 234:114-124.

REESE, A.M. 1913. The histology of the enteron of the Florida alligator. *Anatomical Record*, 7:105-129.

RÖSE, C. 1893. Über die Nasendrüse und die Gaumendrüsen von *Crocodilus porosus*. *Anatomischer Anzeiger*, 8:745-751.

STEEL, R. 1989. Anatomy of a living fossil, in *Crocodiles*. London: Christopher Helm: 12-36.

SUES, H-D. 1989. Tooth replacement in crocodilians, in *Crocodiles and alligators*, edited by C.A. Ross & Ganett. London: Meerhurst Press: 57.

TAGUCHI, H. 1920. Beiträge zur Kenntnis über die feinere Struktur der Eingeweideorgane der Krokodile. *Mitteilungen aus der Medizinischen Fakultät der Kaiserlichen Universität zu Tokyo*: 25:119-188.

TAPLIN, L. 1984. Evolution and zoogeography of crocodilians: a new look at an ancient order, in *Vertebrate Evolution and Zoogeography in Australia*, edited by M. Archer, & G. Clayton. Hesperian Press: Perth: 361-370.

TAPLIN, L.E. 1988. Osmoregulation in crocodilians. *Biological Reviews*, 63:333-377.

TAPLIN, L.E. & GRIGG, G.C. 1981. Salt glands in the tongue of the estuarine crocodile *Crocodylus porosus*. *Science*, 212:1045-1047.

TAPLIN, L.E., GRIGG, G.C. & BEARD, L.A. 1985. Salt gland function in fresh water crocodiles: evidence for a marine phase in eusuchian evolution? in *Biology of Australasian frogs and reptiles*, edited by G.C. Grigg, R. Shine & H. Ehmann. Chipping Norton: Surrey Beatty & Sons with the Royal Zoological Society of New South Wales: 403-410.

TAPLIN, L.E., GRIGG, G.C., HARLOW, P., ELLIS, T.M. & DUNSON, W.A. 1982. Lingual salt glands in *Crocodylus acutus* and *C. johnstoni* and their absence from *Alligator mississippiensis* and *Caiman crocodilus*. *Journal of Comparative Physiology – B*, 149:43-47.

TAPLIN, L.E. & LOVERIDGE, J.P. 1988. Nile crocodiles, *Crocodylus niloticus*, and estuarine crocodiles, *Crocodylus porosus*, show similar osmoregulatory responses on exposure to seawater. *Comparative Biochemistry and Physiology,* 89A:443-448.

TAYLOR, G.C., FRANKLIN, C.E. & GRIGG, G.C. 1995. Salt loading stimulates secretion by the lingual salt glands in unrestrained *Crocodylus porosus*. *The Journal of Experimental Zoology*, 272:490-495.

VON DÜRING, M. 1973. The ultrastructure of lamellated mechanoreceptors in the skin of reptiles. *Zeitschrift für Anatomie und Entwicklungsgeschichte*, 143:81-94.

VON DÜRING, M. & MILLER, M.R. 1979. Sensory nerve endings of the skin and deeper structures, in *Biology of the Reptilia*, *Neurology A*, edited by C. Gans, R.G. Northcutt and P. Ulinski. London: Academic Press: Volume 9:407-442.

WESTERGAARD, B. & FERGUSON, M.W.J. 1986. Development of dentition in *Alligator mississippiensis*: early development of the lower jaw. *Journal of Zoology*, 210:575-597.

WESTERGAARD, B. & FERGUSON, M.W.J. 1987. Development of dentition in *Alligator mississippiensis*: later development in the lower jaws of hatchlings and young juveniles. *Journal of Zoology*, 212:191-222.

WOERDEMAN, M.W. 1920. Über die Gaumendrüsen der Krokodile. *Anatomische Anzeiger*, 53:345-352.

WWW SITE REFERENCE:

http://www.flmnh.ufl.edu/natsci/herpetology/turtcroclist/chklst2.htm Crocodile Specialist Group

Reference to *Crocodilus vulgaris* Cuvier 1807 (=*Crocodylus niloticus* Laurenti, 1768).

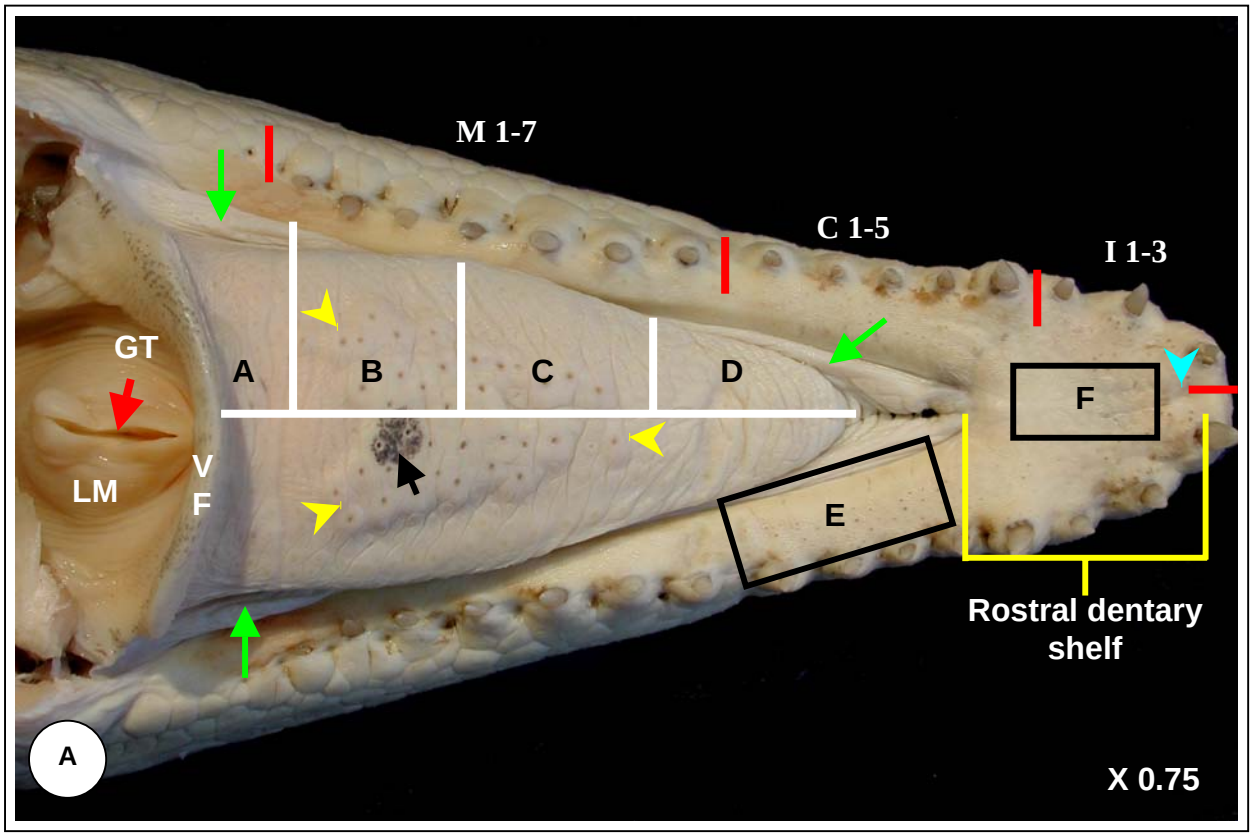

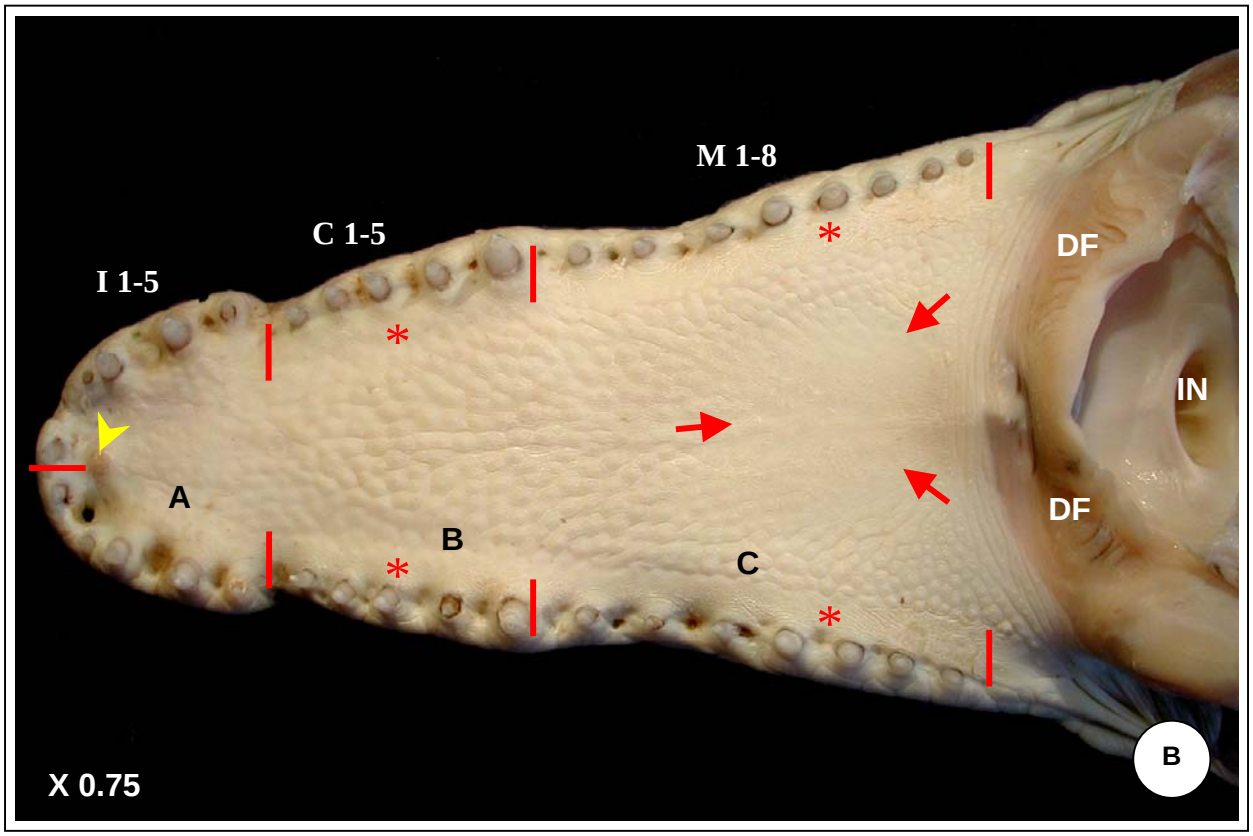

See captions opposite.

CAPTIONS TO FIGURE 1: MACROSCOPIC ANATOMY OF THE ORAL CAVITY

FIG. 1A: Macrophotograph of the mandible with the tongue *in situ* showing the dental arrangement of the incisor (I 1 - 3), canine (C 1 - 5) and molar (M 1 - 7) teeth, demarcated by the red lines. The sampling sites for histology of the tongue (A - D) and the gingivae (E & F) are also indicated. Note the raised appearance of the glandular region on the tongue surface (demarcated by the yellow arrowheads) possibly as a result of formalin fixation, as well as a localised region of pigmentation (black arrow). The fibrous membrane attaching the tongue to the mandible is also obvious in places (green arrows). The rostral dentary shelf is indicated in the region above the symphysis of the dentary bones. The turquoise arrowhead indicates the position of the shallow depression which houses the small, rigid, conically formed process, situated at the base of the I 1 teeth, seen in Fig. 1B. The glottis (GT) and laryngeal mound (LM) are shown *in situ* on the floor of the pharyngeal cavity and the ventral fold (VF) of the gular valve is seen separating the ventral aspects of the oral and pharyngeal cavities. Formalin fixed specimen.

FIG. 1B: Macrophotograph of the maxilla and palate showing the dental arrangement of the incisor (I 1 -5), canine (C 1 - 5) and molar (M 1 - 8) teeth, demarcated by the red lines. The smooth area of the palate, demarcated by the red arrows, lies above the left and right posterior palatine foraminae. The small, rigid, conically formed process, situated at the base of the I 1 teeth, is indicated by the yellow arrowhead. Also note the smooth zone of mucosa forming the gingiva adjacent to the teeth (asterisks) which stretches from approximately I 5 to M 8 on both sides of the maxilla. The common opening of the internal nares (IN) is seen on the roof of the pharyngeal cavity as well as the dorsal fold (DF) of the gular valve which separates the dorsal aspects of the oral and pharyngeal cavities. Samples of the mucosa of the palate and gingiva were removed from regions A, B & C as indicated on the photograph. Formalin fixed specimen.

FIGURE 2: MACROSCOPIC FEATURES

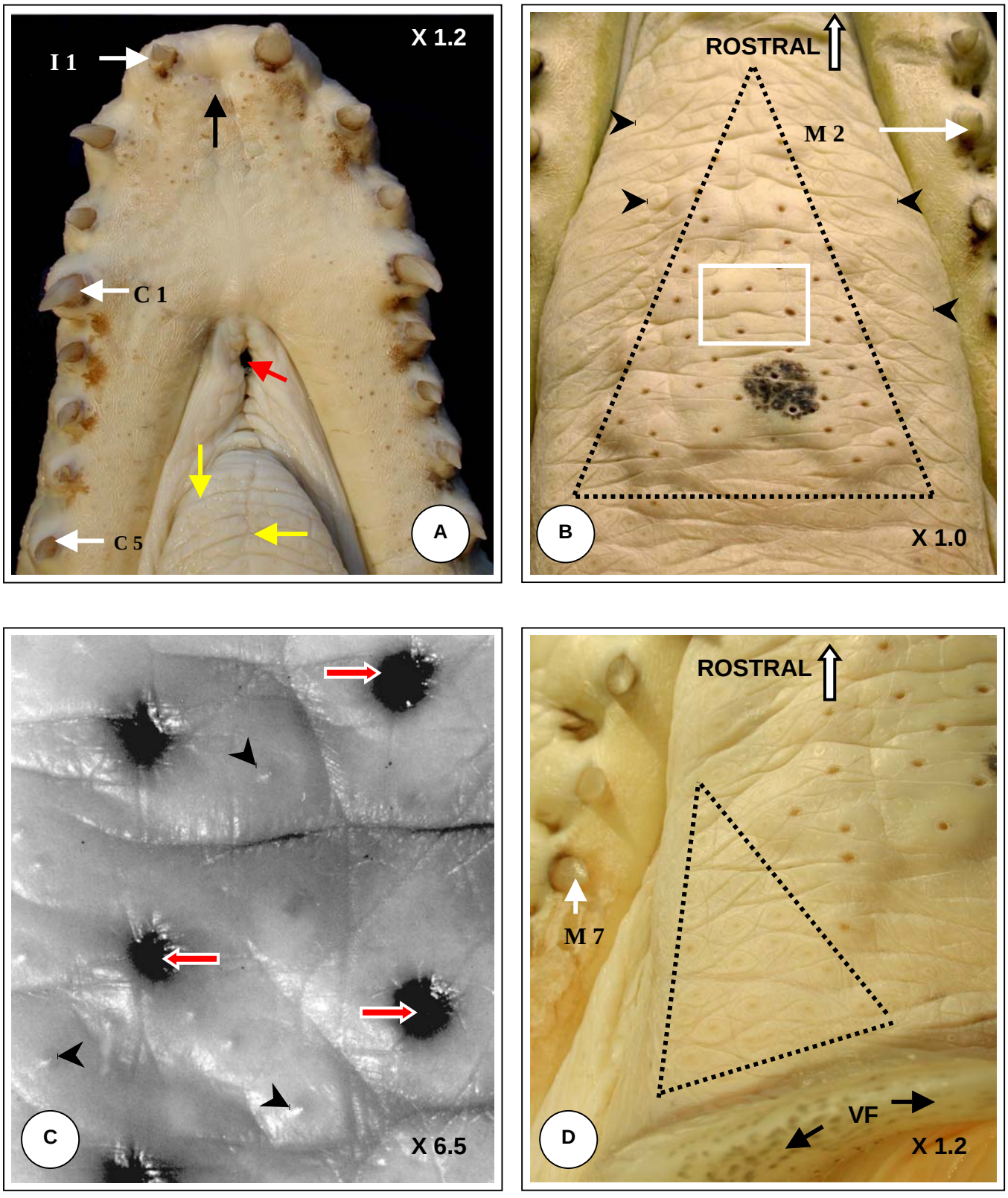

See captions opposite.

CAPTIONS TO FIGURE 2: MACROSCOPICAL CAVITY

FIG. 2A: Macrophotograph of the rostral portion of the mandible (I 1 to C 5) showing the highly folded peripheral membrane around the tip of the tongue. The gingiva is seen to have a slightly cobbled appearance towards the rostral tip above the dentary symphysis. The black arrow indicates a shallow depression which houses the small, rigid, conically-shaped maxillary process seen in Fig. 1B (this chapter). Note the deep transverse and oblique grooves at the tip of the tongue (yellow arrows), possibly accentuated by formalin fixation. The red arrow shows a hole made by the hook in the abattoir when the carcass was suspended during the evisceration process (see Chapter 1, Fig. 1C & D). I 1 = Incisor 1; C 1, C 5 = Canine 1 & 5. Formalin-fixed specimen. X 1.2 .

FIG. 2B: Macrophotograph of the surface of the tongue showing the triangular arrangement of the glandular region (indicated by the dotted line) situated in the posterior two-thirds of the tongue and stretching from approximately M 2 to M 6/7 (not indicated in photograph). The pigmented gland openings are clearly visible. Note the less conspicuous, low-profiled areas (black arrowheads) situated laterally to the glandular region. The rectangular area is enlarged in Fig. C. Formalin-fixed specimen. X 1 .

FIG. 2C: Stereomicrograph of the darkly-pigmented openings to salivary glands (red arrows) on the surface of the tongue. Small nipple-like surface extensions (black arrowheads) are scattered between the openings. Formalin-fixed specimen. X 6.5 .

FIG. 2D: Macrophotograph of the caudo-lateral region of the tongue showing a discrete, triangular region of low-profiled surface extensions at the base of the ventral fold (VF) of the gular valve. M 7 = Molar 7. Formalin-fixed specimen. X 1.2 .

FIGURE 3: HISTOLOGICAL FEATURE

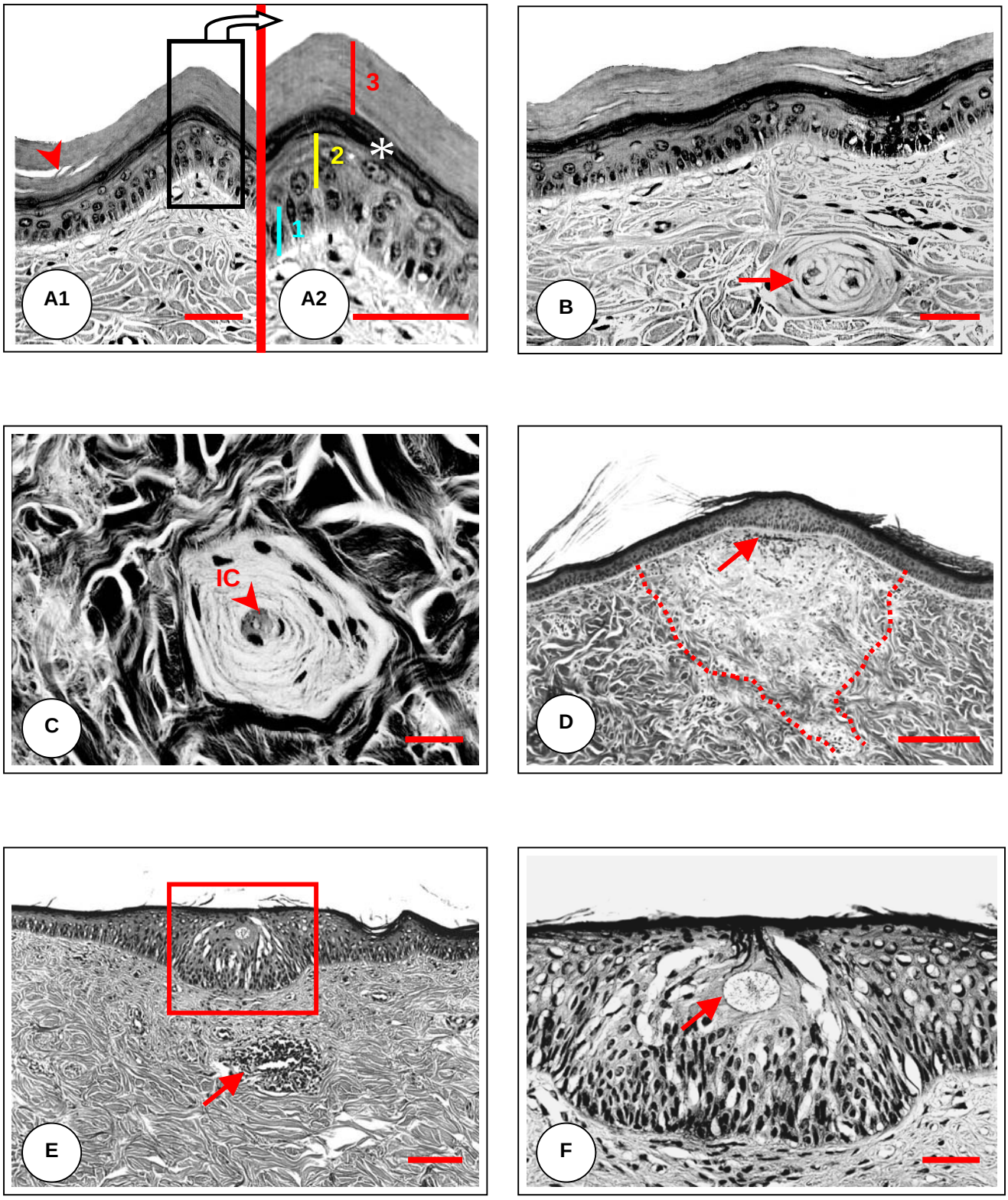

See captions opposite.

CAPTION S TO FIGURE 3: HISTOLOGICA ATE

FIG. 3A1: A pointed elevation of the epithelial lining of the palate supported by subepithelial connective tissue. Note the signs of desquamation of the stratum corneum (arrowhead). H&E-stain. Bar = 100μm.

FIG. 3A2: Enlargement of the rectangle indicated in Fig. 3A1 showing the stratum basale (1), the stratum spinosum (2) the thin stratum granulosum (asterisk) and the superficial stratum corneum (3). Bar = 100μm.

FIG. 3B: Randomly scattered Pacinian-like corpuscles (arrow) were located in the subepithelial connective tissue and often associated with epithelial specialisations. H&E-stain. Bar = 100μm.

FIG. 3C: Typical Pacinian-like corpuscle displaying concentric lamellae around an inner core (IC). Note the thick, fibrous connective tissue capsule surrounding the corpuscle. H&E-stain. Bar = 50μm.

FIG. 3D: Lightmicrograph of an elevated, dome-shaped specialisation commonly found in the rostral and lateral regions of the palate showing a pale connective tissue mass (outlined area) just below the epithelium. Note the localised thickening of the epithelium and the dark, sub-epithelial cellular mass (arrow) H&E-stain. Bar = 500μm.

FIG. 3E: A flattened epithelial specialisation typically found in the mid-, lateral and posterior regions of the palate. Note the dense, dark cellular mass (arrow) in the deeper connective tissue, associated with these receptors and the arrangement of the epithelial cells to form a structure similar to that of a taste bud. H&E-stain. Bar = 250μm.

FIG. 3F: Higher magnification of the epithelial specialisation shown in the rectangle in Fig. 3E. Note the translucent circular structure (arrow) filled with fine fibrillar material. It was not possible to determine the function of this type of corpuscle, but it was thought that they might be associated with taste or osmoreception. H&E-stain. Bar = 100μm.

FIGURE 4: SEM FEATURES OF PAPI : PALATE

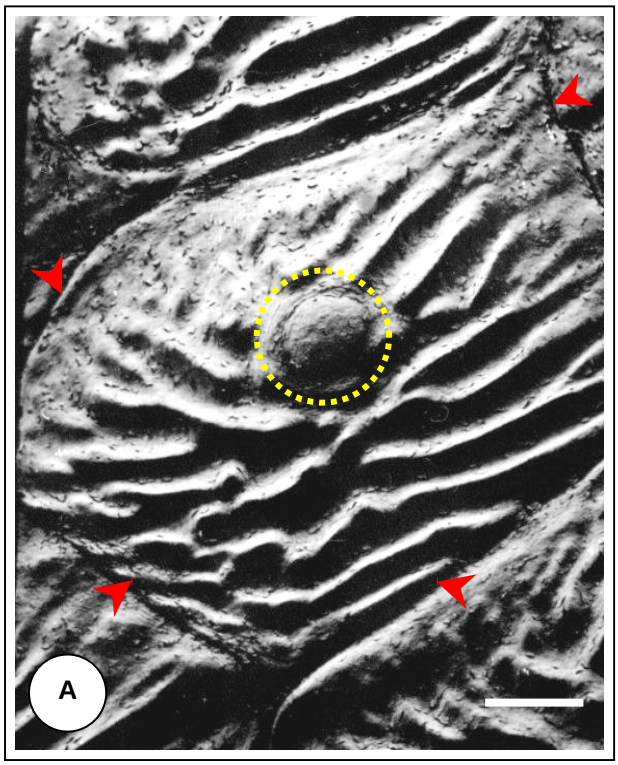

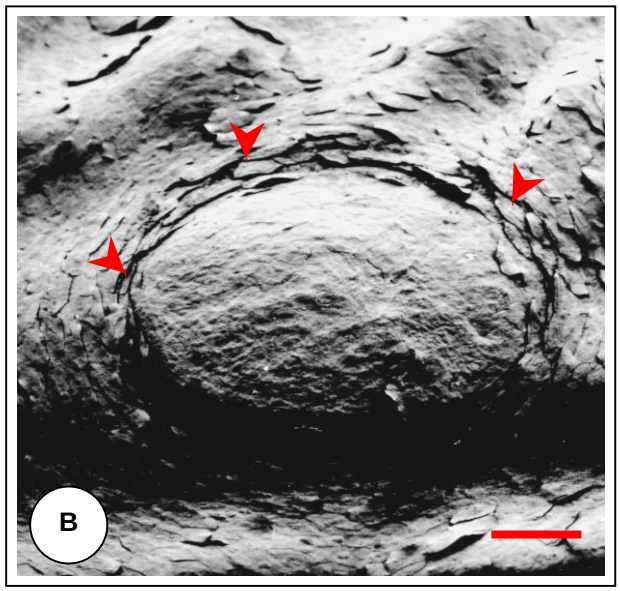

FIG. 4B: Higher magnification of the slightly convex, circular structure circled in Fig. 4A, the surface of which appears featureless. Note the epithelial desquamation (possibly accentuated by SEM processing) around the perimeter of the papilla (arrowheads). Bar = 50μm.

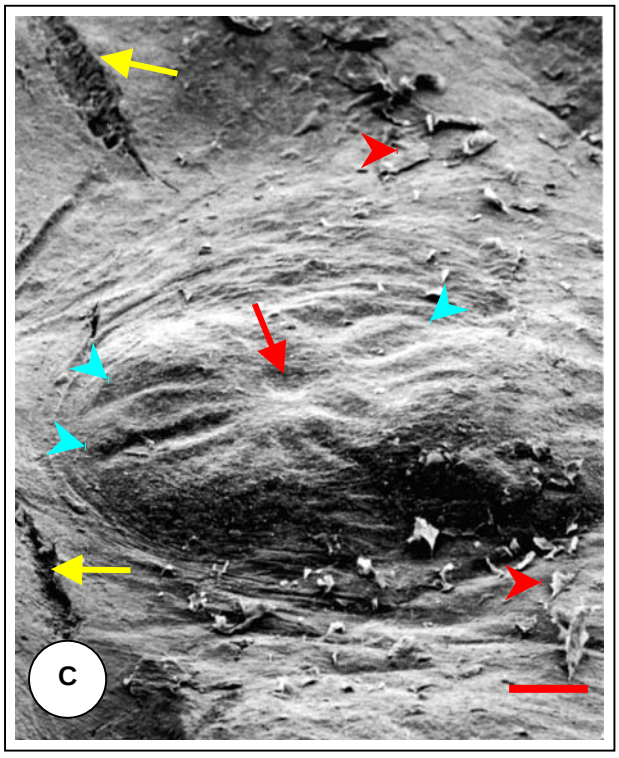

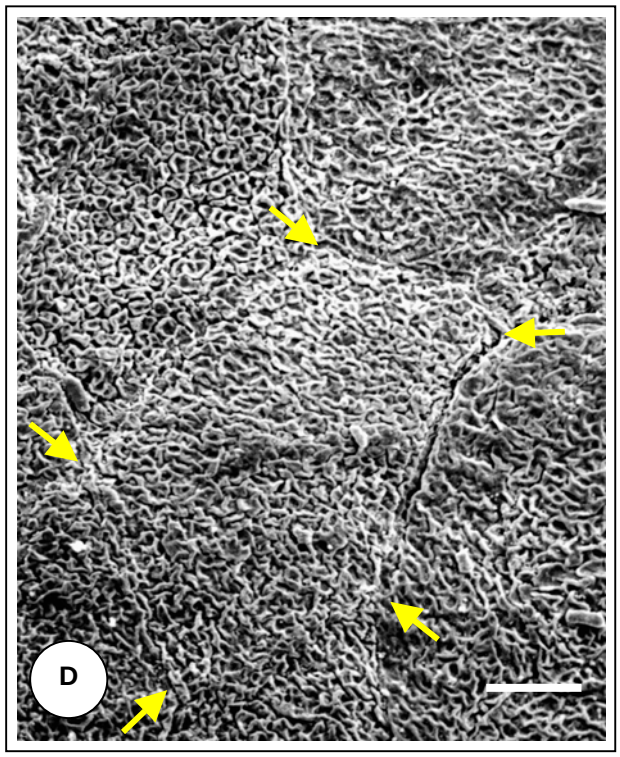

FIG. 4A: SEM-micrograph of a polygonal-shaped cobbled unit (red arrowheads) typical of the surface of the palate. Note the centrally positioned dome-shaped structure (papilla - circled) and the grooved appearance of the surrounding epithelial surface. Bar = 250μm.

FIG. 4C: A convexly raised papilla with a central depression (red arrow) with radiating grooves (blue arrowheads). These papillae were observed in the rostral region of the palate. Light desquamation is also apparent (red arrowheads). The yellow arrows indicate artefacts (cracking of epithelium) probably caused during SEM processing (critical point drying). Bar = 100μm.

FIG. 4D: Higher magnification of the typical cell-surface features seen throughout the palate. The yellow arrows indicate the boundaries of a characteristic polygonal-shaped cell. Note the complex pattern of microridges on the cell surface. Bar = 2μm.

FIGURE 5: MORPHOLOGY OF THE GI

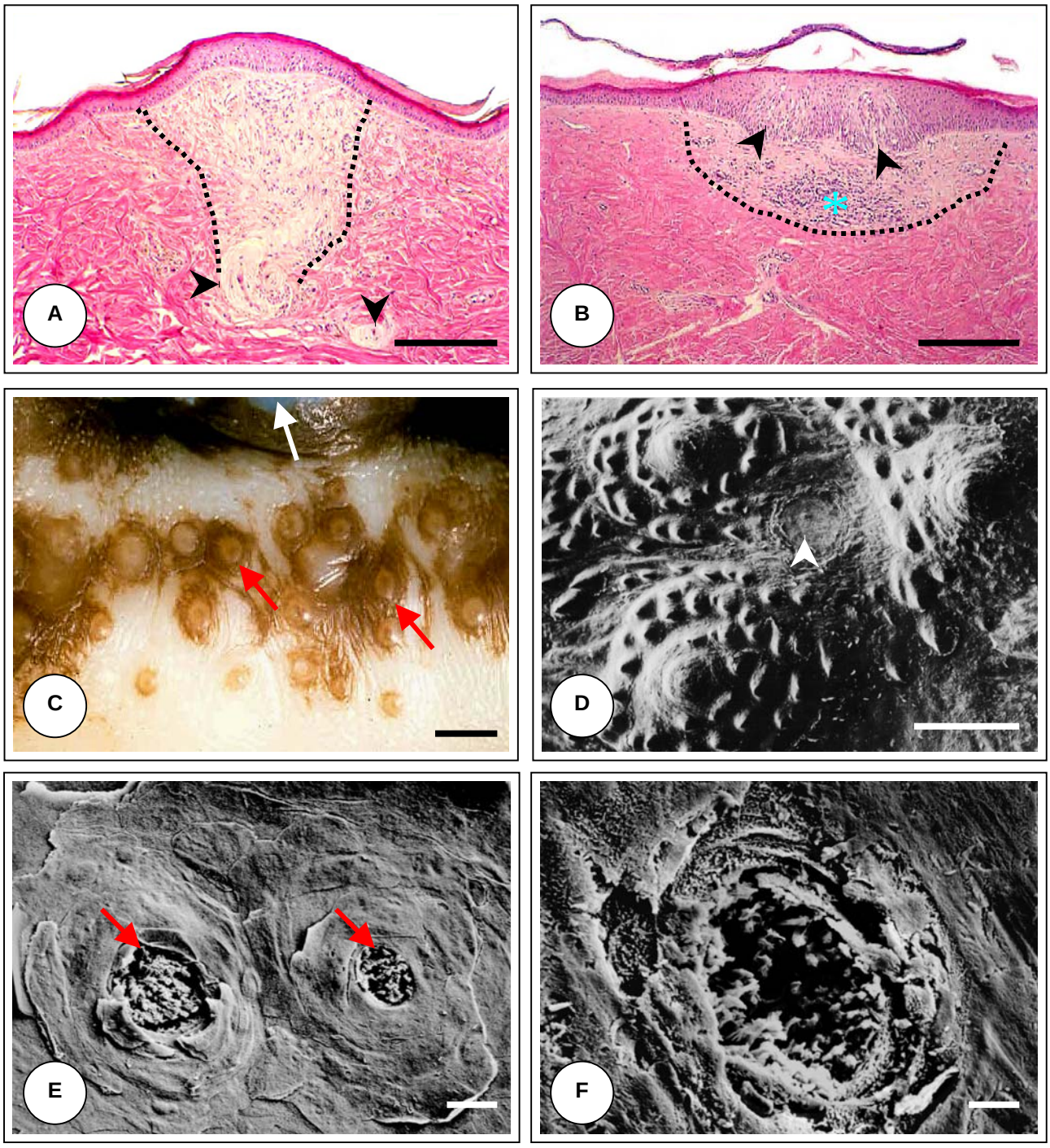

FIG. 5A: Lightmicrograph of a raised sensory unit commonly found in the rostral region of the lower jaw showing a pale connective tissue mass (outlined area) just below the epithelium and at the bottom of which are two Pacinian-like corpuscles (arrowheads). H&E stain. Bar = 500μm.

FIG. 5B: Lightmicrograph of paired sensory units (arrowheads) resembling taste buds within a flattened epithelial specialisation. These structures were generally found in the rostral and mid-lateral gingivae of the lower jaw. Note the similarly pale connective tissue mass (outlined area) below these structures, as seen in Fig. 5A. A basophilic cell rich mass (asterisk) is observed below the sensory units. H&E stain. Bar = 500μm.

FIG. 5C: Stereomicrograph of epithelial specialisations (red arrows) in the rostral region of the gingiva of the lower jaw, normally situated close to teeth (white arrow). Fresh specimen. Bar = 500μm.

FIG. 5D: SEM-micrograph of a group of epithelial specialisations, similarly situated to those shown in Fig. 5C. Each dome-shaped papilla is in turn surrounded by rosettes of conical epithelial projections. Note the flattened circular area (arrowhead) in the centre of the group of papillae, similar to those seen in Figs. 5E & F. Bar = 500μm.

FIG. 5E: SEM-micrograph of paired pores (arrows) associated with the taste buds contained within flattened epithelial specialisations shown in Figs. 5B & 5D. Bar = 10μm.

FIG. 5F: Higher magnification SEM-micrograph of a sensory pore seen in Fig. 5E showing exposed fimbriae. Bar = 5μm.

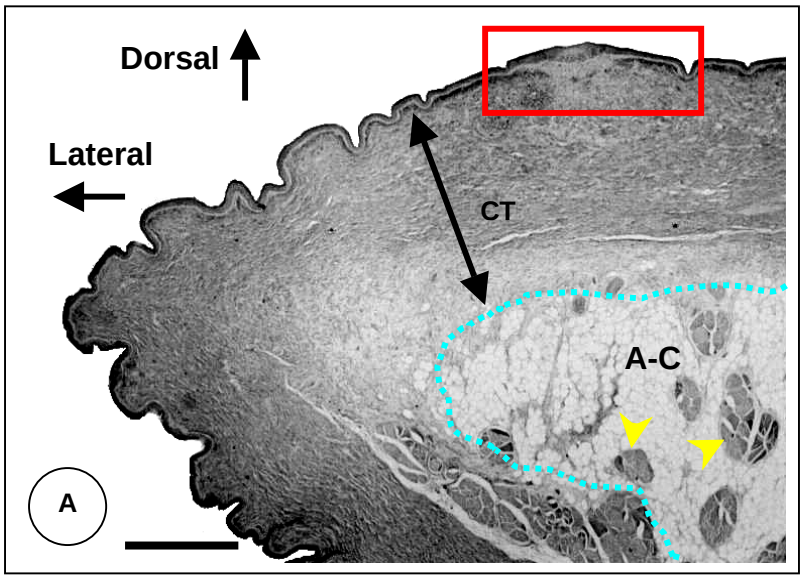

FIG. 6A: Cross-section of the rostral part of the tongue illustrating the lateral aspect. Note the increase in the number of folds on the lateral surface, the thick layer of irregular dense subepithelial connective tissue (CT) and the adipose tissue core (A-C) (approximately following the blue dotted out-line) containing scattered bundles of striated muscle fibres (yellow arrowheads). The blocked area shows an epithelial specialisation. H&E-stain. Bar = 2mm.

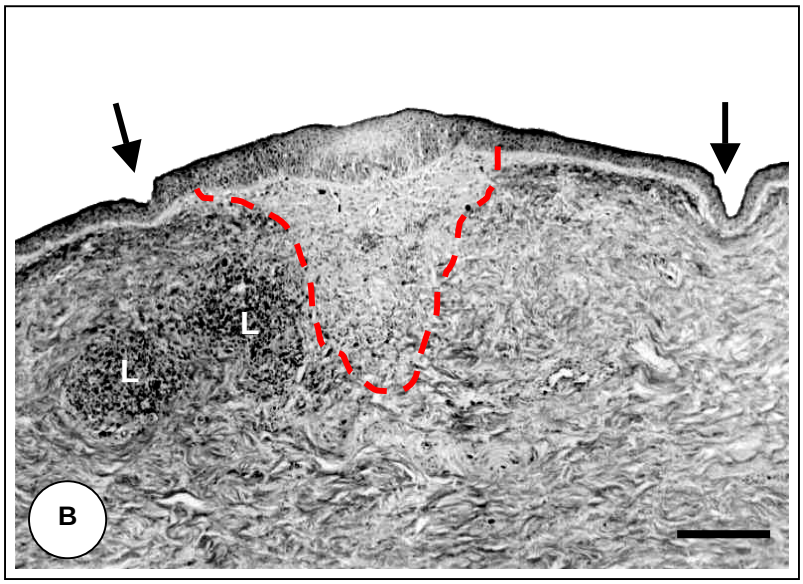

FIG. 6B: An enlargement of the epithelial specialisation (blocked area) shown in Fig. 6A above. Note the thickened epithelium, the characteristic, pale, conical zone of modified subepithelial connective tissue (outlined) and the closely associated lymphocytic aggregations (L). The black arrows indicate the groove/trough often seen surrounding these structures. H&E-stain. Bar = 500μm.

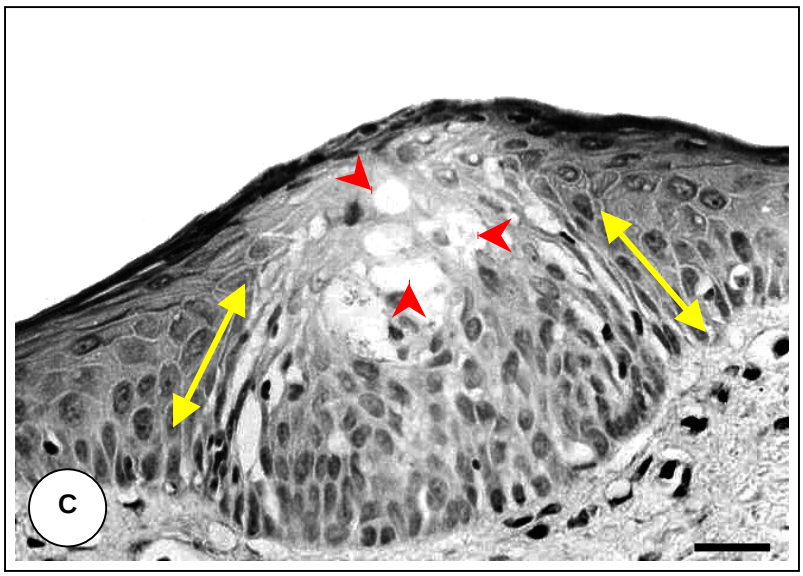

FIG. 6C: Modification of the thickened epithelium of the specialisation to form an enlarged oval core reminiscent of a taste bud. Note the vertical orientation of the core cells (arrows) and the more substantial stratum spinosum surrounding the taste bud. Vacuolation is apparent in the superficial region of the receptor (arrowheads). H&E-stain. Bar = 50μm.

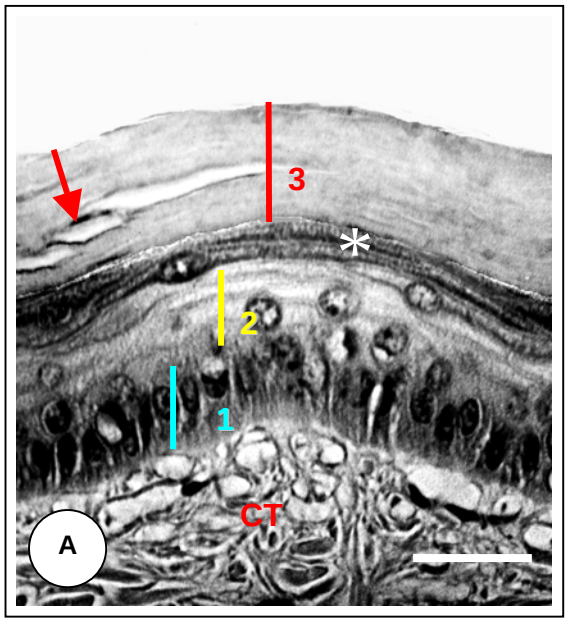

FIG. 7A: Enlargement of the epithelial covering of the tongue surface showing the single layer of vertically oriented cells forming the stratum basale (1), the narrow stratum spinosum (2), the darkly staining stratum granulosum (asterisk) and the superficial stratum corneum (3) which shows signs of desquamation (arrow). The epithelium is supported by irregular dense connective tissue (CT). H&E-stain. Bar = 50μm.

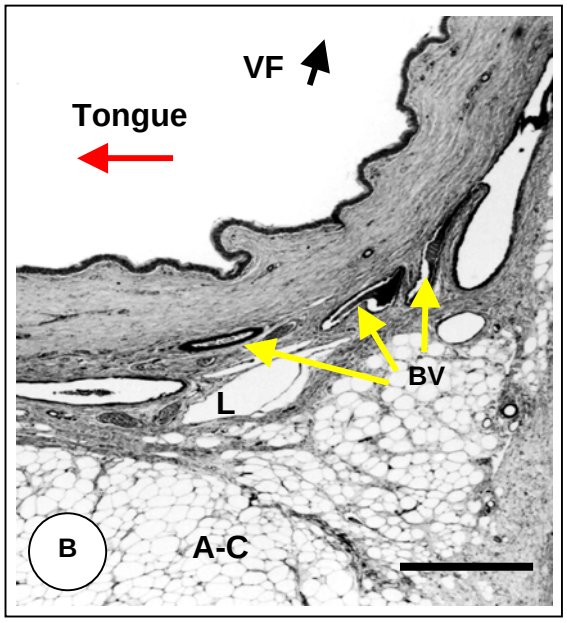

FIG. 7B: Caudal limit of the tongue where it abuts the ventral fold (VF) of the gular valve. Note the large lymphatic (L) and vascular (BV) plexus in this region as well as the underlying adipose tissue core (A-C) of the tongue. See also Fig. 6A – this chapter. H&E-stain. Bar = 1mm.

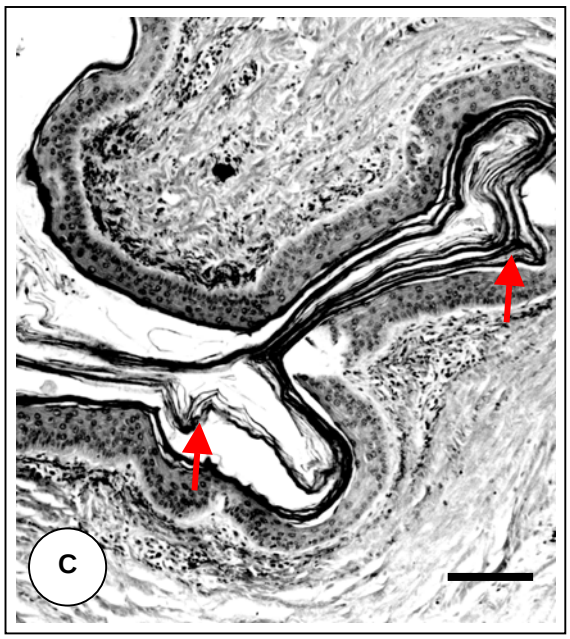

FIG. 7C: Lateral wall of the tongue illustrating the highly folded nature of the surface and the greater degree of desquamation of the surface layers of the epithelium in this region (arrows). H&E-stain. Bar = 250μm.

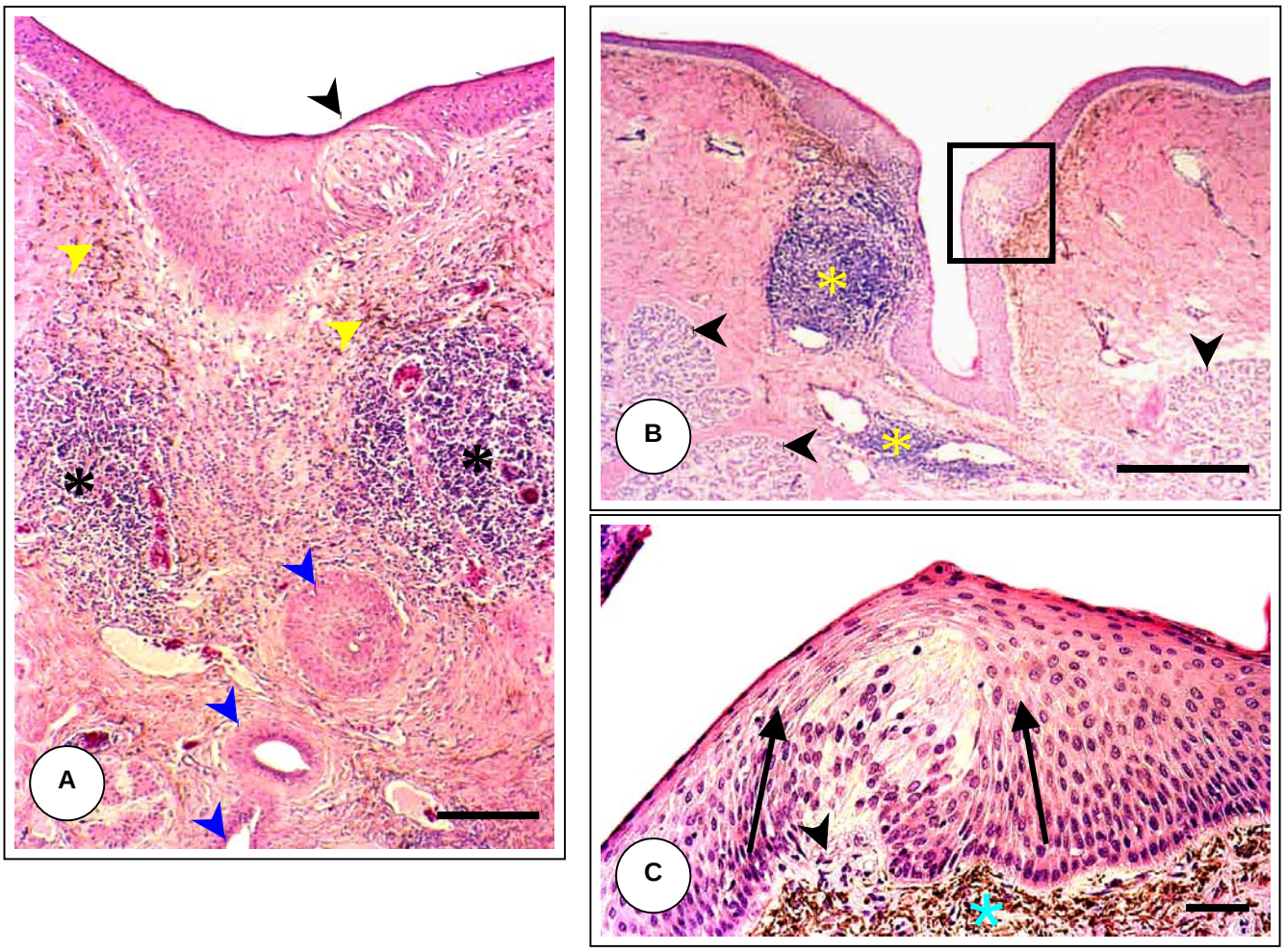

FIG. 8A: Lightmicrograph of an oblique section through the secretory duct of an underlying salivary gland. Note the taste bud (black arrowhead) situated in the wall of the pore opening onto the tongue surface (see also Fig. 8B). Oblique sections of the duct (blue arrowheads) can be seen in close proximity to the glandular tissue (not shown). Lymphocytic aggregations (asterisks) are closely associated with the secretory duct and the secretory pore (see Fig. 8B). Note also the sparse layer of melanin pigmentation in close proximity to the base of the epithelium (yellow arrowheads). Bar = 500μm.

FIG. 8B: Low-power micrograph of a region similar to that shown in Fig. 8A, but showing more detail of the structure of the secretory duct. A taste bud (rectangle) is similarly positioned to the one shown in Fig. 8A. Note the lymphatic aggregations (yellow asterisks) and the secretory units of glandular tissue (arrowheads). Bar = 1mm.

FIG. 8C: Enlargement of the taste bud indicated in Fig. 8B. Note the vertical orientation of the epithelial cells (arrows) and the more substantial stratum spinosum surrounding the taste bud. At the base of the specialisation is an apparent nerve plexus (arrowhead) seen to penetrate below the epithelium into the melanin layer (asterisk). Bar = 100μm.

FIGURE 9: HISTOLOGICAL FEATURES OF THE TONGUE

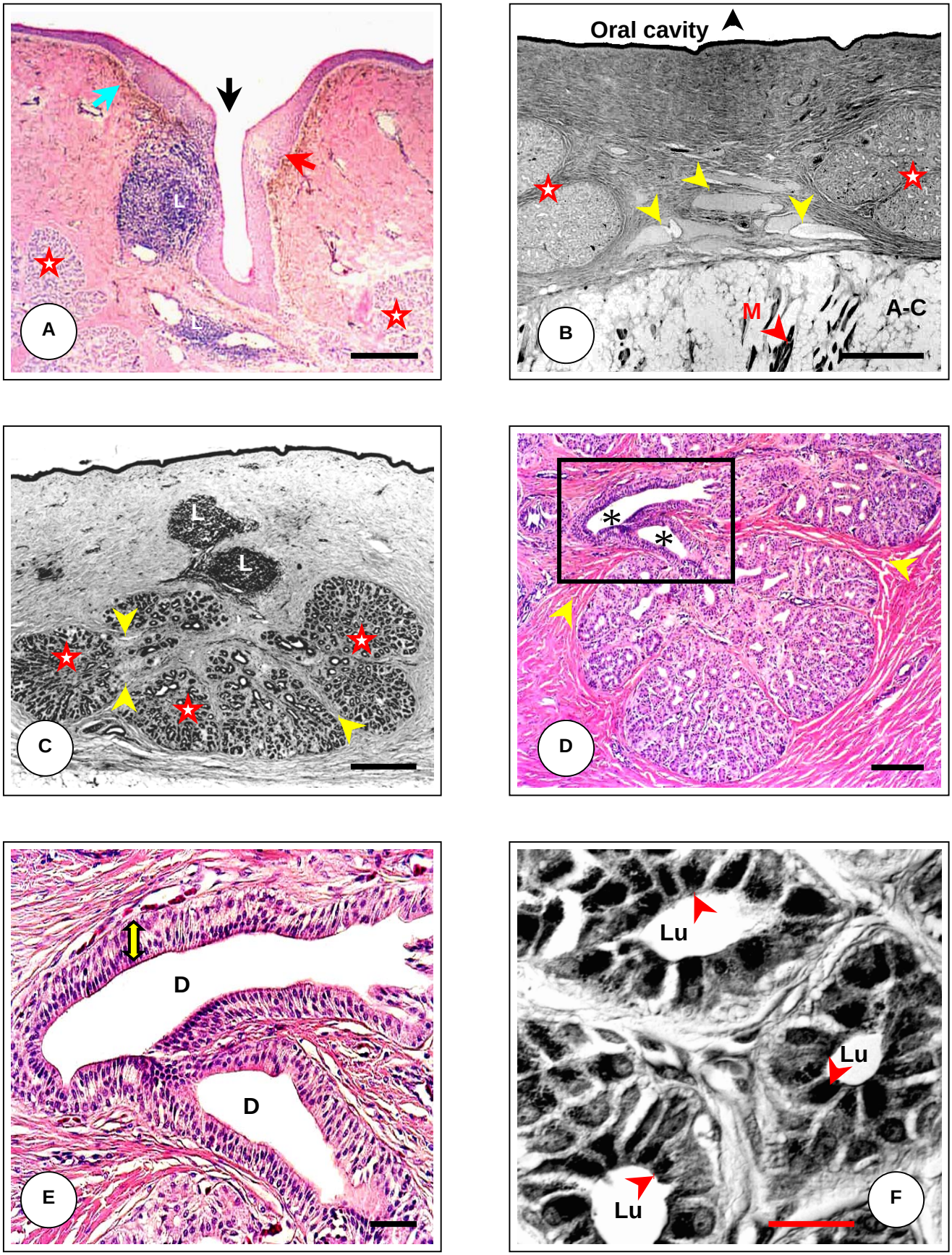

See captions opposite.

CAPTIONS TO FIGURE 9: HISTOLOGIC SALIVARY GLANDS OF THE TONGUE

FIG. 9A: Low magnification of the secretory duct of a deeper lying salivary gland (see Fig. 9C). The duct opens onto the tongue surface by means of a pore (arrow). The duct is not entirely visible due to the slightly oblique plane of the section towards its base. Note the lymphoid aggregation (L) associated with the duct. A taste bud (red arrow) is observed towards the opening of the duct (see also Figs. 8A-C – this chapter). Note the thin, but prominent layer of melanin pigmentation (blue arrow) immediately below the epithelium. A portion of the secretory units (stars) of a salivary gland is also visible in the micrograph. H&E-stain. Bar = 500μm.

FIG. 9B: Secretory units (stars) of the two lingual salivary glands separated by a well-developed vascular and lymphatic plexus (yellow arrowheads). The glandular tissue is positioned deep within the subepithelial connective tissue, close to the adipose tissue core (A-C). Striated lingual muscle (M). H&E-stain. Bar = 2mm.

FIG. 9C: An example of a typical lingual salivary gland. Note the separation of the glandular tissue into lobules (stars) by wide tracts of connective tissue (arrowheads). The main secretory duct does not appear in the section although some lymphoid tissue (L) is visible. PAS-stain. Bar = 1mm.

FIG. 9D: A lobule of a lingual salivary gland unit. Secondary or tertiary branches (asterisks) of the main secretory duct, displaying a wide lumen, can be observed in the rectangle (enlarged in Fig. 9E). Wide connective tissue tracts (arrowheads) can be seen between the lobules of the salivary gland. H&E-stain. Bar = 500μm.

FIG. 9E: Higher magnification of the rectangle in Fig. 9D showing the double columnar nature of the duct epithelium (double-headed arrow) and the wide lumen of the ducts (D). H&E-stain. Bar = 1mm.

FIG. 9F: Higher magnification of a group of secretory tubules of the branched coiled tubular units of the gland demonstrating the PAS-positive granules (arrowheads) observed in the apical cytoplasm of the cells. However, this was not a consistent feature. Note the wide lumen (Lu) of the tubules. PAS-stain. Bar = 50μm.

FIGURE 10: SEM FEATURES OF THE

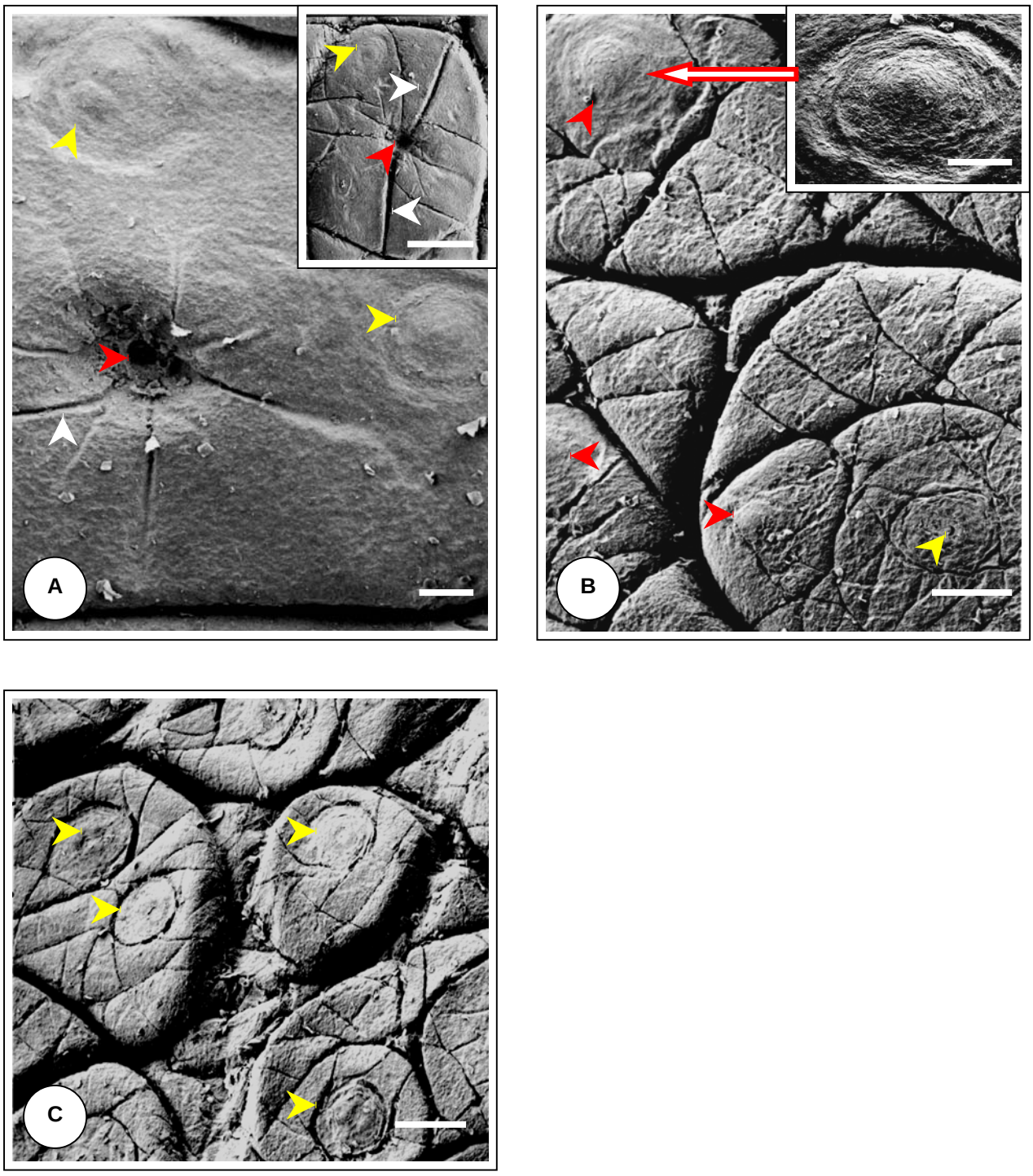

FIG. 10A: A surface unit found on the glandular area of the tongue. Note the large, centrally-positioned gland opening (red arrowhead), the radiating epithelial grooves (white arrowheads) and the dome-shaped structures (yellow arrowheads). Bar = 100μm.

Inset: Overview of another surface unit demonstrating longer epithelial grooves (white arrowheads) and similar features (gland opening – red arrowhead and dome-shaped structures – yellow arrow-head) to those seen in the main micrograph. Bar = 500μm.

FIG. 10B: Typical surface units found in the mid-lateral region of the tongue showing a mosaic pattern of grooves. Flat disc-shaped structure (possible taste receptor – yellow arrowhead) and raised dome-shaped structures (possible pressure receptors – red arrowheads) are present. Bar = 250μm.

Inset: Enlargement of the dome-shaped structure indicated by the outlined arrow. Bar = 100μm.

FIG. 10C: A group of caudo-laterally situated surface units (see Fig. 2D) showing flat disc-shaped structures (arrowheads). Two of these discs are situated on the same unit. Bar = 250μm.

FIGURE 11: SEM FEATURES OF A TOR AREA

FIG. 11A: Enlargement of a disc-shaped structure from the caudo-lateral aspect of the tongue showing the central pore (white arrow) and the concentric rings of loosened, desquamating surface epithelial cells (arrowheads). Bar = 100μm.

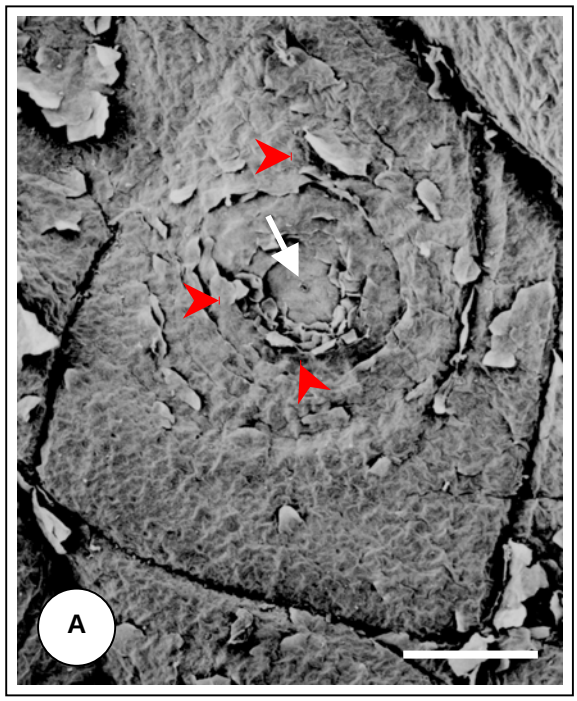

FIG. 11B: Higher magnification of the central pore to show the protruding cellular processes (arrowhead). Note the spongy appearance of surrounding epithelial cells. Bar = 10μm.

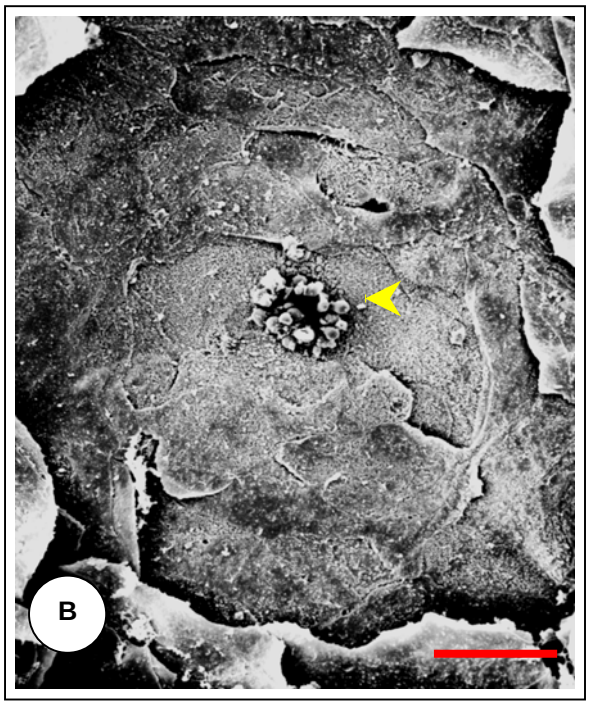

FIG. 11C: An oblique view of clavate cellular processes (arrowheads) which protrude for only a short distance above the surface. The surrounding epithelial cells display a complex arrangement of microridges. Bar = 5μm.

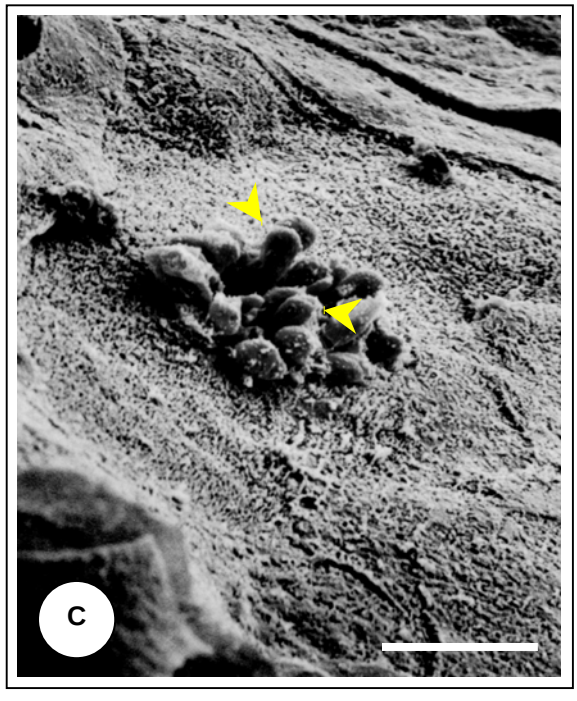

CHAPTER 3

MORPHOLOGY OF THE GULAR VALVE AND PHARYNGEAL CAVITY

INTRODUCTION

A comprehensive description of the anatomy of the pharyngeal region in Crocodilia is not available and only superficial and fleeting reference to this part of the digestive tract has been presented in the literature, (Fuchs, 1908, cited by Barge, 1937; Storer & Usinger, 1961; Chiasson, 1962; Bellairs, 1969; Gans, 1976; Pooley and Gans, 1976; Luppa, 1977; Ferguson, 1979; Evans, 1986; Steel, 1989; Buffetaut, 1989; Mazzotti, 1989; Grigg and Gans, 1993). This situation is further complicated by the variable terminology used to describe anatomical structures in this part of the upper digestive tract. For example, the pair of tissue folds, which effectively isolate the oral cavity from the pharyngeal cavity in Crocodilia when the mouth is closed or gaping, have been given a variety of names or descriptions (Fuchs, 1908, cited by Barge, 1937; Taguchi, 1920; Chiasson, 1962; Bellairs, 1969; Gans, 1976; Pooley and Gans, 1976; Luppa, 1977; Ferguson, 1979; Evans, 1986; Steel, 1989; Buffetaut, 1989; Mazzotti, 1989; Grigg and Gans, 1993). The unit formed by these folds is referred to throughout this chapter as the "gular valve" (F.W. Huchzermeyer, personal communication 1999).

In contrast to the lack of gross anatomical information, the histology of the pharynx has been compared in some detail by Taguchi (1920) in three species of Crocodilia, namely, *Alligator sinensis, Crocodylus porosus* and *Crocodylus niloticus*.

In view of the inconsistency in terminology applied to this region, and considering the paucity of anatomical information, this chapter describes the topography and morphology of the gular valve and pharyngeal cavity in the Nile crocodile, *Crocodylus niloticus* (Laurenti, 1768). The histological features of this region are compared with the findings of Taguchi (1920) and supplemented by information supplied by scanning electron microscopy (SEM).

MATERIALS AND METHODS

Experimental animals

Six clinically healthy 2.5 - 3 year-old (1.2 - 1.5 m in length) and two approximately two year-old (1 m in length) *C. niloticus* specimens of either sex were obtained from a breeding farm where they were slaughtered commercially for their skins and meat. Animals were shot in the brain (see Chapter 1, Fig. 1B) at close range using a .22 calibre rifle. Although death was instantaneous, carcasses were left until all obvious signs of post mortem tremor had ceased before commencing the skinning process. There was therefore an unavoidable delay of approximately 45 minutes before the tissue could be fixed for microscopy. The heads were removed from the skinned carcasses, photographed, and immersion fixed in a large volume of 10 % phosphate-buffered formalin in plastic buckets for a minimum of 48 hours. Care was taken to exclude air from the oral and pharyngeal cavities by wedging a small block of wood in the angle of the mouth prior to immersion in the fixative.

Topography

All six heads from the older animals were utilised for a description of the gross anatomical features and topographical relationships of the structures in the pharyngeal region prior to sampling for microscopy. To assist in the topographic description, two of the heads were cut longitudinally along the midline using a band saw. Two skulls from similarly aged specimens were also examined to provide supporting evidence for the anatomical description.

Light microscopy (LM)

Tissue samples for LM were taken from the dorsal and ventral folds of the gular valve and from the roof and floor of the pharyngeal cavity from four heads (see Figs. 2A & C). All samples were dehydrated through 70, 80, 96 and 2X 100 % ethanol. Samples were further processed through 50 : 50 ethanol : xylol, 2X xylol and 2X paraffin wax (60 - 120 minutes per step) using a Shandon model 2LE Automatic Tissue Processor (Shandon, Pittsburgh, PA, USA). Tissue samples were finally embedded manually into paraffin wax in brass moulds and sectioned at 4 - 6 μm. The sections were stained with haematoxylin and eosin (H&E) (Luna,

1968) or periodic acid-Schiff (PAS) (Pearse, 1985) and viewed and micrographed using a Reichert Polyvar (Reichert, Austria) compound light microscope fitted with a differential interference contrast (DIC) prism.

Scanning electron microscopy (SEM)

In order to examine the mucosal surface of the entire pharyngeal region for possible transition zones, the complete pharynx (including the dorsal and ventral folds of the gular valve) was removed from the heads of the two younger formalin-fixed specimens using a band saw. Each pharynx was divided into its respective dorsal and ventral components and trimmed of excess skin and fascia. Samples were rinsed for six hours in water to remove traces of phosphate buffer after which they were routinely dehydrated through an ascending ethanol series (50, 70, 90, 95 and 3X 100 % - 120 minutes per step due to their large size) and critical point dried from 100 % ethanol through liquid-CO_2 in a Polaron Critical Point Drier (Polaron, Watford, England). Dried samples were mounted (mucosal surface uppermost) onto brass or aluminium viewing stubs with a conductive carbon paste (carbon dag) and sputter coated with gold using a Balzers 020 Sputter Coater (Balzers Union, Liechtenstein). The specimens were first examined and micrographed using a stereomicroscope (Wild Photomakroskop M-400, Heerbrugg, Switzerland) to obtain an overview of their topography prior to being viewed and photographed using a Hitachi S-2500 Scanning Electron Microscope (Hitachi, Tokyo, Japan) operated at 8 kV.

After viewing the bulk samples (dorsal and ventral components) of the pharynx, they were carefully subdivided into smaller, more manageable samples in order to facilitate examination of areas which had previously been inaccessible when viewed in the SEM. These samples were re-mounted to permit viewing at acute angles and from multiple directions.

In order to examine the inner surface of the glottis, the laryngeal mound, including a portion of the underlying basihyal cartilage was excised from the floor of the pharynx of one of the 2.5 - 3 year-old specimens. The mound was then separated into left and right halves by means of two longitudinal midline incisions; one just cranial to the glottis and the other caudal to the glottis along the laryngeal fissure (Figs. 7A & D). This exposed the inner surface of the glottis without causing physical damage. Each half of the laryngeal mound was then processed for SEM and mounted for viewing as outlined above.

RESULTS

Macroscopic features

The pharyngeal cavity was dorso-ventrally flattened and occupied the caudo-ventral part of the head (Fig. 1). The cavity was widened rostrally and narrowed caudally where it became continuous with the entrance to the oesophagus. The rostral boundary was demarcated by the dorsal and ventral folds of the gular valve (Figs. 1, 2B, 2D & 3A) which effectively isolated the pharyngeal cavity from the oral cavity (see Figs. 1 & 3A).

The common opening of the internal nares was located in the roof of the pharyngeal cavity approximately 15 mm caudal to the dorsal fold (Figs. 1 and 2D). This opening was medially positioned and partially divided by low dorsal and ventral median bony ridges which fused rostrally (approximately in line with the base of the tongue - see sagittal section of the head, Fig. 1) to form the nasal septum. The Eustachian tubes (*Tuba auditiva*) opened into the pharynx approximately 5 mm caudal to the internal nares as a common median aperture protected by a tightly fitting fibrous plug (Fig. 1, 2D & 13A). This opening lay at the suture of the basioccipital and basisphenoid bones and was separated rostrally from the opening of the internal nares by a slightly raised, crescent-shaped structure composed of fibrous tissue (Figs. 1, 2D & 13A). In sagittal sections of the head, this fibrous tissue was observed to line the rostral lip of the common opening of the Eustachian tubes, effecting tight seating of the fibrous plug within the entrance of the aperture (Fig. 1). Immediately caudal to the opening of the Eustachian tubes, and continuous with the fibrous plug, was a medially positioned tract of smooth mucosa which demonstrated fine longitudinal ridges and grooves. The mucosa on either side of the medial tract was thrown into numerous coarse longitudinal folds and deep intervening crypts and clefts (Figs. 2D & 13A). Nodular protrusions typical of tonsillar tissue were associated with the crypts (Figs. 2D & 13A). The lymphoid nature of the nodules was confirmed by LM (Fig. 13C). The medial tract and adjacent zones of tonsillar tissue merged medio-caudally to form a stretch of delicately folded mucosa continuous with the lining of the oesophagus.

The dorsal fold of the gular valve was crescent-shaped (with its convex surface facing rostrally) and extended across the roof of the pharynx (following the suture line between the pterygoid, transpalatine and palatine bones) to form the dorsal boundary between the oral and pharyngeal cavities. The fold was caudally inclined and characteristically displayed a shallow, median apical notch (Figs. 2D, 3A & C). It varied

between 12 to 15 mm in height, displayed a broad fleshy base of attachment and narrowed progressively towards its free end or apex. The oral surface of the dorsal fold revealed numerous, well-defined longitudinal mucosal folds which extended from just below the apex to just above the base. A number of prominent transverse mucosal folds were present at the base of the fold and were continuous with similar folds lining the dorso-caudal aspect of the roof of the oral cavity (Figs. 2D, 3A-C). The pharyngeal surface was smoother and displayed a series of fine longitudinal mucosal folds which followed the contours of the dorsal fold i.e., the mucosal folds tended to radiate laterally from their origin at the base of the dorsal fold. On its pharyngeal aspect, the base of the dorsal fold was supported by a pair of relatively large secondary transverse folds. These folds extended from the lateral extremities of the dorsal fold (where they were well developed) to the middle of the fold (where they petered out). Smaller, additional pairs of folds (tertiary folds) were generally observed caudal to the original pair.

The floor of the pharyngeal cavity was dominated by the laryngeal mound. This elevated almond-shaped or ovoid structure occupied a large proportion of the pharyngeal cavity floor. Medially situated on the mound, and extending along much of its length, was the slit-like glottis (Figs. 2B & 7A). The lips of the glottis were prominent and elevated above the surface of the mound. Anteriorly, the lips formed part of a wedge-shaped structure which protruded rostrally beyond the laryngeal mound, ending in close proximity to the base of the ventral fold of the gular valve. The glottis continued caudally as a laryngeal fissure or sulcus (*sulcus laryngis*) (White, 1975) which was shallow and did not open into the larynx (Figs. 2B & 7A). A short rostral fissure, also continuous with the glottis, was present on the wedge-shaped tip of the laryngeal mound. It was obvious in sagittal sections of the head that the laryngeal mound elevated the glottis into the pharyngeal cavity, positioning it in close proximity to the opening of the dorsally situated internal nares when the mouth was closed (see Fig. 1).

The mucosal lining of the floor of the pharyngeal cavity displayed a series of U-shaped folds, the arms of which merged with the longitudinal folds of the oesophagus (Figs. 2B & I5A). The apex of the folds curved around the rostral extremity of the pharyngeal floor and also ran transversely across the pharyngeal surface of the ventral fold of the gular valve (Figs. 15A & B). Similar folds were also obvious on the surface of the laryngeal mound, although they were more delicate in appearance. The continuity of the folds was sometimes broken by the rostral projection of the glottis. The smooth mucosa lining the pharyngeal floor was continuous with, and similar in appearance to, the mucosa lining the compressed lateral walls of the

pharynx where the folds appeared to have a higher profile. This mucosa was continued onto the pharyngeal roof, broken only by the substantial zones of tonsillar mucosa described above.

The ventral fold of the gular valve was formed by the mucosa-covered rostral extremity of the plate-like basihyoid cartilage. The convexly-curved tip of this cartilage extended the width of the base of the tongue and, together with its attached lateral mucosal folds (see below), formed an almost semi-circular barrier which divided the floor of the pharyngeal cavity from that of the oral cavity (Figs. 2B & 3A). The ventral fold was inclined rostrally and extended a variable height above the surface of the tongue (depending on the positioning of the hyoid apparatus). The basihyoid cartilage also formed a point of attachment for the base of the tongue and extended caudally as deep support for the floor of the pharynx (Fig. 1). Mucosal folds were not obvious on the oral surface of the ventral fold but when present were transversely arranged.

It was clear from sagittal sections of the heads examined (Fig. 1) that when the mouth was closed the two components of the gular valve formed a close association, with the more rigid ventral fold being positioned in front of the dorsal fold. The rostral and caudal orientation of the ventral and dorsal folds respectively, further enhanced this close relationship. The effective seal formed by this structural arrangement was also promoted by the fact that the radius of curvature of the ventral fold, together with its additional folds, was greater than that of the dorsal fold, allowing the dorsal fold to be completely accommodated immediately caudal to the ventral fold.

At the corners of the mouth where the arms of the dorsal and ventral folds terminated, a system of smaller, additional mucosal folds linked the two components of the gular valve to each other and to the corners of the mouth, completing the seal. A substantial additional fold extended from the caudo-lateral aspect of the ventral gular fold, attached laterally to the mandible and ran freely across the lateral surface of the transpalatine and pterygoid bones to merge with the broad sheet of fibrous tissue at the angle of the upper and lower jaw (Fig. 3A). A smaller additional fold linked the rostro-lateral aspect of the dorsal gular fold to the base of the pharyngeal aspect of the ventral gular fold just medially to the origin of the larger additional fold. A sheet of mucosa continuous with that of the pharyngeal cavity connected the base of the two folds, forming a shallow, trapezoid recess. The floor of the recess continued caudally, freely covering the rostro-lateral aspect of the transpalatine and pterygoid bones and forming a deep recess between itself and the mucosa-covered bones.

Although there was variation among specimens examined, the colour of the dorsal gular fold varied from a pale brown to yellow in the fresh state. Mottled, dark pigmentation occurred over both the oral and pharyngeal surfaces, but concentrations of pigment were more prominent on the oral surface, particularly at its basal attachment to the palate. The ventral fold also showed individual variation, but was generally of similar colouration to that of the tongue *viz*., creamy-yellow. This fold frequently showed a brownish pigmentation on its oral surface, mainly at its basal mergence with the tongue and in the apical mid-region. On its pharyngeal surface, mottled pigmentation was often seen to be present over the breadth of the fold and progressed in small patches onto the pharyngeal floor, and on occasion, onto the laryngeal mound.

Light microscopy

Dorsal gular fold and roof of the pharyngeal cavity

Sagittal sections of the dorsal fold revealed a tapered, almost triangular structure with a broad base of attachment to the roof of the oral/pharyngeal cavity (Fig. 4A). At its base, the oral aspect of the fold demonstrated a sharp transition from the thin, lightly keratinised, stratified squamous epithelium of the palate to a thick, non-keratinised stratified squamous epithelium with prominent epithelial and connective tissue papillae. This transition was marked by the presence of large nodular accumulations of lymphoid tissue situated in the underlying connective tissue (Fig. 4C). At the point of transition between the two epithelial types, PAS-stained sections revealed the gradual accumulation of PAS-positive granules in the cells of the non-keratinised stratified squamous epithelium. These granules made their appearance in the more superficial layers of the stratum spinosum and extended to the surface of the epithelium. The granules in individual cells were initially relatively few in number but accumulated dramatically with increased distance from the point of transition. This phenomenon was accompanied by inclusion of almost the entire stratum spinosum in granule formation. Cells of the stratum basale were devoid of granules. The initial appearance and subsequent accumulation of granules demonstrated a distinct polarity, with the granules being positioned in the apical cytoplasm of the cells and forming a cap-like structure around the apical aspect of the nucleus. The granules were evenly distributed throughout the cytoplasm of the flattened, more superficial cells of the stratum corneum (Fig. 4D).

After a short distance, the epithelium was seen to thin and the surface cells adopted a more cuboidal appearance. In PAS-stained sections, isolated goblet cells were observed sandwiched between the PAS-

positive epithelial cells. Whether the goblet cells originated independently or through transformation of the epithelial cells, could not be determined. Continued thinning of the epithelium resulted in the formation of a typical respiratory epithelium which covered the remaining oral aspect as well as the tip and pharyngeal aspect of the dorsal fold. This epithelium was typically pseudo-stratified columnar in nature, densely ciliated and displayed a high concentration of goblet cells (Fig. 5D). Ciliation and the accumulation of goblet cells was accompanied by the appearance of large branched tubulo-alveolar, mucus secreting glands (Figs. 4A-C & 5A-C) which stretched deeply into the underlying connective tissue. Some of the branched tubular portions of the glands demonstrated coiling or spiralling. The ducts of the glands generally opened into the base of relatively deep epithelial folds and a distinct demarcation between the ciliated surface epithelium and the non-ciliated duct lining cells could be observed. The secretory portion of the glands, as well as the duct system, were lined by a single layer of columnar cells with basally compressed nuclei (Fig. 4B). The lumen of the glands was very wide. The cytoplasm of the lining cells was filled with mucigen granules and stained PAS-positive (Figs. 4A & 5A-C). The mucus-secreting glands were found throughout the dorsal fold but appeared to be larger and more numerous towards the lateral aspects. The glands lining the pharyngeal surface of the fold were confined to a narrow zone immediately beneath the epithelium and did not extend as deeply into the underlying connective tissue as the glands lining the oral aspect of the fold (Fig. 4A). Scattered between the glands were diffuse and nodular accumulations of lymphoid tissue. This tissue was confined to the supporting connective tissue beneath the basement membrane and generally, with the exception of occasional individual cells, did not appear to infiltrate the respiratory epithelium.

The supporting tissue of the dorsal fold consisted of irregular dense connective tissue. Due to the absence of a muscularis mucosae, no clear distinction could be made between a lamina propria and submucosa. However, the connective tissue immediately beneath the epithelium was more compactly arranged and could be readily distinguished from the more loosely arranged tissue of the deeper regions. A large vascular complex, originating from the base of the fold, supplied the core of the fold and a smaller superficial plexus was present in the lamina propria, particularly in and around the glands and immediately beneath the epithelium. Blood vessels were observed to penetrate between the alveoli via connective tissue septae (Fig. 4B). Non-myelinated nerves were seen to accompany the blood vessels. In some sections a scattering of melanocytes was observed in the region of the basement membrane, particularly on the oral surface.

The roof of the pharynx could be divided into two distinct regions based on histological features. The peripheral areas of the roof continuous with the walls of the pharynx, the dorsal fold and the entrance to the

oesophagus displayed the typical respiratory epithelium described on the dorsal fold. The supporting connective tissue was also similar in structure and basic organisation to that of the dorsal fold. In some sections, however, large lymphatic vessels were observed in the deeper connective tissue layer. A second region occupied the medial aspect of the pharyngeal roof caudal to the opening of the Eustachian tubes and revealed a complex arrangement of mucosal folds and deep intervening clefts. The primary folds displayed secondary and tertiary branching and were supported by a richly vascularised connective tissue core (Fig. 13C). The mucosa was characterised by large accumulations of lymphoid tissue, forming a typical pharyngeal tonsil. The arrangement of the lymphoid tissue on either side of some mucosal clefts resulted in the formation of prominent tonsillar crypts (Fig. 13C). In most instances, the lymphoid tissue was observed to infiltrate the overlying respiratory epithelium, obliterating the regular arrangement of this tissue. The ciliated surface cells of the respiratory epithelium ended abruptly at the periphery of areas of lymphocytic infiltration and it appeared as if some lymphocytes were exposed at the epithelial surface. PAS-stained sections, however, revealed that only a thin layer of surface epithelial tissue, not infiltrated by lymphocytes covered the lymphoid nodules (see inset, Fig. 13C). This region was divided along the midline by a tract of smooth mucosa discussed earlier (see above). The mucosal tract was covered by respiratory epithelium and the underlying connective tissue displayed a longitudinally positioned band of striated muscle, presumably to control the opening and closing of the Eustachian aperture.

Ventral gular fold and floor of pharyngeal cavity

The ventral fold of the gular valve differed in shape in sagittal section depending on the degree of extension of the structure above the floor of the oral cavity at the time of fixation. In the extended position the fold was a slender, tapered structure which was intimately associated with the base of the tongue on its oral aspect and continuous with the floor of the pharyngeal cavity on the pharyngeal aspect (Figs. 1 & 6A). The highly folded non- to lightly keratinised stratified squamous epithelium covering of the tongue was continued onto the oral surface of the fold. This epithelium was relatively thin and generally consisted of between four to six layers of cells. At a variable distance from the base of the fold this epithelium was observed to thicken appreciably, although it remained non- to lightly keratinised in nature (Fig. 6B). In PAS-stained sections this transition was marked by the presence of PAS-positive granules within the cells. The progressive accumulation of these granules within the epithelial cells with increased distance from the point of transition, as well as their specific intra-cytoplasmic orientation, was similar to that described in the dorsal fold (see Fig. 4D). The epithelium displaying mucus transformation was continued over the tip of the ventral fold and

extended over approximately one third to half of the pharyngeal surface. At this point isolated goblet cells were observed between the PAS-positive epithelial cells. As in the dorsal fold the goblet cells rapidly increased in number and were seen to be associated with ciliated columnar elements of the stratified epithelium. Progressive thinning of the epithelium resulted in the formation of a typical respiratory epithelium. The accumulation of goblet cells coincided with the appearance of shallow transverse epithelial grooves. These grooves were generally lined by masses of goblet cells, creating the appearance of intra-epithelial glands (Fig. 6C). In some sections the orientation and positioning of the grooves created intervening epithelial ridges which appeared palmate or leaf-shaped in cross-section. Coiled tubular, mucus secreting glands were associated with the base of some of the epithelial folds. The glandular tissue was confined to the region immediately beneath the epithelium owing to the dense nature of the supporting connective tissue. Towards the base of the fold on the pharyngeal aspect (where the supporting tissue was more loosely arranged) the glands were larger and more complex with coiling and branching being observed. The features of the glandular tissue were similar to those observed in the dorsal fold.

The core of the fold was formed by a tapered hyaline cartilage representing the apical part of the basihyoid cartilage (Fig. 6A). The cartilage was surrounded by a thick perichondrium composed of a sheet of regular dense connective tissue. Between the perichondrium and the epithelium was a less compactly arranged layer of regular dense connective tissue which displayed numerous blood vessels and some non-medullated nerves situated between bundles of parallel-oriented collagen fibres (Fig. 6C). The connective tissue beneath the epithelium was similarly arranged but appeared more cellular in nature, although in some sections it presented as a region of irregular dense connective tissue. A well-developed vascular plexus lay immediately beneath the epithelium (Fig. 6B) and surrounded the glandular tissue. The ventral fold contained very little lymphoid tissue although diffuse patches and the occasional nodule were present towards the base on the pharyngeal aspect, particularly in the region of glandular tissue. Groups of melanocytes were also observed beneath the epithelium on either aspect of the fold.

At the lateral extremities of the ventral fold the non-keratinised stratified squamous epithelium extended further along the pharyngeal aspect before transforming into respiratory epithelium. The supporting connective tissue in this part of the fold also contained large lymphatic vessels and was, in parts, more loosely arranged than in more medially positioned segments of the fold.

The floor of the pharyngeal cavity was exclusively lined by respiratory epithelium. Cross sections of the laryngeal mound (Figs. 7B, C & 8A) revealed a relatively thick respiratory epithelium containing masses of goblet cells lining the pharyngeal surface. The goblet cells were often grouped into units forming typical intra-epithelial glands (Figs. 7B, C & 8A, C). Numerous shallow, longitudinal epithelial folds were present with intra-epithelial glands generally lining the base of the folds. Simple tubular (occasionally coiled) mucus-secreting glands were observed to open at the base of some of the deeper folds (Figs. 8A & B). The respiratory epithelium continued over the lips of the glottis but thinned markedly on the actual surface of the glottis, forming, in parts, a thin, three-cell layer-thick respiratory epithelium devoid of intraepithelial glands or mucus-secreting glands. This particular arrangement of the epithelium and glandular tissue was particularly apparent in the central part (middle) of the glottis (Fig. 8A). The lining of the rostral and caudal aspects of the glottis (including the caudal laryngeal fissure), however, revealed a relatively thick respiratory epithelium and associated intraepithelial and mucus-secreting glands (Fig. 7B). The epithelial lining of the laryngeal mound was supported by a thick, compact sheet of irregular dense connective tissue. Numerous nodular and diffuse lymphoid accumulations were situated in this layer but did not, with the exception of occasional individual lymphocytes, penetrate into the overlying epithelium. A large vascular plexus occupied the deeper layers of the supporting connective tissue and a second plexus of smaller vessels was intimately associated with the epithelial lining. The laryngeal wall was supported by laryngeal cartilages (hyaline) and a striated laryngeal musculature (Figs. 7D & 8A). The connective tissue supporting the lips of the glottis was loosely arranged and more cellular in nature than that found in other parts of the laryngeal mound and displayed no lymphoid tissue.

The lining of the rostral fissure (sulcus) was characterised by arrays of closely packed, oblique and longitudinal mucosal folds. The oblique folds were concentrated on the upper (dorsal) half of the fissure, whereas the longitudinal folds occupied the deeper (ventral) part (Fig. 7D). The epithelium was similar in nature to the lining of the pharyngeal surface of the laryngeal mound, but was thinner and practically devoid of underlying mucus secreting glands (Fig. 7B). No laryngeal cartilages were present and the space between the compact sub-epithelial connective tissue and the perichondrium of the basihyoid cartilage was filled with a loosely arranged irregular dense connective tissue.

Dorsal gular fold and roof of the pharynx

Due to the presence of the median apical notch (Figs. 2D, 3A & 10A) the pattern of mucosal folds on the oral surface of the dorsal gular fold showed evidence of bilateral symmetry. Stereomicroscopy of the samples prepared for SEM revealed basic features similar to those identified macroscopically, i.e., a series of longitudinal mucosal folds extending from the apex of the fold to its base, and a further series of transverse (horizontal) mucosal folds situated at the base. The longitudinal mucosal folds displayed regional peculiarities. At the lateral extremities of the dorsal fold where it merged with the corners of the mouth, the longitudinal mucosal folds were obliquely arranged in a compact group (Fig. 9A). Individual folds were relatively narrow, occasionally branched and anastomosed and were separated by deep intervening clefts (Figs. 9A & B). Higher magnification SEM-imaging of this area showed a complex system of smaller mucosal folds situated on the floor of the clefts and which emanated from the deeper aspects of the primary folds. The smaller folds emerged at an angle from the primary folds and branched and anastomosed, forming an intricate network which enclosed numerous small openings (Fig. 9B). This entire region, including all the aspects of the mucosal folds, was densely ciliated (Fig. 9D) although a reduction in density was observed towards the base of the dorsal fold (Fig. 9C). Between this region and the median apical notch was a series of between 3 to 5 equally spaced, deep longitudinal grooves which divided this area into a number of broad folds (Figs. 3A, B & 9A). SEM-imaging revealed that the sides of these folds (the walls of the grooves) were adorned with smaller folds which branched and anastomosed (Fig. 10C). The longitudinal folds varied in length and generally extended from the smooth, rounded apex of the dorsal gular fold to the region of transverse folds where they ended abruptly (Fig. 9A).

A clear distinction could readily be made between the lining of the palate and that of the oral surface of the dorsal gular fold. At low magnification the surface of the palate adjacent to the dorsal fold was seen to consist of a series of transverse folds and numerous oblique folds, giving this area a cobbled appearance (Figs. 11B & E). The epithelium of the palate showed a high degree of cell sloughing (Figs. 11B & E). This was confirmed by LM which indicated that the epithelium was lightly keratinised. The epithelial cells varied in shape, but were generally polygonal in outline. The surface of the cells had a honeycomb appearance with little indication of characteristic surface projections such as microvilli. There was an abrupt transition

between the surface of the palate and the surface of the dorsal fold which, although it also consisted of delicate transverse folds, appeared smooth (Figs. 11A & B). Individual cells were more clearly defined and a limited degree of cell sloughing was evident. Desquamating cells were scale-like in appearance (Fig. 11D) and also displayed a honeycomb appearance at higher magnification (Fig. 10D).

Bordering the region of smooth epithelium was a zone of fine, transverse epithelial folds, characterised by the presence of ciliated cells, goblet cells and epithelial cells bearing microvilli (Figs. 11A & C). The transition between the two regions appeared gradual in histological preparations, but showed an abrupt transition when viewed by SEM (see Fig. 11A). The surface cell composition of this region varied between the specific part of the fold being examined and between different specimens. However, the general tendency was for ciliated cells to concentrate on the lateral aspects of the fold and to thin markedly towards the median notch. This phenomenon was also obvious on the apical ridge of the fold.

The region in the vicinity of the median notch was dominated by dome-shaped epithelial cells and also showed signs of cellular erosion. Very few ciliated cells were observed. Numerous large cavities which formed clusters were also observed in this region (Figs. 10A & B). The cavities were considered to represent gland duct openings and were often filled with debris or mucus.

The pharyngeal surface of the dorsal fold displayed numerous longitudinal and oblique mucosal folds, with a dramatic increase in number being obvious at the lateral extremities of the fold. A series of deep mucosal folds converged from the base of the median notch towards the midline and extended to the base of the dorsal fold (Fig. 12A). These folds typically branched and anastomosed. At the median apical notch there were similar signs of erosion to that seen on the oral surface. The epithelial cells in this area were dome-shaped and were covered by short microvilli. Numerous pore-like openings (Figs. 12A & B), which were normally surrounded by ciliated epithelium, appeared singly or in groups. Ciliation was evident in the vicinity of the median notch and progressively increased in density towards the lateral aspects of the fold. Goblet cells were associated with the ciliated cells (Figs. 12B & D). In the densely ciliated mid- to extreme lateral regions of the fold, occasional non-ciliated cellular eruptions, which may have been associated with deeper lying lymphoid tissue, were observed. Small mucus-like droplets on the apical surface indicated that these were probably goblet cells (Fig. 12D).

The mucosal folds situated on the roof of the pharyngeal cavity were longitudinally oriented, although in the vicinity of the common opening of the Eustachian ducts and the internal nares they curved medially to form complete and incomplete U-shaped structures (Figs. 2D & 13A). This phenomenon was particularly obvious rostral to the opening of the internal nares. The mucosal folds thus tended to follow the contours of the pharyngeal cavity. A smooth region (including the crescent-shaped structure located rostral to the opening of the Eustachian tubes – see Figs. 2D & 13A), which was devoid of folds, was present in the immediate vicinity of the opening of the internal nares. In addition to the ubiquitous ciliated cells observed throughout the roof of the pharynx, the smooth region demonstrated small patches of non-ciliated, polygonal cells with microvilli and prominent bordering microridges. These localised, non-ciliated areas became more conspicuous (increased in number) towards the base of the dorsal gular fold. The epithelium at the periphery of the internal nares and within its opening, was densely ciliated. The surface of the smooth crescent-shaped structure lying rostral to the opening of the Eustachian ducts was also densely ciliated. As noted above, the lateral areas of the roof, as well as a narrow, medially positioned tract of mucosa, demonstrated fine mucosal folds. The fine, longitudinal folds on the medial tract of mucosa were continued onto the plug of tissue sealing the common opening of the Eustachian tubes (Figs. 2D & 13A). Although fine, these folds displayed a high profile and were seen to branch and anastomose. Caudally, these folds merged with the series of laterally positioned folds to form a zone characterised by an increased number of folds of lower profile. This zone indicated the beginning of the oesophagus. The folds situated on the lateral borders of the smooth medial tract merged with the adjoining tonsillar region.

Sandwiched between the medial and lateral zones of fine mucosal folds were the two areas of deep folds identified by LM as tonsillar regions (Figs. 2D & 13A-D). SEM revealed the densely ciliated nature of the mucosal folds in this region and, in addition, identified localised areas of cellular specialisation (Figs. 13A & B). These specialised areas were ellipsoid in form and displayed little or no ciliation. Their boundaries were demarcated by densely ciliated epithelium and a number of cell profiles were obvious. Some cells presented a ruptured surface typical of mature goblet cells releasing their contents (Fig. 13D). These cells were generally surrounded by non-ruptured (intact) cells displaying microvilli and probably represented goblet cells in various stages of development (Fig. 13D). A number of rounded cell profiles characterised by numerous cell projections were also observed. Whether these represented lymphocytes or non-ciliated epithelial cells, could not be determined. Clusters of elongated, more flattened cells covered with short, stubby microvilli and occasional isolated groups of ciliated cells were

also typical features. These specialised areas represented the tonsillar nodules identified by LM (Fig. 13C).

Ventral gular fold and floor of the pharynx

Stereomicroscopy of samples of the ventral fold and floor of the pharynx prepared for SEM revealed basic features similar to those identified macroscopically (see above). The oral surface of the ventral fold displayed a series of relatively uncomplicated transverse mucosal folds which originated close to the base of the fold and stretched to the apex of the fold which appeared smooth and slightly rounded (Fig. 14A). The additional mucosal folds emanating from the caudo-lateral aspect of the ventral fold (see macroscopic description above) typically showed fine, vertical folds, particularly at their origin.

At low magnification a distinct and abrupt transition between the surface epithelium of the tongue and that of the oral surface of the ventral fold, was obvious (Figs. 14A & B). The surface of the tongue appeared cobbled and desquamating cells were observed. At the base of the ventral fold the epithelium showed a smooth transition zone (Fig. 14B) before being thrown into a series of fine to coarse horizontal folds (Figs. 14A & E). At higher magnification no variation in cell surface morphology could be observed between the various regions. All cells appeared polygonal in shape with individual cells studded with short, stubby microvilli, varying in density. Cells with a honeycomb surface appearance were also evident (Figs. 14C & D). Towards the apex of the fold, signs of cell sloughing became apparent. No ciliation was observed on the oral aspect of the ventral fold.

Stereomicroscopy and low magnification SEM confirmed that a series of U-shaped mucosal folds lined the floor of the pharyngeal cavity. The arms of the folds merged with the longitudinal folds of the oesophagus (Figs. 2B & 15A) while the apex of the fold curved around the rostral extremity of the pharyngeal floor and also ran transversely across the pharyngeal surface of the ventral gular fold (Fig. 15A). The folds, as in other parts of the pharyngeal cavity, remained relatively constant in width for a given area, but freely branched and anastomosed (Fig. 15B). Laterally, where the ventral fold merged with the additional folds at the corner of the mouth and pharynx, the folding pattern appeared complex.

Higher magnification SEM clearly revealed two types of epithelium covering the pharyngeal surface of the ventral fold. Non-ciliated cells occupied the apical region of the fold and also extended in a variably

wide band down the middle of the fold. The cells along the apical surface showed signs of erosion while the medially positioned cells had a slightly more rounded appearance (Fig. 15C) than those found on the oral surface of the fold. These cells, however, also displayed the short, stubby microvilli seen on the oral surface of the fold. The remaining surface of the fold was covered by a ciliated epithelium. The transition between the two cell types was gradual with ciliation becoming increasingly denser towards the base and sides of the fold. The densely ciliated epithelium, which was associated with the numerous goblet cells (Fig. 15D) continued onto the floor and walls of the pharyngeal cavity. The surface of the laryngeal mound was also exclusively lined by densely ciliated epithelium.

DISCUSSION

The pharyngeal cavity and associated gular valve of the crocodilia, including *C. niloticus*, have received little attention in the literature. The pharynx is mentioned briefly in some publications, generally in connection with descriptions of the upper respiratory tract, and simply glossed over in others. Gans (1976), for example, notes that in crocodilians, the trachea terminates “anteriorly at the closable glottis which lies on the floor of the posterior pharyngeal cavity” and that the “internal nares open at the top of a dome in the roof of the pharyngeal cavity”. In similar vein, Storer and Usinger (1961) point out that from “each tympanic cavity a Eustachian tube leads medially, the two having a common opening on the roof of the pharynx behind the internal nares”, whereas Chiasson (1962) mentions that the “glottis is the opening into the larynx from the pharynx”. Steel (1989) states that “the nasal passages are carried to the back of the throat, eventually opening into the pharynx behind the slit-like glottis and the basihyal valve, immediately above the windpipe”. Evans (1986) simply notes that the caudal boundary of the oral cavity (the dorsal and ventral components of the gular valve) “can be constricted to occlude the nasopharynx” while Pooley and Gans (1976) remark that “the mouth of the crocodile can be completely isolated from the pharynx by the gular fold.”

As far as could be ascertained, none of the earlier literature describes the gross anatomy of the crocodilian pharyngeal cavity and even more recent publications make scant reference to this region. Although he discusses the structure of the palate of the adult American alligator, Ferguson (1979) fails to mention the pharynx, stating only that the “basihyal” (gular) valve, “together with the extensive secondary palate, enables the Alligator to isolate its mouth from the nasal passages, trachea and oesophagus.” Grigg and Gans (1993) note that food is generally picked up near the tip of the jaws and then “repositioned and shifted toward the oesophagus”. They also briefly describe the mechanism of

ventilation and the movement of the glottis "into close proximity to the internal nares", and that during ingestion or the swallowing of food, "the glottis is closed and depressed and the palatal flap opened". Luppa (1977) is equally silent on the existence of a pharynx, reporting only that the oesophagus (and the entrance to the trachea) is separated from the oral cavity by the dorsal and ventral folds of the gular valve. The comprehensive study of the reptilian digestive tract by Parsons and Cameron (1977), although containing topographical and gross anatomical information, starts from the oesophagus. This lack of information on the structure of the crocodilian pharynx stems, at least in part, from the view that the digestive tract in this group of animals "starts just beyond the entrance to the trachea." (Pooley and Gans, 1976).

The present study not only confirmed the presence and positioning of pharyngeal structures like the internal nares and common opening of the Eustachian tubes, but also revealed for the first time the anatomical complexity of the region and the specialisation of the mucosal lining. Important features identified during this study included the valve-like structure at the common entrance to the Eustachian tubes and the region of tonsillar tissue in the roof of the pharynx. It has been proposed that the valve-like structure, which functions as a "ball-valve", be termed the "dorsopharyngeal valve" (F.W. Huchzermeyer, personal communication, 2002). Furthermore, the longitudinal, highly folded nature of the mucosa allows for expansion (as is the case in the oesophagus – see Chapter 4) of the region during swallowing of large chunks of food.

The isolating structure between the oral and pharyngeal cavities occurs in the form of dorsal and ventral folds, which together create a valve-like structure. When the folds are in close association with each other they form a closure or seal which effectively isolates the internal nares, the opening to the trachea (glottis), the opening to the Eustachian ducts and the entrance to the oesophagus from the oral cavity. The valve is functional when the animal is semi-submerged in water with its valved external nares above the surface of the water. This is made possible by the fact that the nasal passage extends along the full length of the snout, from the external nares to the internal nares situated on the roof of the pharynx in close proximity to the raised glottis. This successful structural adaptation of the Crocodilia is also described by Romer (1966) who emphasises that the development and caudal elongation of a secondary palate made this adaptation possible.

In the Crocodilia the gular valve has frequently been mentioned in descriptions pertaining to feeding habits (Pooley and Gans, 1976; Ferguson, 1979), respiration (Romer, 1966; Bellairs, 1969; Gans, 1976; Ferguson, 1979; Evans, 1986; Buffetaut, 1989) and the alimentary canal (Gans, 1976; Pooley and Gans, 1976; Evans, 1986). However, there is a distinct inconsistency regarding the terminology used to describe this structure. This situation is further complicated by the fact that some papers refer to components of the gular valve individually while others refer to the combined structure. The dorsal component of the valve has been described by Taguchi (1920) as “a dorsal velum"; by Chiasson (1962) as "the velum palatinum, two large transverse folds from the palate between the oral cavity and pharynx”; by Bellairs (1969) as “A flap or valve of soft tissue”; by Gans (1976) as "a shorter fold, descending from the cranial floor"; by Evans (1986) as “the palatine velum”; by Steel (1989) as "a valve-like glottis (velum palati, or palatal valve)”; by Mazzotti (1989) as "a fleshy fold at the back of the palate" and by Grigg and Gans (1993) as "a palatal flap".

The ventral component has been referred to by Chiasson (1962) as "a transverse fold from the base of the tongue"; by Bellairs (1969) as “the basihyal valve, which projects upwards from the floor of the mouth in front of the glottis” (Bellairs further refers to the ventral fold as “ the muscular basihyal valve”); by Pooley and Gans (1976) as “a gular fold"; by Gans (1976) as "a transverse fold which projects from the floor of the mouth"; by Evans (1986) as "a transverse fold at the base of the tongue"; by Steel (1989) as "the ventral basihyal valve, a muscular structure at the back of the tongue" and by Mazzotti (1989) as "a fleshy fold on the tongue".

Both dorsal and ventral components, as a unit, are referred to by Fuchs (1908, cited by Barge, 1937), as "choanal folds" and "the palatopterygoid folds"; by Gans (1976) as "pharyngeal folds"; by Buffetaut (1989) as "a throat valve"; by Grigg and Gans (1993) as "the palato-buccal valve" and by Pooley and Gans (1976) as “the gular fold, a tissue that can rise from the floor of the mouth to overlap a bony fold on the roof of the mouth” and by Ferguson (1979) as “a system of muscular flaps - the basihyal valve". Romer (1966) simply notes that the throat can be “closed off by a flap of skin.”

It is suggested in the present study that, for simplicity, the structure isolating the oral cavity from the pharyngeal cavity be termed the gular valve, based on the Latin word for throat, “gula” and that the individual components be called the dorsal and ventral folds, respectively. Buffetaut (1989) used a similar term for this structure, referring to it as "a throat valve". The individual dorsal and ventral components should

certainly not be referred to as valves (Bellairs, 1969; Steel, 1989), as it is only when the two structures function together that they constitute a valve.

Chiasson's (1962) description of the dorsal fold (velum palatinum) of the alligator as "two large transverse folds from the palate" is misleading. Although the presence of a median apical notch in the dorsal fold creates the impression of a divided fold (two folds), the notch is shallow (at least in the Nile crocodile) and the fold is continuous. Photographs of the oral cavity of the alligator (Mazzotti, 1989) would seem to confirm this observation. It would be interesting to determine whether the fold originates embryologically as twin structures which meet at the midline.

Ferguson (1979) refers to the gular valve as "a system of muscular flaps" while Steel (1989) describes the ventral fold as "a muscular structure at the back of the tongue". In the Nile crocodile, neither the dorsal nor ventral components of the gular valve revealed any muscular tissue. The closest muscular tissue to the folds were striated elements of the lingual musculature situated at the base of the tongue where it abuts the ventral fold. The dorsal fold can thus be regarded as a passive structure as it appeared not to be influenced by muscular activity and was simply a large tissue fold attached to the bony palate. Bellairs (1969) also confirmed the absence of muscular tissue in the dorsal fold of crocodilians, but stated that there was a muscular "basihyal valve" which "can be thrust up in front of it (the palatal valve) so that the two form an effective partition between the mouth and the pharynx". Although the ventral fold itself is not a muscular structure it would, as part of the hyoid apparatus, and due to its association with the base of the tongue, be controlled by combined or individual muscle activity. It should be noted, however, that Taguchi (1920) describes a striated muscle in the submucosa of the dorsal gular fold in *C. porosus* which he suggests is equivalent to the *musculus pharyngo-palatinus* of higher animals. There is thus some evidence to suggest that species differences between crocodilians exist. Mazzotti (1989) terms the ventral fold "a fleshy fold on the tongue". It was clear from the present study, however, that the ventral fold formed a rigid yet flexible structure as it was internally supported by the rostral aspect of the basihyal plate which formed a hyaline cartilage core.

LM examination revealed that the base of the oral surface of the dorsal and ventral folds of the gular valve was covered by a lightly keratinised squamous epithelium which abruptly transformed into a thicker stratified squamous epithelium. This epithelium, in turn, displayed a progressive transformation to a mucus producing epithelium. This phenomenon was described by Taguchi (1920), who used the term

"Schleimmetamorphose", or mucus metamorphosis to describe the transition zone in two of the crocodilian species he examined, *viz.*, *Crocodylus niloticus* and *Alligator sinensis.* Luppa (1977) also described a similar transition of epithelium in the oral cavity of the lizard *Lacerta agilis*, but avoided using the term mucus transformation. In the present study, the ventral fold displayed this type of transformation on its oral surface, over its apex and onto the pharyngeal surface, whereas it was restricted only to a specific zone on the oral surface of the dorsal fold. Taguchi (1920) notes that the region of "mucometamorphosis" in *A. sinensis* and *C. niloticus* occurs on the lower surface (floor) of the pharynx, but makes no mention of a similar phenomenon in *C. porosus*. In this study it was shown that the region of mucus transformation extended a considerable distance along the pharyngeal surface of the ventral gular fold which, to a certain extent, agrees with Taguchi's (1920) observations.

The transformation of a stratified epithelium into a mucus-producing epithelium is certainly an exceptional occurrence in the pharynx (gular valve) of the Nile crocodile. However, earlier studies on man and the monkey (Wislocki, Fawcett, & Dempsey, 1951) have demonstrated that stratified squamous epithelia (particularly mucus membranes) are capable of producing mucopolysaccharides.

In cited literature, no SEM or stereomicroscopic study of the crocodilian pharyngeal cavity is mentioned. It was thus not possible during this study to make comparative comments regarding structures or features seen using these forms of microscopy. The SEM study however confirmed much of what was observed using LM. This was illustrated in Figs. 11A - E where the transition of epithelium on the oral surface of the dorsal fold of the gular valve was seen to progress from the lightly keratinised nature of the palate epithelium to a smoother non-keratinised epithelium and the almost abrupt transition to a glandular epithelium displaying goblet cells and ciliated cells. Stereomicroscopy also gave an insight into the surface features of the folds of the gular valve and that of the entire pharyngeal cavity. Stereomicroscopy further served as an intermediary between LM and SEM and provided gross morphological information not obtainable by SEM due to the wider optical field of the stereomicroscope. It was also found convenient while viewing with SEM to have stereomicrographs available for orientation purposes.

SEM also clearly revealed the extent of ciliation in the pharyngeal cavity of the Nile crocodile. With the exception of restricted areas on the pharyngeal surface of the dorsal and ventral components of the gular valve and in the tonsillar region, the entire surface of the pharyngeal cavity and the pharyngeal aspect of the gular valve, was densely ciliated. Taguchi (1920) describes ciliation on the pharyngeal

surface of the dorsal gular fold [Taguchi (1920) used the term “des Gaumensegels” which literally means “palate sails” (F.W. Huchzermeyer, personal communication, 2002) and it must be assumed that here he is referring to the dorsal fold of the gular valve or, as Taguchi (1920) also applied the term, the dorsal velum (“velum” is Latin for sail)] and on the floor of the pharynx in *C. porosus*, ciliation only in the region of the laryngeal opening in *A. sinensis* and ciliation on the pharyngeal surface of the dorsal gular fold and at the entrance to the larynx in *C. niloticus*. This discrepancy between ciliation in the pharynx of *C. niloticus* in this study and the data of Taguchi (1920) in the same species, may be due to the limited information provided by a histological study as opposed to the greater overall view provided by SEM. Furthermore, the existence of a number of subspecies (the place of collection of Taguchi’s specimens is unknown) could contribute to the above discrepancies. It should also be noted that Taguchi (1920) only studied a total of five specimens of the three species and that no indication of their age is provided.

Another important feature of the pharynx of the Nile crocodile was the immense potential for mucus production, in the form of goblet cells and mucus-secreting glandular tissue. All of the pharyngeal surfaces examined, including those of the dorsal and ventral components of the gular valve, displayed arrays of goblet cells. SEM of the ciliated epithelium which lined most of the pharyngeal cavity also revealed masses of goblet cells (some actively secreting) interspersed between the ciliated cells (see Figs. 11C & 15D). Mucus production by the goblet cells was further enhanced by the formation of intraepithelial glands (see Figs. 6C, 8A & C). These structures were prominent on the floor of the pharyngeal cavity and on the pharyngeal surface of the ventral gular fold. Numerous mucus-secreting glands were also present throughout the pharyngeal cavity, being particularly obvious on both surfaces of the dorsal gular fold (see Figs. 4A & 5A-C) where they formed large, branched tubulo-alveolar glands. The various mucus-producing structures observed in the present study were also described by Taguchi (1920) in the three crocodilian species investigated. It would appear as if crocodiles require large amounts of lubricant to assist in the swallowing of food, as it has been documented (Pooley and Gans, 1976, Grigg and Gans, 1993) that crocodiles do not chew their food, but swallow pieces, torn off large prey, whole.

It is difficult to explain why a region which would obviously be subject to a great deal of wear and tear during the ingestion of food, should be almost exclusively lined by a ciliated epithelium. It could be argued that the cilia are necessary to retain a constant layer of surface mucus as a lubricant or to move the excess mucus towards the oesophagus during the lengthy fasting periods of the animals.

In Taguchi's (1920) examination of three crocodilian species he encountered a sparse distribution of taste receptors on the oral and pharyngeal surfaces of the dorsal fold and on the floor of the pharynx. In his specimens of the Nile crocodile however, no receptors were seen on the dorsal fold (oral or pharyngeal surfaces) of the gular valve, although five such receptors were noted on the floor of the pharynx ("Unterfläche des Pharynx") and only a single receptor in the cranial region of the oesophagus. In this study, structures resembling taste receptors were observed in the oral cavity and which fitted the description of those described by Bath (1905) and Taguchi (1920) – (see Chapter 2). Although numerous histological sections and gross specimens were examined using LM, SEM and stereomicroscopy, none of these forms of microscopy, as used in this investigation, revealed any structures resembling taste receptors in the pharyngeal region.

The dorsal surface of the pharyngeal cavity could be divided into two distinct regions based on histological features. Peripheral areas of the roof continuous with the walls of the pharynx, the dorsal fold and the entrance to the oesophagus, as well as a median tract of smooth mucosa, displayed typical respiratory epithelium. A second region occupied the medio-lateral aspect of the pharyngeal roof caudal to the opening of the Eustachian tubes and revealed complex mucosal folds with deep intervening clefts. The mucosa was characterised by large accumulations of lymphoid tissue, forming a typical pharyngeal tonsil. With the exception of a reference to a tonsillar region in the pharynx of *C. niloticus* during a study employing histoenzymology by Arvy and Bonichon (1958), no record of tonsillar tissue has been made in any of the cited literature. This region was also not described by Taguchi (1920). This study clearly revealed the extent of the tonsillar region in the Nile crocodile, but to what extent a similar region is present in other crocodilian species is unknown. However, the illustration and description of swollen tissue in a young crocodilian (no species mentioned) by Youngprapakorn, Ousavaplangchai and Kanchanapangka (1994), which may in fact indicate a "tonsillitis", points to the clinical importance of this tonsillar tissue in the pharynx of Crocodilia. Youngprapakorn, *et al*. (1994) identified the condition in this young specimen as "rhinopharyngitis".

Taguchi (1920) also described the presence of "Holl's glandular apparatuses" (Hollschen Drüsenapparaten – Holl, 1888) in the pharynx of the three species he examined. In this investigation "Holl's glandular apparatuses" were assumed to be the well developed and widely distributed intra-epithelial glands (Figs. 8A & C) seen in histological section. Although differing marginally in their distribution, and assuming that "*K. vulgaris*" represents the Nile crocodile, the epithelial types (and associated glandular and supporting tissues) described by Taguchi (1920) generally agreed with the observations of the present study.

The larynx manifests itself in the form of a prominent laryngeal mound which occupies much of the floor of the pharynx. In this study it was seen to be raised above the floor, as it is in birds. Detailed reviews and informative anatomical descriptions of the oral and pharyngeal cavities in *Gallus domesticus* (*Gallus gallus* [*var. domesticus*]) have been given by Calhoun (1933) and in other avian species by White (1975) and McLelland (1979, 1989). The laryngeal mound (*mons laryngealis*) (White, 1975; McLelland, 1979, 1989) in the domestic fowl is heart-shaped, displays medial and caudal papillae and projects into the pharyngeal cavity as a mound. There are also visible openings to lateral and caudal salivary glands, the so-called cricoarytenoid glands of Calhoun (White 1975). In the young (ca. 2.5 - 3 year-old) Nile crocodile the laryngeal mound was similarly elevated to that found in birds, but it was almond-shaped or ovoid and did not have papillae or macroscopically visible salivary gland openings as in the domestic fowl (McLelland, 1989). Furthermore, the laryngeal sulcus or laryngeal fissure (*sulcus laryngis*) (White, 1975) which occurs in birds was also seen to occur in the Nile crocodile. In addition, a short rostral sulcus was present at the tip of the laryngeal mound, an additional feature which has not previously been reported.

It should be emphasised that the results obtained from this study reflect the morphology of relatively young (sub-adult) animals of between 2.5 – 3 years of age. Crocodiles only attain sexual maturity at approximately 12 - 15 years of age and therefore the measurements presented in this chapter would obviously only be valid for younger specimens. It is, however, unlikely that the basic structure of the tissues examined would change appreciably with age (J.T. Soley, personal communication, 2002).

Artifacts in most forms of microscopy are inevitable, whether they result from fixation, dehydration, embedding or staining. The waiting period of 45 minutes prior to fixation of specimens for any form of microscopy used in this investigation became mandatory in the abattoir. This was necessary to enable the carcasses to overcome the post mortem tremor phase. As the animals were slaughtered for their skins, any sudden reflex movement by the carcass during the skinning process might have caused a nick or cut to the skin, thus reducing its market value. Certain artifacts may therefore have been inadvertently introduced in the tissue samples examined.

Shrinkage after any form of drying is a factor which has to be considered when describing biological structures. Although every attempt was made to limit shrinkage during the processing of specimens, it would appear as if certain features were adversely affected by the drying process. In Fig. 13A, for example, the fibrous plug which seals the common opening of the Eustachian tubes has shrunk away from the opening, leaving an artificial gap.

REFERENCES

ARVY, L. & BONICHON, A. 1958. Contribution a l'histoenzymologie de *Crocodylus niloticus* Laurenti. *Zeitschrift für Zellforschung*, 48:519-535.

BARGE, J.A.J. 1937. Mundhöhlendach und Gaumen, in *Handbuch der vergleichenden Anatomie der Wirbeltiere,* edited by L. Bolk, E. Göppert, E. Kallius and W. Lubosch. Berlin and Vienna: Urban and Schwarzenberg: Volume 3:29-48.

BATH, W. 1905. Über das Vorkommen von Geschmacksorganen in der Mundhöhle von *Krokodilus niloticus* Laur. *Zoologischer Anzeiger*. 29:352-353.

BELLAIRS, A. d'A. 1969. The life of reptiles. The Weidenfeld and Nicolson Natural History. London. Volume 1:234-239.

BUFFETAUT, E. 1989. Evolution, in *Crocodiles and alligators*, edited by C.A. Ross and S. Garnett. London: Merehurst Press: 26-41.

CALHOUN, M.L. 1933. The microscopic anatomy of the digestive tract of *Gallus domesticus*. Reprinted from: *Iowa State College Journal of Science,* 7:261-382.

CHIASSON, R.B. 1962. *Laboratory anatomy of the alligator*. Dubuque, Iowa: WM.C. Brown Company Publishers. 3-38.

EVANS, H.E. 1986. Introduction and anatomy, in *Zoo and Wild Animal Medicine*, 2nd ed., edited by M.E. Fowler. Morris Animal Foundation, Denver: W.B. Saunders Company: 109-132.

FERGUSON, M.W.J. 1979. The American alligator (*Alligator mississippiensis*): A new model for investigating developmental mechanisms in normal and abnormal palate formation. *Medical Hypotheses*, 5:1079-1090.

GANS, C. 1976. Ventilatory mechanisms and problems in some amphibious aspiration breathers (*Chelydra, Caiman* – Reptilia), in *Respiration in Lower Vertebrates*, edited by G.M. Hughes. New York: Academic Press: 357-374.

GRIGG, G.C. & GANS, C. 1993. Morphology and physiology of the crocodilia, in *Fauna of Australia - Amphibia and Reptilia*, edited by C.J. Glasby, G.J.B. Ross and P.L. Beesley. Canberra: Australian Government Publishing Service: Volume 2A:326-336.

HOLL, M. 1888. Zur Anatomie der Mundhöhle von *Lacerta agilis*. *Sitzungberichte der Kaiserlichen Akademie der Wissenschaften*: Wien Akademie 3:(96):161-169.

LUNA, L.G. (Ed.) 1968. *Manual of histologic staining methods of the armed forces institute of pathology.* 3rd ed., American Registry of Pathology. New York: McGraw-Hill Book Company.

LUPPA, H. 1977. Histology of the digestive tract, in *Biology of the Reptilia*, *Morphology E*, edited by C. Gans, and T.S. Parsons. London: Academic Press: Volume 6:225-313.

MAZZOTTI, F.J. 1989. Structure and function, in *Crocodiles and alligators*, edited by C.A. Ross and S. Garnett. London: Merehurst Press: 42-57.

McLELLAND, J. 1979. Digestive system, in *Form and function in birds*, edited by A.S. King and J. McLelland. London: Academic Press: Volume 1:69-73.

McLELLAND, J. 1989. Larynx and trachea, in *Form and function in birds*, edited by A.S. King and J. McLelland. London: Academic Press. Volume 4:69-71.

PARSONS, T.S. and CAMERON, J.E. 1977. Internal relief of the digestive tract, in *Biology of the Reptilia*, *Morphology E*, edited by C. Gans, and T.S. Parsons. London: Academic Press: Volume 6:159-223.

PEARSE, A.G.E. 1985. *Histochemistry. Theoretical and applied*. *Analytical technology*. 4th ed. Volume 2, New York: Churchill Livingston.

POOLEY, A.C. and GANS, C. 1976. The Nile crocodile, *Scientific American*, 234:114-124.

ROMER, A.S. 1966. *Vertebrate paleontology*. 3rd ed. Chicago: The University of Chicago Press: 102-111.

STEEL, R. 1989. Anatomy of a living fossil, in *Crocodiles*. London: Christopher Helm: 12-36.

STORER, T.I. & USINGER, R.L. 1961. *Elements of zoology*. 2nd ed. New York: McGraw-Hill Book Company, Inc.: 376-380.

TAGUCHI, H. 1920. Beiträge zur Kenntnis über die feinere Struktur der Eingeweideorgane der Krokodile. Mitteilungen aus der Medizinischen Fakultät der Kaiserlichen Universität zu Tokyo. 25:119-188.

WHITE, S.S. 1975. Larynx, in *Sisson and Grossman's The anatomy of the domestic animals,* 5th ed., edited by R. Getty. Philadelphia: W.B. Saunders Company: Volume 2:1891-1897.

WISLOCKI, G.B., FAWCETT, D.W. & DEMPSEY, E.W. 1951. Staining of stratified squamous epithelium of mucous membranes and skin of man and monkey by the periodic acid-Schiff method. *Anatomical Record*, 110:359-375.

YOUNGPRAPAKORN, P., OUSAVAPLANGCHAI, L. & KANCHANAPANGKA, S. 1994. *A colour atlas of diseases of the crocodile*. Thailand, Style Creative House Co., Ltd.: 19.

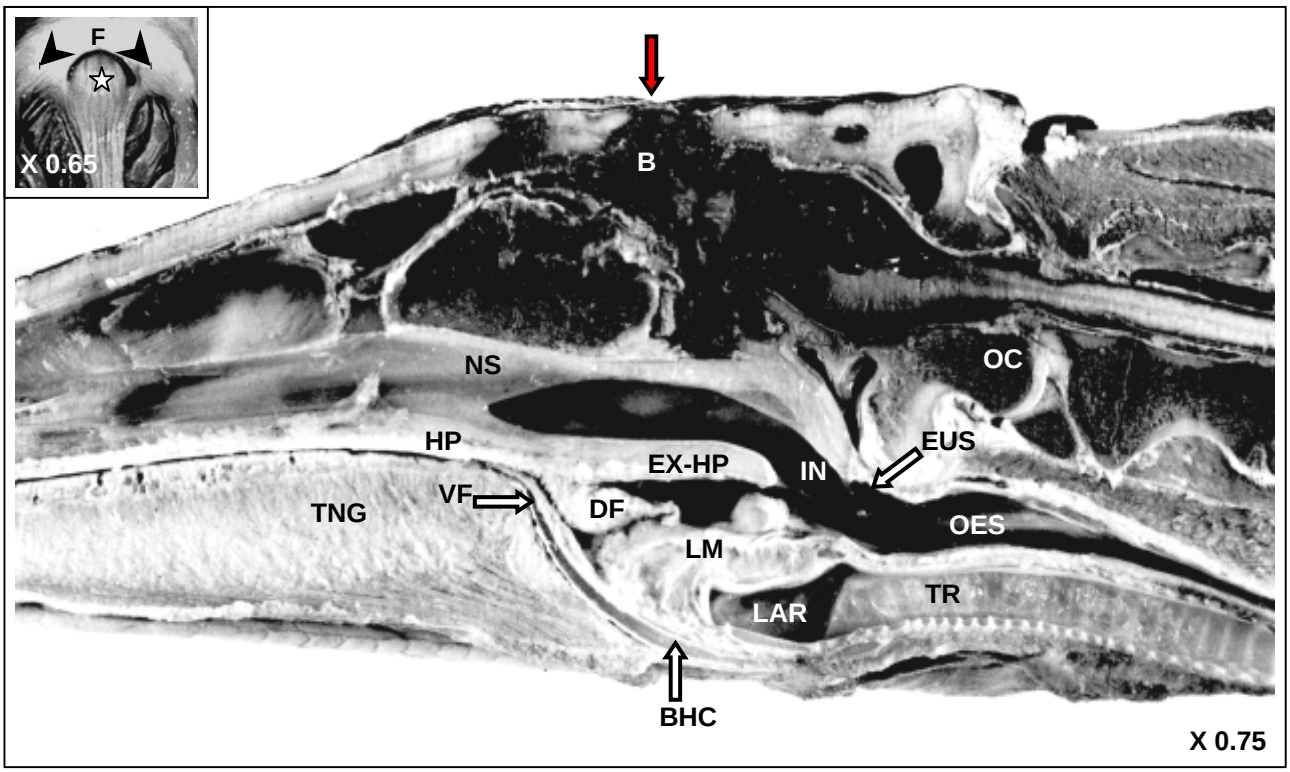

FIG. 1: Mid-sagittal section through the head of a young (ca. 3 year-old and 1.5m length) Nile crocodile showing the topographical relationships between components of the digestive and respiratory tracts. Damage to the brain (B) is caused by the entry (red arrow) of a bullet during the slaughter process. Tongue (TNG); hard palate (HP); nasal septum (NS); extension of hard palate forming part of the roof of the pharynx (EX-HP); opening of internal nares (IN); common opening of Eustachian tubes (EUS); ventral fold of the gular valve (VF); dorsal fold of the gular valve (DF); laryngeal mound (LM); laryngeal cavity (LAR); oesophagus (OES); trachea (TR); occipital condyle (OC); basihyal cartilage (BHC). Formalin fixed specimen. X 0.75 .

Inset: *en face* view of the tightly fitting plug (star) sealing the common opening of the Eustachian tubes. The opening of the Eustachian tubes is surrounded rostrally by a raised, crescent-shaped, fibrous structure (F). X 0.65 .

FIGURE 2: LOCATION OF SAMPLING SITES FROM THE VENTRAL AND DORSAL ASPECTS OF THE PHARYNGEAL CAVITY AND CORRESPONDING MACROSCOPIC FEATURES

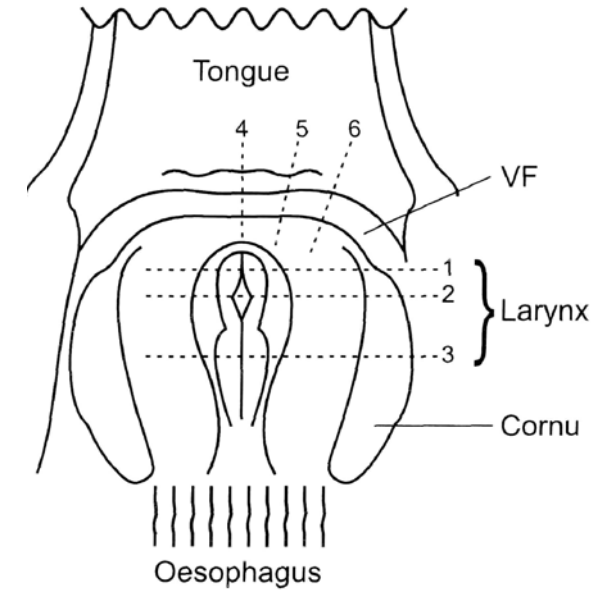

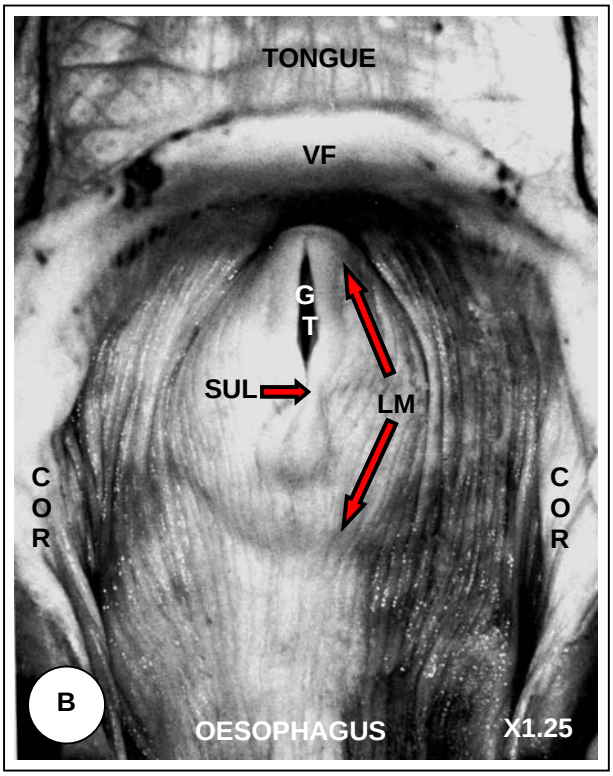

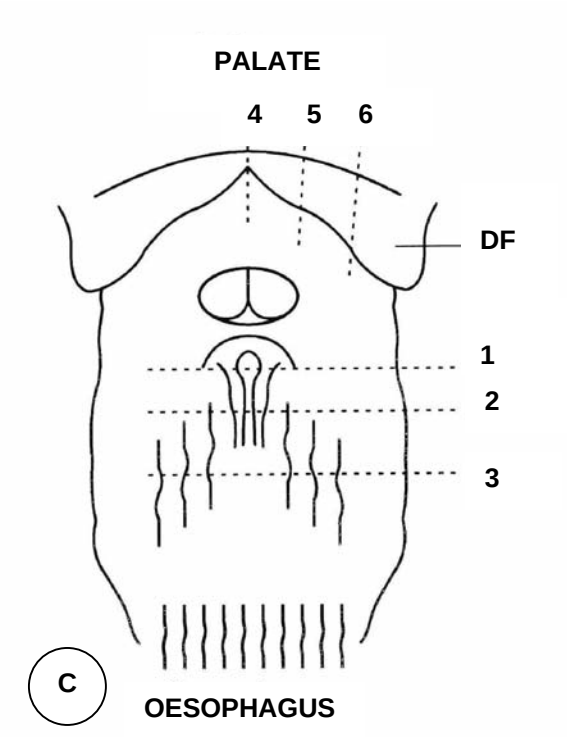

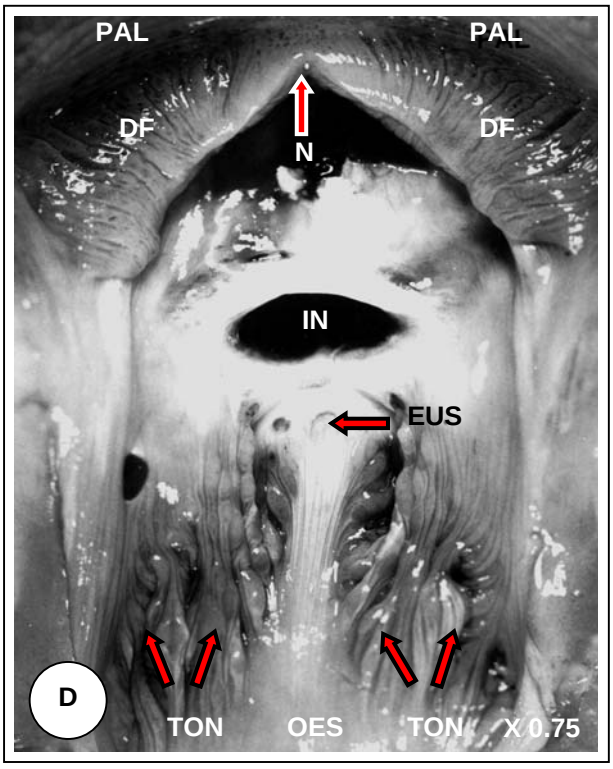

FIG. 2A: Diagrammatic representation of the ventral aspect of the pharynx showing the location of the various regions (1-6) sampled for light microscopic examination. Ventral fold (VF) of the gular valve.

FIG. 2B: Macrophotograph of the ventral aspect of the pharynx. Ventral fold of gular valve (VF); glottis (GT); laryngeal mound (LM); cornuae (COR); laryngeal sulcus (SUL). Formalin fixed specimen. X 1.25 .

FIG. 2C: Diagrammatic representation of the dorsal aspect of the pharynx showing the location of the various regions (1-6) sampled for light microscopic examination. Dorsal fold (DF) of the gular valve.

FIG. 2D: Macrophotograph of the dorsal aspect of the pharynx. Palate (PAL); dorsal fold of the gular valve (DF); median apical notch (N); opening to internal nares (IN); fibrous plug covering the common opening of the Eustachian tubes (EUS); tonsillar region (TON); entrance to the oesophagus (OES). Fresh specimen. X 0.75 .

FIGURE 3: MACROSCOPIC VIEW OF THE GULAR VALVE AND ITS DORSAL FOLD

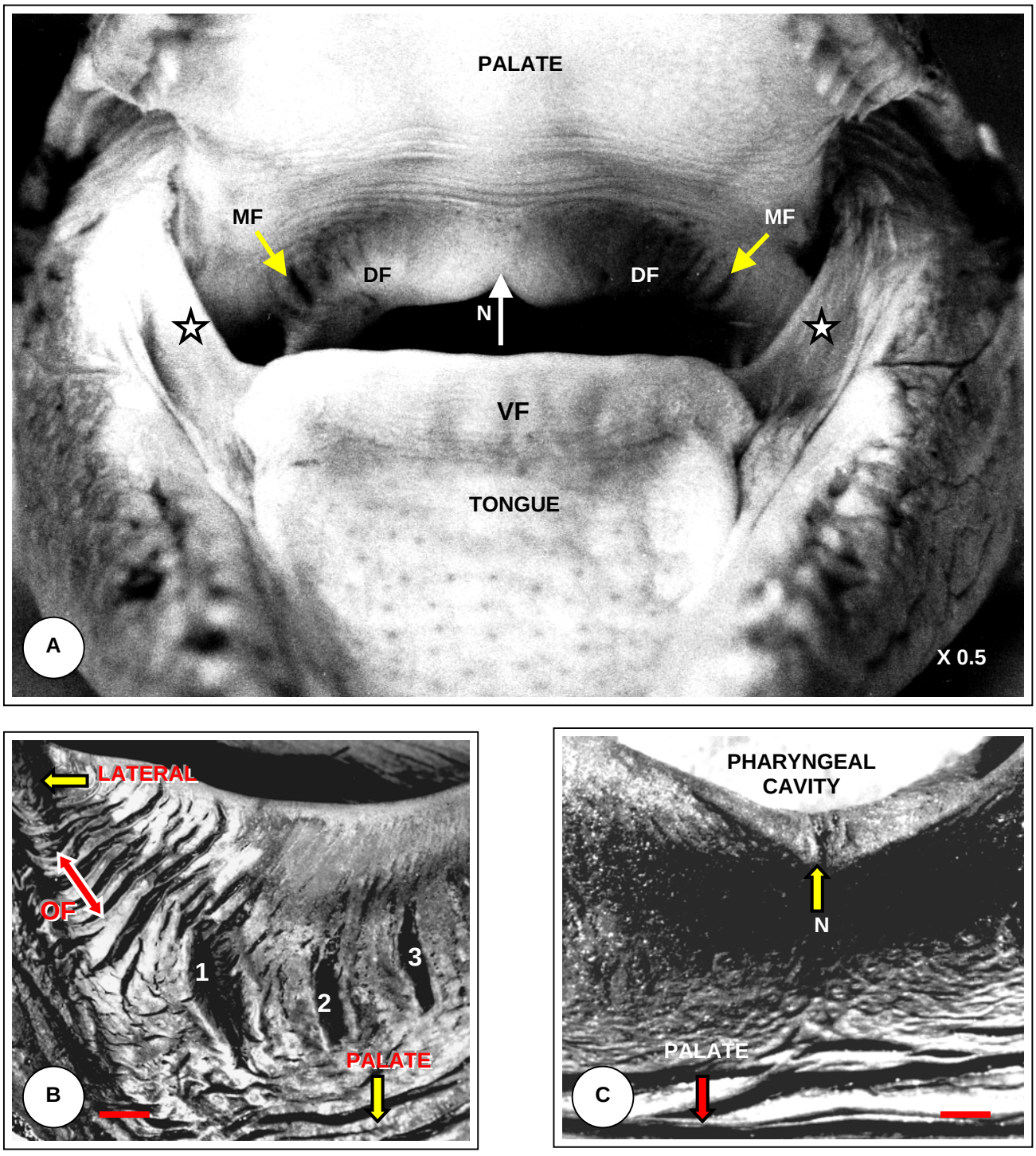

FIG. 3A: Frontal view of the oral cavity and pharynx showing the relationship of the dorsal and ventral folds of the gular valve in an open state. Dorsal fold (DF) of the gular valve; ventral fold (VF) of the gular valve; median apical notch (N) in the dorsal fold; deep mucosal folds (MF). The substantial additional folds (stars) sealing the corners of the mouth are obvious. Fresh specimen. X 0.5 .

FIG. 3B: Stereomicrograph of the extreme lateral and mid-region (oral surface) of the dorsal fold (dorsoventrally inverted) showing the arrangement of the longitudinal mucosal folds. Note the deep vertical mucosal folds (1, 2 & 3) and the compact group of oblique folds (OF) in the lateral region. Specimen prepared for SEM viewing. Bar = 500μm.

FIG. 3C: Stereomicrograph of the median apical notch (N) of the dorsal fold (dorsoventrally inverted) of the gular valve (oral surface). Specimen prepared for SEM viewing. Bar = 500μm.

FIGURE 4: HISTOLOGICAL FEATU .D OF THE GULAR VALVE

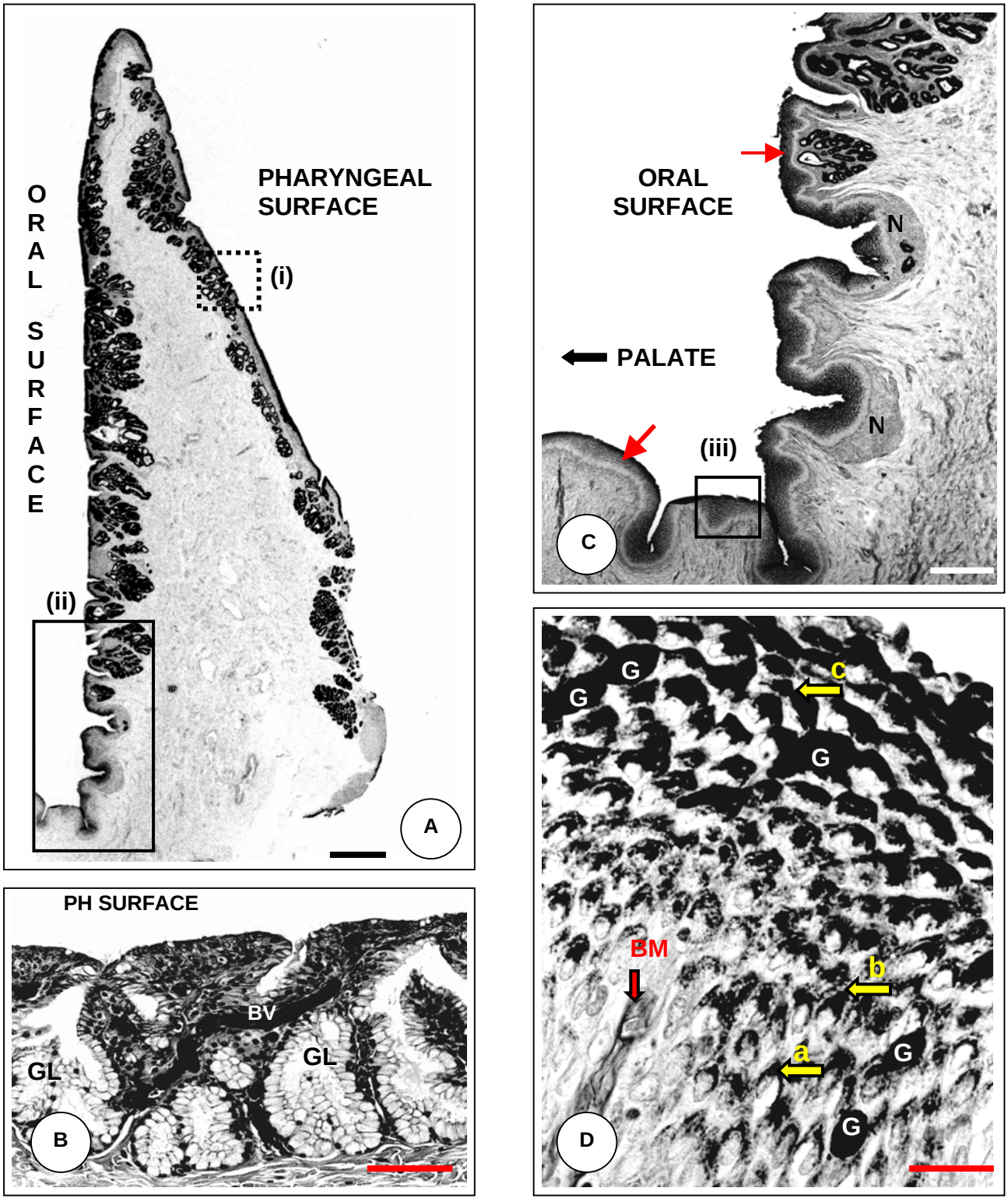

FIG. 4A: Lightmicrograph of a sagittal section from the mid-lateral region of the dorsal fold of the gular valve. PAS-stain demonstrating the distribution of glandular tissue over both the oral and pharyngeal surfaces. Rectangle (i) enlarged in Fig. 4B. Rectangle (ii) enlarged in Fig. 4C. Bar = 2.5mm.

FIG. 4B: Lightmicrograph of the glandular epithelium on the pharyngeal surface (PH SURFACE) of the dorsal fold. Note intimate association of blood vessel (BV) with the epithelium. Branched tubulo-alveolar, mucus secreting glands (GL). H&E stain. Bar = 1mm.

FIG. 4C: Enlargement of the rectangle (ii) in Fig. 4A showing the change of epithelial types from the palate to the base of the dorsal fold. Lymphocytic nodules (N). Region of mucous transformation between red arrows. PAS-stain. Bar = 1mm.

FIG. 4D: Enlargement of the rectangle (iii) in Fig. 4C. The PAS-positive stained stratified squamous epithelium shows signs of mucus transformation at the base of the dorsal fold of the gular valve. (a), (b) and (c) show the increase of PAS-positive granules in the apices of the non-keratinised cells. Accumulation of granules increases from the stratum spinosum to the surface of the epithelium. Basement membrane (BM) associated with a slim connective tissue papilla; goblet cells (G). DIC-imaging. PAS-stain. Bar = 50μm.

FIGURE 5: HISTOLOGICAL FEATU TISSUE AND SURFACE EPITHELIUM OF THE PHARYNGEAL SURFACE OF THE DORSAL GULAR FOLD

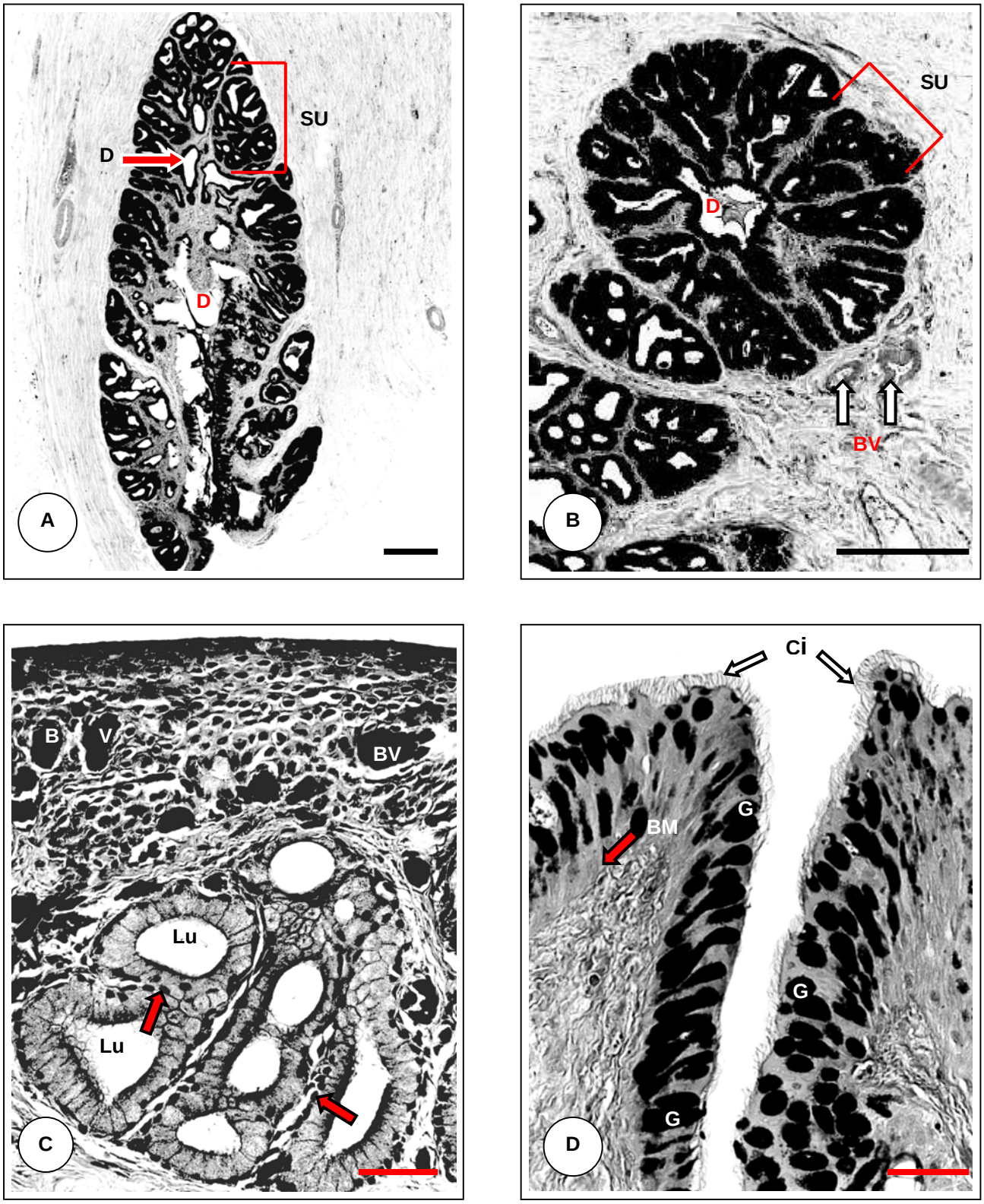

See captions opposite.

CAPTIONS TO FIGURE 5: HISTOLOGICAL FEATURES OF THE GLANDULAR TISSUE AND SURFACE EPITHELIUM OF THE PHARYNGEAL SURFACE OF THE DORSAL GULAR FOLD

FIG. 5A: Lightmicrograph of a longitudinal section through a large, branched tubulo-alveolar mucus-secreting gland situated at the base of the dorsal fold on the pharyngeal surface. Secretory unit (SU); central duct (D) of gland. PAS-stain. Bar = 0.5mm.

FIG. 5B: Lightmicrograph of a transverse section through a gland similar to that in Fig. 5A. Note the wedge-shaped secretory units (SU) arranged around a central duct (D) and the close proximity of blood vessels (BV) to the gland. PAS-stain. Bar = 0.5mm.

FIG. 5C: Lightmicrograph of a tubulo-alveolar mucus-secreting gland showing the high profile of secretory cells with basally situated nuclei (arrows). Note the penetration of blood vessels (BV) between alveoli via connective tissue septae. Gland lumen (LU). H&E-stain. Bar = 100μm.

FIG. 5D: Lightmicrograph of mucosal folds on the pharyngeal surface of the dorsal gular fold showing pseudostratified columnar ciliated (Ci) epithelium with goblet cells (G) (respiratory epithelium). Basement membrane (BM). PAS-stain. Bar = 100μm.

FIGURE 6: HISTOLOGICAL FEATURES OF THE VENTRAL FOLD OF THE GULAR VALVE

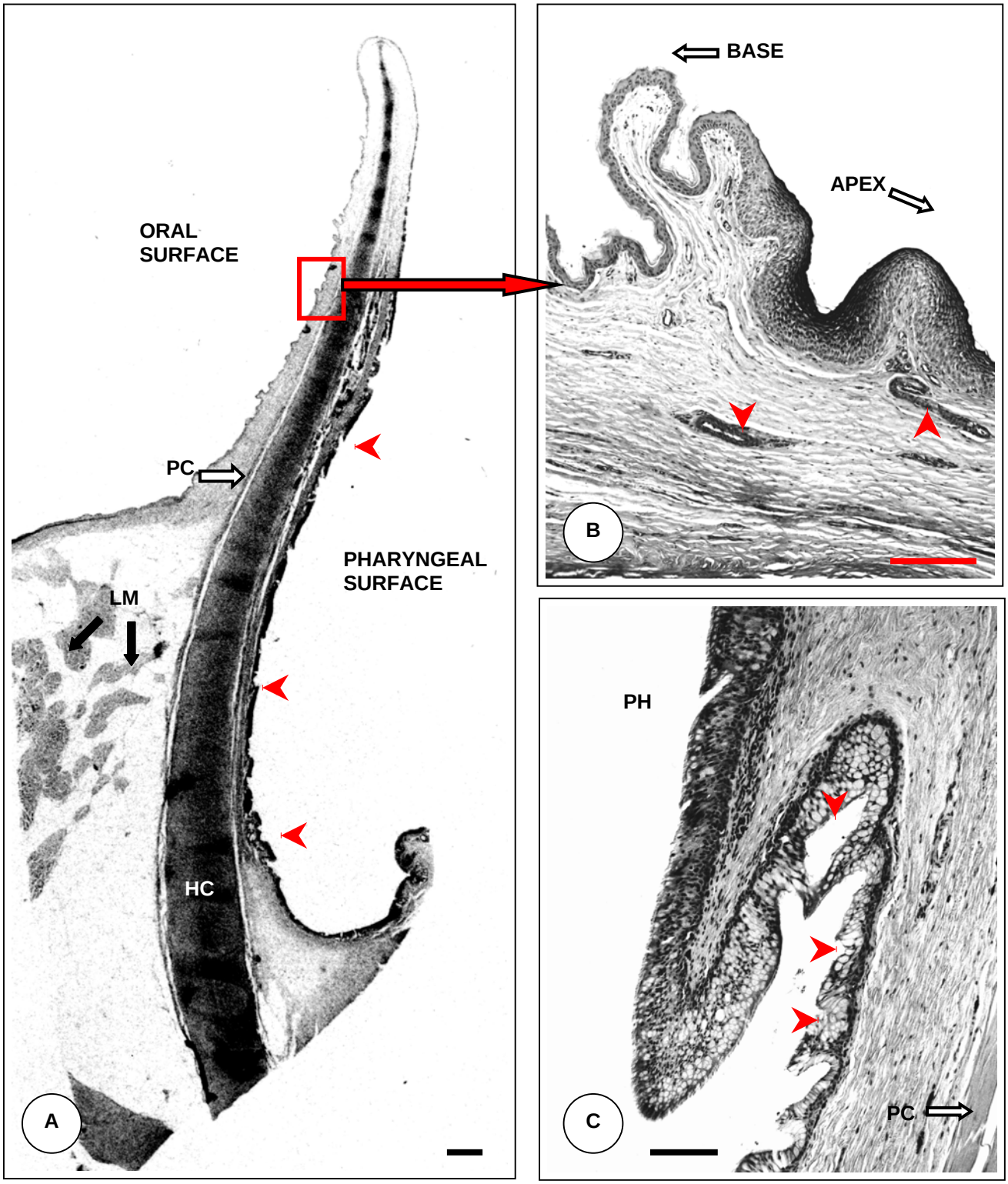

FIG. 6A: Lightmicrograph of a sagittal section through the mid-region of the ventral fold of the gular valve. Note the discrete epithelial folds (arrowheads) on the pharyngeal surface. Striated lingual musculature (LM) of the tongue; perichondrium (PC); hyaline cartilage of the basihyal plate (HC). Rectangle enlarged in Fig. 6B. H&E-stain. Bar = 1mm.

FIG. 6B: Lightmicrograph showing the transition of the epithelium on the oral surface of the ventral fold from lightly keratinised stratified squamous epithelium to thicker non-keratinised stratified squamous epithelium. The superficial and deep vascular plexuses are also visible (arrowheads). DIC-image. H&E-stain. Bar = 500μm.

FIG. 6C: Lightmicrograph of the ventral fold of the gular valve showing an epithelial fold on the pharyngeal surface (PH). Note the masses of goblet cells (arrowheads) lining the groove and the regular nature of the supporting collagen fibres. Perichondrium (PC). H&E-stain. Bar = 250μm.

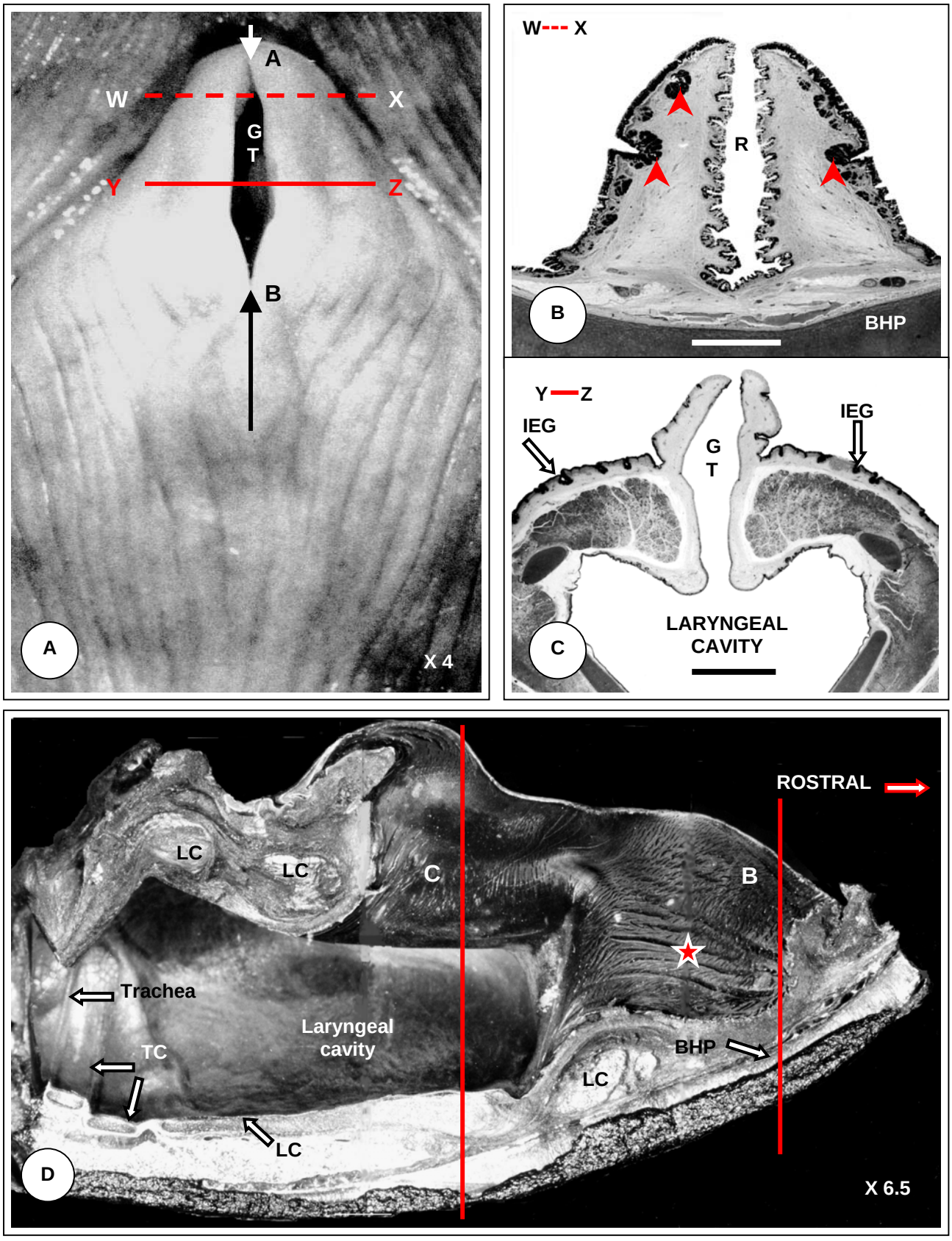

See captions opposite.

CAPTIONS TO FIGURE 7: MORPHOLOGY OF THE LARYNGEAL MOUND

FIG. 7A: Macrophotograph of the laryngeal mound and glottis showing the direction of the longitudinal incisions (white and black arrows) made to separate the left and right halves of the glottis. Dashed line W-X and solid line Y-Z are regions from which the histological sections in Figs. 7B & 7C were taken respectively. The black arrow B lies on the laryngeal sulcus. Glottis (GT). Formalin-fixed specimen. X 4 .

FIG. 7B: Transverse histological section of the rostral tip of the laryngeal mound (section W – X shown in Fig. 7A) showing the glandular nature (arrowheads) of the pharyngeal surface. Rostral sulcus (R) with longitudinal folds. Basihyal cartilage plate (BHP). PAS-stain. Bar = 1mm.

FIG. 7C: Transverse histological section of the mid-region of the glottis showing a decrease in glandular secretory activity and intra-epithelial glands (IEG) on the pharyngeal surface of the laryngeal mound relative to the rostral tip illustrated in Fig. 7B. Glottis (GT). PAS-stain. Bar = 1mm.

FIG. 7D: Montage stereomicrograph of the left half of the laryngeal mound exposed after longitudinal sectioning as shown in Fig. 7A. Lines B & C correspond to histological sections in Figs. 7B & 7C respectively. Tracheal cartilage rings (TC); laryngeal cartilages (LC) making up the support frame of the laryngeal mound. Basihyal cartilage plate (BHP). Note the oblique and longitudinal folds lining the rostral sulcus (star). Specimen prepared for SEM-viewing. X 6.5 .

FIGURE 8: HISTOLOGICAL FEATURES OF THE MID-REGION OF THE GLOTTIS

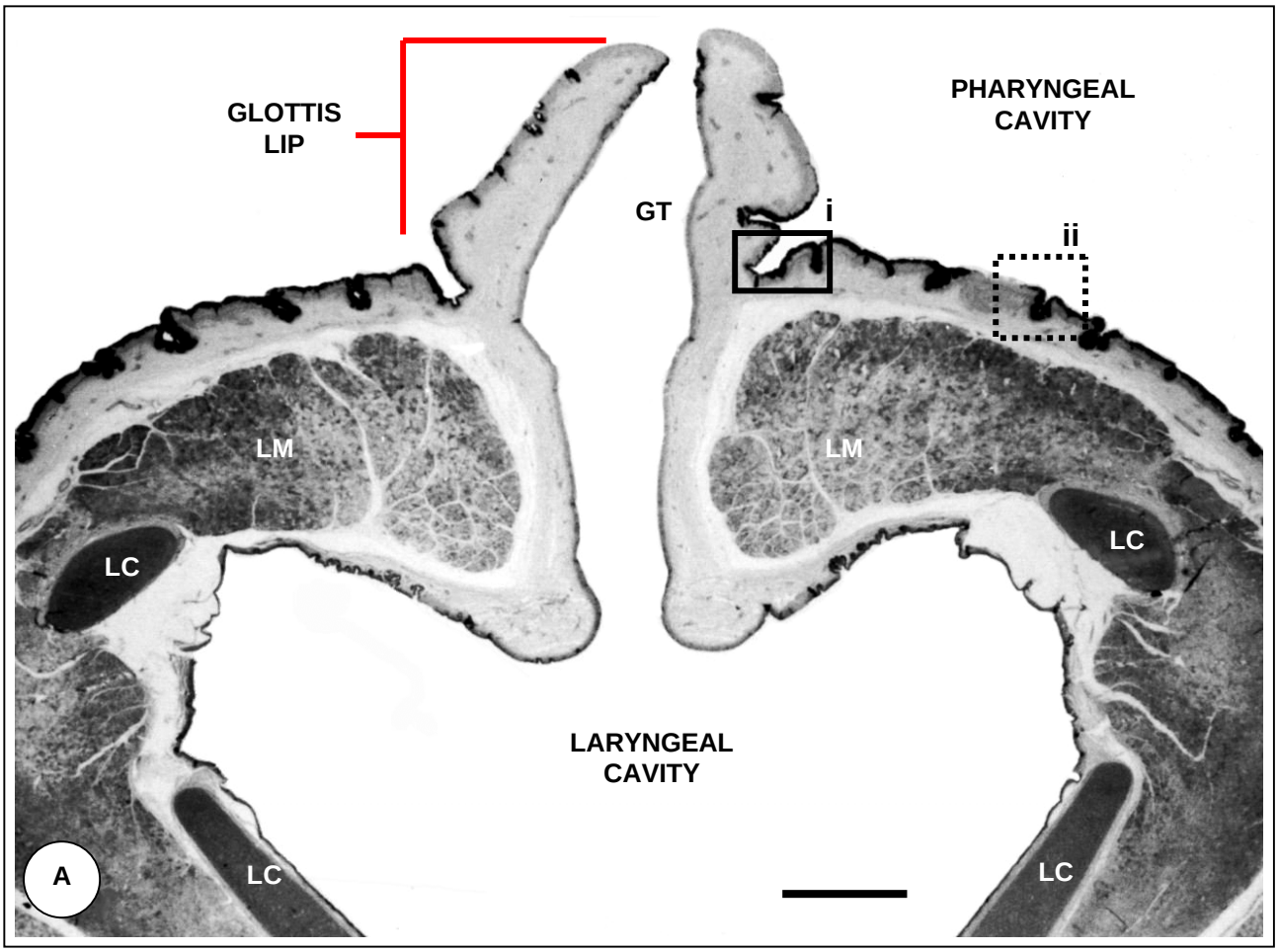

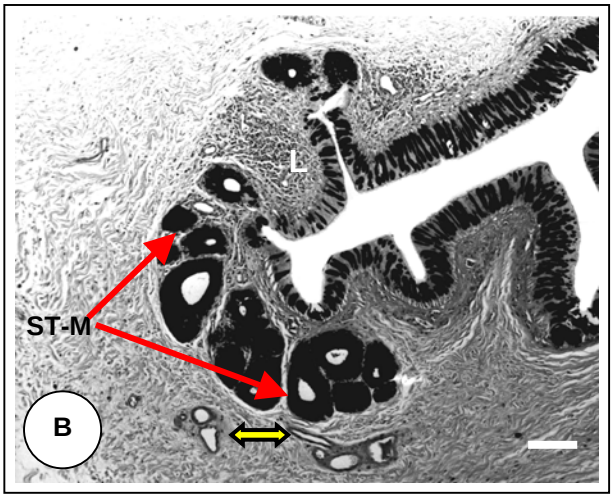

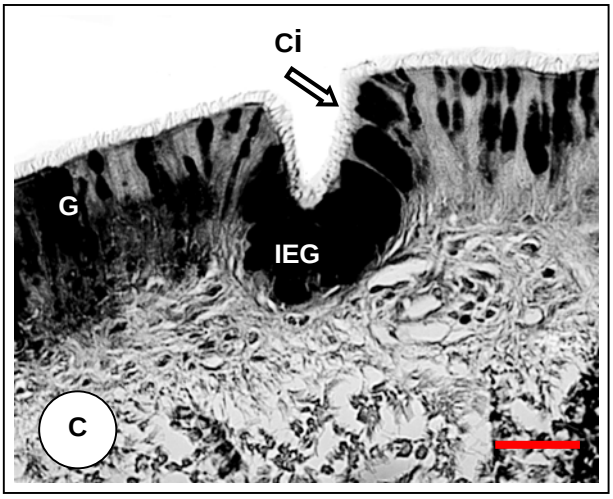

FIG. 8A: Stereomicrograph of a histological cross section through the mid-region of the glottis (GT). Blocks (i) and (ii) are represented in Figs. 8B & 8C respectively. Laryngeal (hyaline) cartilages (LC) supporting the laryngeal mound. Laryngeal musculature (LM). PAS-stain. Bar = 500μm.

FIG. 8B: Lightmicrograph of a simple coiled tubular mucus-secreting gland (ST-M) opening at the bottom of a deep epithelial fold situated at the base of the glottis (GT) lip as shown in rectangle (i) in Fig. 8A. Note the close proximity of blood vessels (double headed arrow) to the glandular tissue. Lymphocytic aggregation (L). PAS-stain. Bar = 250μm.

FIG. 8C: Lightmicrograph of the highly glandular epithelium on the pharyngeal surface of the laryngeal mound as shown in rectangle (ii) in Fig. 8A. Note the high concentration of goblet cells (G) and the dense ciliation (Ci). Intra-epithelial gland (IEG). PAS-stain. Bar = 100μm.

FIGURE 9: 3-DIMENSIONAL FEATURES OF THE ORAL SURFACE OF THE DORSAL FOLD OF THE GULAR VALVE

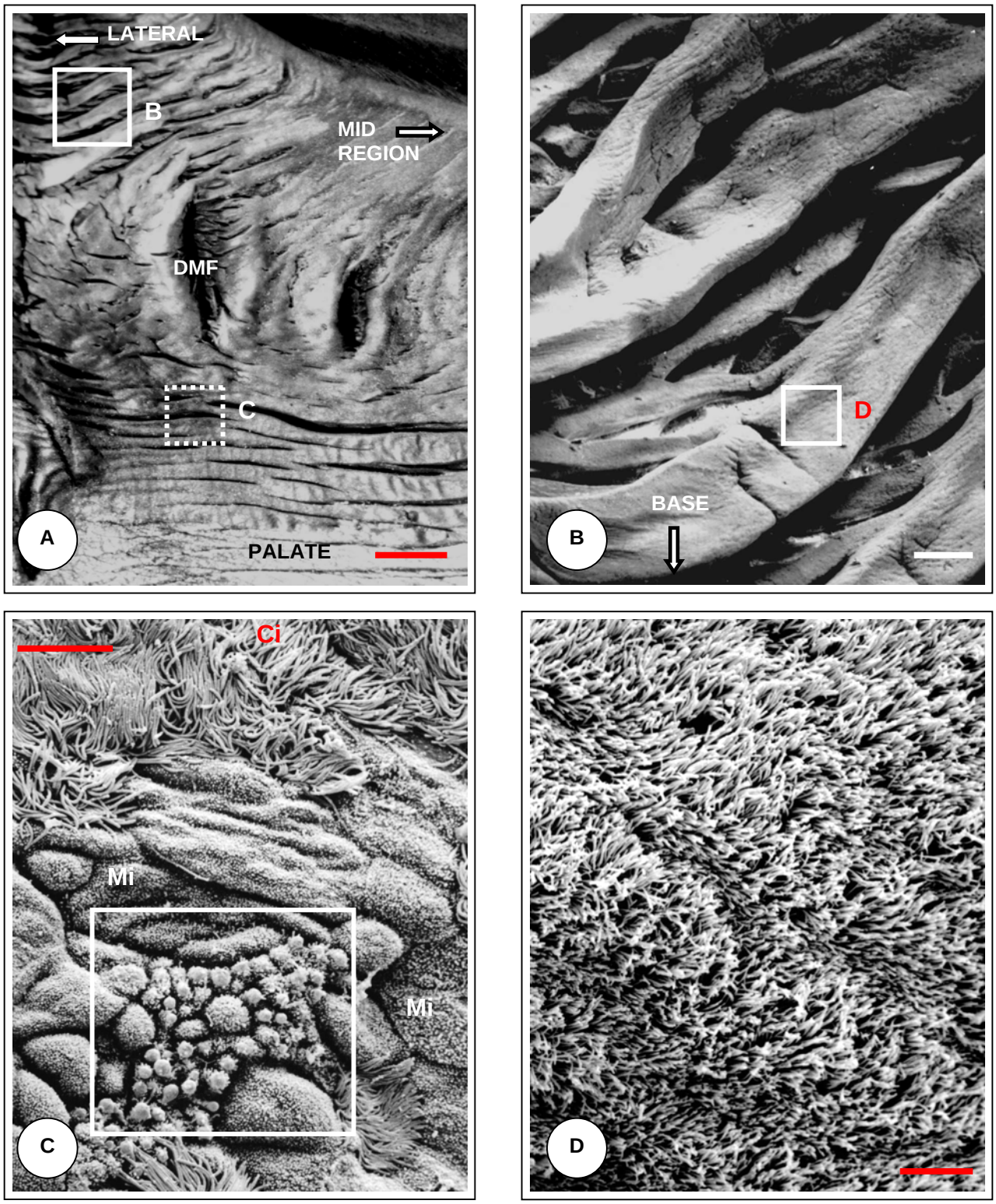

FIG. 9A: Stereomicrograph of the lateral to mid-lateral region of the oral surface of the dorsal fold of the gular valve. Note the compact group of longitudinal mucosal folds situated at the corner of the fold (rectangle B shown in Fig. 9B) and the deep mucosal folds (DMF) adjacent to them. Rectangle C enlarged in Fig. 9C. Specimen critical point dried and Au-coated in preparation for SEM viewing. Bar = 500μm.

FIG. 9B: SEM-micrograph of the compact group of longitudinal folds shown in Fig. 9A. Note the complicated branching and anastomosing of the mucosal folds. Base of dorsal fold in the direction of the arrow. Rectangle D enlarged in Fig. 9D. Bar = 100μm.

FIG. 9C: SEM-micrograph representing the type of epithelium present at the base of the dorsal gular fold shown in rectangle C, Fig. 9A. The blocked area represents an undetermined cellular eruption not seen during histological examination. Microvillous covered cells (Mi); ciliated cells (Ci). Bar = 5μm.

FIG. 9D: SEM-micrograph of the densely ciliated epithelium present on all surfaces of the mucosal folds in the lateral region of the dorsal gular fold. Enlarged from rectangle D in Fig. 9B. Bar = 5μm.

FIGURE 10: SCANNING ELECTRON MICROGRAPHS OF THE ORAL SURFACE OF THE DORSAL FOLD OF THE GULAR VALVE

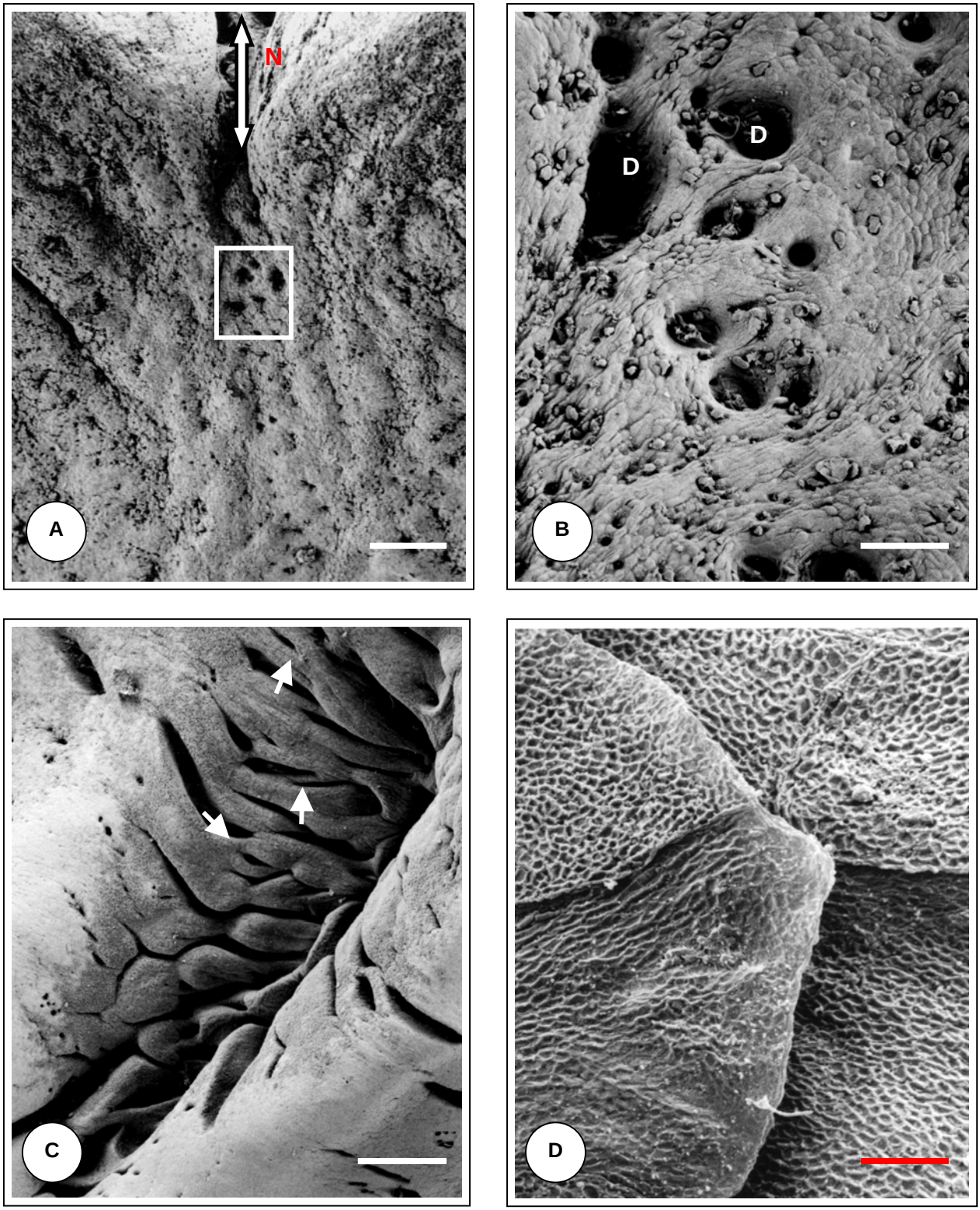

FIG. 10A: Low magnification of the median apical notch (N) showing a large number of duct openings from the underlying glandular tissue. Rectangle enlarged in Fig. 10B. Bar = 250μm.

FIG. 10B: The duct openings (D) are surrounded by masses of non-ciliated, dome-shaped epithelial cells. Bar = 20μm.

FIG. 10C: View of the wall of one of the deep mucosal folds in the mid-lateral region of the dorsal gular fold. See also Fig. 9A (this chapter). Note the intricate branching and anastomosing (arrows) of the mucosal folds. Bar = 250μm.

FIG. 10D: Higher magnification SEM-micrograph showing the honeycomb appearance of surface cells in the region of "smooth" epithelium situated near the base of the fold. See also Fig. 11D (this chapter). Bar = 2.5μm.

FIGURE 11: EPITHELIAL TRANSITION OF THE DORSAL FOLD OF THE GULAR VALVE

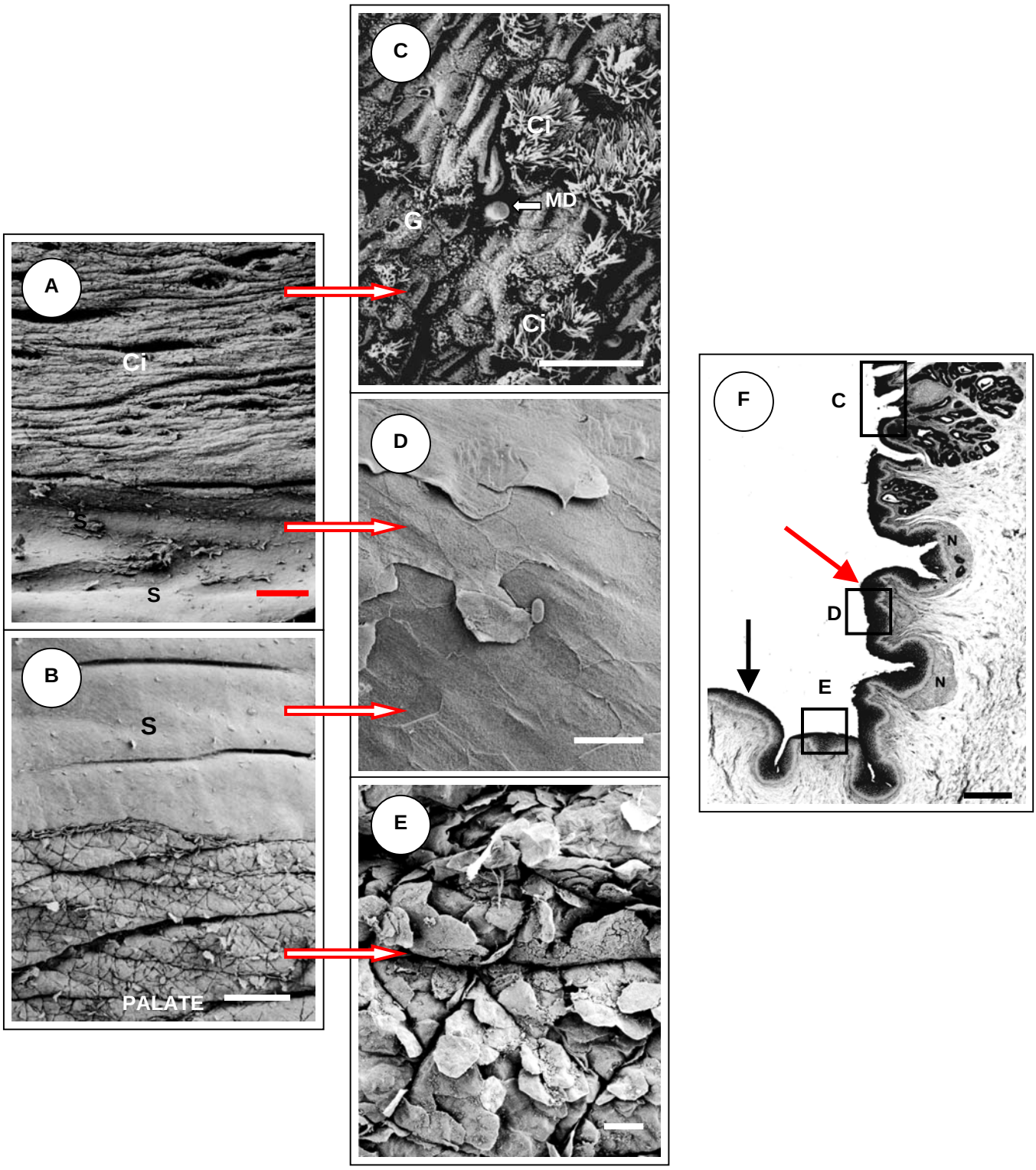

SEM-micrographs of the basal region of the oral surface of the dorsal fold showing the transition of epithelial types from the palate onto the fold. The histological section (Fig. 11F) can be used for orientation purposes.

FIG. 11A: Transition between the non-ciliated smooth epithelium (S) and the ciliated (glandular) epithelium (Ci). Bar = 250μm.

FIG. 11B: Transition between the "cobbled" epithelium of the palate and the "smooth" epithelium (S) at the base of the dorsal fold. Bar = 250μm.

FIG. 11C: Glandular epithelium showing ciliation (Ci) and goblet cells (G). Mucus droplet (MD). Bar = 10μm.

FIG. 11D: Smooth epithelium situated between the palate and the glandular epithelium. Note the polygonal outline of the surface epithelial cells and cell loosening. Bar = 20μm.

FIG. 11E: Lightly keratinised epithelium of the palate showing the "flaky" (desquamating) appearance of the epithelium. Bar = 20μm.

FIG. 11F: Orientation lightmicrograph of the basal region (red arrow) of the dorsal fold and its junction with the palate (black arrow). Rectangles C, D & E are represented by SEM-micrograph Figs. 11C, 11D & 11E respectively. PAS-stain. Bar = 1mm.

FIGURE 12: SCANNING ELECTRON MICROGRAPHS OF THE PHARYNGEAL SURFACE OF THE DORSAL FOLD OF THE GULAR VALVE

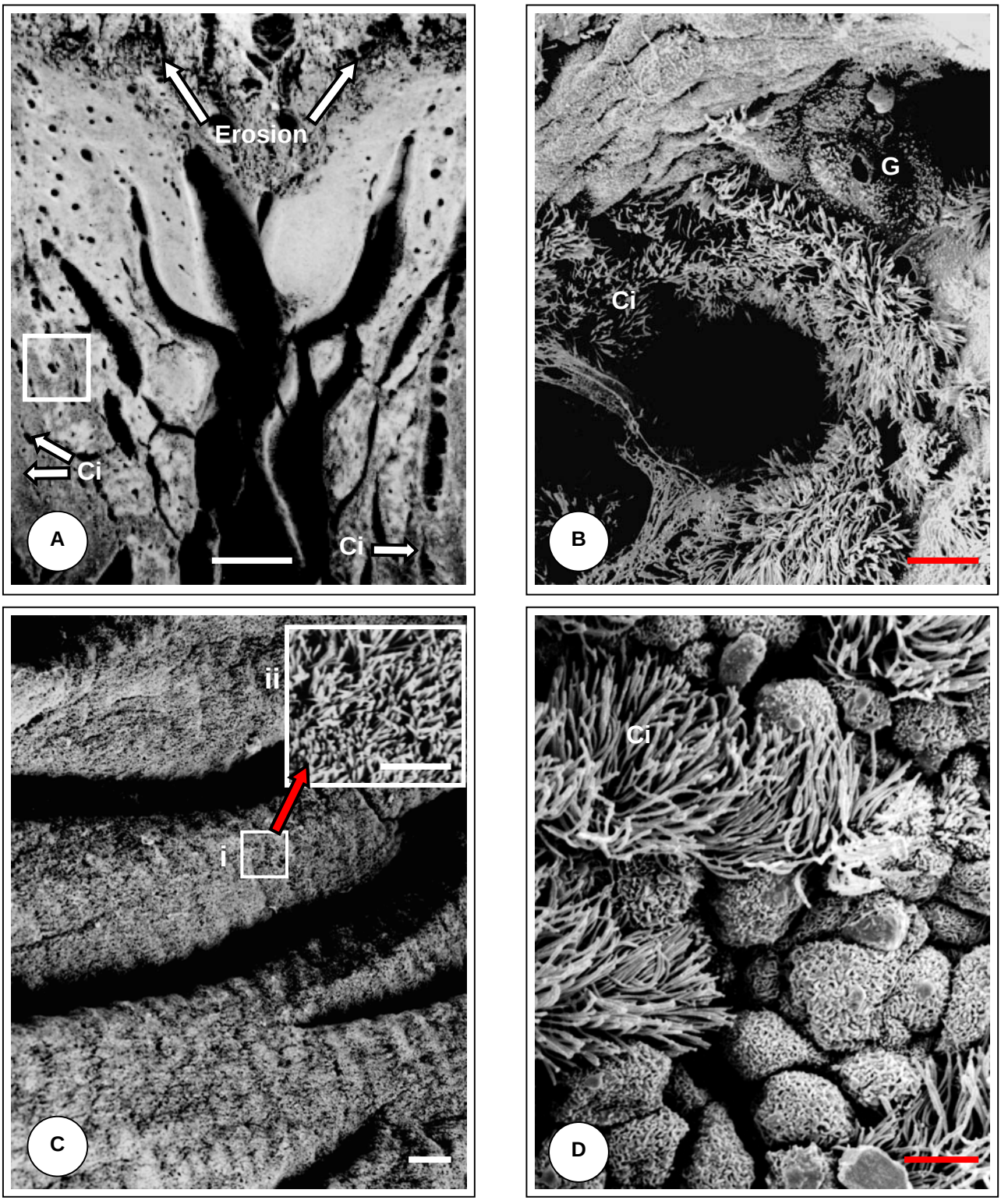

FIG. 12A: SEM-micrograph showing the collection of converging folds situated at the base of the median apical notch on the pharyngeal surface of the dorsal gular fold. Note the numerous duct openings emanating from the underlying glandular tissue. Rectangle enlarged in Fig. 12B. Bar = 250μm.

FIG. 12B: SEM-micrograph of the rectangle indicated in Fig. 12A showing the ciliated nature of the epithelium surrounding the openings to deeper lying glandular tissue. This is a common, but not constant feature. Goblet cell (G); ciliation (Ci). Bar = 5μm.

FIG. 12C: SEM-micrograph of the densely ciliated epithelium seen in the mid- to extreme lateral region of the pharyngeal surface of the dorsal gular fold. The inset shows an enlargement of the ciliated epithelium. Bar = 20μm; Inset bar = 5μm.

FIG. 12D: Occasional non-ciliated cellular eruptions are seen between the ciliated cells. These eruptions may be associated with deeper lying lymphocytic activity and probably represent goblet cells. Ciliation (ci). Bar = 2.5μm.

FIGURE 13: MORPHOLOGY OF THE [illegible] AND TONSILLAR REGION

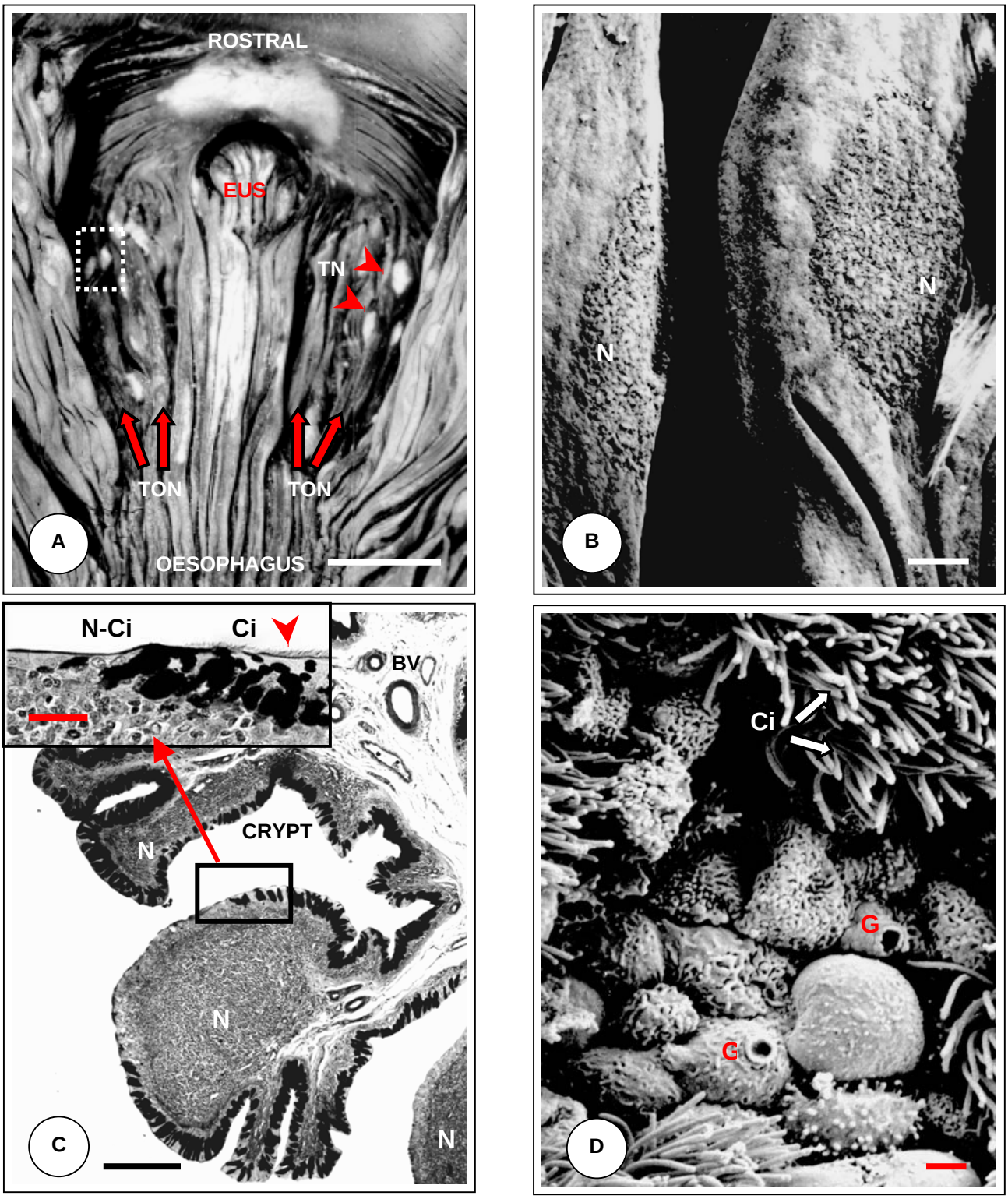

See captions opposite.

CAPTIONS TO FIGURE 13: MORPHOLOGY OF THE PHARYNGEAL ROOF AND TONSILLAR REGION

FIG. 13A: Stereomicrograph of the tightly fitting fibrous plug (EUS) covering the common entrance to the Eustachian tubes on the roof of the pharynx, bordered by tonsillar tissue (TON). Typical tonsillar nodules (TN). Rectangle enlarged in Fig. 13B. The gap between the fibrous plug and the aperture is an artifact caused by shrinkage during the critical point drying process. Specimen prepared for SEM-viewing. Bar = 1mm.

FIG. 13B: SEM-micrograph of tonsillar nodules (N) situated in the tonsillar region seen in Fig. 13A. The abrupt difference in surface features between the lymphoid (tonsillar) tissue and the ciliated surface lining is obvious. Bar = 100μm.

FIG. 13C: Light micrograph of tonsillar nodules (N) and a typical tonsillar crypt. Note the vascular complex (BV) within the connective tissue at the base of the folds. The inset (Bar = 10μm) illustrates the typical histological surface features seen on some tonsillar nodules. Note the progression from ciliated (Ci) to non-ciliated (N-Ci) epithelium on the surface of the nodule and the thin, continuous epithelial lining (see p. 57). Goblet cells (G). PAS-stain. Bar = 500μm.

FIG. 13D: SEM-micrograph of part of a tonsillar nodule bordered by dense ciliation (Ci). Goblet cells (G). Bar = 1μm.

FIGURE 14: MORPHOLOGY OF THE VENTRAL FOLD OF THE GULAR VALVE

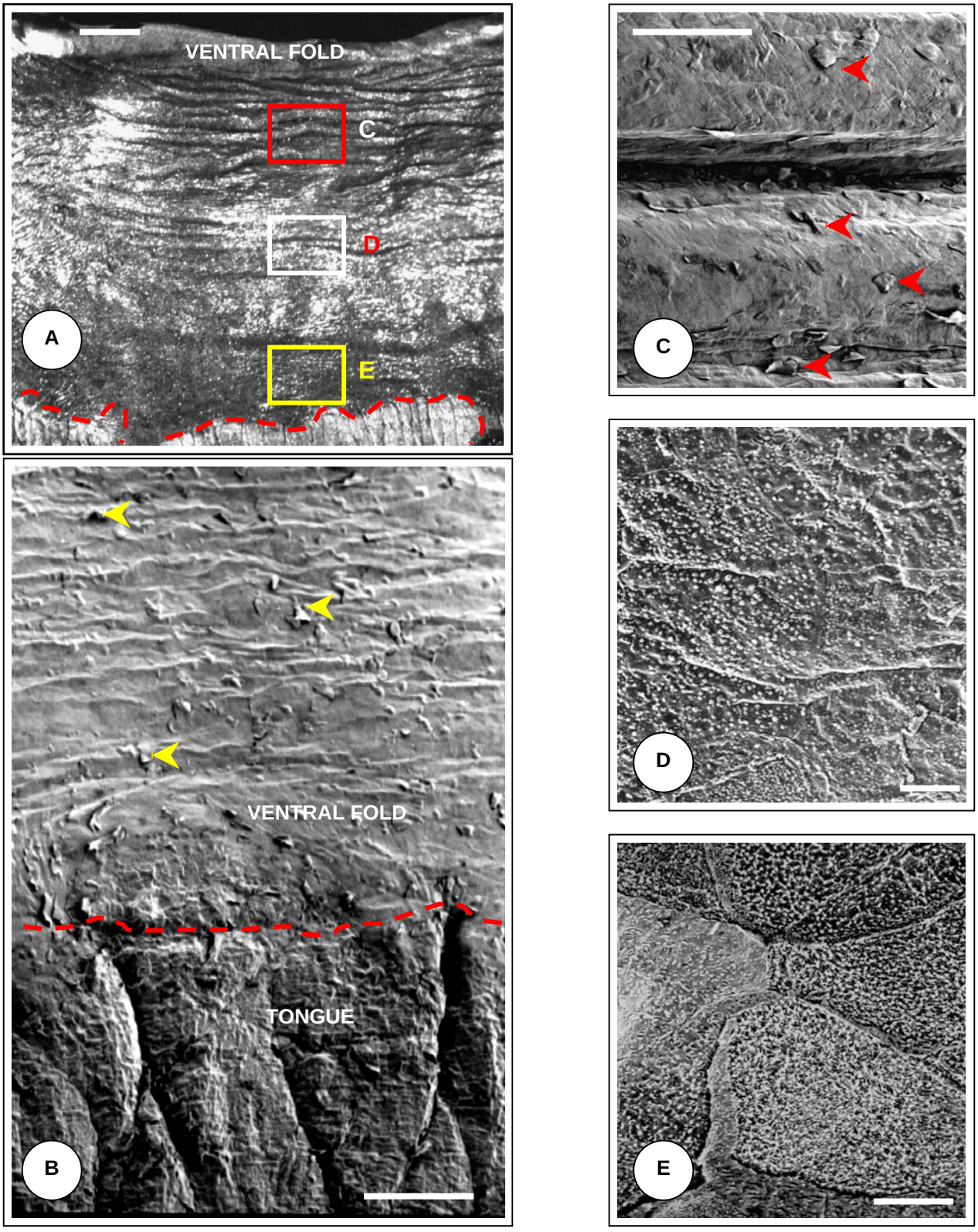

See captions opposite.

CAPTIONS TO FIGURE 14: MORPHOLOGY OF THE ORAL SURFACE OF THE VENTRAL FOLD OF THE GULAR VALVE

FIG. 14A: Stereomicrograph of the oral surface of the ventral fold of the gular valve showing the distinct transition from the surface of the tongue to the fold (red dashed line). Transverse folds are obvious towards the apex of the fold. The rectangles C, D and E are represented in figs. 14C, 14D and 14E respectively. Bar = 500μm.

FIG. 14B: Higher magnification of the transition area shown in Fig. 14A above. Note the smooth appearance of the epithelium of the fold in contrast to that on the tongue surface. The dashed red line indicates the boundary. A few desquamating cells can also be seen (arrowheads) Bar = 250μm.

FIG. 14C: Higher magnification of the transverse mucosal folds occurring towards the apex of the ventral gular fold indicated by the rectangle C in Fig. 14A. A few desquamating cells are present (arrowheads). Bar = 50μm.

FIG. 14D: SEM-micrograph representative of the epithelium observed on the ventral gular fold in the region indicated by the rectangle D in Fig. 14A. Note the occurrence, in varying densities, of short stubby microvilli on the cell surfaces Bar = 2.5μm.

FIG. 14E: SEM-micrograph representative of the epithelium observed at the base of the ventral gular fold at its junction with the tongue in the region indicated by the rectangle E in Fig. 14A. Note the cell surfaces adorned with microridges giving them a honeycomb appearance. Bar = 5μm.

FIGURE 15: MORPHOLOGY OF THE [illegible] OF THE VENTRAL FOLD OF THE GULAR VALVE

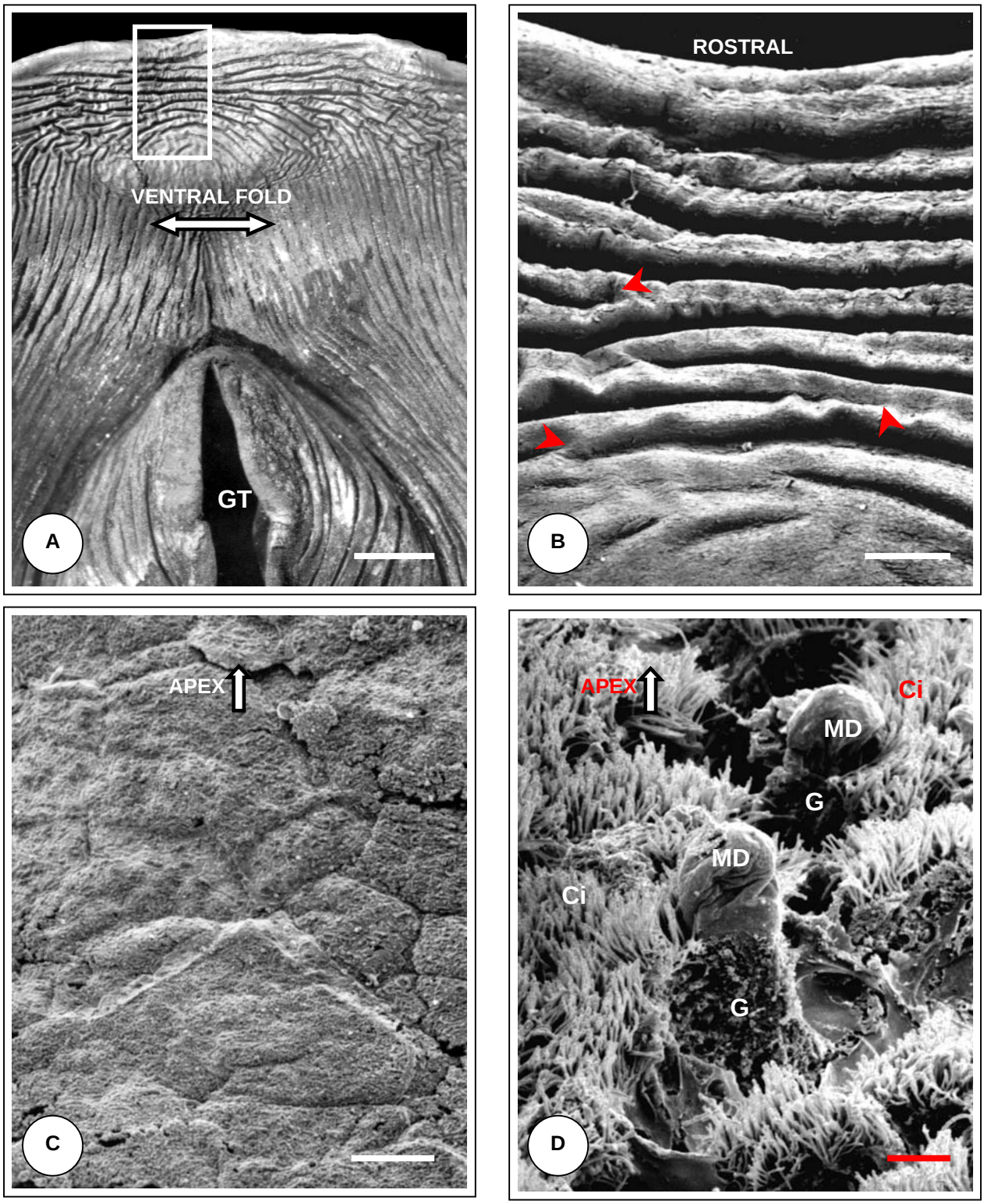

FIG. 15A: Montage stereomicrograph of the rostral region of the larynx and mid-region of the ventral fold of the gular valve showing the regular pattern of mucosal folds around the laryngeal mound. The blocked area is enlarged in Fig. 15B. Glottis (GT). Specimen prepared for SEM viewing. Bar = 1mm.

FIG. 15B: SEM-micrograph of the blocked area shown in Fig. 15A demonstrating the regular pattern of mucosal folds in the mid-region of the ventral fold of the gular valve. Note the branching and anastomosing of the mucosal folds (arrowheads). Bar = 250μm.

FIG. 15C: SEM-micrograph of a characteristic non-ciliated area near the apex on the pharyngeal surface of the ventral gular fold. Note the polygonal shape and slightly raised profile of the cells. Bar = 5μm.

FIG. 15D: SEM-micrograph of a ciliated area on the pharyngeal surface, found laterally and towards the base of the ventral fold. Note the densely ciliated cells (Ci) and the goblet cells (G) with erupting mucus droplets (MD). Bar = 2,5μm.

CHAPTER 4

MORPHOLOGY OF THE OESOPHAGUS

INTRODUCTION

The morphology of the reptilian oesophagus has received a great deal of attention in the literature (for reviews see Luppa 1977 and Parsons and Cameron 1977). Many of these studies concentrated on a description of the internal relief of the oesophagus and the pattern of mucosal folds observed in various groups of reptiles such as turtles, lizards and snakes has been carefully documented (Parsons & Cameron, 1977).

The oesophageal relief of the Crocodilia has also been studied in a number of species including *Alligator mississippiensis* (Parsons & Cameron, 1977), *Caiman crocodilus* (Jacobshagen, 1920; Parsons & Cameron, 1977), *Caiman crocodilus fuscus*, *Caiman latirostris* (Parsons & Cameron, 1977), *Crocodylus acutus*, *Crocodylus niloticus* (Jacobshagen, 1920), *Crocodylus porosus* (Parsons & Cameron, 1977), *Osteolaemus tetraspis* (Jacobshagen, 1920) and *Tomistoma schlegelii* (Parsons & Cameron, 1977) and a general pattern of longitudinal folds has been described (Parsons & Cameron, 1977). Parsons & Cameron (1977), however, have cautioned against accepting the accuracy of these studies as they were often based on single specimens which were not always optimally preserved. Moreover, the specimens studied by Parsons & Cameron (1977) were small (indicating young animals) and the possibility exists that the pattern of mucosal folds may change or differ with age.

The histological structure of the reptilian oesophagus has likewise been studied in a variety of species, including representatives of the Crocodilia (Luppa, 1977). Reese (1913) described the histology of the "Florida alligator", while Taguchi (1920) compared this region in three species of Crocodilia, namely, *Alligator sinensis*, *Crocodylus porosus* and *Crocodylus niloticus*. Taguchi (1920) also described the presence of taste receptors/buds in the proximal region of the oesophagus of *Crocodylus niloticus*, an

observation supported in an earlier study by Bath (1905) who identified taste buds in the upper oesophagus of *C. niloticus*.

The oesophageal epithelium of the Crocodilia is composed of variably distributed ciliated cells and goblet cells (Béguin, 1904; Taguchi, 1920; Pernkopf & Lehner, 1937; Luppa, 1977). However, conflicting reports have been presented regarding the relative numbers of the two cell types along the length of the oesophagus (Béguin, 1904; Taguchi, 1920; Pernkopf & Lehner, 1937). The occurrence of oesophageal glands has likewise elicited contrasting opinions, with some authors reporting their presence (Eisler, 1889; Taguchi, 1920) and others noting their absence (Béguin, 1904). Oppel, (1900, cited by Luppa, 1977) noted that oesophageal glands are present in *Alligator* and absent in *Crocodylus*. Histochemical studies have demonstrated the presence of non-specific alkaline phosphatase in the ciliated cells of the oesophageal epithelium of *Crocodylus* (Arvy, 1962; Arvy & Bonichon, 1958).

Although some information has been provided on the morphology of the oesophagus of the Nile crocodile (Béguin, 1904; Taguchi, 1920; Jacobshagen, 1920), a comprehensive histological description of this part of the upper digestive tract is not available. This situation is further complicated by the lack of adequate numbers of specimens used in the earlier studies, often coupled with inadequate fixation of the tissue samples.

This chapter presents a detailed description of the macroscopic, microscopic and some ultrastructural features of the oesophagus of the Nile crocodile, *Crocodylus niloticus* (Laurenti, 1768) and compares the results with published information on this species and other Crocodilia.

MATERIALS AND METHODS

Experimental animals

Whole oesophagi were obtained from twelve, 2.5 – 3 year-old clinically healthy *C. niloticus* specimens, of either sex, which had been raised on a breeding farm and were slaughtered commercially for their skins and meat. The length of animals ranged between 1.2 – 1.5 m. To limit rapid degenerative changes after death, samples were collected on site at the abattoir. Animals were shot in the brain at close range using a .22 calibre rifle (see Chapter 1 – Fig. 1B). Although death was instantaneous, carcasses were left until all

obvious signs of post mortem tremor had ceased before commencing the skinning process. All oesophagi were thus removed from carcasses after the skinning process had been completed, resulting in an unavoidable delay of approximately 45 minutes before the tissue could be fixed for microscopy. During evisceration, the oesophagus and trachea were severed at the pharynx or in some instances were removed with the tongue and pharynx attached. The oesophagi were isolated from the pharynx and the stomach, trimmed of excess fascia and further processed for light microscopy (LM), scanning electron microscopy (SEM) and transmission electron microscopy (TEM) as detailed below. An additional three fixed specimens of similar age which had been skinned, but not eviscerated, were obtained from the Department of Anatomy and Physiology, Faculty of Veterinary Science, University of Pretoria and dissected to provide topographical data.

Topography

The three fixed, non-eviscerated specimens were carefully dissected to provide a description of the gross anatomical features and topographical relationships of the oesophagus and associated structures. This information was compared in the fresh specimens prior to evisceration. All the oesophagi were measured from the termination of the pharynx to the gastro-oesophageal junction. The splayed-open oesophagi prepared for LM (n = 3) and SEM (n = 3) were utilised for a description of the luminal relief (mucosal fold pattern) prior to fixation.

Light microscopy

Six oesophagi were used for light microscopy. All samples were immersion-fixed in 10 % phosphate buffered formalin for a minimum period of 48 hours. Three oesophagi were left intact and irrigated with fixative solution from both cut ends using a syringe and immersed in a fixative bath for the minimum fixation period. They were subsequently divided, post fixation, into nine equal, transversely cut segments (Fig. 2B). Three other oesophagi were slit longitudinally, carefully splayed open and pinned, mucosa uppermost, onto cork sheets and immersed, oesophagus down, in a fixative bath for the minimum period. These samples were then also divided into nine segments, post fixation. All samples were dehydrated through 70, 80, 96 and 2X 100 % ethanol and further processed through 50 : 50 ethanol : xylol, 2X xylol and 2X paraffin wax (60 - 120 minutes per step) using a Shandon model 2LE Automatic Tissue Processor (Shandon, Pittsburgh, PA, USA). Tissue samples were finally embedded manually into paraffin wax in brass moulds. Sections

were cut at 4 - 6 μm, stained with haematoxylin-eosin (H&E) (Luna, 1968), periodic acid-Schiff (PAS) (Pearse, 1985) or Verhoeff's elastic stain (Bancroft & Cook, 1994) and viewed and micrographed using a Reichert Polyvar (Reichert, Austria) compound light microscope fitted with a differential interference contrast (DIC) prism.

Scanning electron microscopy (SEM)

Six oesophagi were used for SEM description of the mucosal surface and mucosal relief. Three oesophagi were slit along their length and rinsed several times in Ringer lactate solution to remove adhering mucus and detritus. The oesophagi were splayed open along their length and pinned onto cork sheets, mucosa uppermost, with care being taken to avoid stretching the specimens. Small wax discs were placed between the cork sheet and the oesophagus in each of the nine regions equivalent to those sampled for LM. The tissue in contact with each disc was pinned to the wax and excised around the perimeter. The pinned tissue discs were then immersion fixed in 4 % glutaraldehyde in 0.2 M sodium cacodylate buffer (pH 7.2 – 7.4) for a minimum of 48 hours. The fixed samples were rinsed twice in 0.2 M sodium cacodylate buffer (pH 7.2 – 7.4) and routinely dehydrated through an ascending ethanol series (50, 70, 90, 95 and 3X 100 % - 30 minutes per step). Material was then critical point dried from 100 % ethanol through liquid-CO_2 in a Polaron Critical Point Drier (Polaron, Watford, England). The samples were mounted onto brass or aluminium viewing stubs with a conductive paste (carbon dag) and sputter coated with gold using a Balzers 020 Sputter Coater (Balzers Union, Liechtenstein). Specimens were viewed and photographed using a Hitachi S-2500 Scanning Electron Microscope (Hitachi, Tokyo, Japan) operated at 8 kV.

A further three oesophagi were left unslit after removal and pinned to their original length onto cork sheets. These specimens were irrigated several times from both cut ends with 4 % glutaraldehyde in 0.2 M sodium cacodylate buffer (pH 7.2 – 7.4) using a syringe and immersion fixed, oesophagus down, for another 4 hours in a 4 % glutaraldehyde fixative bath. Each oesophagus was divided into nine equal segments and each segment was cut longitudinally to expose the luminal surface. These were then rinsed in 0.2 M sodium cacodylate buffer (pH 7.2 – 7.4) and processed further for SEM viewing as indicated above.

Transmission electron microscopy (TEM)

Preliminary LM and SEM findings obtained from the nine regions examined indicated that the oesophagus, based on peculiarities in the surface relief and variations in the surface cell population of the epithelium, could be divided into three broad regions (cranial, mid and caudal) exhibiting similar characteristics. After an initial fixation period of 3 hours, glutaraldehyde-fixed SEM samples representing the three main regions identified above were trimmed to supply small blocks of tissue for TEM. A total of three oesophagi were therefore utilised for TEM and the samples were processed according to the protocol outlined below.

Samples were rinsed twice in 0.2 M sodium cacodylate buffer (pH 7.2 – 7.4) and post fixed in 0.2 M sodium cacodylate-buffered 1 % osmium tetroxide for 3 - 4 hours. After two further rinses in sodium cacodylate buffer, the tissue was routinely dehydrated through an ascending ethanol series (50, 70, 90, 95 and 3 X 100 % - 20 minutes per step). After one change of 100 % ethanol : 100 % acetone and 2 X 100% acetone, there followed three transition steps to resin through 30 : 70, 50 : 50, 70 : 30 acetone : resin mixtures (2 hours per step). Tissues were then taken through 2 X 100 % resin changes (3 hours per step) and embedded in Embed-812/Araldite Resin (EM Corp., Chestnut Hill, MA, USA) according to Cross (1989). Semi-thin sections (0.3 – 0.5 μm) were cut with glass knives and stained with Toluidine Blue-O (E. Merck, Darmstadt) for light microscopic evaluation. Ultra-thin sections (0.06 – 0.075 μm) were cut with a Microstar Diamond Knife (Micro Engineering Inc., Huntsville, Texas, USA) using a Reichert Ultracut Ultramicrotome (Reichert, Austria) and stained with 2 % aqueous uranyl acetate (Watson, 1958) for 10 - 15 minutes and Reynolds' lead citrate (Reynolds, 1963) for 3 - 5 minutes. Sections were viewed and photographed using a Jeol 1200EX Mk-I Transmission Electron Microscope (Jeol Ltd., Tokyo, Japan) operated at 80 kV.

RESULTS

Macroscopic features

The oesophagus lay along the midline of the body and extended from the base of the basihyoid plate to the clearly defined, ridged gastro-oesophageal junction (Fig. 3A & Inset Fig. 1A). It was superficially situated close to the ventral body wall within the mediastinum and was closely related to the trachea. The latter lay ventral to the oesophagus for a short distance after leaving the larynx before swinging to the left border of the oesophagus where it continued caudally for most of its length. At the cranial border of the lungs the

trachea crossed sharply to the right over the ventral aspect of the oesophagus before dividing into two primary bronchi (Fig. 1A).

The oesophagus was exceptionally wide and flaccid along most of its length and averaged approximately 3.5 cm in width (Fig. 1A). At the bifurcation of the trachea, however, it narrowed appreciably to approximately 1.5 cm and was firmer indicating a greater muscular component. This segment was approximately one-third the length of the oesophagus and corresponded to the caudal region identified by histology (see below). It passed dorsally to the heart and through two membranes, *viz*., a post pulmonary membrane situated at the base of the lungs and to which the pericardial sac was attached, and the post hepatic membrane positioned apically to the heart. Fat tissue containing the thymus, thyroid and parathyroid glands surrounded the oesophagus and trachea at the bifurcation of the trachea at the base of the heart (Huchzermeyer, 1995). The length of the dissected oesophagi examined was 27 - 32 cm.

Macroscopically, the entire luminal surface of the oesophagus presented a series of longitudinal folds (Fig. 2A & 2B[i]). Three regional sub-divisions could be distinguished (cranial, mid and caudal) which were based on the nature of the folding, in both profile and number of folds in each region (Fig. 2A). The most cranial region consisted of numerous fine anastomosing and branching, longitudinal folds which converged from the pharyngeal region. In the mid-region these folds were consolidated into 12 – 14 widely spaced folds which occasionally adopted a zigzag course. In the caudal region the folds appeared to condense, forming approximately 10 highly convoluted, tightly packed folds which exhibited a relatively low profile. Subepithelial nodules (shown by LM to be lymphoid accumulations) were visible throughout the oesophagus but increased in number in the caudal region, particularly in the immediate vicinity of the cardiac sphincter of the stomach. A prominently ridged cardiac sphincter occurred at the gastro-oesophageal junction which was clearly defined in terms of both colour and appearance. The cream coloured oesophagus was grooved in appearance compared to the reddish-brown and relatively smooth textured stomach (see inset Fig. 1A & Fig. 3A).

Light microscopy (LM)

Based on the macroscopic features outlined above and a preliminary histological examination, the nine segments of the oesophagus initially sampled for LM and scanning and transmission electron microscopy (see Materials and Methods above) could be grouped into three regions based on morphological

similarities. The cranial region comprised four segments (totalling 12 to 14 cm in length), the mid-region two segments (this was considered to represent a transitional region between the cranial and caudal regions and totalled between 6 to 7 cm in length), and the caudal region represented by three segments (totalling 9 to 10.5 cm in length). These figures were based on an average oesophageal length of 27 to 32 cm. The cranial region therefore made up approximately 43 % of the total length of the oesophagus, the mid-region 22 % and the caudal region 35 %.

The wall of the oesophagus was composed of a mucosa, submucosa, tunica muscularis (consisting of inner circular- and an outer longitudinal layers) and an adventitia (Figs. 1B & C & 4A). In cross sections of all regions of intact oesophagi, the mucosa displayed a series of alternating major and minor folds which jutted into the lumen (Figs. 1B & 2C-E). The number of folds was relatively constant in the cranial and mid-regions of the oesophagus (± 14), but tended to diminish in number towards the caudal region (± 10). The detailed histological description which follows was based on transverse sections of oesophagi to facilitate easier orientation.

In the cranial region of the oesophagus the major mucosal folds appeared elaborate and consisted of primary folds, secondary folds and frequently tertiary folds (Figs. 2C, 4A, 5B & 6A). The broad-based primary folds were composed of a thick, ciliated epithelium supported by a well developed lamina propria. The muscularis mucosae, which was variably developed throughout the cranial region, only extended for a short distance into the base of the primary folds (Fig. 4A). Secondary folds (typically devoid of a muscularis mucosae) extended from the sides and tips of the primary folds at regular intervals and in turn gave origin to smaller, more delicate tertiary folds supported only by a thin layer of the lamina propria. The minor mucosal folds also displayed a broad base, but tapered markedly towards the apex, forming short, triangular structures. Again, small secondary folds extended from the primary fold. Although all the components of the minor folds were supported by the lamina propria, no involvement of the muscularis mucosae was observed.

The epithelial lining of the oesophagus in the cranial region consisted of typical respiratory epithelium, *viz.* pseudostratified, columnar ciliated epithelium with goblet cells (Figs. 4B–D & 5A). However, in many parts of the material studied the epithelium was composed of numerous cell layers, creating the impression of a stratified columnar epithelium (Figs. 4B & D). This situation was confirmed by transmission electron microscopy (see below). PAS-staining indicated an extremely high concentration of goblet cells in the

epithelium. These cells had a plain, granular cytoplasm and a basally compressed nucleus. The cells were strongly PAS-positive indicating a high concentration of muco-polysaccharides and were bulbous in shape with only a narrow strip of apical cytoplasm in contact with the luminal surface. Situated between the goblet cells were numerous ciliated cells which stained pink/red in H&E-stained sections. The apical surface of these cells was expanded and formed an almost solid cytoplasmic layer through which the goblet cells made narrow points of contact with the lumen (Fig. 4D). The long cilia were heavily concentrated and ubiquitous in the cranial region (Figs. 4B,C & 6C).

In those parts of the mucosa containing a typical respiratory epithelium, the nuclei were arranged in two layers (Fig. 4C). The nuclei of the basal layer were dense and round and this layer was clearly demarcated. The second nuclear layer was more diffuse and exhibited elongated, vesicular nuclei oriented parallel to the long axis of the cells. In stratified columnar regions of the mucosa, the number of nuclear layers was increased (Figs. 4B & D). The basal layer of epithelial cells rested on a basal lamina which was conspicuous in PAS-stained sections and appeared undulated.

Typical flask-shaped intra-epithelial glands were common throughout the cranial region of the oesophagus and were found on and between the various types of mucosal folds. These structures were located exclusively within the pseudostratified/stratified columnar epithelium and were sometimes associated with localised epithelial thickenings. The gland was composed of a crypt-like epithelial fold, the base of which was lined by a layer of goblet cells resting on the basement membrane (Figs. 4B & D). Ciliated cells, when present, were restricted to the neck of the gland.

The lamina propria was well developed and stretched from the basal lamina to the muscularis mucosae (Fig. 4A). In the absence of the muscularis mucosae (at the most cranial aspect of the oesophagus) the lamina propria and submucosa formed a continuous connective tissue layer. In some sections, the lamina propria appeared to consist of two distinct layers. Immediately beneath the basal lamina was a thin band of reticular connective tissue and collagen fibres which closely followed the basal contours of the epithelium. This layer appeared pale in colour using both Verhoeff's elastic- and H&E-stains. Beneath the band was a thicker layer of irregular dense connective tissue which formed the core of the various mucosal folds and extended to the muscularis mucosae. There was a very sparse distribution of elastic fibres in the lamina propria. Immediately beneath the epithelium was an extensive capillary plexus which was linked to a network of larger vessels situated in the irregular dense connective tissue

layer of the lamina propria. The larger vessels were particularly obvious at the centre of the mucosal folds. Mast cells were occasionally noted and occurred either singly or in small groups of three to four and were generally associated with small blood vessels in the sub-epithelial plexus. Deeper regions of the lamina propria, muscularis mucosae and submucosa did not reveal any Mast cell activity. These cells appeared morphologically similar to those observed in the oral cavity (see Chapter 3).

The most cranial aspect of the oesophagus was devoid of a muscularis mucosae which first appeared towards the middle of the cranial segment as sparsely distributed thin strands and small bundles of smooth muscle. At the apex of some of the larger folds, similar collections of smooth muscle fibres were observed, possibly indicating an extension of the muscularis mucosae. This layer rapidly established itself as a solid band of smooth muscle oriented in an extended spiral throughout the remainder of the cranial region. The submucosa exhibited similar features to the fibrous layer of the lamina propria. As described above, the submucosa and lamina propria were continuous at the cranial aspect of the oesophagus. In the area where the smooth muscle bundles of the muscularis mucosae made their appearance, the submucosa was more loosely arranged and relatively wide. In the more distal portion of the cranial region this layer became appreciably thinner and denser in nature, being sandwiched between the ever-thickening muscularis mucosae and tunica muscularis. A large submucosal vascular plexus was present with distributing vessels to the lamina propria and, through connective tissue channels between the smooth muscle bundles of the tunica muscularis, to the adventitia.

The tunica muscularis was composed of an inner circular layer and outer longitudinal layer of smooth muscle (Fig. 4A). The two layers were separated by a thin band of irregular dense connective tissue. The muscular tunic appeared poorly developed in the cranial aspect of the cranial region and appeared in the form of small bundles of longitudinally oriented fibres separated by intermuscular tracts of connective tissue. The inner circular muscle layer was reinforced more caudally by the addition of a superficially positioned thin band of transversely oriented muscle bundles. In the cranial region both the inner circular and outer longitudinal muscle layers, although well developed, generally remained incomplete and never formed solid layers.

Bundles of non-medullated nerve fibres and neurons were associated with the appearance of the inner circular muscle layer, being situated towards the periphery of the oesophagus in the region of the adventitia. The peripheral location of the nerve cells and fibres was maintained even after the

establishment of the outer longitudinal muscle layer, with neural elements being present between the muscle bundles. The adventitia was in the form of a loose connective tissue which housed an extensive arterial and venous plexus.

The mucosal folds in the mid-region of the oesophagus were similar in basic appearance and arrangement to those located in the cranial region. The major folds were less elaborate, however, and showed little sign of tertiary branching (Figs. 1C & 2D). Histologically, the mid-region exhibited similar morphological features to those seen in the cranial region. The epithelial lining was similar to that described above although this region appeared to have a higher density of goblet cells (Figs. 5C & D). Fewer intra-epithelial glands were present compared to the cranial region, although the mid-region overall showed a strong PAS-positive reaction.

Lymphoid tissue occurred in the form of small, sub-epithelial aggregations, immediately below the basement membrane in the lamina propria of the folds. In the cranial region, these nodules were sparsely distributed, but showed an increase in occurrence from the lower mid-region of the oesophagus towards the caudal region where the nodules became particularly prominent adjacent to the stomach. The nodules were observed in the apical region of the folds, but also occurred in the basal regions of some folds. A few lymphocytes were seen to penetrate the epithelial layer where the nodules occurred. The penetration of migratory lymphocytes into the epithelial layer was also seen in TEM sections (see Fig. 10B).

Ciliation throughout the mid-region appeared to vary amongst specimens and sections examined. In some sections, ciliation appeared evenly distributed and consistent throughout the region (Fig. 5C), while in other sections, the ciliation diminished and even disappeared in the more caudal aspects of the segment. The disappearance or depletion of ciliation in some samples thus created the impression that the mid-region was a transition zone.

The muscularis mucosae was better developed and more compact in appearance with less intermuscular connective tissue. It was seen to penetrate deeper into primary mucosal folds, but not into the secondary divisions (Fig. 1C). The submucosa also appeared more compressed/thinner than in the cranial region. The extensive capillary and larger blood vessel plexuses retained their respective positions, similar to the pattern seen in the cranial region.

Clearly demarcated groups of neurons and associated non-medullated nerves were present throughout the mid-region in the connective tissue band located between the circular- and longitudinal layers of the tunica muscularis, forming a typical myenteric plexus. This plexus became progressively better developed further caudally along the oesophagus where it was linked to a less prominent submucosal plexus. The tunica muscularis itself differed little in structure to that in the cranial region.

In the caudal region of the oesophagus the alternating pattern of major and minor folds was again observed. However, the folds were generally fewer in number and displayed less subdivision than the cranial and mid-regions (Figs. 2E & 5F). The microscopic structure of this region was similar to that of the mid-region, except that the tunica muscularis was thicker and more compactly arranged. Ciliation was observed in most sections but was sometimes patchy (Fig. 5E). Very few intra-epithelial glands were seen. The transition between the oesophagus and the stomach was abrupt and was indicated by a marked thinning of the epithelial lining as well as by a number of mucosal folds representing the ridged gastro-oesophageal junction (Figs. 3A-C). The pseudostratified/stratified oesophageal epithelium was replaced by a simple columnar epithelium which remained non-glandular for a short distance (Figs. 3B & C). The glandular region of the stomach contained simple tubular glands.

Although elastic fibres were observed in larger blood vessels and in the adventitia in all regions examined in Verhoeff's stained sections, they appeared very sparsely distributed or absent in the submucosa and circular layer of the tunica muscularis. The lamina propria appeared to be devoid of any elastic fibres.

Scanning electron microscopy (SEM)

Based on the findings of the histological study and on the pattern of luminal mucosal folds observed macroscopically, the specimens for SEM were also divided into cranial, mid- and caudal regions.

Cross-sections of the cranial region viewed obliquely revealed similar features to those observed by LM. The alternating major and minor mucosal folds, and the subdivision of the former into primary, secondary and tertiary folds, could be clearly discerned. The various connective tissue and muscular components (except the muscularis mucosae) of the oesophageal wall could also be clearly seen (Fig. 6A). In pinned specimens this region displayed a series of low-profiled, fine, closely packed longitudinal folds which branched and anastomosed at regular intervals throughout the length of the sample (Fig.

6B). Numerous fine longitudinal grooves were apparent on the larger folds and represented the borders of the secondary and tertiary folds seen in unpinned samples.

Higher magnification of the mucosal folds revealed a densely ciliated surface covering all aspects of the folds. The cilia appeared long and of similar diameter, and were generally evenly distributed. Occasional tufts of cilia, probably originating from a single cell, were also observed (Figs. 6C & D). Randomly distributed small gaps were present between the ciliated cells, probably indicating the site of goblet cells (Figs. 6C & D). The latter were often difficult to resolve due to the dense ciliation. Larger islands of non-ciliated cells were also apparent. These cells displayed round to oval surface profiles and were covered by numerous thick, stubby microvilli of variable diameter. Strands of mucus were trapped on the surface of the cells and some showed crater-like openings indicative of goblet cells (Fig. 6D). Based on LM observations, the non-ciliated cells probably represent goblet cells. The intra-epithelial glands which were widely distributed in the cranial region could not be seen by SEM in the pinned samples. This could be due to stretching of the mucosa during pinning, thus obliterating the grooves forming the intra-epithelial glands. The groups of non-ciliated cells surrounded by ciliated elements may even represent the goblet cells found at the base of the glands and now exposed due to the stretching of the epithelium.

The pattern of folds in the mid-region was again similar to that seen by LM. In cross-sections of this region the major mucosal folds appeared more robust than those in the cranial region and jutted prominently into the lumen. The primary folds divided into numbers of secondary folds, but very few tertiary folds were obvious (Fig. 7A). Pinned samples of the mid-region revealed a limited number of prominent longitudinal folds and intervening smooth areas. The folds showed only a few fine longitudinal grooves and rarely branched and anastomosed. Fine cross-striations were observed which probably represented a shrinkage artifact (Fig. 7B).

In the samples studied, only randomly distributed concentrations of ciliated cells were observed, mainly on the ridges of folds. The vertical sides and troughs of the folds showed only isolated ciliated cells. Between the pockets of ciliated cells were sheets of slightly raised polygonal cells and rounded goblet cells (Fig. D). The polygonal cells were studded with variable numbers of short microvilli and ridge-like concentrations of microvilli, occurring at the perimeter of the cells, accentuated the shape of the cells. The obvious goblet cells were characterised by a crater-like opening and a paucity of microvilli. Mucus droplets were sometimes associated with the goblet cells (Fig. 7D). However, some of the cells showed

features typical of both cell types, that is, a part of the cell surface was adorned with microvilli, while the rest of the surface was represented by a smoother area with a crater-like opening (Fig. 7D). These observations would suggest that all or most of the non-ciliated cells represented varying stages of goblet cell development. Towards the caudal aspect of the mid-region a number of completely or partially eroded cells appeared. The mid-region overall, appeared to represent a transition zone from a ciliated to a non-ciliated epithelium.

The longitudinal mucosal folds in the caudal region displayed a simple structure in cross-section with the major folds giving rise to fewer secondary folds (Fig. 8A). Near the gastro-oesophageal junction the folds adopted a wavy appearance (Fig. 8B), believed to be the result of post mortem contraction or shrinkage during specimen preparation. Numerous low-profiled transverse folds were also present (Fig. 8B) at the junction, confirming the macroscopic observations (see Fig. 3A). The honeycomb appearance of the luminal surface, indicating the cardiac region of the stomach, appeared abruptly (Fig. 8B). The epithelium in the caudal region displayed large areas of cellular erosion (Fig. 8C), with cells in various stages of degeneration (Figs. 8D & E), indicated by the appearance of holes, cracks, pitting or complete loss of material. Mucus droplets/remnants associated with some of the eroded cells identified them as goblet cells. Sheets of polygonal cells, whose surfaces were either smooth or covered with short, stubby microvilli were randomly distributed throughout the region. As in the mid-region, polygonal cells with distinctly demarcated microvillous borders and goblet cells could be distinguished. No ciliated cells were seen in the caudal aspect of the oesophagus using SEM techniques. Small round to oval, low-profiled nodules were observed in the caudal region and appeared to occur mainly in the troughs between the major mucosal folds. The frequency of the nodules appeared to increase towards the gastric junction and often occurred in pairs (as seen in Fig. 8F). Light microscopy revealed that the nodules (as seen using SEM) were lymphocytic in nature. The epithelium covering the nodules appeared similar in nature to the surrounding non-ciliated and often eroded epithelium of the region.

Transmission electron microscopy (TEM)

TEM was employed to provide detailed information on the structure of the ciliated epithelium lining the oesophagus and to highlight certain cellular characteristics. This technique revealed that, although in parts, the epithelium appeared typically pseudostratified ciliated in nature, it generally adopted the form

of a stratified columnar epithelium. This appearance was sometimes accentuated by the plane of section.

The cells situated at the base of the epithelium varied in shape. Many of these cells were tall columnar elements which stretched for a variable distance into the upper layers of the epithelium (Fig. 9A). Other cells adopted a variety of shapes ranging from round/cuboidal to angular with numerous cytoplasmic processes and were confined to the immediate vicinity of the basal lamina. Despite their differences in shape, all the basal cells exhibited similar cytoplasmic characteristics and it was not always possible to distinguish ciliated cells from developing goblet cells. All the basal cells generally displayed a broad base of contact with the basal lamina to which they were firmly attached by hemi-desmosomes. These structures revealed the classical features of this anchoring device, viz., a localised density situated at the cytoplasmic face of the basal plasmalemma and connected to the cytoplasm by radiating microfilaments. The area of contact was further increased by numerous cytoplasmic extensions of the epithelial cells which interdigitated with similar structures formed by the lamina propria (Figs. 10A & B).

The well-developed basal lamina closely followed the basal contours of the epithelial cells and consisted of an electron dense lamina densa separated from the plasmalemma by a relatively clear zone, the lamina rara. Fine microfilaments were seen to transverse the lamina rara, connecting the lamina densa to the plasmalemma. Immediately beneath the lamina densa was a poorly demarcated lamina reticularis which, with the basal lamina (see inset, Fig. 10A), constituted the basement membrane seen by LM. The fine reticular fibres of the lamina reticularis were intermingled with variably sized collagen fibres of the lamina propria. The collagen fibres were oriented in various directions, although sheets of parallel oriented collagen fibres, often alternating in direction, were a feature of the deeper layers of the lamina propria. Rows of stellate fibroblasts with attenuated cytoplasmic processes were situated in the lamina propria between sheets of collagen fibres. Typical features of these cells included an elongated nucleus with a distinct layer of marginal heterochromatin, and cytoplasm filled with profiles of granular endoplasmic reticulum (Fig. 12A). Numerous capillaries were situated just beneath the basement membrane and on occasion were seen within the connective tissue papillae pushing into the epithelium (Fig. 10B). The thin endothelial lining of the capillaries displayed numerous micropinocytotic vesicles indicating active transfer of substances between the blood vessels and the surrounding tissue. The endothelial cells were also enclosed by a basal lamina of similar structure and dimensions to that underlying the epithelium.

The nucleus of the columnar basal cells were elongated and oriented parallel to the long axis of the cell. It was generally situated closer to the base of the cell and displayed a number of nuclear membrane folds. The karyoplasm was vesicular in nature with small, moderately electron-dense accumulations of marginal chromatin sometimes being observed. A large, dense nucleolus was a consistent feature (Fig. 11A). The nuclei of the smaller basal cells exhibited similar properties, but were more compressed.

The homogeneous cytoplasm was filled with free ribosomes which gave the cells a relatively dense appearance. Large round to oval mitochondria with lamellar cristae were often concentrated at the base of the cells, although these organelles were also encountered in groups at the apical pole of the nucleus and scattered throughout the cytoplasm. Large numbers of microfilaments were also present. These supporting elements were frequently arranged in bundles and generally oriented parallel to the long axis of the cell. Scattered strands of granular endoplasmic reticulum (GER) and isolated lipid droplets were also consistent features (Figs. 9A & 14A).

The supranuclear region of many of the columnar cells showed features typical of developing goblet cells. Numerous profiles of the Golgi apparatus could be identified and small moderately electron-dense bodies (mucigen granules) were seen to be surrounded by, or lay adjacent to, the cisternae. In more advanced stages of development, the mucigen granules were observed to have increased in size and number, but were restricted to a particular location in the supranuclear cytoplasm (Fig. 11B). These granules were filled with moderately electron-dense homogenous material and appeared to be membrane-bound, although it was not possible to resolve the membrane in the material studied. Many of the granules were flattened or comma-shaped and often closely aligned (Figs. 12A & B). Continued aggregation and growth of the granules made it progressively more difficult to identify elements of the Golgi apparatus and other cytoplasmic organelles. When present, the organelles were found at the periphery of the goblet cells.

Profiles of GER were sometimes seen lying between the mucigen granules and mitochondria trapped at the cell periphery appeared thin and elongated. The accumulation of mucigen granules was accompanied by a gradual shortening of the cell and a change in shape of the nucleus from elongated to more flattened forms. In some cells the nuclear surface abutting the region of granules became cup-shaped. The cytoplasm also increased in density due to the compression effect of the increasing numbers of mucigen granules (Figs. 12A & B).

Mature goblet cells were typically large, oval-shaped structures which were completely filled with mucigen granules. The granules were surrounded by a thin rim of dense cytoplasm displaying a paucity of organelles. The nucleus was compressed against the basal plasmalemma and was relatively electron-dense. Most of the granules were round and pale in appearance. Coalescence of the granules was seldom observed. Goblet cells were present in all strata of the epithelium (Figs. 9A & 12A), but were particularly obvious in the more superficial layers. The areas of contact of the goblet cells with the oesophageal lumen was small and the narrow apical plasmalemma was adorned with microvilli. The apico-lateral plasmalemma was attached to neighbouring ciliated cells and/or goblet cells by junctional complexes (Fig. 12B) similar to those described below between ciliated cells. In some sections the apical region of cells, which appeared to be developing goblet cells, formed large luminal protrusions, separated from the main body of the cell by a layer of junctional complexes (Fig. 9B). This observation possibly indicates that the protrusions are, in fact, complete cells in the process of being released from the surface of the epithelium. Some of the protrusions appeared to lie free in the lumen, but this effect could be due to the plane of section. The apical cytoplasm of the parent cells and the protrusions were filled with fine homogeneous material and large numbers of relatively small mucigen granules similar to those described in earlier stages of goblet cell formation. Very few cytoplasmic organelles were observed and the cells and projections were covered by short microvilli.

The apical cytoplasm of the ciliated cells was dominated by a row of basal bodies which were situated just beneath the plasmalemma and gave rise to the cilia (Figs. 12B, 13A, B & D). The dense wall of the basal bodies displayed nine sets of triplet microtubules which were continued as the nine outer microtubular doublets of the cilium. The two central microtubules of the cilia emanated from a collection of dense material situated at the apical end of the basal body. The lumen of the basal bodies appeared “empty” in some instances while in others it was filled, or partially filled, with a block of dense material. Long striated ciliary rootlets extended deeply into the apical cytoplasm from the base of each basal body. In some instances the rootlets appeared spiralled or were extremely long (Figs. 13A & B). In cross-section the cilia revealed the typical 9 X 2 + 2 microtubular arrangement and protein structures (dynein arms, radial spokes, etc.) associated with the axoneme. Situated between the cilia were numerous short microvilli which in cross-section contained a core of microfilaments. A glycocalyx was associated with the surface of the microvilli (Fig. 13C & Fig. 13C inset). The cytoplasm in the immediate vicinity of the basal bodies was relatively free of cytoplasmic organelles but did contain apparently randomly oriented microtubules and microfilaments. Immediately beneath this zone was a concentration

of large, pale mitochondria with numerous, well-developed, lamellar cristae. The ciliated cells often occurred in groups and were separated from each other by typical junctional complexes composed of more superficially positioned tight junctions (*zonula occludens*) and gap junctions (*nexus*) and deeper bands of desmosomes (*zonula adherens*). It was obvious at low magnification that the cells towards the base of the epithelium were separated by wide intercellular spaces (Fig. 9A), whereas the more superficially positioned cells were more intimately connected (Figs. 13A & D). This phenomenon could have been the result of the delay in fixing the tissue or by inadequate penetration of the fixative solution into the deeper tissue layers. The basal cells were connected to each other at regular intervals by relatively large lateral cytoplasmic extensions emanating from each cell and which displayed one or more desmosomes at the point of contact (Figs. 9A & 14A & B). The larger intercellular gaps so created were filled with numerous slender cytoplasmic projections which interdigitated with each other. In the deeper layers of the epithelium both the lateral cell membranes and the apical plasmalemma were involved in the form of cell contact described above. Although the more superficial cell layers did not reveal exaggerated intercellular spaces, the slender cell processes were still well-developed and numerous and intimately linked neighbouring cells. Mature goblet cells revealed less complex lateral cellular interdigitations.

Migratory lymphocytes were regularly encountered in the deeper layers of the epithelium. These cells exhibited a spherical profile characterised by a large round nucleus which occupied much of the cell (Fig. 10B). The karyoplasm was extremely electron-dense and characterised by dense marginal blocks of heterochromatin and a distinct nucleolus. The thin rim of pale cytoplasm revealed scattered free ribosomes and a few mitochondria. A centriole and some short strands of GER were also sometimes seen. The plasmalemma was observed to make contact with surrounding cells by means of short, stubby processes creating a “halo” effect between the lymphocyte and the surrounding cells. No cell junctions were ever observed between the lymphocytes and surrounding cells. Occasional large cells, identified as macrophages, were also seen in the epithelium. The nucleus was generally oval to slightly elongated and appeared vesicular with very little chromatin condensation. A distinct nucleolus was observed. The homogenous, finely granular cytoplasm contained numerous mitochondria, a few short profiles of GER, some structures resembling primary lysosomes, an occasional secondary lysosome and myelin figures. The secondary lysosomes, when present, were filled with heterogeneous, moderately osmiophilic material as well as some very dense particles and pale lipid droplets. The cytoplasm extended numerous processes into the intercellular spaces. Some were relatively thick and

long, resembling pseudopodia, while others were slender structures similar to those formed by the epithelial cells. Organelles were generally restricted to the cell body and not found in the cell processes. The wandering macrophages, like the migratory lymphocytes, did not form junctional complexes with surrounding epithelial cells. Although no Langerhans (Birbeck) granules were ever seen in the migratory cells in the material studied, their morphological features suggest that they are typical Langerhans cells (antigen detectors) previously described pervading stratified squamous epithelia (Gerneke, 1980).

DISCUSSION

Anatomical descriptions of the crocodilian oesophagus are sketchy and incomplete. Van der Merwe and Kotzé (1993) simply note, in the Nile crocodile, that “at the thoracic inlet the trachea is situated to the left of the oesophagus which lies in the midline within the dorsal mesentery”, and illustrate the posterior segment of this organ as a straight tube of constant diameter. The illustration of the digestive tract of the “Florida alligator” (Reese, 1913) also depicts the oesophagus, with the exception of its origin from the pharynx, as a straight tube of equal width. In contrast, the present study demonstrated that the oesophagus of the Nile crocodile can be divided into two anatomically distinct regions. The long anterior segment, which stretches from the pharynx to the bifurcation of the trachea is wide and flaccid, whereas the shorter posterior segment which enters the stomach is narrower, firm and round.

Luppa (1977) divides the oesophagus of reptiles in general, into two regions, noting that “the more extensive anterior section is sharply differentiated from the shorter, posterior esophageal section which enters the visceral cavity dorsal to the pericardio-peritoneal septum.” However, no indication of a morphological distinction between the two sections is given. In the Nile crocodile, the oesophagus has to pass through two membranes (the post-pulmonary and post-hepatic membranes) to reach the stomach, although this point does not coincide with the change in calibre which is observed. In the alligator, the oesophagus is described as stretching from the pharynx to the stomach (Chiasson, 1962). In the specimens of the Nile crocodile examined, the oesophagus originated at the base of the cartilaginous basihyal plate (which forms a support for the floor of the pharynx) and terminated at the prominent, internally ridged gastro-oesophageal junction.

Parsons and Cameron (1977) described the internal relief of the reptilian oesophagus in a large number of species, including representatives of the Crocodilia. They noted that in the Crocodilia the typical

pattern of oesophageal relief was one of “long, straight, smooth-surfaced longitudinal folds which are very prominent and un-branched.” However, a distinction was made between the Alligatorinae which typically displayed longitudinal folds of similar diameter along their complete length, and the Crocodylinae where the longitudinal folds were “generally broader, rougher and more irregular than in the Alligatorinae.” In addition these folds were stated to “branch and fuse more frequently and have variable diameters.” These observations were confirmed in the present study which clearly revealed branching and anastomosing of the longitudinal folds (particularly in the more anterior part of the oesophagus) as well as variability in the diameter of the folds. Reese (1913), in his study of the “Florida alligator”, simply noted that the epithelium and submucosa of the anterior region were thrown into complicated folds with less complicated folds being present more distally. Chiasson (1962) merely states that “the mucous lining of the esophagus is thrown into longitudinal folds throughout its entire length.”

Although recognising the occurrence of longitudinal folds, none of the earlier studies presented specific observations on the nature of the folds or utilised morphological peculiarities to divide the oesophagus into specific regions or zones. The most striking feature observed in the present study was the consistent occurrence, throughout the oesophagus, of alternating major and minor folds. This was particularly obvious in cross-sections of the oesophagus prepared for LM, but could also be seen in SEM preparations. Moreover, both sets of folds displayed a regional variation in their complexity and number, making it possible to divide the oesophagus into three distinct zones based on these criteria.

The cranial zone or region exhibited a number (± 12 - 14) of fine, low profiled, longitudinal folds which freely branched and anastomosed. These folds represented the continuation of the more numerous fine folds found throughout the pharyngeal region (see Chapter 3). The major folds (and to a lesser extent the minor folds) in this region displayed a high degree of secondary and tertiary folding, a phenomenon not observed in the rest of the oesophagus.

The mid-region displayed a similar number of folds, although these were less complex in design than those encountered in the cranial region. The major folds were more robust in appearance, jutted appreciably into the oesophageal lumen and showed a limited degree of secondary folding. There was a reduction in the number of folds in the caudal region (± 10 folds). Although they differed little in structure from those in the mid-region, the formation of secondary folds was severely limited. In SEM samples the longitudinal folds in the caudal region were seen to adopt a zigzag course. This phenomenon was also

observed in fresh samples when the oesophagus was removed from the carcass, leading to the suggestion that zigzag folding of the caudal region simply represents a post mortem artifact which, in SEM samples, is possibly accentuated by the degree of shrinkage generally associated with this technique. The prominent transverse creases seen on the longitudinal folds throughout the mid-region are probably also indicative of post mortem/preparatory technique artifacts. It should be noted, however, that SEM revealed a narrow region at the gastro-oesophageal junction where transversely oriented mucosal folds were clearly present. During their examination of a small specimen of *Caiman crocodilus*, Parsons and Cameron (1977) described the presence of definite transverse ridges situated between the longitudinal folds in the distal region of the oesophagus. These ridges were described as “little more than striations” which may in fact have represented part of the gastric relief. According to Parsons and Cameron (1977) the existence of transverse or oblique folds would only serve to impede the passage of food through the oesophagus and are therefore rarely encountered in reptiles. The possibility exists that the ridges seen in the present study, as well as those seen by Parsons and Cameron (1977) in *C. crocodilus* are formed as a result of post mortem/fixation contraction of the substantial smooth muscle layers present in the region of the oesophageal-gastric junction.

The occurrence of longitudinal folds throughout the oesophagus of the Nile crocodile is typical of reptiles in general and has also been described in other Crocodilia (Béguin, 1904; Taguchi, 1920; Chiasson, 1962; Parsons & Cameron, 1977; Steel, 1989). Parsons and Cameron (1977) correctly point out that most reptiles swallow large chunks of food without chewing it. The oesophagus merely conveys the food to the stomach and digestion commences in this organ. It is obvious, therefore, that the oesophagus needs to be capable of dramatic distension to accommodate the passage of these large food masses. The distensability of the oesophagus is provided by the longitudinal mucosal folds.

The histological features of the oesophagus of the Nile crocodile agree broadly with those reported in other Crocodilia (Béguin 1904; Taguchi, 1920; Pernkopf & Lehner, 1937; Arvy & Bonichon, 1958; Luppa, 1977). The typical tissue layers were a lamina epithelialis, lamina propria, muscularis mucosae, submucosa, tunica muscularis and an adventitia. Some of these layers, however, were poorly developed or absent in the anterior segment of the oesophagus.

The lamina epithelialis in the specimens studied formed a typical respiratory type epithelium (pseudostratified, columnar ciliated epithelium with goblet cells) within which the nuclei were arranged in

two layers. In many parts of the oesophagus however, the epithelium was composed of numerous cell layers which created the impression of a stratified columnar epithelium. Goblet cells and ciliated cells found throughout the epithelium, lined the lumen. Luppa (1977), in his generalised description of the reptilian oesophagus, states that the epithelium is mainly two cells thick and contains variably distributed ciliated cells and goblet cells. Béguin (1904) described the oesophageal epithelium of the alligator as consisting of two to three layers of cells. Reese (1913), in contrast, in his study of *A. mississippiensis*, describes "twenty-five or thirty layers of cells", but adds that the nuclei of these cells were "arranged in two dense, irregular groups, one along the base of the epithelium, the other about two-thirds of the distance from the base of the free border." Taguchi (1920) does not discuss the number of epithelial cell layers, but describes the epithelium as a "stratified ciliated epithelium with many goblet cells". Pernkopf and Lehner (1937) also generalise their description of the reptilian oesophageal epithelium, stating that the mucosa is similar to that found in the amphibia and consists of ciliated and goblet cells "in two steps" and that the ciliated cells increase in number towards the hind end of the oesophagus. It was clear from the present study, and taking the plane of section into consideration, that the epithelial lining of the oesophagus varied in thickness. However, the combination of ciliated cells and goblet cells forming the superficial layer of the epithelial lining remained a consistent feature.

Taguchi (1920) compared the oesophagus in *A. sinensis*, C. *porosus* and *C. niloticus* and divided the oesophagus into three basic regions, based on the distribution and density of the ciliated cells and goblet cells within the epithelium and also the relative thickness of the muscularis mucosae throughout the length of the oesophagus. These three regions were termed the proximal- (cranial end), mid- and distal (gastric end) regions by Taguchi (1920), but he failed to define them more clearly than the description given above. Both Béguin (1904) and Taguchi (1920) found ciliation to be present throughout the oesophagus. Taguchi (1920) reported that the cilia in the distal region of the three species examined by him were "shorter and less distinct than in the proximal and mid-region" but that the ciliated cells in his specimen from *Alligator sinensis* were more common than the goblet cells in the distal portion of the oesophagus. Béguin (1904), who also described the oesophagus of the alligator (no species is named by Béguin [1904]), stated that the distal end of the oesophagus displayed a ciliated epithelium, but that there were larger numbers of goblet cells and fewer ciliated cells present. Taguchi (1920) explained this discrepancy as possibly indicating that the two types of cells could change from one cell type to the other, which he said, had been stated by many authors, although he does not elucidate further as to who these authors were. However, Taguchi (1920) also examined the distal oesophagus of *C. niloticus* and reported similar findings to those of Béguin (1904)

in the alligator, that is, the presence of fewer ciliated cells and more abundant goblet cells. Reese (1913), who sampled the oesophagus of *A. mississippiensis* from two regions, anterior (12,5 mm caudal to the pharynx) and posterior (12,5 mm cranially to the cardiac sphincter of the stomach), found that the epithelium in the anterior region was partially ciliated and that cilia were entirely lacking in the posterior region. Pernkopf and Lehner (1937) also noted that ciliation increased towards the distal portion of the oesophagus, but their description, like that of Luppa (1977) is a generalised one regarding the reptilia, in which they fleetingly refer to the crocodiles without mentioning any species. Romer (1962) states that ciliation occurs in all reptilian oesophagi, except in the case of turtles, where there is a unique presence of cornified papillae. The present investigation revealed that the oesophagus of the Nile crocodile could be divided into three regions (cranial-, mid- and caudal) based on the number of ciliated cells present on the luminal surface. Dense ciliation was always present in the cranial and upper mid-regions examined, but showed diminishing density progressively towards the stomach. In some sections, the ciliation appeared to diminish in the distal portion of the mid-region and was totally absent (with pronounced desquamation of the epithelium) in the caudal region. In these instances, the mid-region was presumed to be a transition zone between the cranial and caudal regions where the cilia gradually disappeared. In other sections however, ciliation appeared throughout the length of the oesophagus, but showed a reduction in density and length of cilia from the cranial to the caudal region. This phenomenon may simply reflect individual variation between the specimens examined. The desquamation of surface epithelial cells observed in a large number of the sections examined, and which is not mentioned by either Béguin (1904), Reese (1913) or Taguchi (1920), was attributed to possible post mortem reflux of stomach contents and/or the manner in which carcasses were handled during the slaughter and skinning process. To what extent the effect of the commercial diet (pellets) on which the animals utilised in this study were raised may have contributed to this phenomenon, could not be determined.

Although it is clear from the above discussion that conflicting reports exist regarding the extent of ciliation of the crocodilian oesophagus, the present study on the Nile crocodile, supported by observations in certain other species (Béguin, 1904; Reese, 1913; Taguchi, 1920) would appear to suggest that there is a general decrease in the number of ciliated cells lining the oesophagus from the cranial to the caudal aspects of the organ. Concomitantly, at least in the Nile crocodile and in alligators, there appears to be an increase in the density of the goblet cell component (This study; Béguin, 1904; Taguchi, 1920).

The SEM findings of the present study support the general tendency regarding ciliation outlined above. In the material studied (three oesophagi) the cranial region showed dense ciliation, the mid-region patchy ciliation and the caudal region no ciliation. This discrepancy between the SEM findings and the LM observations regarding ciliation of the caudal region could be due to individual differences in the specific batch of animals used for SEM. It is also possible that the delay between obtaining the samples and fixing them for SEM, combined with the handling of the carcasses during skinning, and evisceration possibly leading to reflux of stomach contents, could have resulted in the loss of the surface epithelium in this specific region. It is interesting that Reese (1913) also failed to find ciliation in the posterior region of the oesophagus of *A. mississippiensis*, but no indication is given regarding possible reasons.

The typical flask-shaped intra-epithelial glands found commonly throughout the cranial- and upper mid-regions of the oesophagus of the Nile crocodile were distributed on and between the mucosal folds and were sometimes found to be associated with localised epithelial thickenings. The gland was composed of a crypt-like epithelial fold, the base of which was lined by a layer of goblet cells resting on the basement membrane. Ciliated cells, when present, were restricted to the neck of the gland. Béguin (1904) described goblet cells in the alligator as “caliciform” cells and stated that they were most numerous in the valleys of the folds and that in some instances these cells lined the bottom of the folds. Whether or not Béguin (1904) was referring to intra-epithelial glands, could not be determined. Taguchi (1920) simply described the intra-epithelial glands as crypts consisting of large numbers of goblet cells and stated that they occurred in the proximal and mid-regions of the specimens examined. However, these crypts appeared to be fewer in number in *C. porosus* than in *C. niloticus* and *A. sinensis*.

Only Bath (1905, 1906) and Taguchi (1920) have described taste receptors in the oesophagus of the Nile crocodile, specifically in the cranial region. Bath (1905, 1906) described the taste receptors as being similar to those described by Merkel (1880, cited by Bath, 1905, 1906) in the lizard, *Lacerta agilis*, and concluded that the taste buds in crocodiles were also similar to those of higher vertebrates. Taguchi (1920) only rarely found taste receptors in the proximal region of the oesophagus of *C. niloticus*. The other two species of Crocodilia studied by Taguchi (1920) (*C. porosus* and *A. sinen*sis) did not show taste receptors in any region of the oesophagus. Although numerous histological sections of the proximal (cranial) region of the oesophagus were examined during this investigation, no structures remotely resembling taste receptors were observed. SEM also failed to detect any structures in this region which morphologically resembled taste receptors.

Oppel (1900, cited by Luppa, 1977) drew up a long list of species (it is not specified by Luppa as to which Class, Order or Family Oppel referred to) whose oesophagi contain glands and noted that glands occurred in the oesophagus of *Alligator*, but that they were absent in *Crocodylus*. Eisler (1889) also described glands in the caudal region of the oesophagus at the gastro-oesophageal junction of the alligator. Andrew (1959) stated that glands only occur in the oesophagus of Reptilia in exceptional cases and that where they do occur, as in *Testudo graeca*, these glands are purely mucigenic in nature. Oesophageal glands are particularly prevalent in turtles (Gabe, 1971). Béguin (1904) reviewed the earlier literature and emphasised the confusion amongst authors pertaining to the presence or absence of glandular tissue and the presence or absence of a cardiac sphincter in certain of the reptilia, including *C. niloticus*. Béguin (1904), who only examined a single, young alligator (95 cm), disputed the findings of Eisler (1889), claiming that Eisler had been incorrectly assuming that the highly/tightly folded mucosa in the caudal region of the oesophagus of the alligator, were glands. Béguin (1904) also stated that Jäger (no reference was given by Béguin (1904) in this citation) observed oesophageal glands in *C. niloticus*. Taguchi (1920) also described oesophageal glands in the three species of Crocodilia he studied and noted that in the specimen of *C. niloticus* the glands were of the simple branched tubular type and limited to a short portion in the cardiac region (referred to as the caudal region in this study) of the oesophagus. Illustrations given by Taguchi (1920) indicate clearly that he is referring to the gastro-oesophageal junction. The glands Taguchi (1920) identified in *A. sinensis* and *C. porosus* were simple un-branched tubular glands and occupied a narrow area at the distal end of the oesophagus close to the stomach.

This study revealed that the transition between the oesophagus and the stomach was abrupt and that the junction was indicated by a marked thinning of the epithelial lining. There were also a number of mucosal folds representing the ridged gastro-oesophageal junction. The pseudostratified/stratified oesophageal epithelium was replaced by a simple columnar epithelium which remained non-glandular for a short distance, but soon merged with the glandular region of the stomach which contained simple tubular glands. No glands were observed to be associated with the oesophagus of *C. niloticus* in the numerous specimens examined during the present study. The fact that the earlier studies identified glands in the more caudal aspects of the oesophagus, close to the stomach and that the glands were either of the simple tubular or simple branched tubular variety, suggests that these authors may have been describing cardiac glands of the stomach. The age of the specimens examined may also have further complicated these observations.

Luppa (1977), quoting Prenant (1896) and Gianelli & Giacomini (1896), notes that lymphocytes penetrate either individually or in aggregates from the lamina propria into the epithelium of the oesophagus in most reptiles. This investigation essentially revealed similar findings in the Nile crocodile, except that an increase in the occurrence of lymphocytic accumulations was observed from the lower mid-region of the oesophagus towards the stomach. The nodules were generally observed at the apex of the mucosal folds, but also occurred at the base of some folds. Where nodules did occur, little lymphocytic penetration of the epithelial layer was seen and most lymphocytes were restricted to the lamina propria, that is, they did not penetrate the basal lamina. However, migratory lymphocytes were seen to penetrate the epithelial layer in TEM sections, but were generally restricted to the basal layers of the epithelium (see TEM Results). Taguchi (1920) only noted accumulations of lymphocytic cells in the tunica (lamina) propria in his specimen of *A. sinensis*. Béguin (1904), although not referring to lymphocytic nodules *per se*, does mention that the “chorion” was seen to contain large accumulations of leucocytes with some degree of epithelial infiltration. Reese (1913) makes no mention of lymphocytic infiltration in his study of *A. mississippiensis*.

The presence of mast cells is an indication of allergic reactions as these cells, like basophils, contain histamine and heparin (Fawcett, 1986). Taguchi (1920) describes the presence of these cells in varying numbers in the tunica (lamina) propria, submucosa and muscularis mucosae of the oesophagus in the three species of Crocodilia studied. However, this observation should be regarded with caution, as the origin or habitat from which these specimens originated and their condition was not mentioned in his manuscript and could have influenced the numbers and occurrence of the mast cells (F.W. Huchzermeyer, personal communication, 1999). Mast cells were also observed in varying numbers in histological sections (H&E-stained) examined during this study, but were not regarded as having any particular relevance.

Van Aswegen (1975) has described the muscularis mucosae in reptiles as a poorly developed layer consisting only of a few “visceral muscle fibres”, and usually only seen in the posterior portion of the oesophagus. In turtles, the musclaris mucosae is completely lacking and in the gecko (*Tarentola annulata*) this layer is only seen during early embryological development. In the Nile crocodile it was noted that the muscularis mucosae was absent in the most cranial aspect of the oesophagus and first appeared in the middle of the cranial region in the form of sparsely distributed, small bundles of smooth muscle fibres. However, it soon established itself as a solid band of smooth muscle which extended throughout the rest of

the oesophagus. It was seen to penetrate into the primary mucosal folds, but not into the secondary divisions. A similar situation has been described in other Crocodilia. Taguchi (1920) described the muscularis mucosae in the three species studied as running the entire length of the oesophagus, but that it was less developed in the cranial region than in the distal portion. He further stated that smooth muscle bundles could be seen close to the apex in some of the larger folds, indicating extension of the muscularis mucosae into the mucosal folds. Béguin (1904) stated that the muscularis mucosae was represented only from the mid-region by smooth muscle fibres dispersed near the base of the epithelium and that these fibres multiplied towards the end of the oesophagus but did not become a well-defined layer. Taguchi (1920) ascribed this discrepancy as possibly being due to Béguin's specimen being too young. Reese (1913) also noted a few scattered muscle bundles in the cranial region of the oesophagus and referred to them as "probably" representing the muscularis mucosae, which in his specimen appeared well developed in the posterior region.

This study revealed that the submucosa occurred as a continuous connective tissue layer throughout the oesophagus, being loose in the more cranial region, but becoming thinner (denser) and more compressed from the upper mid-region towards the stomach where it became sandwiched between the ever-thickening muscularis mucosae and tunica muscularis. It was observed that in the absence of the muscularis mucosae (at the most cranial aspect of the oesophagus), the lamina propria and submucosa merged into a single connective tissue layer. This is consistent with the findings of Béguin (1904) who only examined a single small specimen of an alligator and Taguchi (1920) who examined three species of Crocodilia, viz., *C. porosus*, *A. sinen*sis and *C. niloticus*. In sections examined during this study, a large submucosal vascular plexus was present with distributing vessels to the lamina propria and, through connective tissue channels between the smooth muscle bundles of the tunica muscularis, to the adventitia. This observation was confirmed by Béguin (1904) who stated that the "chorion [assumed to represent the lamina propria and submucosa in this study] is very strongly vascularised" and by Reese (1913) who described the submucosa as being "a fairly dense mass of connective tissue, mainly of elastic fibres, through which are scattered small blood vessels." Taguchi (1920) however, does not mention vascularisation in any of the species he studied.

In the Nile crocodile, the tunica muscularis was composed of an inner circular layer and outer longitudinal layer of smooth muscle, the two layers being separated by a thin band of irregular dense connective tissue. Cranially, the tunic appeared as small bundles of longitudinally oriented fibres

separated by intermuscular tracts of connective tissue, but remained incomplete and never formed solid layers. More caudally, the inner circular muscle layer was reinforced by the addition of a thin band of transversely oriented muscle bundles. The tunica muscularis, as with the muscularis mucosae, also changed in complexity (thickness) along the length of the oesophagus, from the cranial to the caudal regions. Unlike the muscularis mucosae however, it was present in the more cranial aspect of the oesophagus, but only as a poorly developed layer.

Little is recorded in the literature regarding the structure of the tunica muscularis in the Crocodilia. Taguchi (1920) simply mentions the two layers of the tunic, whereas Béguin (1904) ends his histological description of the oesophagus at the muscularis mucosae. However, the general tendency observed in the present study for the tunica muscularis to increase in complexity towards the caudal aspect follows the pattern observed in reptiles. Pernkopf and Lehner (1937), for example, state that the “muscularis propria consists of an inner circular and an outer, weak longitudinal muscle and the latter often stretches along the whole oesophagus but only forms a complete layer in the lowest part.” Gegenbaur (1901, cited by Luppa, 1977), similarly notes that “the tunica muscularis consists of two layers of smooth muscle fibres”, but that “the external longitudinal one may be completely missing in the anterior portion of the esophagus”.

Equally little is mentioned about the external covering layer of the oesophagus. Reese (1913), in his study of the *A. mississippiensis*, describes the existence of a serosa in the posterior region of the oesophagus which he notes is “a varying but fairly thick layer” and that “it consists of the usual connective tissue groundwork with scattered blood vessels”. Taguchi (1920) only mentions an adventitia which is described as “a loose connective tissue layer which connects the organ to the body wall and the neighbouring organs.” This study revealed only the existence of an adventitia which appeared to be represented along the entire length of the oesophagus. It occurred in the form of a loose connective tissue which housed an extensive arterial and venous plexus. No sign of an outer mesothelial layer was observed in any of the sections examined during this study.

Neither Béguin (1904), Taguchi (1920), Pernkopf and Lehner (1937) or Luppa (1977) make any mention of innervation of the oesophagus, in either crocodiles, or in other reptiles examined by them. It was found during this investigation that bundles of non-medullated nerve fibres and neurons were situated near the periphery of the oesophagus in the region of the adventitia and were associated with the

appearance of the inner circular muscle layer. The nerve cells and fibres remained peripherally located even after the establishment of the outer longitudinal muscle layer, with neural elements being present between the muscle bundles. Prominent groups of neurons and associated non-medullated nerves were present throughout the mid-region of the oesophagus in the connective tissue band between the inner circular and outer longitudinal layers of the tunica muscularis and formed a typical myenteric plexus. This plexus became progressively better developed further caudally along the oesophagus where it was linked to a less prominent submucosal plexus.

No SEM study has previously been undertaken of the Nile crocodile oesophagus and it is therefore not possible to make comparative comments regarding the results obtained in this investigation. However, the results obtained by SEM confirmed the majority of the LM findings regarding the surface (luminal) morphology of the oesophagus. The lack of ciliation and the apparent erosion of cellular surfaces of the lower mid- to caudal regions encountered in the SEM samples, as opposed to the LM findings, may be attributable to individual variation or post mortem reflux of stomach contents, or both. SEM did however reveal the fine branching and anastomosing of the mucosal folds in the cranial region and to a lesser extent in the mid-region, which confirms the macroscopic findings of Parsons and Cameron (1977). The openings of the intraepithelial glands, which were observed frequently in LM sections of the cranial region and less frequently in the lower mid-region of the oesophagi examined, could not be seen by the SEM techniques used during this investigation. In the cranial region in particular, this was probably due to the density of the ciliation. Shrinkage of the tissue due to SEM preparation techniques (dehydration and critical point drying processes) may also have played a role in this phenomenon.

No ultrastructural observations of the cell types lining the oesophagus of Crocodilia have been reported. However, Luppa (1977) studied the ultrastructure of the oesophageal epithelium of the lizard, *Lacerta agilis* and gave a brief description of the ciliated cells and goblet cells present. The basic ultrastructural features of the ciliated cells and goblet cells observed in the oesophagus of the Nile crocodile agree broadly with the findings of Luppa (1977) and illustrate the structural similarity of the oesophagus which exists in the Reptilia. The organelle content, as well as the specific location of certain organelles, was identical for both cell types in *Lacerta* and *Crocodylus niloticus*. For example, in the ciliated cells of both species, the apical cytoplasm was dominated by a row of basal bodies anchored by ciliary rootlets, immediately beneath which was a zone rich in mitochondria. In addition to the general ultrastructural features of the two basic cell types, this study describes the interface between the base of the epithelial cells

and the supporting connective tissue elements which was characterised by the classical arrangement of the lamina rara, lamina densa and lamina reticularis. These components were seen to make up the basement membrane observed in LM sections. Interdigitations between cytoplasmic projections of the basal cells and the lamina propria were a particularly prominent feature in the Nile crocodile. Although Luppa (1977) mentions “well marked desmosomes in the apical region”, he does not elucidate further regarding other types of cell contacts in the various strata of the epithelium and which were observed in this study, *viz*., superficially positioned tight junctions and gap junctions in addition to the deeper situated desmosomes. This study also revealed that lateral attachment of both ciliated cells and goblet cells was effected through wide, regularly positioned cytoplasmic projections connected by desmosomes. Between these sites of contact the cells typically displayed numerous slender cytoplasmic projections which interdigitated with each other. The present TEM study also confirmed the stratified nature of the epithelium seen by LM in parts of the oesophagus. In these regions, not all the layers of cells were seen to attach to the basal lamina. The more superficially situated cells were coupled to the apical surface of the deeper cell layers via desmosomes and interdigitating cytoplasmic processes.

Due to the fact that all material used in this investigation came from similarly aged animals, it cannot be assumed that patterns seen in this study are consistent throughout the life of the animal or that these animals, which were raised intensively in hot house conditions, are similar to wild specimens. It should be emphasised that the results obtained from this study reflect the morphology of relatively young (sub-adult) animals of between 2.5 – 3 years of age. Crocodiles only attain sexual maturity at approximately 12 – 15 years of age and therefore the measurements presented in this chapter would obviously only be valid for younger specimens. It is, however, unlikely that the basic structure of the tissues examined would change appreciably with age (J.T. Soley, personal communication, 2002).

REFERENCES

ANDREW, W. 1959. *Textbook of comparative histology*, 1st ed. New York: Oxford University Press.

ARVY, L. 1962. Histochimie des enzymes impliqués dans la digestion, dans la série animale, in *Handbuch der Histochemie*, edited by W. Graumann and K.H. Neumann. Stuttgart: Gustav Fischer. Chapter 7:154-303.

ARVY, L. & BONICHON, A. 1958. Contribution a l'histoenzymologie de *Crocodylus niloticus* Laurenti. *Zeitschrift für Zellforschung*: 48:519-535.

BANCROFT, J.D. & COOK, H.C. (Eds) 1994. *Manual of histological techniques and their diagnostic application*. Edinburgh: Churchill Livingstone.

BATH, W. 1905. Über das Vorkommen von Geschmacksorganen in der Mundhöhle von *Krokodilus niloticus* Laur. *Zoologisches Anzeiger*, 29:352-353.

BATH, W. 1906. Die Geschmacksorgane der Vögel und Krokodile, *Archiv für Biontologie*, 1:4-52.

BÉGUIN, F. 1904. La muqueuse oesophagienne et ses glandes chez les reptiles. *Anatomischer Anzeiger*, 24:337-356.

CHIASSON, R.B. 1962. *Laboratory anatomy of the alligator*. Dubuque, Iowa: WM.C. Brown Company Publishers. 3-38.

CROSS, R.H.M. 1989. A reliable epoxy resin mixture and its application in routine biological transmission electron microscopy. *Micron and Microscopica Acta*, 20:1-7.

EISLER, P. 1889. Zur Kenntnis der Histologie des Alligatormagens. *Archiv für mikroskopische Anatomie*, 34:1-10.

FAWCETT, D.W. 1986. *Bloom and Fawcett. A textbook of histology*, 11th ed. Philadelphia: W.B. Saunders Co.:619-624.

GABE, M. 1971. Répartition des cellules histaminergiques dans le parvis gastrique de quelqués reptiles. Comptes Rendus Hebdomadaires des Séances de L'Académie des Sciences, Paris: Série D, 273:2287-2289.

GERNEKE, W.H. 1980. The origin and significance of the Langerhans cell granules. *Journal of the South African Veterinary Association*, 51:137-142.

HUCHZERMEYER, F.W. 1995. The topography of some endocrine organs in the Nile crocodile. *Zimbabwe Veterinary Journal*, 26:11-18.

JACOBSHAGEN, E. 1920. Zur Morphologie des Oberflächenreliefs der Rumpfdarmschleimhaut der Reptilien. *Jenaische Zeitschrift für Naturwissenschaften*, 56:361-430.

LUNA, L.G. (Ed.) 1968. *Manual of histologic staining methods of the Armed Forces Institute of Pathology.* 3rd ed. American Registry of Pathology. New York: McGraw-Hill Book Company.

LUPPA, H. 1977. Histology of the digestive tract, in *Biology of the Reptilia*, *Morphology E*, edited by C. Gans, & T.S. Parsons. London: Academic Press. Volume 6:225-313.

PARSONS, T.S. & CAMERON, J.E. 1977. Internal relief of the digestive tract, in *Biology of the Reptilia*, *Morphology E*, edited by C. Gans, & T.S. Parsons. London: Academic Press. Volume 6:159-223.

PEARSE, A.G.E. 1985. *Histochemistry. Theoretical and applied*. *Analytical technology*. 4th ed. Volume 2, Edinburgh: Churchill Livingston.

PERNKOPF, E. & LEHNER, J. 1937. Vergleichende Beschreibung des Vorderdarms bei den einzelnen Klassen der Kranioten, in *Handbuch der vergleichenden Anatomie der Wirbeltiere* edited by L. Bolk, E. Göppert, E. Kallius and W. Lubosch. Berlin: Urban and Schwarzenberg, Volume 3:349-476.

REESE, A.M. 1913. The histology of the enteron of the Florida alligator. *Anatomical Record*, 7:105-129.

REYNOLDS, E.S. 1963. The use of lead citrate at high pH as an electron-opaque stain in electron microscopy. *Journal of Cell Biology*, 17:208-212.

ROMER, A.S. 1962. *The vertebrate body*, 3rd ed., Philadelphia: W.B. Saunders.

STEEL, R. 1989. Anatomy of a living fossil, in *Crocodiles*. London: Christopher Helm: 12-36.

TAGUCHI, H. 1920. Beiträge zur Kenntnis über die feinere Struktur der Eingeweideorgane der Krokodile. Mitteilungen aus der Medizinischen Fakultät der Kaiserlichen Universität zu Tokyo, 25:119-188.

VAN ASWEGEN, G. 1975. Die mikroanatomie van die maag en dermkanaal van die pofadder (*Bitis arietans*). M.Sc. Thesis, University of Pretoria.

VAN DER MERWE N.J. & KOTZÉ, S.H. 1993. The topography of the thoracic and abdominal organs of the Nile crocodile (*Crocodylus niloticus*). *Onderstepoort Journal of Veterinary Research*, 60:219-222.

WATSON, M.L. 1958. Staining of tissue sections for electron microscopy with heavy metals. *Journal of Biophysical and Biochemical Cytology*, 4:475-478.

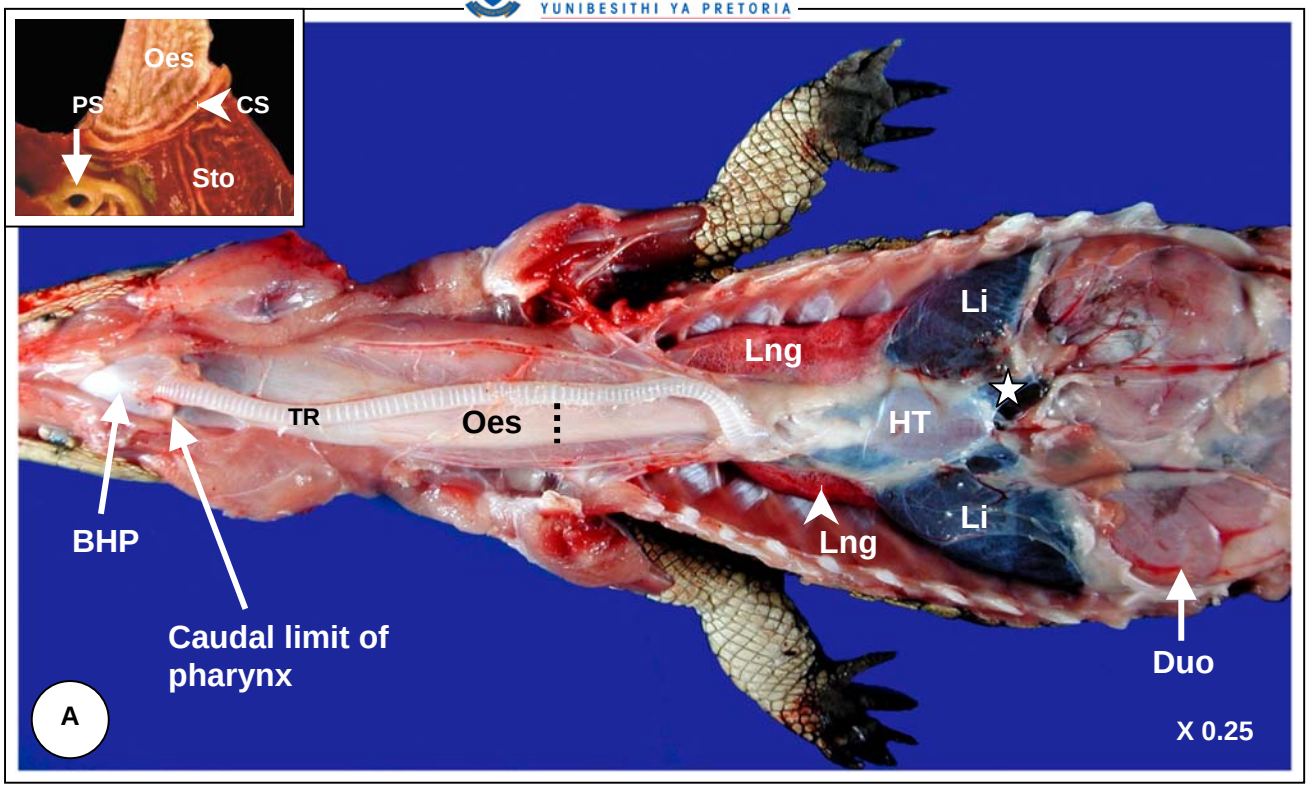

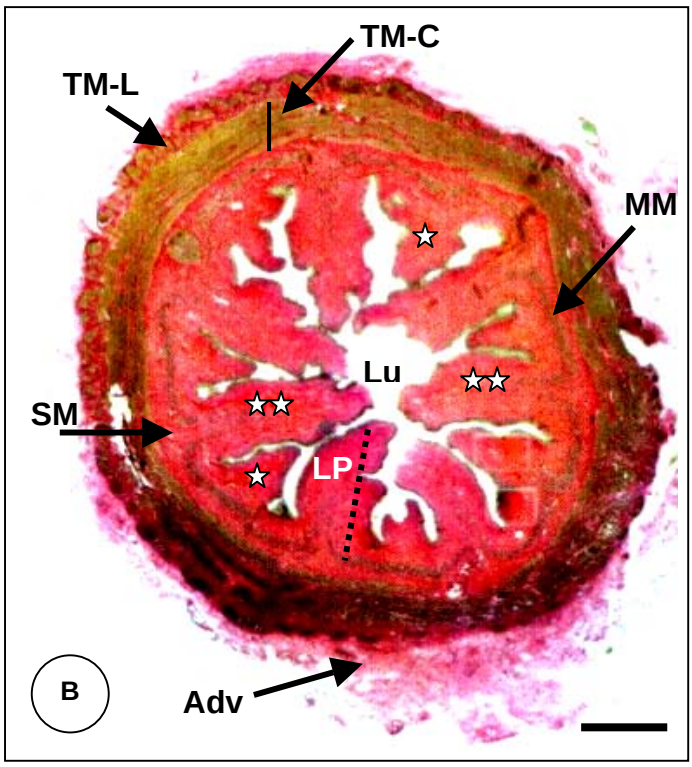

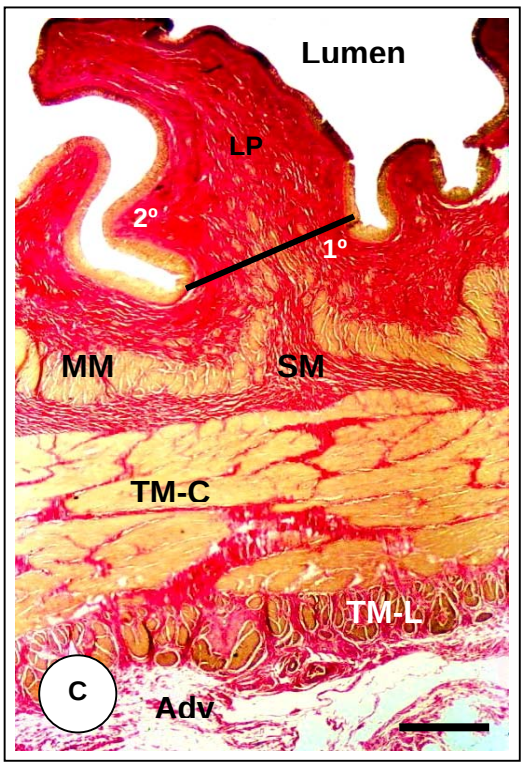

FIG. 1A: Macrophotograph of the torso of *C. niloticus* (ca. 3 year-old) showing the *in situ* position of the basihyal plate (BHP), oesophagus (Oes), trachea (TR), lungs (Lng), heart (HT), liver (Li) and duodenum (Duo). The dotted black line indicates the approximate region from which the cross sections illustrated in Figs. 1B & 1C were taken. The star represents the approximate position of entry of the oesophagus into the stomach.

Inset: Macrophotograph showing the prominent cardiac sphincter (CS) between the stomach (Sto) and oesophagus (Oes). Pyloric sphincter (PS). Fresh specimen. X 0.25 .

FIG. 1B: Lightmicrograph of a cross section of the mid-region of the oesophagus (approximately at the level of the black dotted line in Fig. 1A) showing the basic tissue layers. Note the alternating major (two stars) and minor (one star) longitudinal mucosal folds. Lamina propria (LP); muscularis mucosae (MM); submucosa (SM); inner circular layer of the tunica muscularis (TM-C); outer longitudinal layer of the tunica muscularis (TM-L); adventitia (Adv) and oesophageal lumen (LU). Verhoeff's elastic-stain. Bar = 1mm.

FIG. 1C: Higher magnification light micrograph of a section of the mid-region of the oesophagus showing the basic tissue layers and pattern of folds. Lamina propria (LP); muscularis mucosae (MM); submucosa (SM); circular layer of the tunica muscularis (TM-C); longitudinal layer of the tunica muscularis (TM-L); major mucosal fold consisting of primary (1º) and secondary (2º) components. Verhoeff's Elastic stain. Bar = 250μm.

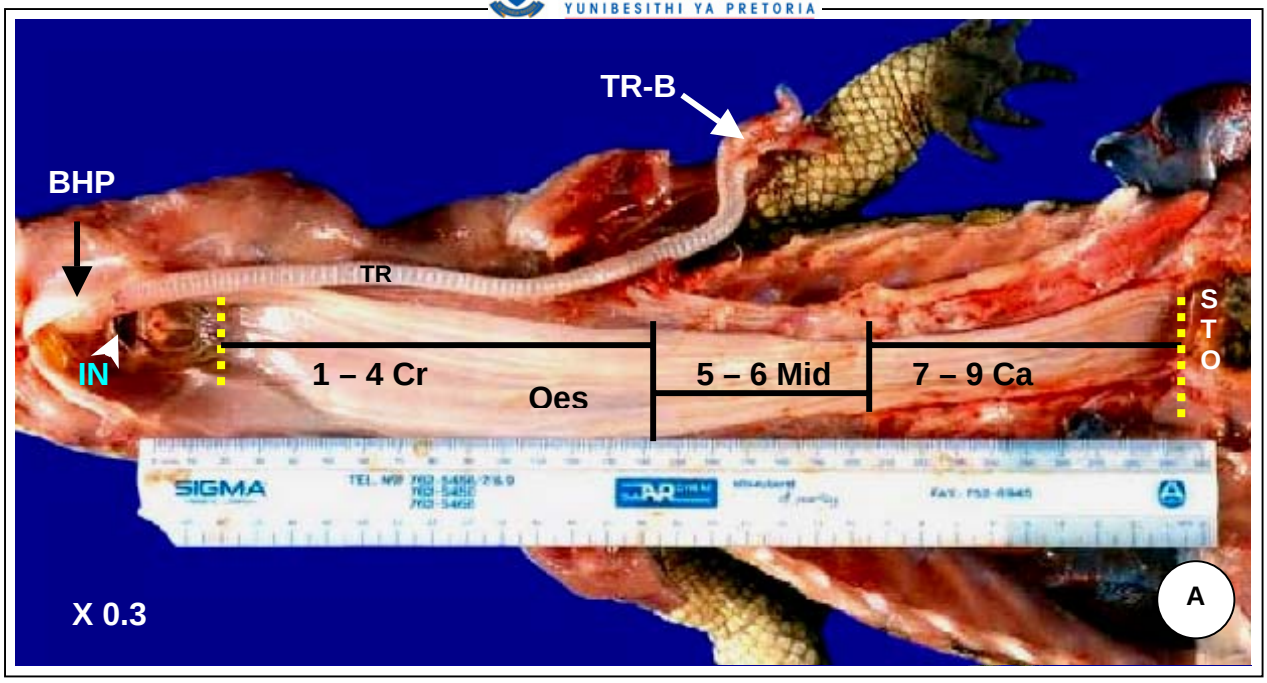

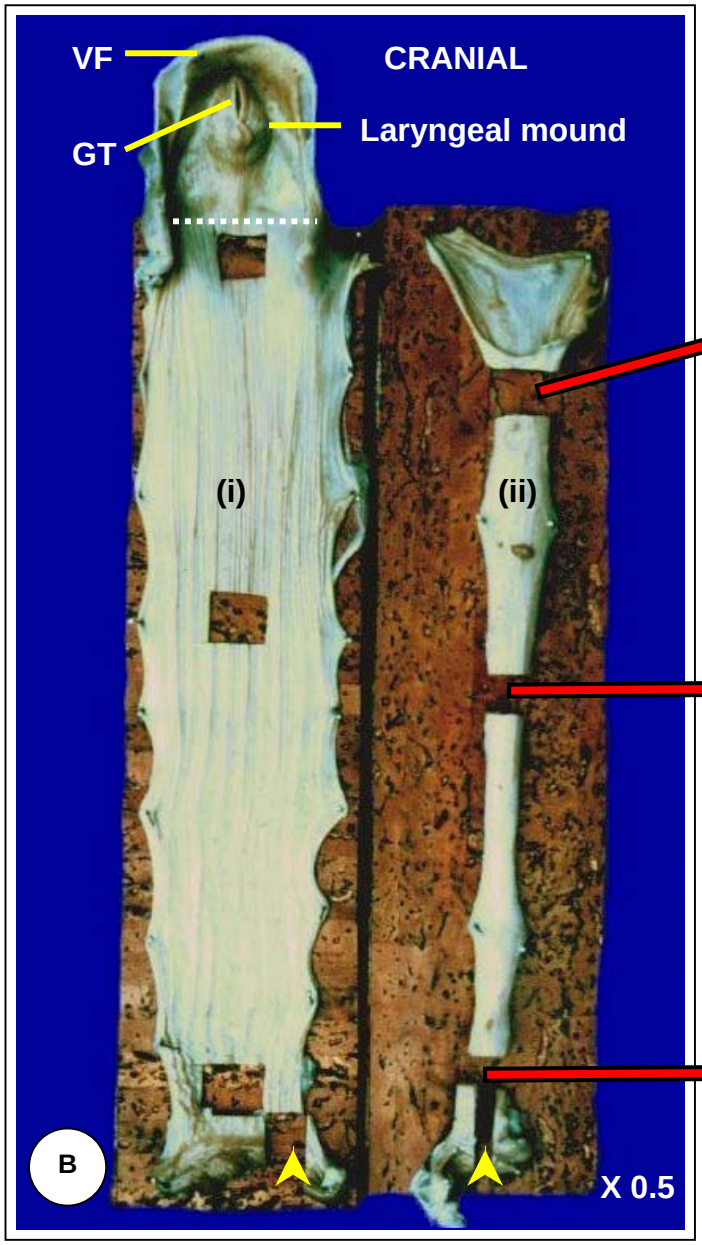

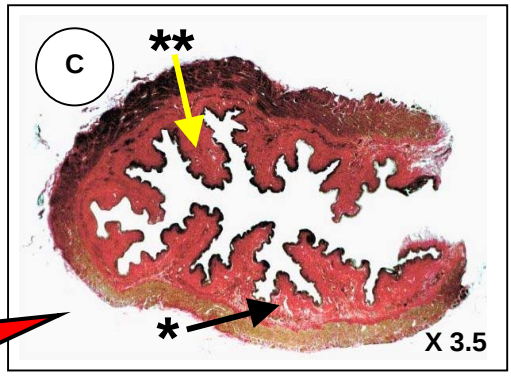

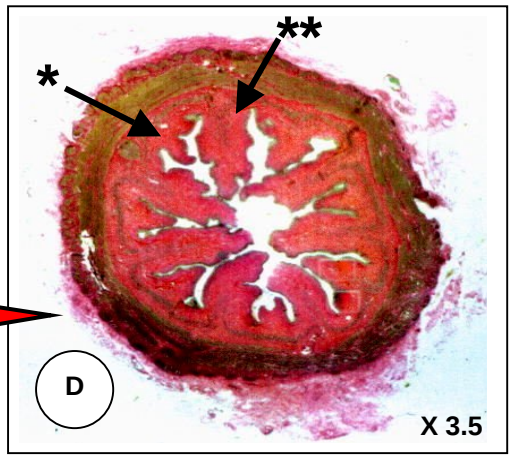

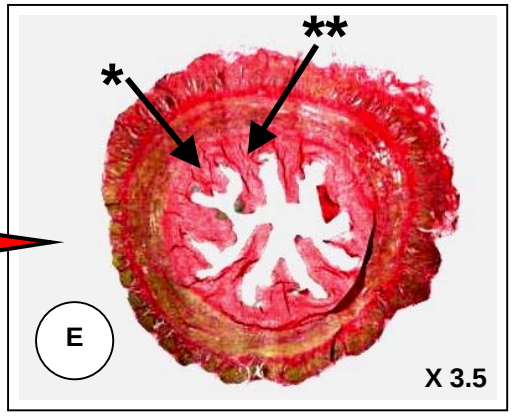

See captions opposite.

CAPTIONS TO FIGURE 2: MACROSCOPIC FEATURES OF THE OESOPHAGUS

FIG. 2A: Macrophotograph of the oesophagus *in situ*, slit longitudinally to reveal the luminal surface, showing the general division of the cranial (1-4CR), mid- (5-6MID) and caudal (7-9CA) regions selected for sampling during this study. The laryngeal mound and trachea have been reflected to illustrate the origin of the oesophagus from the base of the dorsal pharynx (transverse yellow-dotted line) and the median positioning of the oesophagus in the thoracic and abdominal cavities. Basihyal plate (BHP); internal nares (IN); oesophagus (OES); trachea (TR); bifurcation of the trachea (TR-B) stomach (STO). X 0.3 .

FIG. 2B: Macrophotograph of a fixed, splayed, pinned oesophagus (specimen i) and a fixed, pinned, un-slit oesophagus (specimen ii). The sections removed from specimen ii for light microscopy are illustrated in Figs. 2C, D & E respectively. Similar regions were removed from specimen i for SEM examination. Specimen i also shows the transition between the pharynx and the oesophagus, approximately in the region of the dotted line. The ventral fold (VF) of the gular valve and the laryngeal mound with the glottis (GT) are visible on the floor of the pharynx (see also Chapter 3 - Figs. 2A & B). Specimens used for describing the histology of the gastro-oesophageal junction (cardiac sphincter) were taken from the area at the yellow arrowheads. X 0.5 .

FIGS. 2C-E: Stereomicrographs of Verhoeff's elastic-stained cross-sections from the regions shown in Fig. 2B, specimen ii. 2C = cranial region; 2D = mid-region; 2E = caudal region. Note that the number and pattern of the mucosal folds (major [**] and minor [*] folds) remains relatively constant, but that the complexity of the mucosal folds (number of secondary and tertiary folds) decreases from the cranial to caudal regions. For reference see this chapter, Figs. 1B & C. All Figs. X 3.5 .

FIGURE 3: MORPHOLOGICAL FEATURES OF THE GASTRO-OESOPHAGEAL JUNCTION

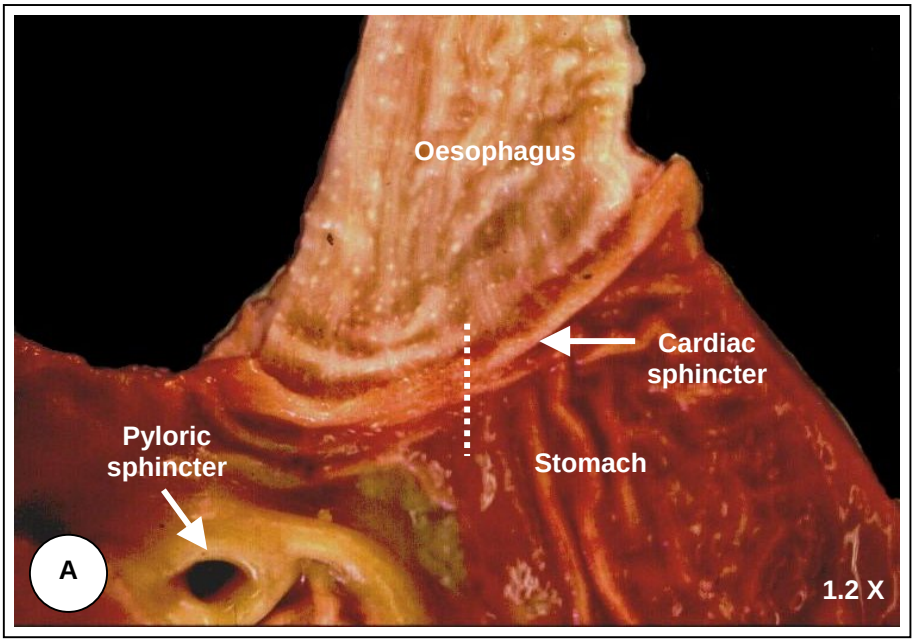

FIG. 3A: Macrophotograph of the gastro - oesophageal junction. The specimen has been splayed open to expose the luminal surfaces of the stomach and oesophagus. Note the distinctive colour transition between the oesophagus and stomach at the cardiac sphincter and also the close proximity of the cardiac and pyloric sphincters. The vertical line indicates the approximate region from where specimens were taken for histological examination. See Figs. 3B & 3C. Fresh specimen. X 1.2 .

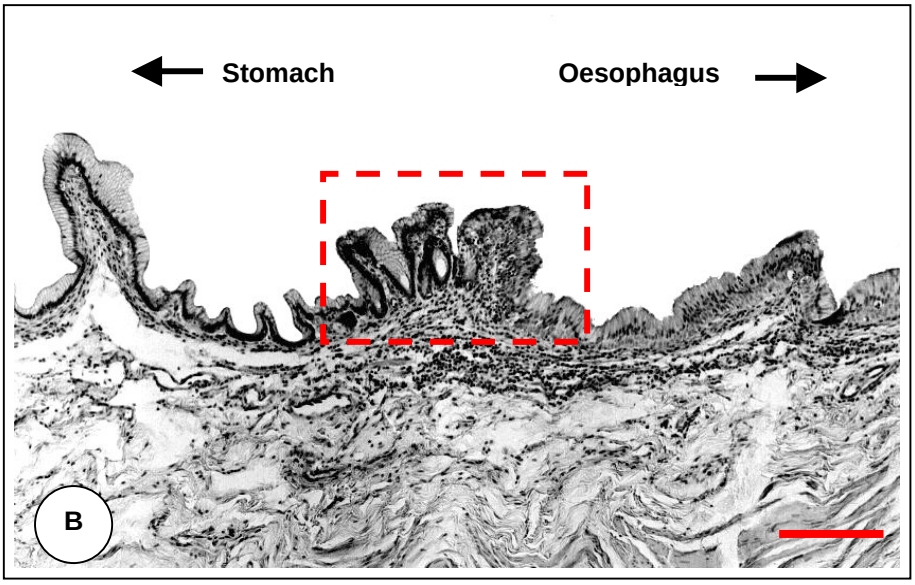

FIG. 3B: Light micrograph of the gastro - oesophageal junction. The mucosal folds within the block correspond to the ridge (cardiac sphincter) seen macroscopically in Fig. 3A. Note the relatively thinner epithelial lining of the stomach compared to that of the oesophagus. H&E-stain. Bar = 500μm.

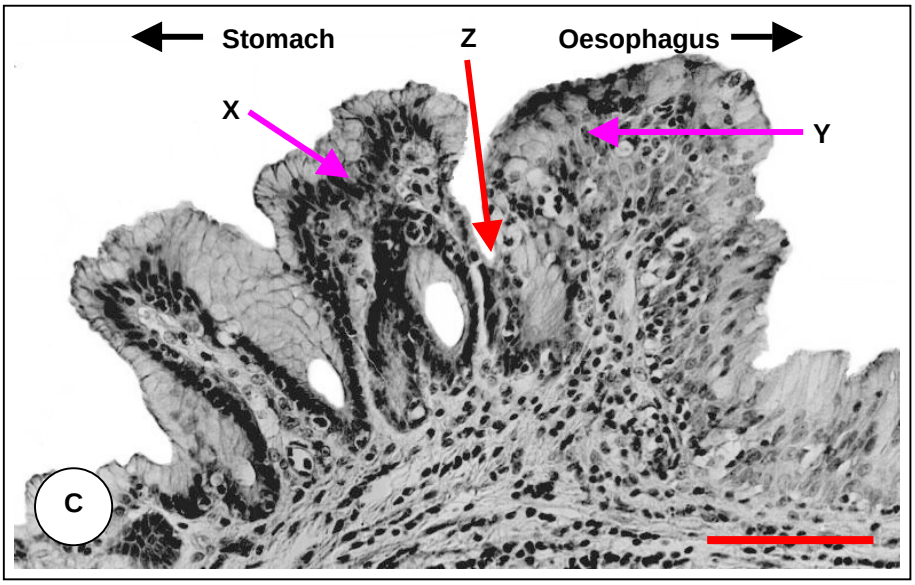

FIG. 3C: Higher magnification light micrograph of the block indicated in Fig. 3B. Note the change from the stratified/pseudostratified columnar epithelium of the oesophagus (Y) to the simple columnar epithelium of the stomach (X). The single row of dark nuclei associated with the simple columnar epithelium is conspicuous. The arrow at Z indicates the point of transition between the two epithelial types. H&E-stain. Bar = 20μm.

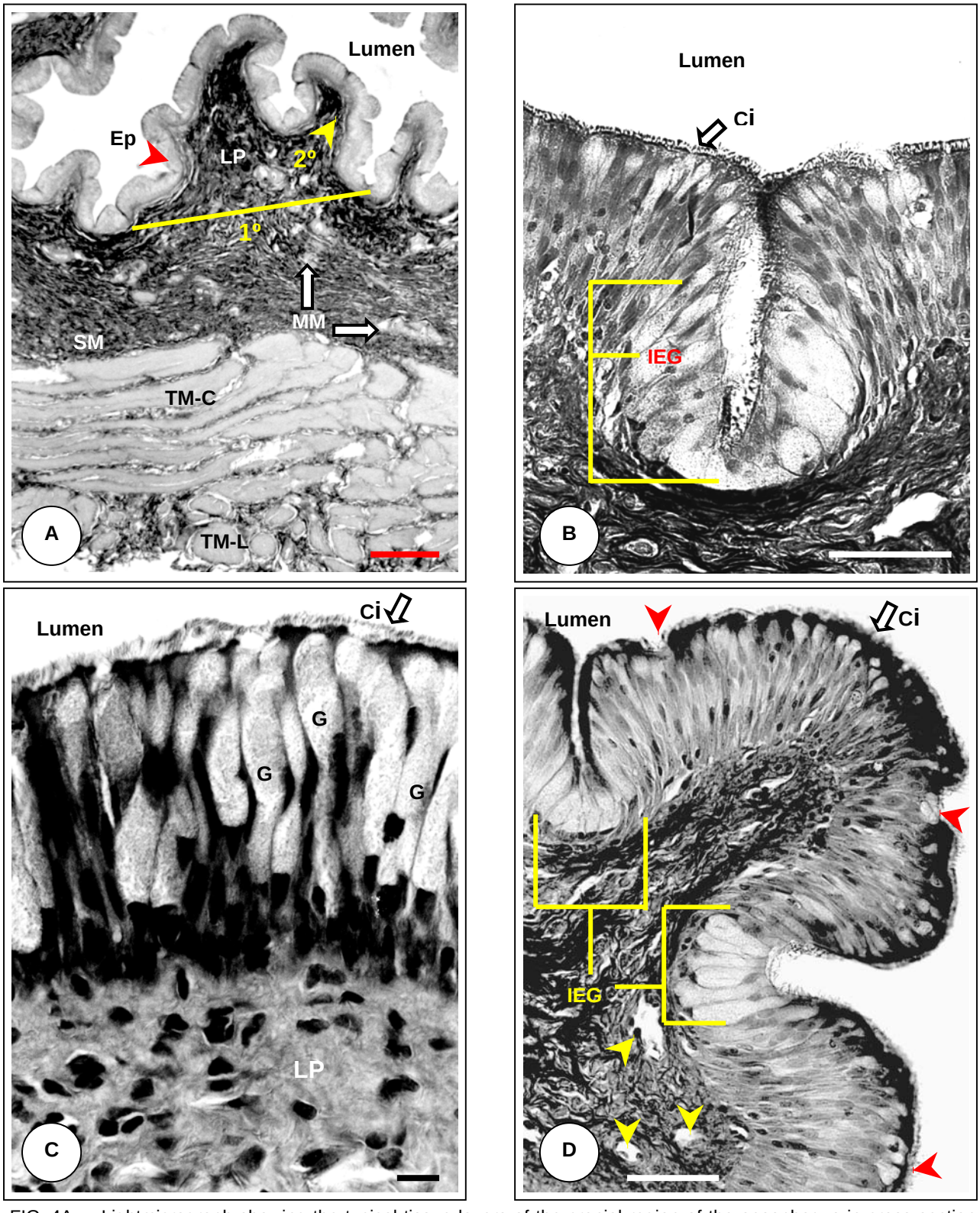

FIG. 4A: Lightmicrograph showing the typical tissue layers of the cranial region of the oesophagus in cross section. Note the poorly developed muscularis mucosae (MM) and the thick circular component (TM-C) of the tunica muscularis. Epithelium (Ep); lamina propria (LP); submucosa (SM); outer longitudinal layer of the tunica muscularis (TM-L); primary fold (1º); secondary fold (2º). Verhoeff's elastic-stain. Bar = 1mm.

FIG. 4B: A typical intra-epithelial gland (IEG) located within the stratified columnar epithelium. The base of the gland is composed exclusively of goblet cells. The luminal surface is densely ciliated (Ci). See Fig. 4D. H&E-stain. Bar = 10μm.

FIG. 4C: A typical pseudostratified columnar region of the epithelium in the cranial oesophagus. The pale, classically-shaped goblet cells (G) display basally compressed nuclei. The ciliated cells appear dark and form a definite surface layer. Lamina propria (LP). H&E-stain. Bar = 10μm.

FIG. 4D: Secondary mucosal folds supported by cores of connective tissue from the lamina propria. Note the blood vessels (yellow arrowheads) situated in close proximity to the epithelium. The dark-staining cytoplasm of the ciliated cells lines the luminal surface, except for narrow points of contact formed by goblet cells (arrows) (see TEM Fig. 12) Intra-epithelial gland (IEG). H&E-stain. Bar = 100μm.

FIGURE 5: CILIATION AND GOBLET C[illegible]: OESOPHAGUS

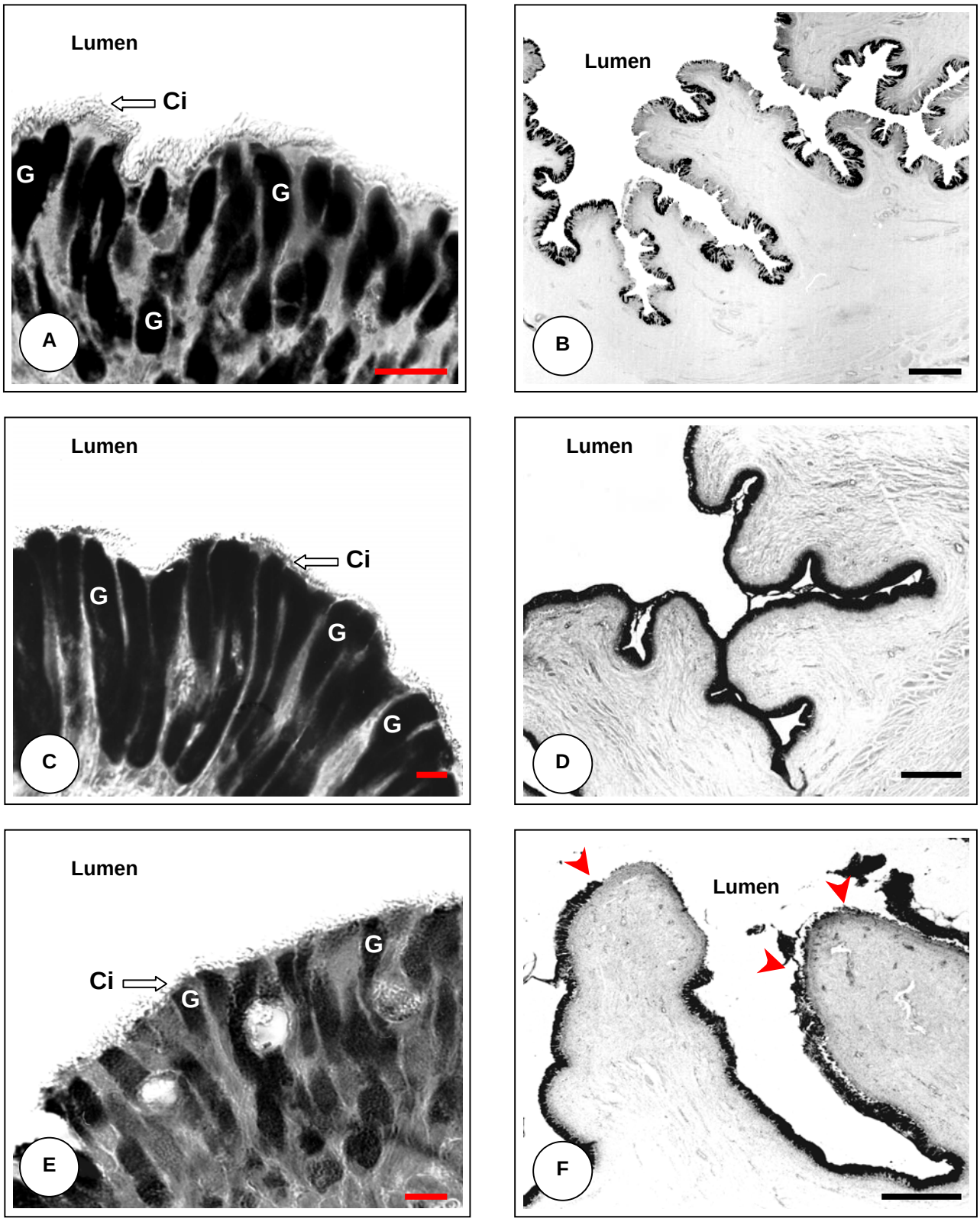

FIGS. 5A, C & E: Light micrographs showing the PAS-positive reaction of the goblet cell-rich epithelium in the cranial (Fig. 5A), mid- (Fig. 5C) and caudal (Fig. 5E) regions of the oesophagus. Note the decrease in density of cilia from the cranial to caudal regions and the greater length of the cilia in the cranial region. PAS-stain. Bar Figs. 5A, C & E = 20μm.

FIGS. 5B, D & F: Low magnification light micrographs showing the relative increase in goblet cell concentration (density) between the cranial region (Fig. 5B) and mid-region (Fig. 5D) seen in PAS-stained sections. No difference is apparent between the mid-region and caudal region (Fig. 5F). Note also the progressive simplification of the mucosal folds from the cranial- to caudal regions (compare with Figs. 5C & D). Cell sloughing is obvious in the caudal region (arrows – Fig. 5F). PAS-stain. Bar Figs. 5B, D & F = 1mm.

FIGURE 6: SEM FEATURES OF THE CRANIAL REGION OF THE OESOPHAGUS

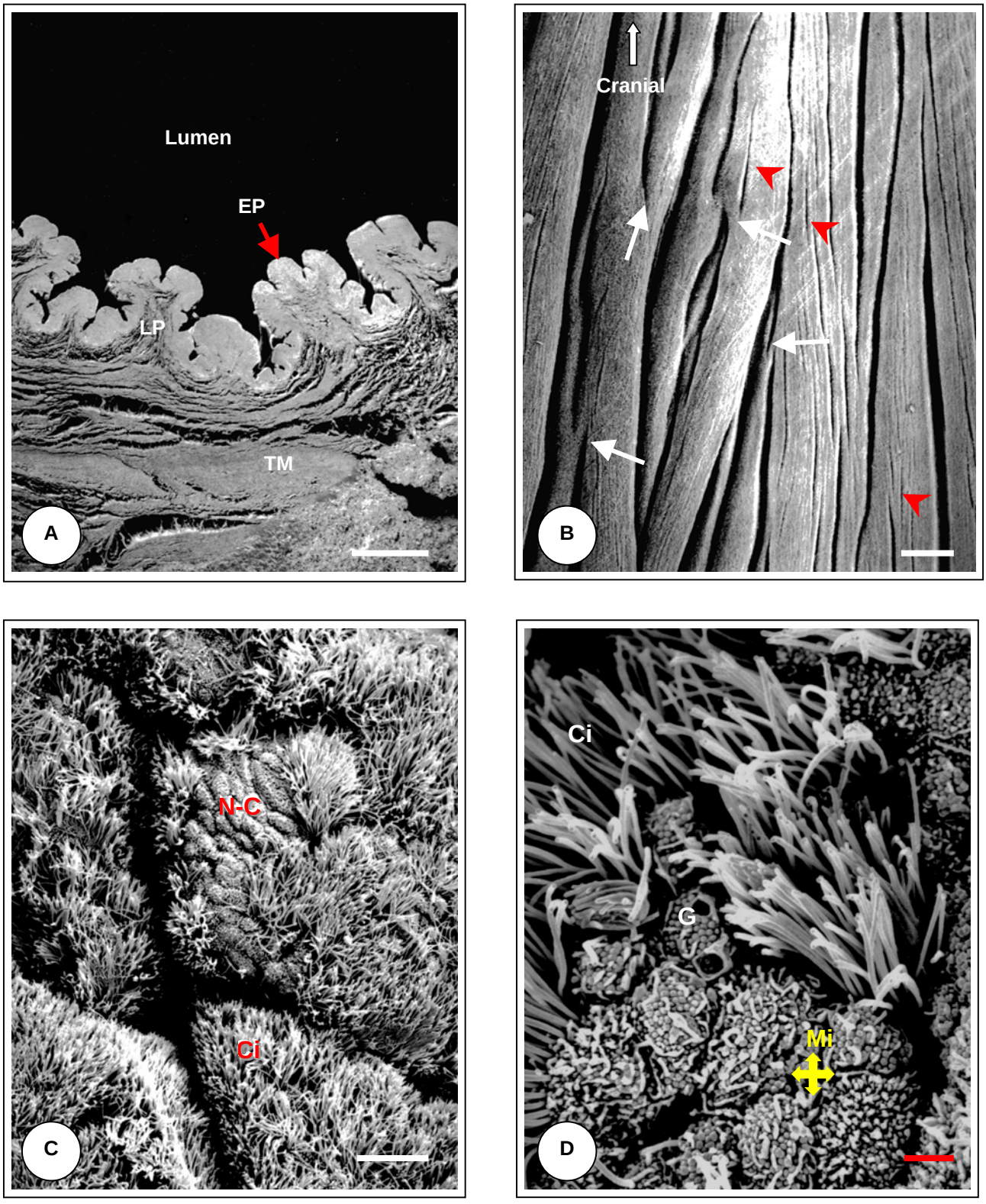

FIG. 6A: SEM-micrograph of a transverse section of the cranial region of the oesophagus. Note the alternating major and minor mucosal folds and secondary and tertiary branching. The muscularis mucosae is not clearly visible in this region. Epithelium (EP); Lamina propria (LP); tunica muscularis (TM). Specimen unpinned. Bar = 250μm.

FIG. 6B: The mucosal relief in the cranial region of the oesophagus. The fine longitudinal folds are closely packed and regularly branch and anastomose (arrows). The fine grooves (arrowheads) represent the borders of secondary and tertiary folds (see Figs. 4A & 6A). Pinned specimen. Bar = 100μm.

FIG. 6C: SEM-micrograph showing the densely ciliated nature of the epithelium covering the folds. Patches of non-ciliated cells (N-C) were also apparent throughout the region. Bar = 5μm.

FIG. 6D: High magnification SEM-micrograph of the cranial region showing ciliated and non-ciliated, microvillous covered cells (Mi). Cilia (Ci); erupted goblet cell (G). The non-ciliated cells probably represent the varying stages of development of the mucigen-filled goblet cells seen by LM (see Figs. 4B–D & 5A). Bar = 1μm.

FIGURE 7: SEM FEATURES OF THE OESOPHAGUS

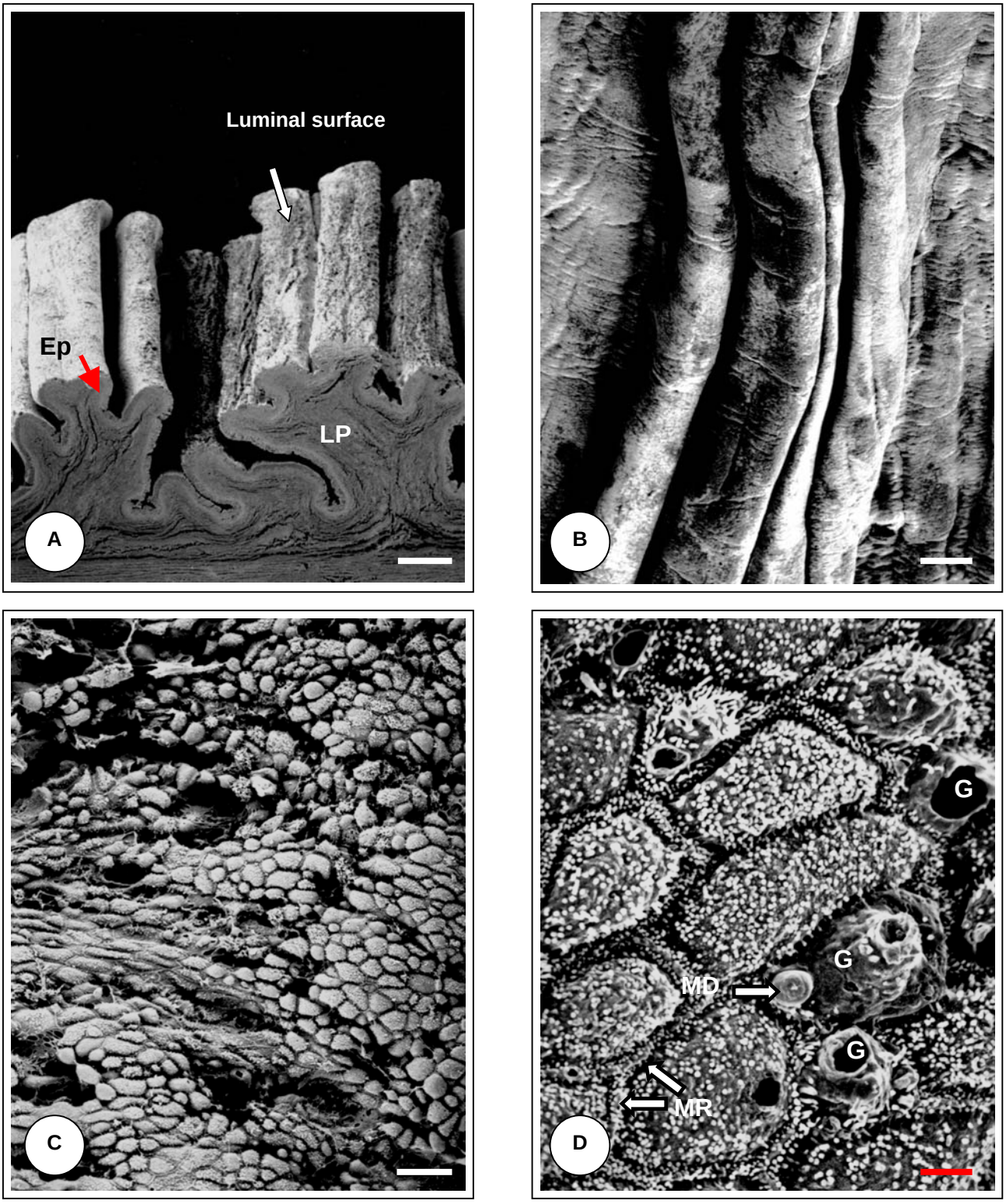

FIG. 7A: An oblique view of a cross section from the mid-region of the oesophagus showing taller, but less complicated (fewer secondary- and tertiary) mucosal folds. The epithelium (EP), and lamina propria (LP) are obvious in this region. The muscularis mucosae is not obvious in this micrograph. Bar = 250μm.

FIG. 7B: The mucosal relief in the mid-region of the oesophagus. The mucosal folds are more pronounced and stretch deeper into the lumen, but show very few longitudinal grooves compared to the cranial region (see Fig. 6B). Bar = 250μm.

FIG. 7C: Low power SEM-micrograph of the epithelium in the mid-region showing the polygonal to elongated surface profiles of the epithelial cells. No ciliated cells are present. Bar = 10μm.

FIG. 7D: SEM-micrograph of microvillous covered cells with microridges (MR) accentuating the polygonal shape of the cells. Erupted goblet cells (G); mucus droplet (MD). Based on LM observations, the non-ciliated cells in this region are probably goblet cells. Bar = 1μm.

FIGURE 8: SEM FEATURES OF THE OESOPHAGUS

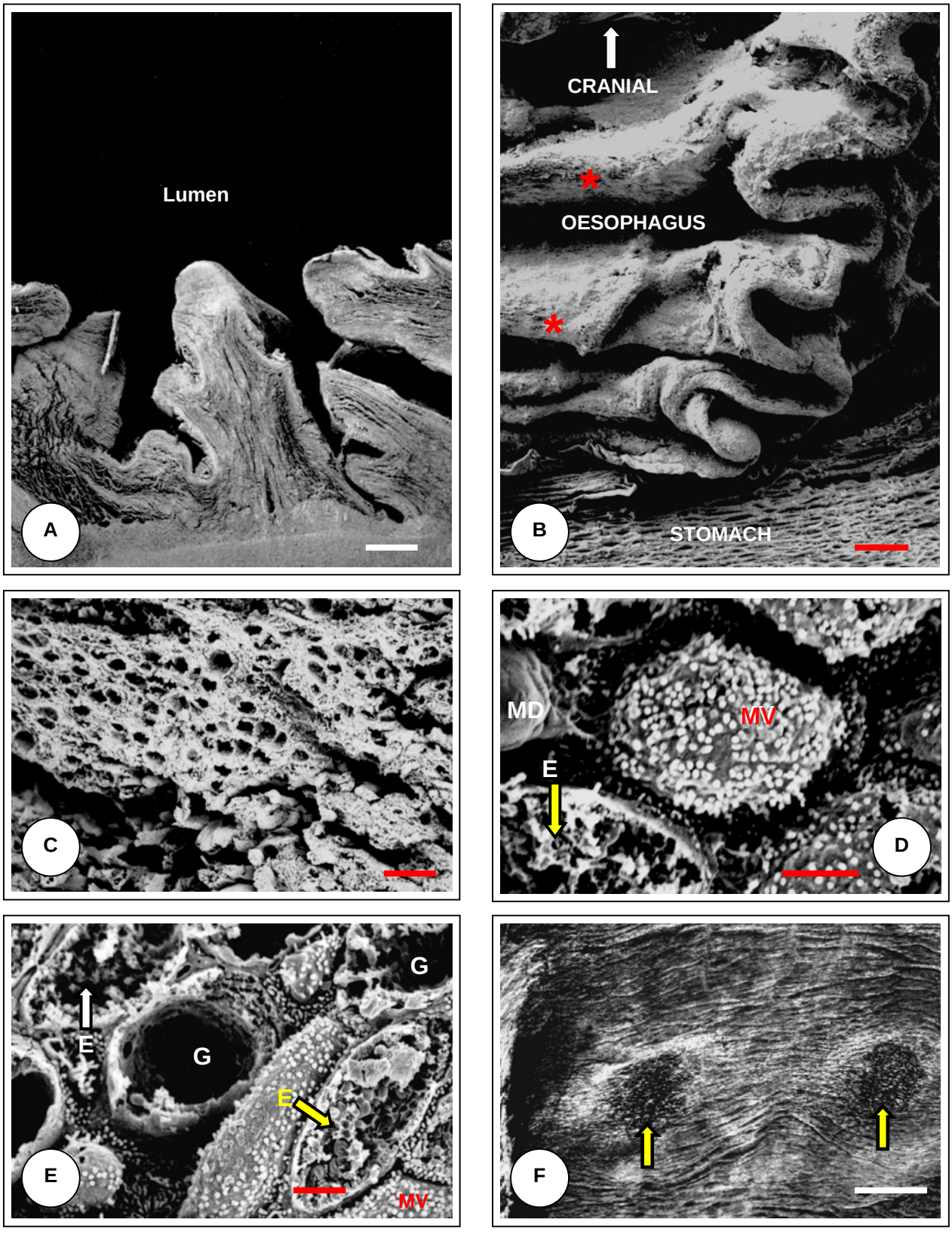

See captions opposite.

CAPTIONS TO FIGURE 8: SEM FEATURES OF THE CAUDAL REGION OF THE OESOPHAGUS

FIG. 8A: SEM-micrograph of a transverse section of the caudal region of the oesophagus. The mucosal folds are tall with only a few secondary folds present. Specimen unpinned. Bar = 250μm.

FIG. 8B: SEM-micrograph at the gastro-oesophageal junction. The wavy pattern of the folds, which makes them appear complex, is possibly due to shrinkage and post mortem contraction. Note the prominent transverse folds (asterisks) found in this region. Bar = 250μm.

FIG. 8C: Low magnification SEM-micrograph showing extensive erosion of the epithelium, possibly due to post mortem reflux of stomach contents. Bar = 10μm.

FIGS. 8D & E: Higher magnification SEM-micrographs of eroded (E) and intact, microvillous (MV) covered cells found in the caudal region of the oesophagus. No ciliated cells were seen by SEM in this region. Most of the cells are probably goblet cells at various stages of development. Some mucus droplets (MD) are visible. Erupted goblet cell (G). Bar = 1μm.

FIG. 8F: SEM-micrograph of subepithelial nodules (arrows) in the caudal region. The nodules became more numerous from the lower mid-region towards the gastro-oesophageal junction. Bar = 250μm.

FIGURE 9: TEM MORPHOLOGY OF THE EPITHELIAL CELLS

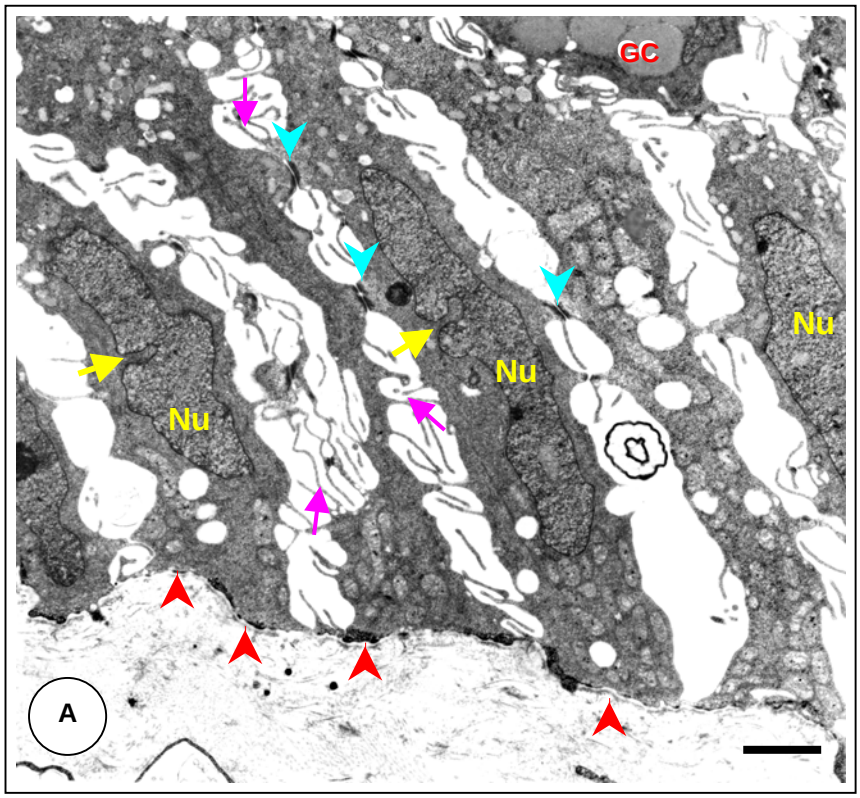

FIG. 9A: Low magnification TEM-micrograph of typical columnar basal epithelial cells with elongated nuclei (NU) displaying nuclear membrane folds (yellow arrows). The cells are firmly attached to the basal lamina (red arrowheads) by hemidesmosomes (see Fig. 10A). A number of desmosomes (blue arrowheads) can be seen which, together with the cytoplasmic processes (purple arrows) from adjacent cells, connect the cells together. The wide intercellular spaces are artefactual, probably as a result of delayed fixation or inadequate penetration of the fixative into the deeper tissue layers. A portion of a goblet cell (GC) can be seen at the top right of the micrograph. Bar = 2μm.

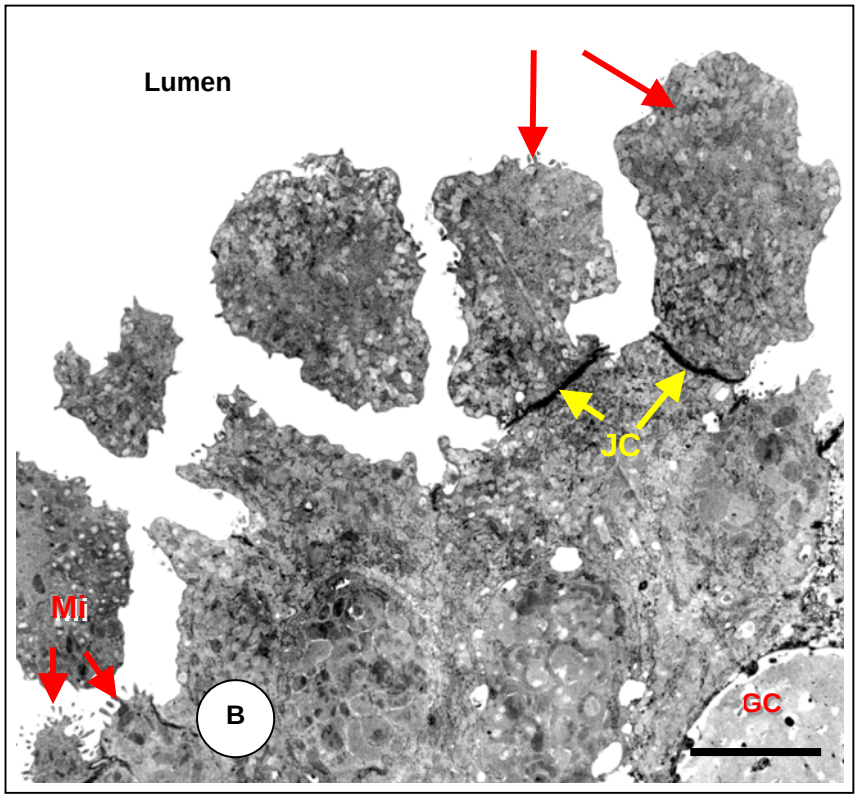

FIG. 9B: Low magnification TEM-micrograph of the luminal surface of the epithelium. Unidentified cells are seen to form large luminal protrusions (red arrows), separated from the main cell body by junctional complexes (JC). This may indicate the release of cytoplasm into the lumen. The cytoplasmic features of the cell protrusions are reminiscent of developing goblet cells. Microvilli (MI) are also associated with the surface of the protrusions. The apparently free-lying protrusions are possibly due to the plane of section. A portion of the apical region of a typical goblet cell (GC) may be seen in the lower right-hand corner of the micrograph. Bar = 5μm.

FIGURE 10: TEM FEATURES OF THE E TISSUE INTERFACE

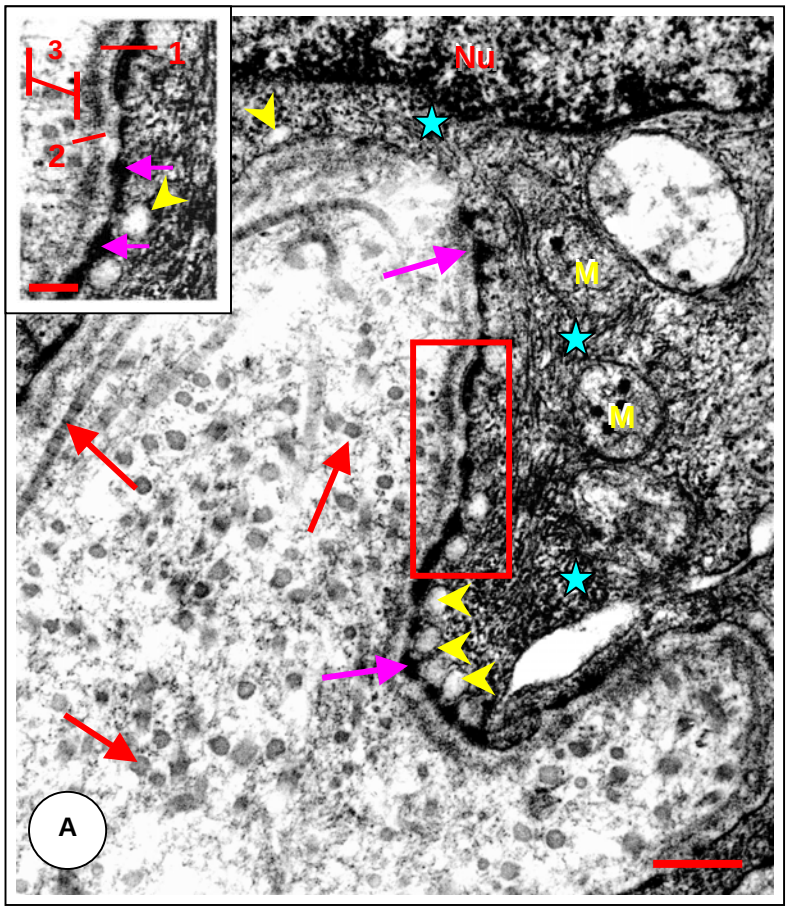

FIG. 10A: TEM-micrograph of the proximal region of a columnar basal cell showing the classical epithelium/basal lamina junction. Hemi-desmosome (purple arrows); nucleus (NU); mitochondria (M); collagen fibres oriented in various directions (red arrows); micro-pinocytotic vesicles (yellow arrowheads); radiating micro-filaments (blue stars). Bar = 250nm.

Inset: Higher magnification of the rectangle showing details of the basement membrane. Lamina densa (1), lamina rara (2), lamina reticularis (3), micro-pinocytotic vesicles (yellow arrowhead) and hemi-desmosomes (purple arrows). Bar = 100nm.

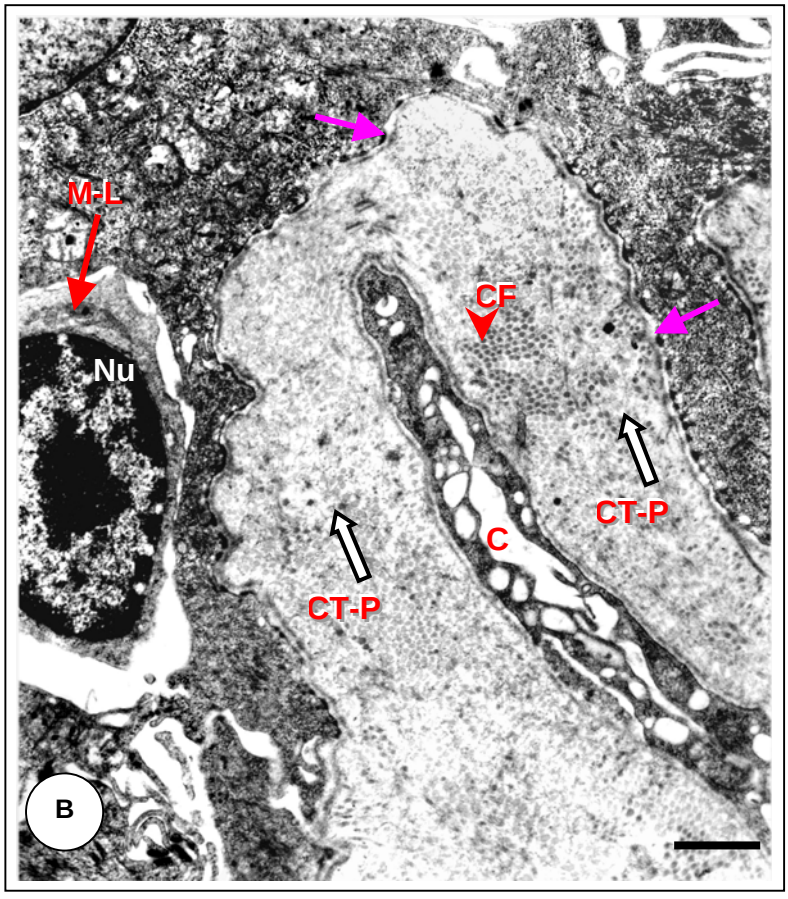

FIG. 10B: TEM-micrograph of a capillary (C) within a connective tissue papilla (CT-P) of the lamina propria and in close association with the basal lamina (purple arrows) of the epithelium. A group of transversely cut collagen fibres (CF) are obvious in the connective tissue papilla. A migratory lymphocyte (M-L) is situated close to the basal lamina. The nucleus (NU) is pycnotic and no cell junctions are formed with adjacent cells. Bar = 1μm.

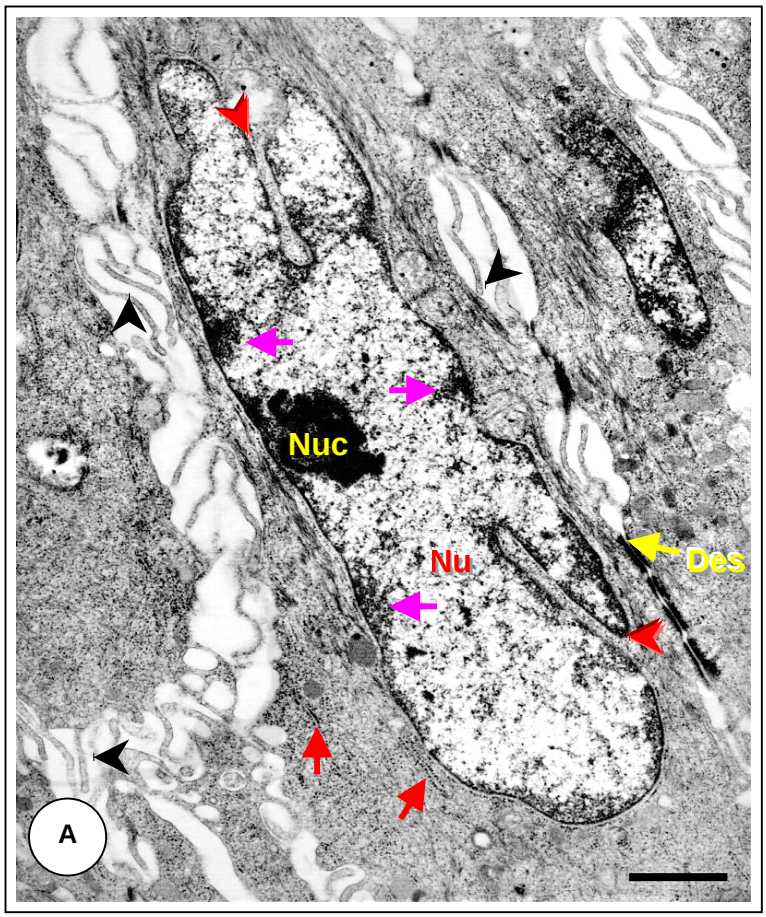

FIG. 11A: TEM-micrograph of an elongated nucleus (NU) of a columnar basal cell showing typical nuclear membrane folds (red arrowheads). The nucleus is oriented parallel to the long axis of the cell and shows small marginal accumulations of electron dense chromatin (purple arrows) and a large, electron-dense nucleolus (NUC). Desmosomal complexes (DES) between adjacent cells and strands of granular endoplasmic reticulum (red arrows) can be seen. Note the numerous, long cellular projections traversing the intercellular spaces (black arrowheads). Bar = 1μm.

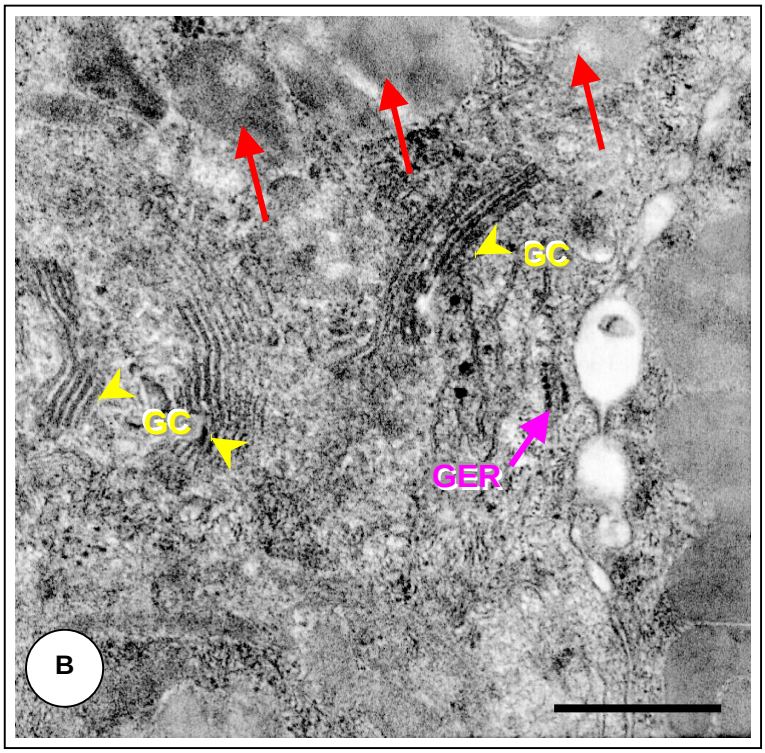

FIG. 11B: An enlargement of the Golgi-rich region located distal to the cell nucleus. Numerous profiles of the Golgi complex (GC) and some moderately electron-dense mucigen granules (red arrows) can be observed. A small strand of granular endoplasmic reticulum (GER) is also present. Bar = 0.5μm.

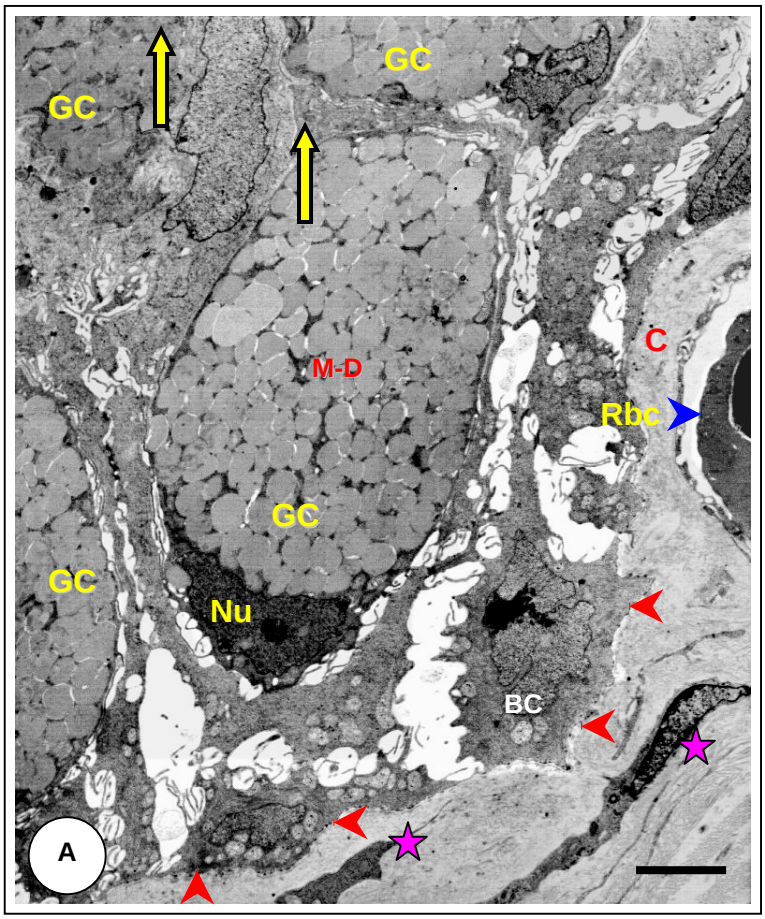

FIG. 12A: TEM-micrograph of a goblet cell (GC) situated near the basal lamina (red arrow-heads) of the epithelium. The cell appears to be migrating in the direction of the yellow arrows towards the luminal surface of the epithelium (see Fig. 12B). Note the com-pressed, electron-dense, cup -shaped nucleus (NU) at the base of the cell and the mass of mucigen droplets (M-D) filling the cytoplasm. Other goblet cells are also apparent at different levels of the epithelium. Note the portion of a capillary (C) at right of the image with a nucleated erythrocyte (Rbc) and a basal cell (BC) attached to the basal lamina. Fibroblasts (stars) are also visible in the lamina propria. Bar = 2.5μm.

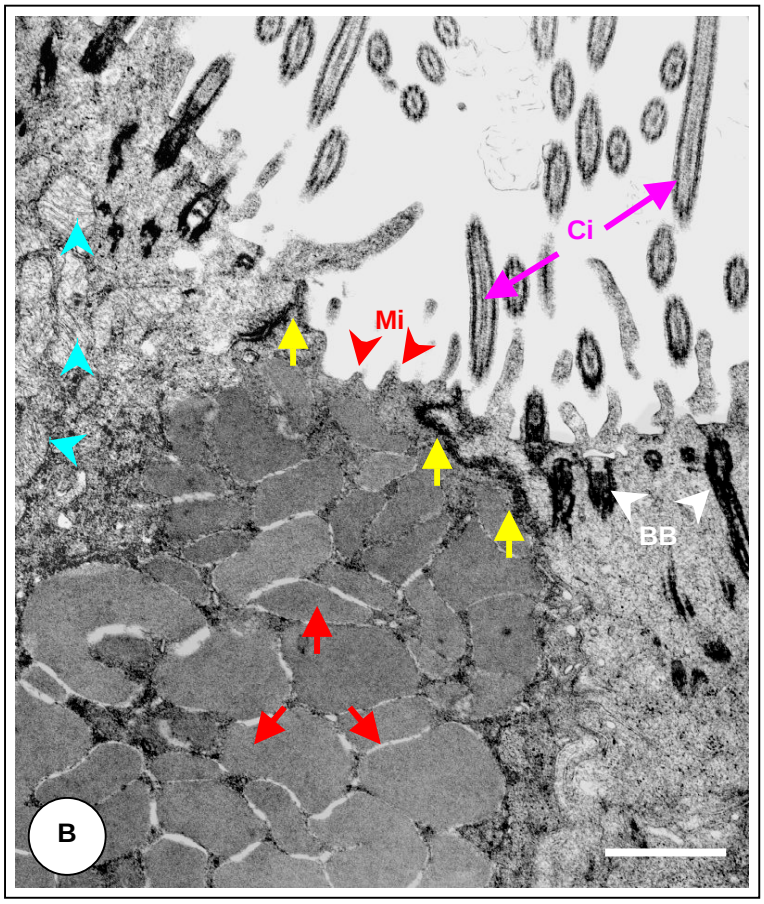

FIG. 12B: TEM-micrograph of the apical portion of a goblet cell. The cell has migrated from the basal region of the epithelium (see Fig. 12A) and lies wedged between two ciliated cells at the luminal surface. The surface of the goblet cell is non-ciliated and shows only a few short, stubby microvilli (Mi). Note the density and range in shape of the mucigen droplets (red arrows) within the goblet cell. The goblet cell is attached to the adjacent cells by apical junctional complexes (yellow arrows). The ciliated cells show an apical row of basal bodies (BB) (see detailed description in Fig. 13B – this chapter). Note the close proximity of mitochondria (blue arrowheads) to the basal bodies. Longitudinally sectioned cilia (Ci). Bar = 1μm.

FIGURE 13: TEM MORPHOLOGY OF THI ES

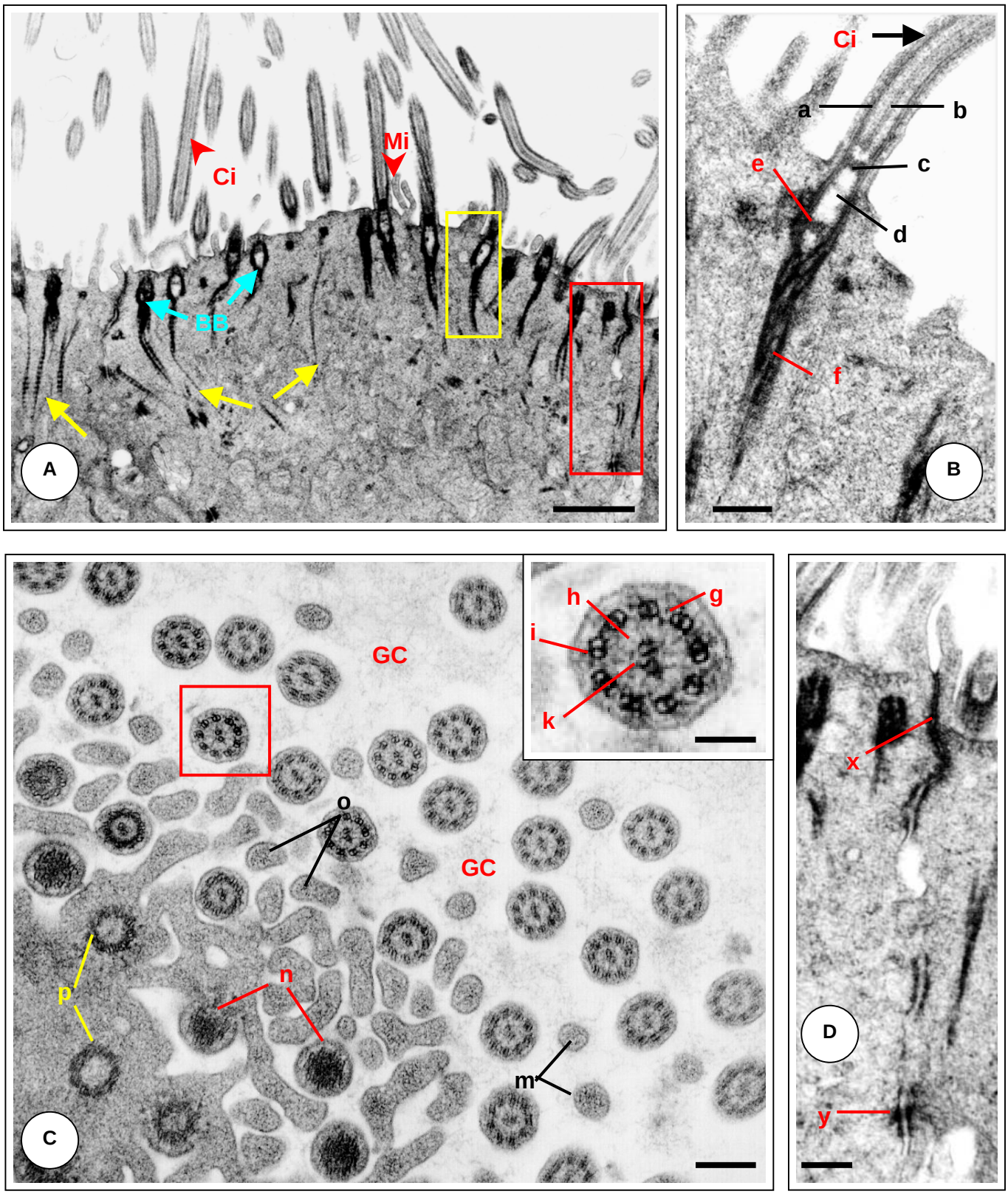

See captions opposite.

CAPTIONS TO FIGURE 13: TEM MORPHOLOGY OF THE CILIA AND BASAL BODIES

FIG. A: Low magnification TEM-micrograph of the apical surface of a ciliated epithelial cell showing a prominent row of basal bodies (BB) which give rise to the cilia (ci) seen in the oesophageal lumen. The rootlets of the basal bodies (yellow arrows) extend deep into the apical cytoplasm of the cell. A basal body and rootlet (yellow rectangle) are detailed in Fig. 13B. The junctional complex (red rectangle) joining adjacent cells is shown in Fig. 13D. A limited number of short microvilli (Mi) also occur between the cilia. Bar = 1μm.

FIG. B: Detailed enlargement of a basal body and rootlet giving rise to a cilium (ci). The outer microtubular doublets (a) of the axial filament complex arise from the wall of the basal body while a block of dense material (c) occupying the apical end of the basal body gives rise to the central pair of microtubules (b). The lumen (d) of the basal body appears “empty”, except for a block of dense material (e) situated towards the base of the lumen. Long ciliary rootlets (f), sometimes showing spiralling, extend deep into the apical cytoplasm of the cell. Note the faint cross striations (also apparent in Fig. 13A) exhibited by the rootlets. Bar = 250nm.

FIG. C: Various structures are illustrated at the apical cytoplasmic/luminal interface of a ciliated cell. A complex of microvilli is observed in cross- (m) and oblique (o) section while basal bodies are seen transected at various levels – (n) is cut through the block of dense material at the tip of the basal body while (p) is sectioned just beneath it and shows an “empty” lumen. A diffuse glycocalyx (GC) is associated with the microvilli and cilia. Bar = 250nm.

Inset: Higher magnification of a cross section of a cilium showing the typical 9 X 2 + 2 microtubular arrangement of the axoneme. Also visible are the dynein arms (g) associated with the 9 sets of peripheral doublets (i) and the radial spokes (h) linking the microtubular doublets to the centrally situated, paired microtubules (k). Bar = 100nm.

FIG. D: Enlargement of the junctional complex binding the apical regions of the cells. Tight junctions (x), and deeper lying desmosomes [zonula adherens] (y) form the junctional complex. Gap junctions are not visible in the micrograph. Bar = 250nm.

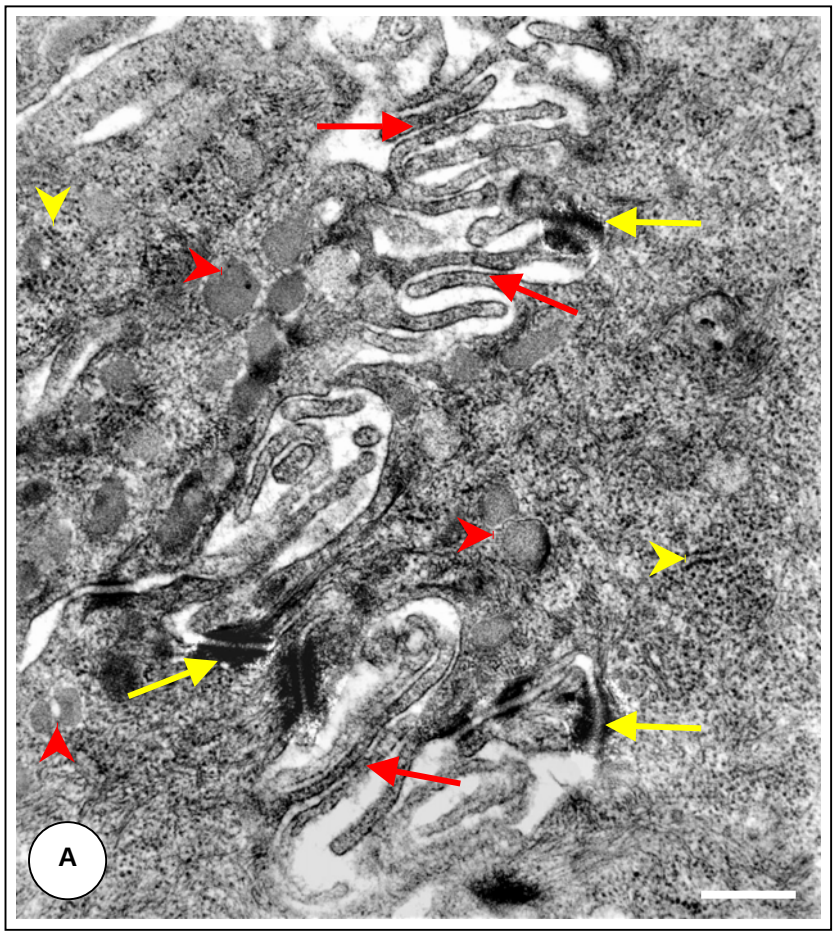

FIG. 14A: TEM-micrograph of deeper lying columnar epithelial cells showing interdigitation of the numerous, long cytoplasmic projections (red arrows) from adjacent cells. Desmosomes (yellow arrows) occur at points of contact along the length of the adjacent cells. The homogenous cytoplasm contains scattered ribosomes, occasional short strands of GER (yellow arrowheads) and scattered mucigen granules (red arrowheads). Bar = 250nm.

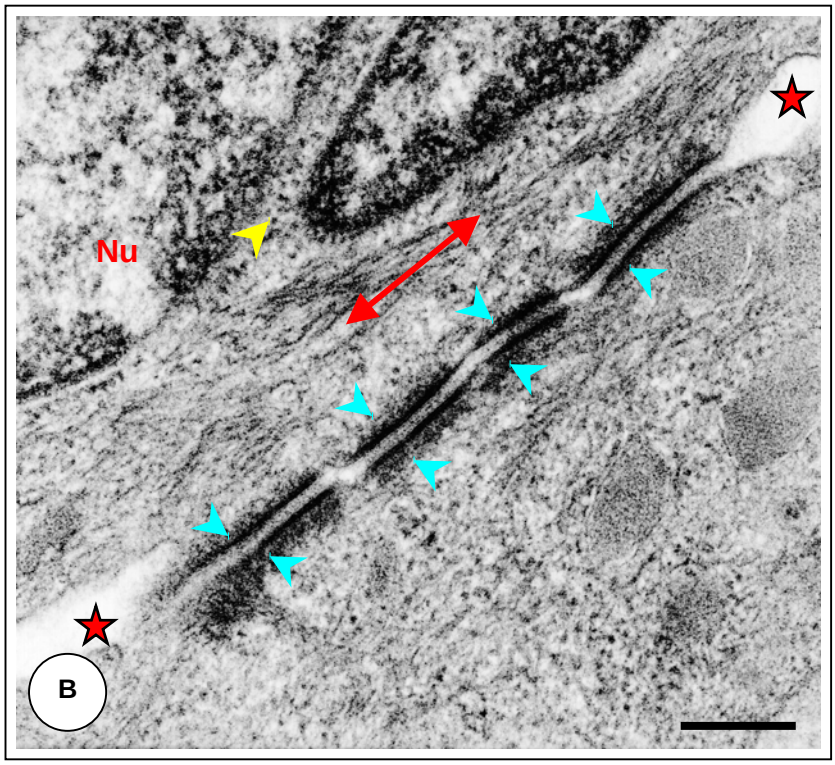

FIG. 14B: TEM-micrograph of a desmosomal band at the point of contact between two adjacent cells. Note the fine, long microfilaments running parallel (double-headed arrow) to the desmosomal band. Note the widening of the inter-cellular space at either end of the complex (stars). A nucleus (NU) showing a portion of a nuclear membrane fold (yellow arrow) is positioned close to the desmosomal complex. The blue arrowheads show the dense material associated with the cytoplasmic face of the desmosomes. Bar = 250nm.

CHAPTER 5

GENERAL CONCLUSIONS

Morphological features in the crocodilian oral and pharyngeal cavities reflect the unique adaptation of these animals to their environment, particularly in respect of their feeding habits. According to the literature, the crocodile, while catching prey in water, would of necessity have to rely on a mechanism to prevent drowning while restraining its prey. The dorsal and ventral mucosal folds located in the gular region provide this mechanism by creating a valve-like seal (the gular valve) between the oral cavity and the pharynx, thus preventing flooding of the pharyngeal region. The extension of the nasal passages from the valved external nares, situated ventrally on the tip of the snout, to the internal nares, an opening situated in the roof of the pharyngeal cavity, is a further adaption to feeding in an aquatic environment. Together with the gular valve, the extended nasal passages provide an unrestricted airflow to the lungs while partially submerged in water. This airflow is further enhanced by the raised glottis, situated dorsally on a laryngeal mound on the floor of the pharyngeal cavity and which positions the larynx in close proximity to the internal nares. However, there are other opinions regarding the involvement of the gular valve during feeding activities in the water (F.W. Huchzermeyer, personal communication, 2002).

These unique morphological features were confirmed in the present study which, in addition, graphically illustrated that the size, positioning and nature of the dorsal and ventral components of the gular valve, together with a set of smaller mucosal folds guarding the lateral boundaries of the valve, provided complete isolation of the oral and pharyngeal cavities. This study also provided information on other distinguishing morphological features of the oral cavity. Although frequently illustrated in the literature, the cobbled appearance of the palate, including the clearly defined median ridge of closely positioned cobbles has not been described. Similarly, the small, rigid, conical process situated at the base of the first incisor teeth of the maxilla, and fitting into an opposing shallow depression in the mandible, has not previously been described.

The epithelial lining of the oral cavity (palate and gingivae) and the tongue showed little variation and revealed features typical of a lightly keratinised stratified squamous epithelium. Contrary to information supplied by some of the earlier literature, no glandular tissue was observed in the palate proper. However, branched tubulo-alveolar glands were present on the oral surface of the dorsal fold of the gular valve and could therefore be construed to be palatine glands.

Two types of specialised sensory structures were seen throughout the oral cavity and were characterised by modification of both the epithelial component and the underlying connective tissue. Each specialisation could be identified by light microscopy (LM) and scanning electron microscopy (SEM). Raised, dome-like structures with a markedly thickened epithelium were often associated with Pacinian-like corpuscles situated in the underlying connective tissue and were believed to represent sensory pressure receptors. Other specialisations, characterised by a flattened, thickened epithelium and the presence of structures within the epithelium resembling taste buds, were considered to be taste receptors. When viewed by SEM, the taste receptors revealed superficial pores with occasional clavate or hair-like processes protruding from them. Taste receptors were particularly obvious on the tongue where they were also associated with the walls of the secretory ducts of the lingual salivary glands where they opened onto the tongue surface.

Lingual salivary glands occurred in the posterior two-thirds of the tongue and displayed a weak PAS-positive reaction, chiefly at the periphery of the secretory lobules. A large volume of literature has speculated/postulated on the presence of salt secreting glands in the Crocodylinae and their absence in the Alligatorinae. Although no physiological studies were carried out during this study, the histological composition of the lingual glands of the Nile crocodile and those described from *Crocodylus porosus* appear similar. It can be concluded, therefore, that the glands occurring in *C. niloticus*, as postulated by certain authors, could be responsible for the secretion of both saliva (mucus secretion) and salt.

The pharyngeal cavity was also dorso-ventrally flattened. It was separated rostrally from the oral cavity by the gular valve and was continuous caudally with the oesophagus. The roof of the pharynx displayed the internal nares linking the pharynx to the nasal cavity and also the common opening to the Eustachian tubes. This study revealed that the latter opening was sealed by a plug of fibrous tissue that was continuous with a median tract of tissue separating the caudo-laterally located pharyngeal tonsils. Within this tissue tract was a longitudinally disposed band of striated muscle, presumably for controlling

the opening and closing of this valve in the aperture to the Eustachian ducts. The tonsillar region displayed a complex arrangement of mucosal folds and deep clefts. Tonsillar nodules were clearly visible and demonstrated a lack of ciliation. This region has only been superficially described in previous studies and its identification and characterisation in the present study could be of clinical importance. The floor of the pharyngeal cavity was dominated by the raised laryngeal mound containing the median, slit-like glottis. The morphological features of this structure have not previously been described but share certain characteristics with the laryngeal mound of birds.

As noted above, the rigid, internally supported ventral gular fold and the more flaccid dorsal fold, together with additional laterally positioned folds formed an effective seal between the oral and pharyngeal cavities. Both folds revealed a gradual transformation of the surface lining from a thin, lightly keratinised stratified squamous epithelium to a thick, non-keratinised stratified squamous epithelium and eventually to a stratified/pseudo-stratified columnar ciliated epithelium with goblet cells. In both folds the conversion to a typical respiratory type of epithelium was accomplished by mucous transformation of the stratified squamous epithelium. In this study the change in epithelial types was clearly illustrated by both light microscopy and scanning electron microscopy, and confirmed, in greater detail, the earlier observations made in the literature.

The epithelium of the pharyngeal cavity was predominantly of the respiratory type. Only the median regions of the dorsal and ventral folds, the caudal rim of the internal choanae and the tonsillar region were devoid of ciliated elements. Signs of cellular erosion, probably due to the passage of food, were seen in places.

The oesophagus could be divided anatomically into two clear regions; a proximal, flaccid region, occupying approximately two-thirds of the oesophageal length and a narrower, firmer, distal region stretching from the bifurcation of the trachea to the stomach entrance. The firming of the distal region was shown by LM to result from a greater smooth muscle component in the wall of the oesophagus. Histologically, the oesophagus could be divided into three regions (cranial, mid- and caudal) based on the proportion of goblet cells and ciliated cells along its length, as well as by progressive development of both the muscularis mucosae and tunica muscularis in a cranial to caudal direction. This study confirmed the general observation in the literature that in crocodilia the ciliated component of the

oesophageal epithelium thins towards the caudal aspect of the organ, together with a concomitant increase in the goblet cell component.

A pattern of longitudinal mucosal folds was a consistent feature throughout the pharyngeal cavity and oesophagus of the Nile crocodile. This arrangement of the mucosa would allow for distension of the upper digestive tract when swallowing large chunks of food which is the feeding habit of this animal. As the crocodile does not chew its food, the additional capacity of these regions to produce large amounts of mucus through the presence of goblet cells, intra-epithelial glands and mucus producing glands would further assist in conveying the food to the stomach.

This study presents baseline morphological information on the nature and composition of the upper digestive tract of the Nile crocodile and provides a point of reference for pathological studies of this region. The work also highlights previously unreported or superficially described features such as the sensory structures in the oral cavity and the pharyngeal tonsils, which will require more detailed study. The complementary nature of simultaneous light microscopical and scanning electron microscopical studies is also emphasised.